EXPLORING THE CROSSTALK BETWEEN ADIPOSE TISSUE AND THE CARDIOVASCULAR SYSTEM

EDITED BY: Nadia Akawi, Elena Sommariva, Kazuo Miyazawa, Hidekazu Kondo, Valerio Azzimato and Ileana Badi

PUBLISHED IN: Frontiers in Cell and Developmental Biology

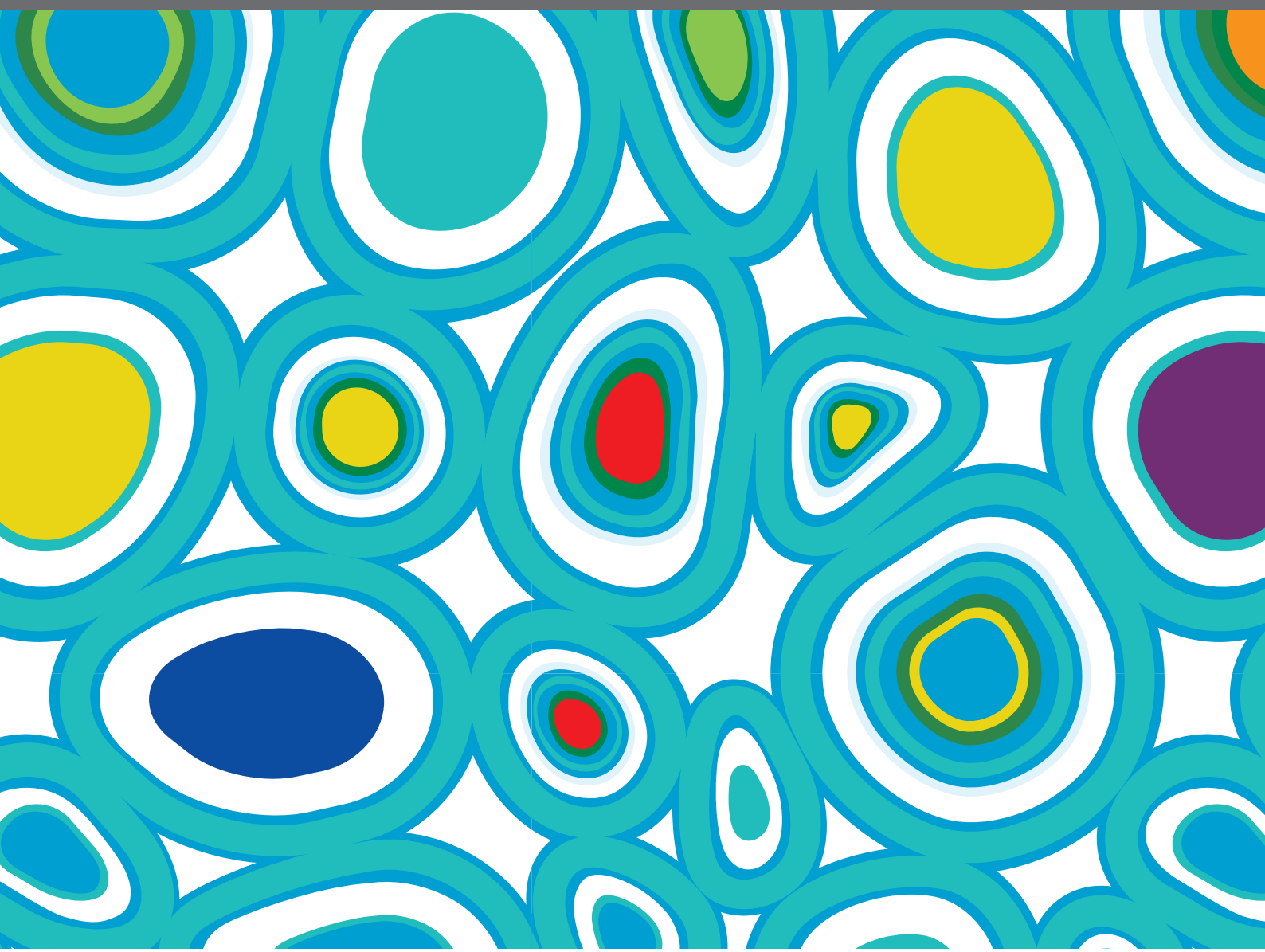

frontiers Research Topics

frontiers

ISSN 1664-8714
ISBN 978-2-88976-764-9
DOI 10.3389/978-2-88976-764-9

About Frontiers

Frontiers is more than just an open-access publisher of scholarly articles: it is a pioneering approach to the world of academia, radically improving the way scholarly research is managed. The grand vision of Frontiers is a world where all people have an equal opportunity to seek, share and generate knowledge. Frontiers provides immediate and permanent online open access to all its publications, but this alone is not enough to realize our grand goals.

Frontiers Journal Series

The Frontiers Journal Series is a multi-tier and interdisciplinary set of open-access, online journals, promising a paradigm shift from the current review, selection and dissemination processes in academic publishing. All Frontiers journals are driven by researchers for researchers; therefore, they constitute a service to the scholarly community. At the same time, the Frontiers Journal Series operates on a revolutionary invention, the tiered publishing system, initially addressing specific communities of scholars, and gradually climbing up to broader public understanding, thus serving the interests of the lay society, too.

Dedication to Quality

Each Frontiers article is a landmark of the highest quality, thanks to genuinely collaborative interactions between authors and review editors, who include some of the world's best academicians. Research must be certified by peers before entering a stream of knowledge that may eventually reach the public - and shape society; therefore, Frontiers only applies the most rigorous and unbiased reviews.
Frontiers revolutionizes research publishing by freely delivering the most outstanding research, evaluated with no bias from both the academic and social point of view. By applying the most advanced information technologies, Frontiers is catapulting scholarly publishing into a new generation.

What are Frontiers Research Topics?

Frontiers Research Topics are very popular trademarks of the Frontiers Journals Series: they are collections of at least ten articles, all centered on a particular subject. With their unique mix of varied contributions from Original Research to Review Articles, Frontiers Research Topics unify the most influential researchers, the latest key findings and historical advances in a hot research area! Find out more on how to host your own Frontiers Research Topic or contribute to one as an author by contacting the Frontiers Editorial Office: frontiersin.org/about/contact

EXPLORING THE CROSSTALK BETWEEN ADIPOSE TISSUE AND THE CARDIOVASCULAR SYSTEM

Topic Editors:
Nadia Akawi, United Arab Emirates University, United Arab Emirates
Elena Sommariva, Monzino Cardiology Center (IRCCS), Italy
Kazuo Miyazawa, RIKEN Yokohama, Japan
Hidekazu Kondo, Oita University, Japan
Valerio Azzimato, Department of Medicine, Huddinge, Karolinska Institutet (KI), Sweden
Ileana Badi, University of Oxford, United Kingdom

Citation: Akawi, N., Sommariva, E., Miyazawa, K., Kondo, H., Azzimato, V., Badi, I., eds. (2022). Exploring the Crosstalk Between Adipose Tissue and the Cardiovascular System. Lausanne: Frontiers Media SA. doi: 10.3389/978-2-88976-764-9

Table of Contents

frontiers | Frontiers in Cell and Developmental Biology

EDITORIAL
published: 15 July 2022
doi: 10.3389/fcell.2022.973135

Editorial: Exploring the Crosstalk Between Adipose Tissue and the Cardiovascular System

Ileana Badi[1]*, *Elena Sommariva*[2], *Kazuo Miyazawa*[3], *Hidekazu Kondo*[4], *Valerio Azzimato*[5] *and Nadia Akawi*[6]*

[1]Division of Cardiovascular Medicine, University of Oxford, Oxford, United Kingdom, [2]Unit of Vascular Biology and Regenerative Medicine, Centro Cardiologico Monzino IRCCS, Milan, Italy, [3]Laboratory for Cardiovascular Genomics and Informatics, RIKEN Center for Integrative Medical Sciences, Yokohama, Japan, [4]Department of Cardiology and Clinical Examination, Faculty of Medicine, Oita University, Yufu, Japan, [5]Center for Infectious Medicine, Department of Medicine Huddinge, Karolinska Institute, Karolinska University Hospital, Stockholm, Sweden, [6]Department of Genetics and Genomics, College of Medicine and Health Sciences, United Arab Emirates University, Al-Ain, United Arab Emirates

Keywords: adipose tissue, cardiovascular system, cardiovascular disease, adipokines, obesity

Editorial on the Research Topic

Exploring the Crosstalk Between Adipose Tissue and the Cardiovascular System

Many studies have confirmed the existence of a bidirectional cross-talk between adipose tissue (AT) and the cardiovascular system, which is crucial to the maintenance of normal physiological function in both tissues (Oikonomou and Antoniades, 2019). AT can be considered an endocrine organ *per se* releasing signaling messengers, such as microvesicles and immunomodulatory factors, that influence the development and progression of cardiovascular diseases (CVD) (Oikonomou and Antoniades, 2019). For instance, the altered structure and function of AT in obesity is accompanied by a dysregulated profile of adipokine secretion and is closely associated with an increased incidence of adverse CVD outcomes (Oikonomou and Antoniades, 2019). Similarly, the cardiovascular system secretes molecules that are detected by the surrounding AT, which "senses" cardiovascular inflammation and modify its secretory profile accordingly (Oikonomou and Antoniades, 2019).

The objective of this Research Topic was to receive studies that describe AT dysfunction in the metabolic syndrome and to delineate the role of AT-derived immunomodulatory factors in the development and progression of CVD. We also shed light on the role of "inside-to-outside" signaling (from the cardiovascular system to AT) in the cross-talk between the myocardium, the vasculature, and AT. Eight submissions were received (two reviews, one perspective and five research articles).

In this Research Topic, two review articles highlighted the role of different molecules in this crosstalk. Shalaby et al. reviewed the detrimental role of ceramides in the pathogenesis of cardiometabolic disorders including CVD, type II diabetes and obesity. In this paper the authors discussed the mechanisms by which ceramides affect endothelial dysfunction (Akawi et al., 2021). Ceramides were also reported to exert their detrimental effects via increasing insulin resistance, dysregulating cardiac muscle dilation and contractility, and augmenting inflammation. They also provided an update regarding possible ceramide-targeted therapies. Soci et al. instead described the current knowledge on the epigenetic role exerted by microRNAs in the cross-talk between AT and the cardiovascular system. They also discussed the latest evidence for heart-enriched microRNAs in cardiovascular diseases as epigenetic biomarkers, which regulate cardiac- and metabolic-related gene expression. This suggests a clinical utility for microRNAs given their predictive and therapeutic potential for cardiovascular diseases.

OPEN ACCESS

Edited and reviewed by:
Cecilia Giulivi,
University of California, Davis, United States

***Correspondence:**
Ileana Badi
ileana.badi@cardiov.ox.ac.uk
Nadia Akawi
nadia.akawi@uaeu.ac.ae

Specialty section:
This article was submitted to Cellular Biochemistry, a section of the journal Frontiers in Cell and Developmental Biology

Received: *19 June 2022*
Accepted: *24 June 2022*
Published: *15 July 2022*

Citation:
Badi I, Sommariva E, Miyazawa K, Kondo H, Azzimato V and Akawi N (2022) Editorial: Exploring the Crosstalk Between Adipose Tissue and the Cardiovascular System. Front. Cell Dev. Biol. 10:973135. doi: 10.3389/fcell.2022.973135

Four articles examined the mechanisms through which dysregulated AT can affect CVD development. Piacentini et al. focused on how innate and adaptive immune cells, present in the perivascular AT (PVAT) of abdominal aortic aneurisms (AAAs), help to sustain a deleterious inflammatory loop. They speculated that trained immunity, which is defined as a form of innate immune memory resulting in enhanced responsiveness to repeated triggers, can be induced and shaped in myeloid progenitor cells by specific innate stimuli and epigenetic and metabolic reprogramming events. This concept was supported by a bioinformatic analysis performed by the authors on AAA human samples and by data from the literature. PVAT also plays an important role in atherosclerosis. For instance, in obesity it promotes the initial step of endothelial dysfunction through mechanisms involving increased oxidative stress and proinflammatory cytokines production (Ketonen et al., 2010). The consequent generation of excess reactive oxygen species and low-density lipoprotein (LDL) oxidation contribute to the progression of atherosclerosis (Poznyak et al., 2021). Li et al. found a mechanistic association in endothelial cells between levels of oxidized LDL (oxLDL) and Neogenin 1 (Neo-1), an inflammatory regulator (Schlegel et al., 2018). OxLDL induced the transactivation of Neo-1 in endothelial cells via enhancing the interaction between CREB1 and BAF47 transcription factors. The authors also revealed that Neo-1 promotes leukocyte adhesion to endothelial cells by modulating the proinflammatory transcription factor NF-κB. Antibody-mediated inhibition of endogenous Neo-1 in mice significantly and markedly reduced atherosclerotic lesions. Using a Mendelian randomization (MR) analysis approach, Huang et al. revealed significant genetic associations between the predicted mass of visceral adiposity and a wide range of traditional metabolic risk factors and endpoints for CVD, including coronary heart disease, cardiac arrhythmias, vascular diseases, and stroke. The authors also conducted a network MR analysis to identify the potential mechanisms linking visceral AT (VAT) with the pathogenesis of CVD. Proteins mainly involved in energy metabolism, inflammation and angiogenesis were highlighted as potential players in the cross-talk between VAT and CVD. Cabaro et al. investigated the paracrine effect of epicardial AT (EAT)-secreted IL-1β on post-operative atrial fibrillation (POAF). They found that patients with POAF had higher IL-1β levels in EAT conditioned medium when compared to the no-POAF group. Furthermore, human atrial fibroblasts exposed to IL-1β and IL-18 showed increased proliferation and migration as well as increased expression levels of proinflammatory and profibrotic genes.

AT can be classified as white AT (WAT) or brown AT (BAT) depending on its metabolic, morphologic, and broader biological phenotype (Badi and Antoniades, 2021). BAT exerts protective effects on cardiometabolic health as well as on the heart (Badi and Antoniades, 2021). Two research articles in this collection focused on understanding the biology of BAT, and WAT browning. Lin et al. observed in a mouse model that the survival of fat grafts for soft-tissue reconstruction is affected by the spontaneous browning of WAT *in situ*. They showed that the local post-transplantation browning of WAT is accompanied by early angiogenesis and superior final graft retention. They proposed that avascularity and hypoxia during the early stage of fat transplantation promote the browning of white adipocytes leading to early revascularization. They also highlighted the beneficial clinical use of browning agents such as CL316243 (Danysz et al., 2018) in improving fat engraftment. Finally, Shaw et al. demonstrated that the beige adipocyte stimulator irisin promotes the release of a novel adipokine, CXCL1, via upregulation of the NF-κB pathway in adipocytes derived from the neck area (which is one of the main sources of BAT). Interestingly, CXCL1 exerted a positive effect on the adhesion of endothelial cells suggesting a possible role for this adipokine in improving tissue vascularization.

Taken together, the articles published within this Research Topic highlighted the importance of deepening our knowledge of the cross-talk between AT and the cardiovascular system in order to assist the development of new and effective therapies for the leading cause of death, CVD.

AUTHOR CONTRIBUTIONS

IB and NA wrote the first draft of the editorial. All authors reviewed and approved the submitted version of the manuscript.

ACKNOWLEDGMENTS

We sincerely thank all authors of this Research Topic for their contributions and we are very grateful to the reviewers for evaluating all manuscripts. We also thank Murray Polkinghorne for proofreading the manuscript.

REFERENCES

Akawi, N., Checa, A., Antonopoulos, A. S., Akoumianakis, I., Daskalaki, E., Kotanidis, C. P., et al. (2021). Fat-secreted Ceramides Regulate Vascular Redox State and Influence Outcomes in Patients with Cardiovascular Disease. *J. Am. Coll. Cardiol.* 77, 2494–2513. doi:10.1016/j.jacc.2021.03.314

Badi, I., and Antoniades, C. (2021). Brown Adipose Tissue and the Take (12,13-di) HOME Message to the Heart. *Circulation* 143, 160–162. doi:10.1161/CIRCULATIONAHA.120.051981

Danysz, W., Han, Y., Li, F., Nicoll, J., Buch, P., Hengl, T., et al. (2018). Browning of White Adipose Tissue Induced by the SS3 Agonist CL-316,243 after Local and Systemic Treatment - PK-PD Relationship. *Biochimica Biophysica Acta (BBA) - Mol. Basis Dis.* 1864, 2972–2982. doi:10.1016/j.bbadis.2018.06.007

Ketonen, J., Shi, J., Martonen, E., and Mervaala, E. (2010). Periadventitial Adipose Tissue Promotes Endothelial Dysfunction via Oxidative Stress in Diet-Induced Obese C57Bl/6 Mice. *Circ. J.* 74, 1479–1487. doi:10.1253/circj.cj-09-0661

Oikonomou, E. K., and Antoniades, C. (2019). The Role of Adipose Tissue in Cardiovascular Health and Disease. *Nat. Rev. Cardiol.* 16, 83–99. doi:10.1038/s41569-018-0097-6

Poznyak, A. V., Nikiforov, N. G., Markin, A. M., Kashirskikh, D. A., Myasoedova, V. A., Gerasimova, E. V., et al. (2021). Overview of OxLDL and its Impact on Cardiovascular Health: Focus on Atherosclerosis. *Front. Pharmacol.* 11, 613780. doi:10.3389/fphar.2020.613780

Schlegel, M., Körner, A., Kaussen, T., Knausberg, U., Gerber, C., Hansmann, G., et al. (2018). Inhibition of Neogenin Fosters Resolution of Inflammation and Tissue Regeneration. *J. Clin. Invest.* 128, 4711–4726. doi:10.1172/JCI96259

Conflict of Interest: The authors declare that the research was conducted in the absence of any commercial or financial relationships that could be construed as a potential conflict of interest.

Publisher's Note: All claims expressed in this article are solely those of the authors and do not necessarily represent those of their affiliated organizations, or those of the publisher, the editors and the reviewers. Any product that may be evaluated in this article, or claim that may be made by its manufacturer, is not guaranteed or endorsed by the publisher.

frontiers in Cell and Developmental Biology

ORIGINAL RESEARCH
published: 11 October 2021
doi: 10.3389/fcell.2021.737872

Irisin Stimulates the Release of CXCL1 From Differentiating Human Subcutaneous and Deep-Neck Derived Adipocytes *via* Upregulation of NFκB Pathway

Abhirup Shaw[1,2†], Beáta B. Tóth[1†], Róbert Király[1], Rini Arianti[1,2], István Csomós[3], Szilárd Póliska[4], Attila Vámos[1,2], Ilma R. Korponay-Szabó[5], Zsolt Bacso[3,6], Ferenc Győry[7], László Fésüs[1‡] and Endre Kristóf[1*‡]*

[1] Laboratory of Cell Biochemistry, Department of Biochemistry and Molecular Biology, Faculty of Medicine, University of Debrecen, Debrecen, Hungary, [2] Doctoral School of Molecular Cell and Immune Biology, University of Debrecen, Debrecen, Hungary, [3] Department of Biophysics and Cell Biology, Faculty of Medicine, University of Debrecen, Debrecen, Hungary, [4] Genomic Medicine and Bioinformatics Core Facility, Department of Biochemistry and Molecular Biology, Faculty of Medicine, University of Debrecen, Debrecen, Hungary, [5] Department of Pediatrics, Faculty of Medicine, University of Debrecen, Debrecen, Hungary, [6] Faculty of Pharmacy, University of Debrecen, Debrecen, Hungary, [7] Department of Surgery, Faculty of Medicine, University of Debrecen, Debrecen, Hungary

Thermogenic brown and beige adipocytes might open up new strategies in combating obesity. Recent studies in rodents and humans have indicated that these adipocytes release cytokines, termed "batokines". Irisin was discovered as a polypeptide regulator of beige adipocytes released by myocytes, primarily during exercise. We performed global RNA sequencing on adipocytes derived from human subcutaneous and deep-neck precursors, which were differentiated in the presence or absence of irisin. Irisin did not exert an effect on the expression of characteristic thermogenic genes, while upregulated genes belonging to various cytokine signaling pathways. Out of the several upregulated cytokines, *CXCL1*, the highest upregulated, was released throughout the entire differentiation period, and predominantly by differentiated adipocytes. Deep-neck area tissue biopsies also showed a significant release of CXCL1 during 24 h irisin treatment. Gene expression data indicated upregulation of the NFκB pathway upon irisin treatment, which was validated by an increase of p50 and decrease of IκBα protein level, respectively. Continuous blocking of the NFκB pathway, using a cell permeable inhibitor of NFκB nuclear translocation, significantly reduced CXCL1 release. The released CXCL1 exerted a positive effect on the adhesion of endothelial cells. Together, our findings demonstrate that irisin stimulates the release of a novel adipokine, CXCL1, *via* upregulation of NFκB pathway in neck area derived adipocytes, which might play an important role in improving tissue vascularization.

Keywords: obesity, adipose tissue, irisin, cytokines, CXCL1, integrins, NFκB, angiogenesis

Abbreviations: BAT, brown adipose tissue; CXCL, C-X-C motif chemokine ligand; DN, deep-neck derived adipocytes; GRO, growth-related oncogene; hASCs, human adipose-derived stromal cells; HUVEC, human umbilical vein endothelial cells; IgG, immunoglobulin G; IL, interleukin; MCP1, monocyte chemoattractant protein 1; NFκB, nuclear factor-κB; PI, propidium iodide; SC, subcutaneous neck derived adipocytes; WAT, white adipose tissue.

OPEN ACCESS

Edited by:
Ileana Badi,
University of Oxford, United Kingdom

Reviewed by:
Amaia Rodríguez,
University of Navarra, Spain
Janne Lebeck,
Aarhus University, Denmark
Rubén Cereijo,
University of Barcelona, Spain

***Correspondence:**
László Fésüs
fesus@med.unideb.hu
Endre Kristóf
kristof.endre@med.unideb.hu

† These authors have contributed equally to this work and share first authorship

‡ These authors have contributed equally to this work and share last authorship

Specialty section:
This article was submitted to Cellular Biochemistry, a section of the journal Frontiers in Cell and Developmental Biology

Received: *07 July 2021*
Accepted: *15 September 2021*
Published: *11 October 2021*

Citation:
Shaw A, Tóth BB, Király R, Arianti R, Csomós I, Póliska S, Vámos A, Korponay-Szabó IR, Bacso Z, Győry F, Fésüs L and Kristóf E (2021) Irisin Stimulates the Release of CXCL1 From Differentiating Human Subcutaneous and Deep-Neck Derived Adipocytes via Upregulation of NFκB Pathway. Front. Cell Dev. Biol. 9:737872. doi: 10.3389/fcell.2021.737872

INTRODUCTION

Recent studies indicated the presence of thermogenic adipose tissue, capable of dissipating energy as heat under sub-thermal conditions in healthy human adults (Cypess et al., 2009; Leitner et al., 2017). These are located in cervical, supraclavicular, axillary, mediastinal, paravertebral, and abdominal depots (Saito et al., 2009; van Marken Lichtenbelt et al., 2009; Virtanen et al., 2009); supraclavicular, deep-neck (DN), and paravertebral having the highest amounts. Together these depots account for 5% of basal metabolic rate in adults, highlighting their importance in combating obesity and type 2 diabetes mellitus (van Marken Lichtenbelt and Schrauwen, 2011). In rodents, these thermogenic adipocytes are either classical brown or beige depending on their origin and distribution (Rosen and Spiegelman, 2014; Kajimura et al., 2015). In addition to their role in thermogenesis, these adipocytes also secrete adipokines, termed "batokines", which have been shown to exert autocrine, paracrine, or endocrine activity (Villarroya et al., 2017). For example, vascular endothelial growth factor A (VEGF-A) secreted by brown adipocytes promotes angiogenesis and vascularization of brown adipose tissue (BAT) (Xue et al., 2009; Sun et al., 2014; Mahdaviani et al., 2016), while Fibroblast growth factor (FGF) 21 enhances the beiging of white adipose tissue (WAT) in animal studies (Cuevas-Ramos et al., 2019) and increases thermogenesis in BAT (Hondares et al., 2011; Wang et al., 2015; Ruan et al., 2018). Understanding the roles of batokines in the human body is an area of active research (Villarroya et al., 2019; Ahmad et al., 2021).

Irisin, a cleaved product of the transmembrane protein Fibronectin Type III domain-containing protein 5 (FNDC5), was discovered as a myokine in mice and was shown to be a browning inducing endocrine hormone (Boström et al., 2012; Zhang et al., 2014), presumably acting *via* integrin receptors (Kim et al., 2018). A recent publication has shown that individuals with obesity exhibited a downregulation of *FNDC5* gene and protein expression in visceral and subcutaneous fat depots (Frühbeck et al., 2020). In mice, irisin secretion was induced by physical exercise and shivering of skeletal myocytes, which induced a beige differentiation program in subcutaneous WAT (Boström et al., 2012). In rats, irisin was also found to be released from cardiomyocytes at much higher amount than skeletal muscles (Aydin et al., 2014). Lower levels of circulating irisin was observed in patients with cardiovascular disease (Polyzos et al., 2018). Irisin has also been shown to improve cardiac function and inhibit pressure overload induced cardiac hypertrophy and fibrosis (Yu et al., 2019). In humans, inconsistent effects were found when adipocytes of different anatomical origins were treated with recombinant irisin (Raschke et al., 2013; Lee et al., 2014; Silva et al., 2014; Kristóf et al., 2015; Klusóczki et al., 2019; Li et al., 2019). How irisin affects the differentiation of the thermogenically prone neck area adipocytes still awaits description. We have previously reported that human DN adipose tissue biopsies released significantly higher amounts of interleukin (IL)-6, IL-8, monocyte chemoattractant protein 1 (MCP1) as compared to subcutaneous ones, which was further enhanced upon irisin treatment (Kristóf et al., 2019).

C-X-C Motif Chemokine Ligand (CXCL) 1, previously known as growth-related oncogene (GRO)-α, is a small peptide belonging to the CXC chemokine family. Newly synthetized CXCL1 by vessel-associated endothelial cells and pericytes facilitates the process of neutrophil diapedesis (Gillitzer and Goebeler, 2001). A recent study showed that the chemokine CXCL14 is secreted by BAT under thermogenic stimulation, which induces browning of WAT by recruitment and activation of M2-macrophages (Cereijo et al., 2018). This study reinforced the fact that chemokines play an important role in thermogenic activation.

In this study, we aimed to get an overview of all the genes in which expression is regulated by irisin. For this, we have performed a global RNA-Sequencing comprising of *ex vivo* differentiated adipocytes of subcutaneous and deep depots of human neck from nine individuals and analyzed the upregulated genes upon irisin treatment. Surprisingly, several genes which encode secreted proteins were upregulated. Out of those, CXCL1 was found to be the highest expressed and a novel adipokine induced in differentiating adipocytes of both origins. The CXCL1 release was stimulated partially *via* the upregulation of nuclear factor-κB (NFκB) pathway. We found that the secreted CXCL1 had an adhesion promoting effect on endothelial cells, supporting that irisin can exert effects not directly linked to heat production.

MATERIALS AND METHODS

Materials

All chemicals were obtained from Sigma Aldrich (Munich, Germany) unless otherwise stated.

Isolation, Cell Culture, Differentiation, and Treatment of hASCs

Human adipose-derived stromal cells (hASCs) were obtained from stromal-vascular fractions of subcutaneous neck (SC) and DN tissues of volunteers, aged between 35–75 years, undergoing planned surgical treatment. A pair of biopsies from SC and DN areas was obtained from the same donor, to avoid inter-individual variations (Sárvári et al., 2015; Kristóf et al., 2019; Tóth et al., 2020). Patients with known diabetes, body mass index > 30, malignant tumor, infection or with abnormal thyroid hormone levels at the time of surgery were excluded from the study. Written informed consent was obtained from all participants before the surgery. Data of the donors included in RNA-sequencing are listed in **Supplementary Table 1**.

hASCs were isolated and cultivated as previously described (Sárvári et al., 2015; Kristóf et al., 2019; Tóth et al., 2020). The absence of mycoplasma was confirmed by PCR analysis (PCR Mycoplasma Test Kit I/C, Promocell, Heidelberg, Germany). Cells were differentiated following a previously described white adipogenic differentiation protocol, with or without the addition of human recombinant irisin (Cayman Chemicals, MI, United States) (provided in 50 mM Tris pH 8.0, 150 mM sodium chloride, and 20% glycerol stocks) at 250 ng/mL (20 nM)

concentration (the stock was diluted 1:6,500) (Fischer-Posovszky et al., 2008; Raschke et al., 2013; Kristóf et al., 2019). Media were changed every 4 days and cells were collected after 14 days of differentiation. In every repetition, untreated and irisin treated samples were obtained from the same donor. Cells were incubated at 5% CO_2 and 37°C. Where indicated, cells were treated with RGDS peptide (10 μg/mL, R&D systems, MN, United States) (Kim et al., 2018) or SN50 (50 μg/mL, Med Chem Express, NJ, United States) (Sárvári et al., 2015).

RNA Isolation, RT-qPCR, and RNA-Sequencing

Cells were collected in Trizol reagent (Thermo Fisher Scientific, MA, United States) and RNA was isolated manually by chloroform extraction and isopropanol precipitation. To obtain global transcriptome data, high throughput mRNA sequencing was performed on Illumina Sequencing platform (Tóth et al., 2020). Total RNA sample quality was checked by Agilent Bioanalyzer using Eukaryotic Total RNA Nano Kit; samples with RNA integrity number >7 were used to prepare the library. Libraries were prepared by NEBNext® Ultra™ II RNA Library Prep for Illumina (New England BioLabs, Ipswich, MA, United States). Sequencing runs were executed on Illumina NextSeq500 using single-end 75 cycles sequencing. The reads were aligned to the GRCh38 reference genome (with EnsEMBL 95 annotation) using STAR aligner (Dobin et al., 2013). To quantify the reads, featureCounts was used (Liao et al., 2014). Gene expression analysis was performed using R. Genes with very low expression and with outlier values were removed from further analysis. To further remove outlier genes, Cook's distance was calculated and genes with Cook's distance higher than 1 were filtered out. PCA analysis did not show any batch effect considering sequencing date and the donor origin, sex or tissue origin (data not shown). DESeq2 algorithm was used to detect the differentially expressed genes based on adjusted p values < 0.05 and log2 fold change threshold >0.85. Grouping was performed based on Panther Reactome pathways[1]. Heatmap visualization was performed on the Morpheus web tool[2] using Pearson correlation of rows and complete linkage based on calculated z-score of DESeq normalized data after $\log_2$ transformation (Tóth et al., 2020). The interaction networks were determined using STRING[3] and constructed using Gephi 0.9.2[4]. The size of the nodes was determined based on fold change (Tóth et al., 2020).

For RT-PCR, RNA quality was evaluated by spectrophotometry and cDNA was generated by TaqMan reverse transcription reagents kit (Thermo Fisher Scientific) followed by qPCR analysis (Szatmári-Tóth et al., 2020). LightCycler 480 (Roche Diagnostics, IN, United States) was used to determine the normalized gene expression using the probes (Applied Biosystems, MA, United States) which are listed in **Supplementary Table 2**. Human *GAPDH* was used as an endogenous control. Samples were run in triplicate and gene expression values were calculated by the comparative cycle threshold (Ct) method. ΔCt represents the Ct of target after deducting the *GAPDH*. Normalized gene expression levels were calculated by $2^{-\Delta Ct}$.

Antibodies and Immunoblotting

Samples were collected, separated by SDS-PAGE, and transferred to PVDF Immobilon-P transfer membrane (Merck-Millipore, Darmstadt, Germany) as previously described (Szatmári-Tóth et al., 2020). The following primary antibodies were used overnight in 1% skimmed milk solution: anti-p50 (1:1,000, 13755, Cayman Chemicals), anti- IκBα (1:1,000, 4812, Cell Signaling Technology, MA, United States), and anti-β-actin (1:5,000, A2066, Novus Biologicals, CO, United States). HRP-conjugated goat anti-rabbit (1:10,000, Advansta, CA, United States, R-05072-500) or anti-mouse (1:5,000, Advansta, R-05071-500) IgG were used as secondary antibodies, respectively. Immobilion western chemiluminescence substrate (Merck-Millipore) was used to visualize the immunoreactive proteins. FIJI was used for densitometry.

Immunostaining Analysis and Image Analysis

hASCs from SC and DN areas were plated and differentiated in eight well Ibidi μ-chambers (Ibidi GmbH, Gräfelfing, Germany). Cells were treated with Brefeldin A (100 ng/mL), an inhibitor of intracellular protein transport, 24 h prior collection to sequester the released CXCL1 (Sárvári et al., 2015; Kristóf et al., 2019). After that, cells were washed with PBS, fixed by 4% paraformaldehyde, permeabilized with 0.1% saponin and blocked by 5% milk as per described protocols (Szatmári-Tóth et al., 2020). The cells were incubated subsequently with anti-CXCL1 primary antibody (1:100, 712317, Thermo Fisher Scientific) and Alexa 488 goat anti-rabbit IgG (1:1,000, A11034, Thermo Fischer Scientific) secondary antibody for 12 and 3 h at room temperature, respectively. Propidium iodide (1.5 μg/mL, 1 h) was used to label the nuclei. A secondary antibody test was also performed where the cells were incubated only with the respective secondary antibodies. Images were acquired with Olympus FluoView 1000 confocal microscope and analyzed by FIJI (Szatmári-Tóth et al., 2020). Boundaries of preadipocytes and differentiated adipocytes were identified manually based on brightfield (BF) images and nuclear staining, followed by quantification of immunostaining intensity. Adipogenic differentiation rate was quantified as described previously (Doan-Xuan et al., 2013; Kristóf et al., 2015).

Determination of the Released Factors

Supernatants of samples from cell culture experiments were collected at regular replacement of media, on days 4, 12, 18, 21 of differentiation, wherever indicated. For SC and DN, supernatants were collected and stored at −20°C from the differentiated cells of the same donor and considered as one repetition, followed by repetition with subsequent donors. For tissues, 10–20 mg of SC and DN tissue samples from the same donor were floated

[1]https://pantherdb.org

[2]https://software.broadinstitute.org/morpheus

[3]https://string-db.org

[4]https://gephi.org

for 24 h in DMEM-F12-HAM medium with or without the presence of 250 ng/mL irisin (Ballak et al., 2013; Kristóf et al., 2019). The release of CXCL1, CX3CL1, IL-32, TNFα, and IL1-β were analyzed from the stored samples using ELISA Kits (R&D systems, MN, United States).

Human Umbilical Vein Endothelial Cell Adhesion Assay

A human umbilical vein endothelial cell (HUVEC) cell line was generated from endothelial cells isolated from the human umbilical cord vein of a healthy newborn by collagenase digestion as described earlier (Palatka et al., 2006). Cells were cultured in M199 medium (Biosera, Nuaille, France) containing 10% FBS (Thermo Fisher Scientific), 10% EGM2 Endothelial Growth Medium (Lonza, Basel, Switzerland), 20 mM HEPES (Biosera), 100 U/mL Penicillin, 100 μg/mL Streptomycin and 2.5 μg/mL Amphotericin B (Biosera), and immortalized by the viral delivery of telomerase gene using pBABE-neo-hTERT (Counter et al., 1998) (gift from Bob Weinberg, 1774, Addgene). The virus packaging was performed in HEK293FT cells (Thermo Fisher Scientific) based on a calcium precipitation method using pUMVC and pCMV-VSV-G vectors (Stewart et al., 2003) (gift from Bob Weinberg, 8449 and 8454, Addgene). The pseudovirion containing supernatant was used for infection, and selection was started 72 h later using 300 μg/mL G418 (Merck-Millipore). Immortalized cells completely retain the morphological properties of primary endothelial cells.

Prior to the adhesion assay, EGM2 was omitted from the standard medium of HUVEC cells and FBS content was decreased to 1% (in which condition cell proliferation is unlikely) for 24 h. 96-well plates (Thermo Fisher Scientific) were precoated with fibronectin (Merck-Millipore) at 1.25 μg/mL concentration in PBS, for 1 h at 37°C and then washed twice with PBS. After centrifugation, trypsinized HUVEC samples were diluted for coating based on counting with three parallels using KOVA Glasstic Slide with Counting Grids (KOVA International, Netherlands). Then cells were plated at 1,000 cells/well density and left to adhere for 2 h in the CO_2-incubator in the mixture (1:1 ratio) of starvation and conditioned media (incubation period from day 8–12 of differentiation) from SC and DN adipocytes, differentiated in the presence or absence of 250 ng/mL irisin, respectively. Where indicated, recombinant human CXCL1 (275-GR, R&D Systems) was used at 2,500 pg/mL, at the highest observed concentration in media of irisin treated *ex vivo* differentiated adipocytes, in starvation media. Unattached cells were removed by once washing with PBS and adhered cells were incubated with starvation media containing CellTiter-Blue Cell Viability reagent (resazurin; Promega, WI, United States; 36 times dilution). To determine the ratio of attached cells in various conditions, the fluorescent intensity change of each well (Ex:530 nm/Em:590 nm), due to the conversion of resazurin to resorufin by cellular metabolism, was measured using Synergy H1 (BioTek, Hungary) plate reader 2, 4, 6, 18, and 24 h after adding resazurin. Fluorescent intensity values were plotted with respect to time, followed by calculation of slope, which gave the relative adhesion values, after subtraction of values for only starvation media without cells. A linear slope was obtained, which suggests that there could be only negligible cell proliferation, and the gained values represent endothelial cell adhesion measuring the attached viable endothelial cells during the treatments. The final value of adhesion was represented in RFU/hr units and taken from the mean of technical parallels with a minimum of three independent repetitions.

Statistics and Image Analysis/Preparation

Results are expressed as mean ± SD for the number of independent repetitions indicated. For multiple comparisons of groups, statistical significance was determined by one- or two-way analysis of variance followed by Tukey *post hoc* test. In comparison of two groups, two-tailed unpaired Student's *t*-test was used. For the design of graphs and evaluation of statistics, Graphpad Prism 9 was used.

RESULTS

Irisin Did Not Change the Differentiation Potential of Adipocytes While Increased the Expression of Integrin Receptor Genes in Both SC and DN Origins

Primary hASCs from nine independent donors were isolated and cultivated from SC and DN area of human neck, as described (Tóth et al., 2020). Adipogenic differentiation was driven by a white adipocyte differentiation medium with or without the presence of irisin for 14 days. Then, the global gene expression pattern of differentiated adipocytes and undifferentiated hASCs were determined by global RNA-sequencing (Tóth et al., 2020). Gene expression of general adipocyte markers (e.g., *FABP4*, *ADIPOQ*) was higher in all differentiated adipocytes as compared to preadipocytes (**Figure 1A**). Quantification of the adipogenic differentiation rate by laser-scanning cytometry (Kristóf et al., 2015) revealed that more than 50% of the cells were differentiated following our 14-days long differentiation protocol (**Figure 1B**). The presence of irisin did not affect the differentiation and gene expression of general adipocyte markers (**Figures 1A,B**). A recent publication proposed the receptors for irisin to be integrins, Integrin subunit alpha V (ITGAV) and Integrin subunit beta (ITGB) 1/3/5 (ITGB1/3/5) (Kim et al., 2018). Hence the expression of *ITGAV* was analyzed from RNA-sequencing data (**Figure 1C**), which revealed that it is expressed in both the preadipocytes and differentiated adipocytes. Upon RT-qPCR validation, a significant increase of *ITGAV* expression was observed in DN adipocytes in response to irisin (**Figure 1D**). RNA-sequencing data showed that *ITGB1*, *3*, and *5* were also expressed at a high extent in preadipocytes and in differentiated adipocytes irrespective of the presence of irisin (**Supplementary Figure 1**).

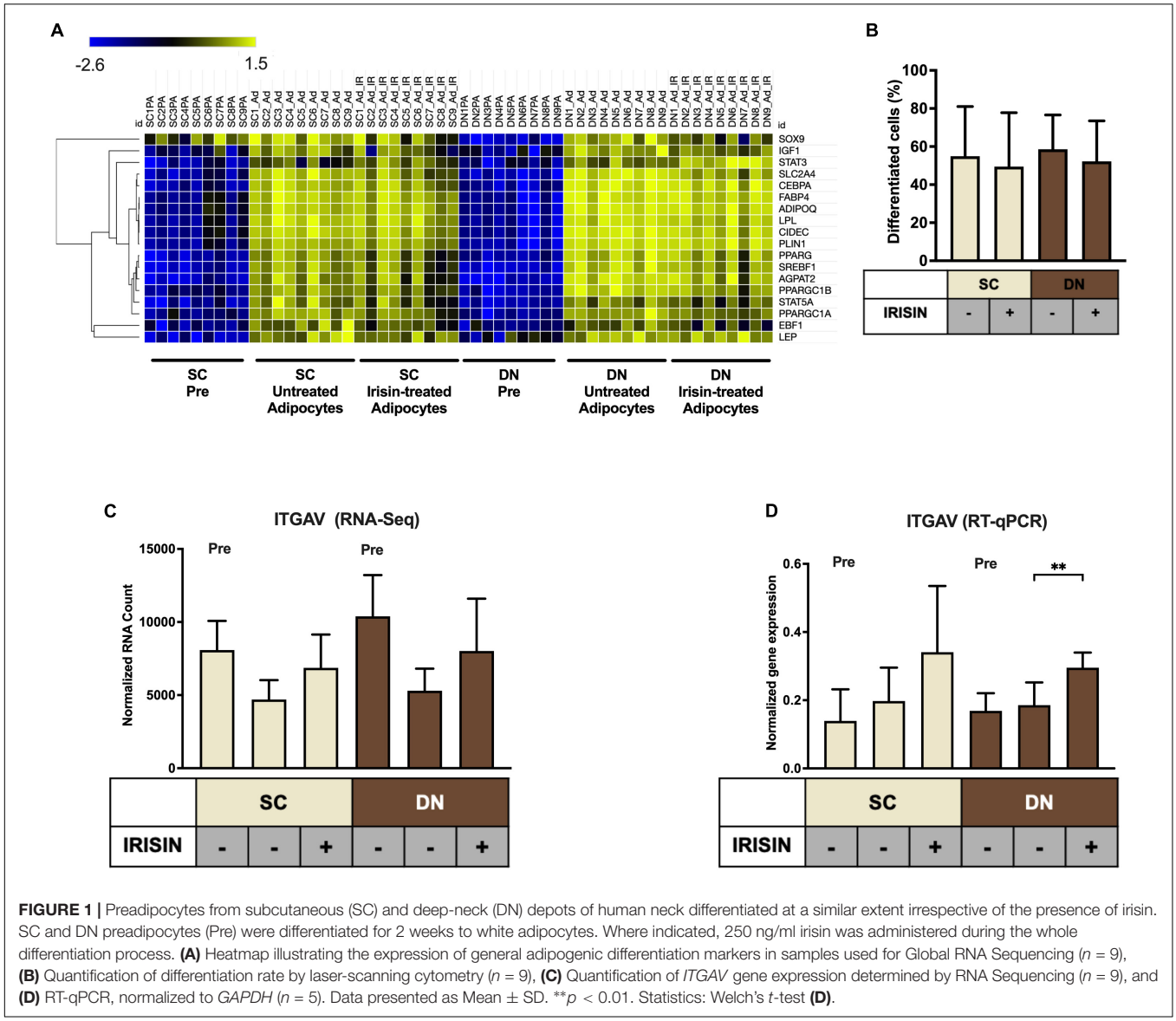

FIGURE 1 | Preadipocytes from subcutaneous (SC) and deep-neck (DN) depots of human neck differentiated at a similar extent irrespective of the presence of irisin. SC and DN preadipocytes (Pre) were differentiated for 2 weeks to white adipocytes. Where indicated, 250 ng/ml irisin was administered during the whole differentiation process. **(A)** Heatmap illustrating the expression of general adipogenic differentiation markers in samples used for Global RNA Sequencing (n = 9), **(B)** Quantification of differentiation rate by laser-scanning cytometry (n = 9), **(C)** Quantification of *ITGAV* gene expression determined by RNA Sequencing (n = 9), and **(D)** RT-qPCR, normalized to *GAPDH* (n = 5). Data presented as Mean ± SD. $^{**}p < 0.01$. Statistics: Welch's t-test **(D)**.

Genes Involved in Chemokine Signaling Pathways Were Upregulated in Adipocytes Differentiated With Irisin

RNA-Sequencing analysis identified 79 genes to be higher expressed upon irisin treatment that are visualized by a Volcano plot (**Figure 2A**). 50 and 66 genes were significantly upregulated in SC and DN area adipocytes, respectively, each of which are listed in **Supplementary Table 3**. 37 genes, including *CXCL1*, *CX3CL1*, *IL32*, *IL34*, *IL6*, and *CCL2* were found to be commonly upregulated in adipocytes of both depots (**Figures 2A,B** and **Supplementary Table 3**). Surprisingly, thermogenic marker genes did not appear among these. Panther enrichment analysis of genes upregulated in both SC and DN adipocytes by irisin treatment revealed pathways such as cytokine signaling (*NFKB2*, *CXCL1*, *CXCL2*, *IL32*, *IL34*, *IL6*, *CCL2*), interleukin-4 and 13 signaling (*IL6*, *CCL2*, *JUNB*, *ICAM1*), and class A/1 rhodopsin like receptors (*CXCL3*, *CXCL5*, *CX3CL1*, *CXCL2*, *CCL2*, *CXCL1*), which were commonly upregulated in both SC and DN adipocytes (**Table 1**). Gephi diagrams illustrate the interaction of upregulated genes that belong to several pathways (**Figures 2C,D**). Interleukin-10 signaling were amongst the upregulated pathways in SC adipocytes (**Figure 2C**), while in DN, G-alpha-I and response to metal ions were upregulated (**Figure 2D**). Cluster analyses and heatmap illustration of the gene expression values of the 79 higher expressed genes upon irisin treatment identified two main clusters: a cluster of 25 genes that were uniquely expressed in irisin treated mature adipocytes, and another group of genes that were expressed highly in preadipocytes, but suppressed in differentiated adipocytes without irisin treatment (**Supplementary Figure 2**). The higher expression of *IL6*, *CCL2*, *CX3CL1*, and *IL32*, cytokine encoding genes was observed by both RNA Sequencing and RT-qPCR analysis (**Supplementary Figure 3**). Next, we investigated if

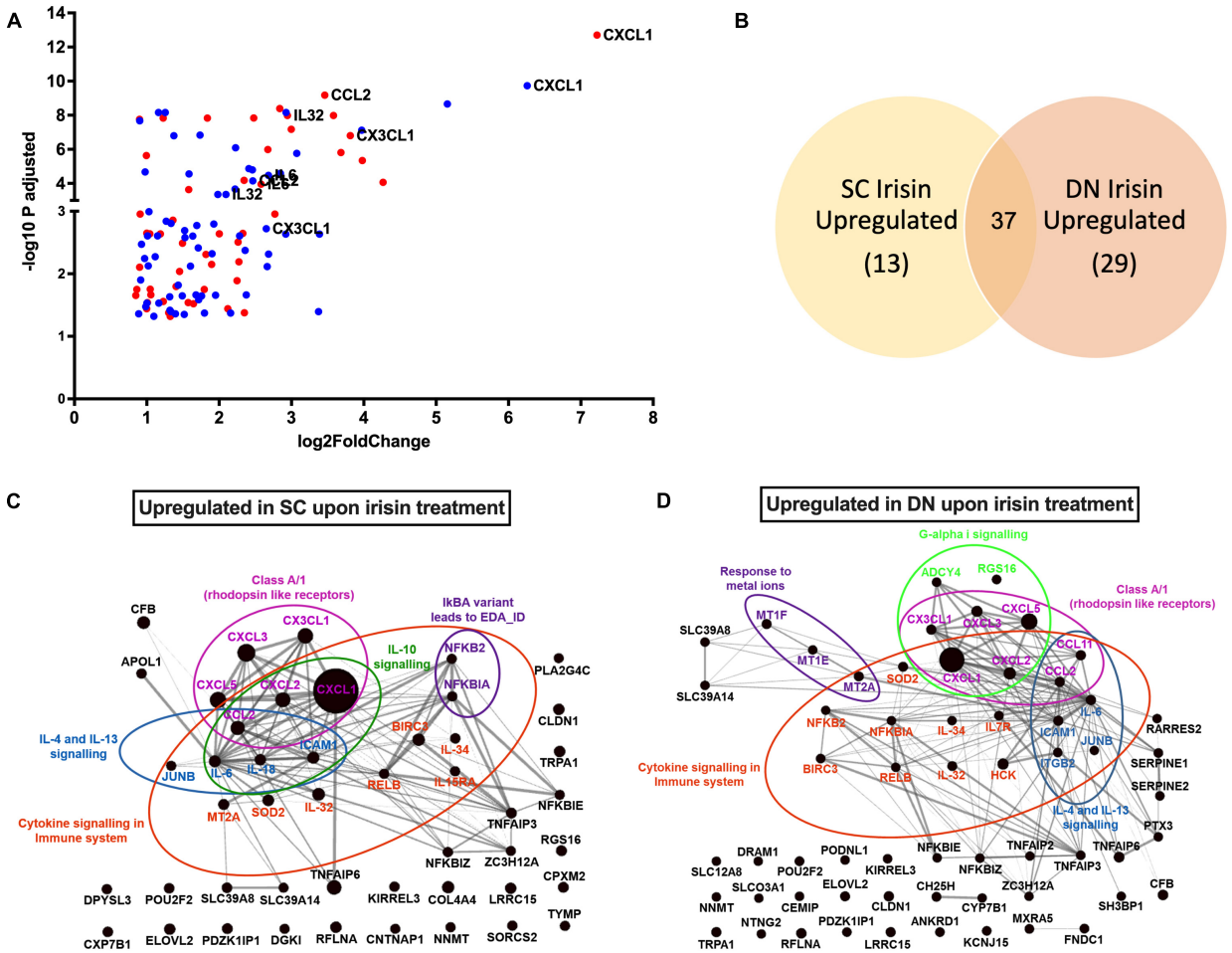

FIGURE 2 | Irisin upregulated similar gene-sets that encode for cytokines in subcutaneous (SC) and deep-neck (DN) depots of human neck area adipocytes. SC and DN preadipocytes were differentiated and treated as in **Figure 1**. **(A)** Volcano plot showing each of the upregulated genes in SC (red) and DN (blue) depots upon irisin treatment; the highest upregulated genes are listed separately, **(B)** Venn-diagram illustrating the genes commonly upregulated by irisin treatment in SC and DN depots. Gephi illustrations highlighting the most important pathways and the interaction of genes upregulated by irisin treatment in SC **(C)** and DN **(D)** derived adipocytes.

fractalkine (encoded by *CX3CL1* gene) and IL-32 were released into the conditioned media collected during the differentiation on days numbers 4 and 12; however, we were unable to detect these factors (data not shown).

Irisin Dependent Induction of CXCL1 Release Occurred Predominantly From Differentiating and Mature Adipocytes

Irisin upregulated *CXCL1* gene expression at the largest extent in both SC and DN area adipocytes (**Figures 2A**, **3A** and **Supplementary Table 3**). This observation was verified by RT-qPCR (**Figure 3B**). As a next step, release of CXCL1 from irisin treated and untreated adipocytes was investigated into the conditioned differentiation media collected on the fourth and twelfth days of differentiation. Irisin treatment resulted in significant increase in CXCL1 secretion at the intervals of days 0–4 and 8–12 in both types of adipocytes (**Figure 3C**).

We aimed to further investigate the dependence of CXCL1 release on the presence of irisin. Therefore, we differentiated hASCs for 21 days, with three sets of samples, each from SC and DN derived adipocytes. Two sets of hASCs were differentiated as previously described, and for the third set, irisin treatment was discontinued after 14 days. Conditioned media were collected on days number 4, 12, 18, 21 and measured for the release of CXCL1. Large amounts of CXCL1 were secreted throughout the differentiation period in the presence of irisin; however, discontinuation of irisin administration led to gradual and significant reduction of the released chemokine (**Figure 3D**).

A recent publication indicated that RGDS peptide, an integrin receptor inhibitor, can potentially inhibit the effect of irisin (Kim et al., 2018). Hence, we checked the effect of this peptide on the release of CXCL1 on top of irisin treatment. RGDS partially reduced the irisin-stimulated release of CXCL1 by DN adipocytes at day 12 of the differentiation period (**Figure 3E**).

TABLE 1 | Pathways of significantly upregulated genes upon irisin treatment during differentiation of subcutaneous (SC) and deep-neck (DN) derived adipocytes.

Panther reactome pathways	Gene name	FDR
SC Irisin upregulated		
IkBA variant leads to EDA-ID	***NFKBIA, NFKB2***	4.49×10^{-2}
Cytokine signaling in immune system	***IL6, NFKBIA, JUNB, IL32, SOD2, MT2A, NFKB2, CXCL2, CCL2,*** *IL15RA*, *IL18*, ***IL34, ICAM1, CXCL1, RELB, BIRC3***	5.23×10^{-8}
Interleukin-10 signaling	***IL6, CXCL2, CCL2,*** *IL18*, ***ICAM1, CXCL1***	1.65×10^{-6}
Class A/1 (Rhodopsin like receptors)	***CXCL3, CXCL5, CX3CL1, CXCL2, CCL2, CXCL1***	3.5×10^{-2}
Interleukin-4 and Interleukin-13 signaling	***IL6, JUNB, CCL2,*** *IL18*, ***ICAM1***	2.3×10^{-3}
DN Irisin Upregulated		
Response to metal ions	***MT2A,*** MT1E, MT1F	4.74×10^{-3}
Class A/1 (Rhodopsin like receptors)	*CCL11*, ***CXCL3, CXCL5, CX3CL1, CXCL2, CCL2, CXCL1***	1.85×10^{-2}
Cytokine signaling in immune system	***IL6,*** *CCL11*, *ITGB2*, ***NFKBIA, JUNB, IL32, SOD2, MT2A, NFKB2,*** *IL7R*, ***CXCL2, CCL2, IL34, ICAM1,*** *HCK*, ***CXCL1, RELB, BIRC3***	5.55×10^{-8}
Interleukin-4 and Interleukin-13 signaling	***IL6,*** *CCL11*, *ITGB2*, ***JUNB, CCL2, ICAM1***	6.33×10^{-4}
G-alpha (i) signaling events	***CXCL3, CXCL5, CX3CL1,*** *ADCY4*, *RGS16*, ***CXCL2, CXCL1***	5.07×10^{-2}

Genes commonly upregulated in both SC and DN area adipocytes are in bold character.
CXCL1 was the highest upregulated gene in both SC and DN area adipocytes.
FDR, false discovery rate.

Release of CXCL1 throughout the whole differentiation period raised a possibility that both undifferentiated preadipocytes and differentiated adipocytes are able to release the chemokine. To investigate this, the secretion machinery of the mixed cell population was inhibited by Brefeldin A, followed by CXCL1 immunostaining and image acquisition by confocal microscopy. Irisin treatment significantly increased CXCL1 immunostaining intensity in both SC (**Figure 4A**) and DN adipocytes (**Figure 4B**). Irisin treated adipocytes accumulated significantly more CXCL1 compared to their preadipocyte counterparts in both SC (**Figure 4A**) and DN areas (**Figure 4B**). A test for the secondary antibody alone confirmed that the applied secondary antibody did not produce a labeling on its own by unspecifically binding to the cells (**Supplementary Figure 4**). Our data suggests that irisin stimulates the release of CXCL1 from differentiating and mature adipocytes which is strongly dependent on the presence of irisin but not prominently on its presumed integrin receptor.

Irisin Stimulates the Release of CXCL1 *via* the Upregulation of NFκB Pathway

Next, we aimed to investigate the molecular mechanisms underlying the irisin-induced CXCL1 release. According to our RNA Sequencing data, irisin treatment resulted in a significant upregulation of *NFKB2* and a very modest trend for an increase in *NFKB1* and *RELA* (**Supplementary Figures 5A–C**) genes. RT-qPCR validation indicated significant upregulation of *NFKB1* (p50 subunit) and *RELA* (p65 subunit) in DN, while an increasing trend was observed in SC adipocytes (**Figures 5A,B**). p50 protein expression was significantly increased in DN and a slightly increasing trend was found in the case of SC adipocytes (**Figure 5C**). Protein expression of IκBα, the inhibitor of NFκB transcription factor, decreased significantly upon irisin treatment in SC and a decreasing trend was observed in DN adipocytes (**Figure 5D**), indicating the upregulation of NFκB pathway.

To prove the direct involvement of the NFκB pathway in adipocyte response to irisin, we applied a cell permeable inhibitor of NFκB nuclear translocation, SN50 (Sárvári et al., 2015), which significantly reduced the release of the chemokine from both types of adipocytes, when it was applied on top of irisin on both the fourth and twelfth days of differentiation, as compared to cells stimulated only by irisin (**Figure 5E**).

The observed effects of irisin are not likely to be caused by any contamination of endotoxins, which is proved by the negligible expression of *TNFα* or *CCL3* genes (**Supplementary Figures 5D,E**), and the decreasing trend of *IL1β* gene expression (**Supplementary Figure 5F**) in irisin treated adipocytes. Furthermore, we did not detect secreted TNFα or IL-1β in the conditioned media of either untreated or irisin treated SC and DN derived adipocytes (data not shown).

CXCL1 Released From Irisin Stimulated Adipocytes and Adipose Tissue Improves the Adhesion Property of Endothelial Cells

Finally, SC and DN paired tissue biopsies were floated in the presence or absence of irisin dissolved in empty media, followed by quantification of CXCL1 release. The secretion of the chemokine was significantly stimulated from DN tissue biopsies upon irisin treatment (**Figure 6A**).

Secretion of CXCL1 plays an important role in wound repair and angiogenesis (Gillitzer and Goebeler, 2001). Angiogenesis is crucial for the thermogenic function of BAT (Cannon and Nedergaard, 2004). Therefore, we intended to detect whether the released chemokine can contribute to increased adhesion ability of endothelial cells. Conditioned media collected on the twelfth day of *ex vivo* differentiation, from untreated and irisin treated SC and DN area adipocytes, were added to HUVECs followed by a resorufin based adhesion assay. The conditioned medium from irisin treated adipocytes, which contains various released factors (including CXCL1) was able to significantly increase the number of attached viable HUVECs, compared to

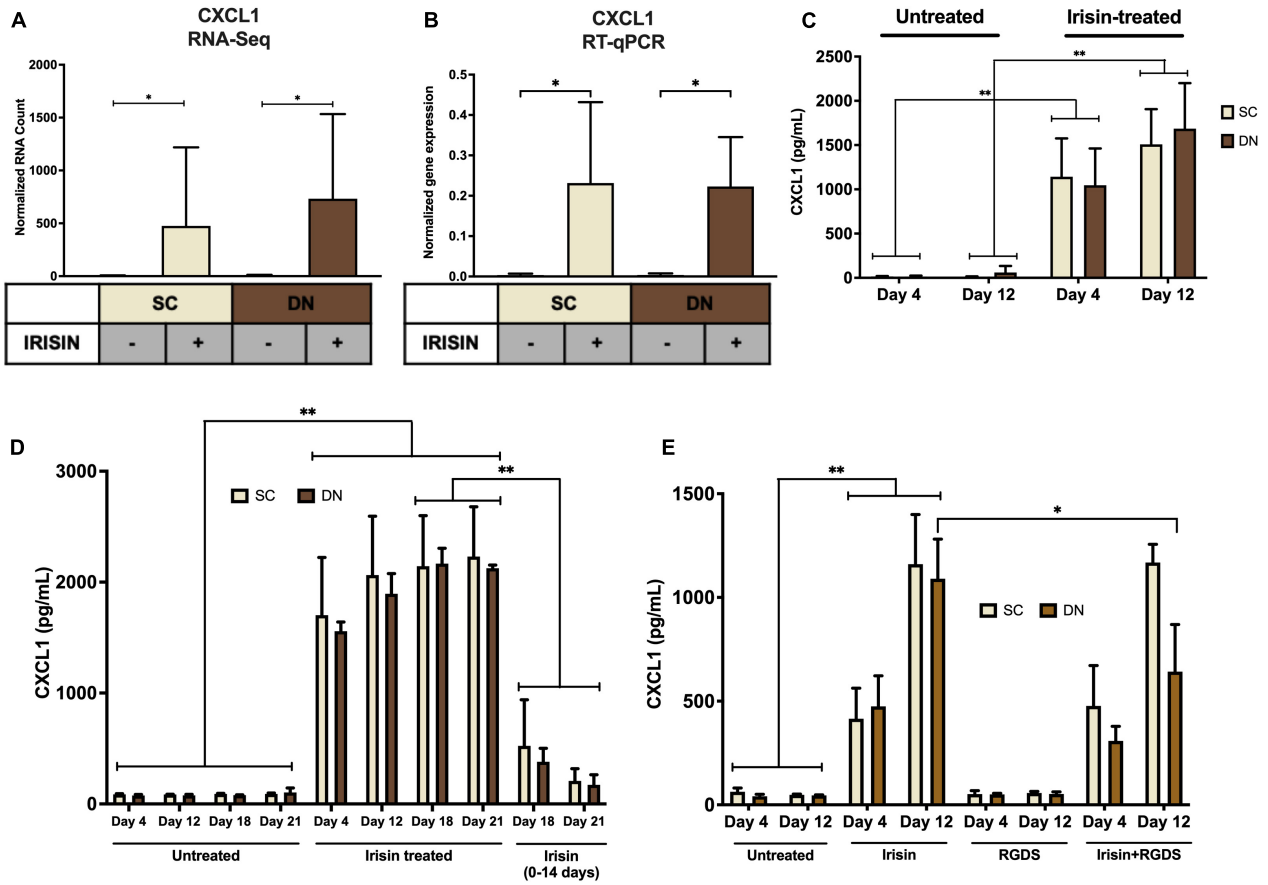

FIGURE 3 | Irisin dependent CXCL1 release was stimulated from differentiating subcutaneous (SC) and deep-neck (DN) area adipocytes. SC and DN preadipocytes were differentiated and treated as in **Figures 1**, **2**. Where indicated, irisin was omitted from the differentiation medium at day 14. Conditioned differentiation media was collected and secreted CXCL1 was measured by sandwich ELISA. **(A)** Quantification of *CXCL1* gene expression as determined by RNA Sequencing ($n = 9$) or RT-qPCR **(B)** normalized to *GAPDH* ($n = 5$), **(C)** CXCL1 release by *ex vivo* differentiating SC and DN adipocytes into the conditioned media collected at the indicated intervals, in the presence or absence of irisin ($n = 4$), **(D)** CXCL1 release in conditioned medium collected at indicated intervals from untreated (21 days) and irisin treated (14 and 21 days as indicated) cell-culture samples ($n = 3$), **(E)** CXCL1 release from differentiating adipocytes with or without irisin treatment, in the presence or absence of 10 μg/ml RGDS ($n = 4$). Comparisons are for the respective days in case of ELISA. Data presented as Mean ± SD. $^*p < 0.05$, $^{**}p < 0.01$. Statistics: GLM **(A)**, One-way ANOVA with Tukey's post-test **(B)**, Two-way ANOVA with Tukey's post-test **(C–E)**.

the conditioned medium of untreated adipocytes (**Figures 6B,C**). When HUVECs were treated with recombinant CXCL1, at the highest observed concentration in media of irisin treated *ex vivo* differentiated adipocytes, their adhesion property was enhanced significantly (**Figure 6D**). This suggests a potential beneficial role of the released CXCL1 in promoting endothelial functions and adipose tissue remodeling to support efficient thermogenesis indirectly by enhancing vascularization.

DISCUSSION

Irisin was discovered as a proteolytic product of FNDC5, released by cardiac and skeletal myocytes, which induces a beige differentiation program in mouse subcutaneous WAT (Boström et al., 2012; Aydin et al., 2014). In humans, adenine has been shown to be replaced by guanine in the start codon of the human *FNDC5* gene, which was shown to result in a shorter precursor protein lacking the part from which irisin is cleaved (Raschke et al., 2013). Despite this, the presence of irisin in human blood plasma could be detected using mass spectrometry or different antibodies at 3–4 ng/mL (Jedrychowski et al., 2015). The reported concentration range, however, is subject to uncertainty even according the authors themselves, who discussed that they could not account for how much irisin was lost during sample preparation (Jedrychowski et al., 2015). A recent publication indicated the level of circulating irisin in mice to be 0.3 ng/mL, which was previously estimated to be 800 ng/mL (Maak et al., 2021). Furthermore, it is present in the cerebrospinal fluid, liver, pancreas, stomach, saliva, and urine (Mahgoub et al., 2018). However, further research and validated commercially available techniques are required to assess the irisin concentration of human samples in a reproducible manner.

The applied concentrations and time intervals of recombinant irisin largely vary in the experiments reported. The effect of irisin

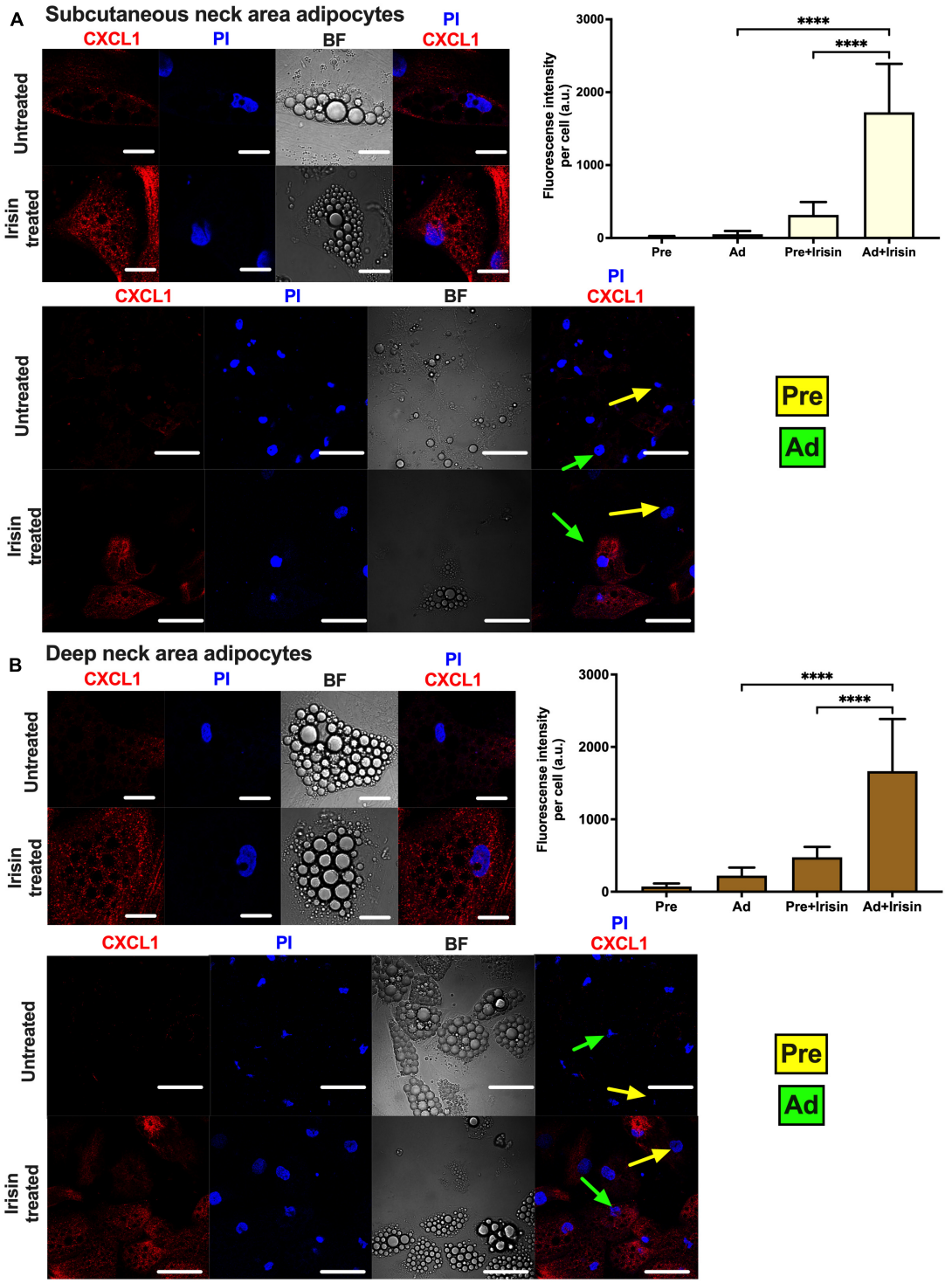

FIGURE 4 | Irisin stimulated CXCL1 release predominantly from subcutaneous **(A)** and deep-neck **(B)** area differentiated adipocytes. Preadipocytes (Pre) were plated and differentiated into adipocytes (Ad) on Ibidi chambers, with or without irisin treatment as in **Figures 1–3**. Cells were treated with 100 ng/ml brefeldin-A for 24 h to block the secretion of CXCL1, which was followed by fixation and image acquisition by confocal microscopy. Propidium Iodide (PI) was used to stain the nucleus. BF represents the bright field image. Confocal images of differentiated adipocytes were shown followed by wider coverage of undifferentiated and differentiated adipocytes. Scale bars represent 10 μm for single differentiated Ad and 30 μm for wider coverage of Pre and Ad. Yellow and green arrows point the undifferentiated preadipocytes and the differentiated adipocytes, respectively. Quantification of fluorescence intensity normalized to per cell are shown on the right bar graphs. Data presented as Mean ± SD. n = 35 cells **(A)** and 50 cells **(B)** from two independent donors. $^{****}p < 0.0001$. Statistics: One-way ANOVA with Tukey's post-test.

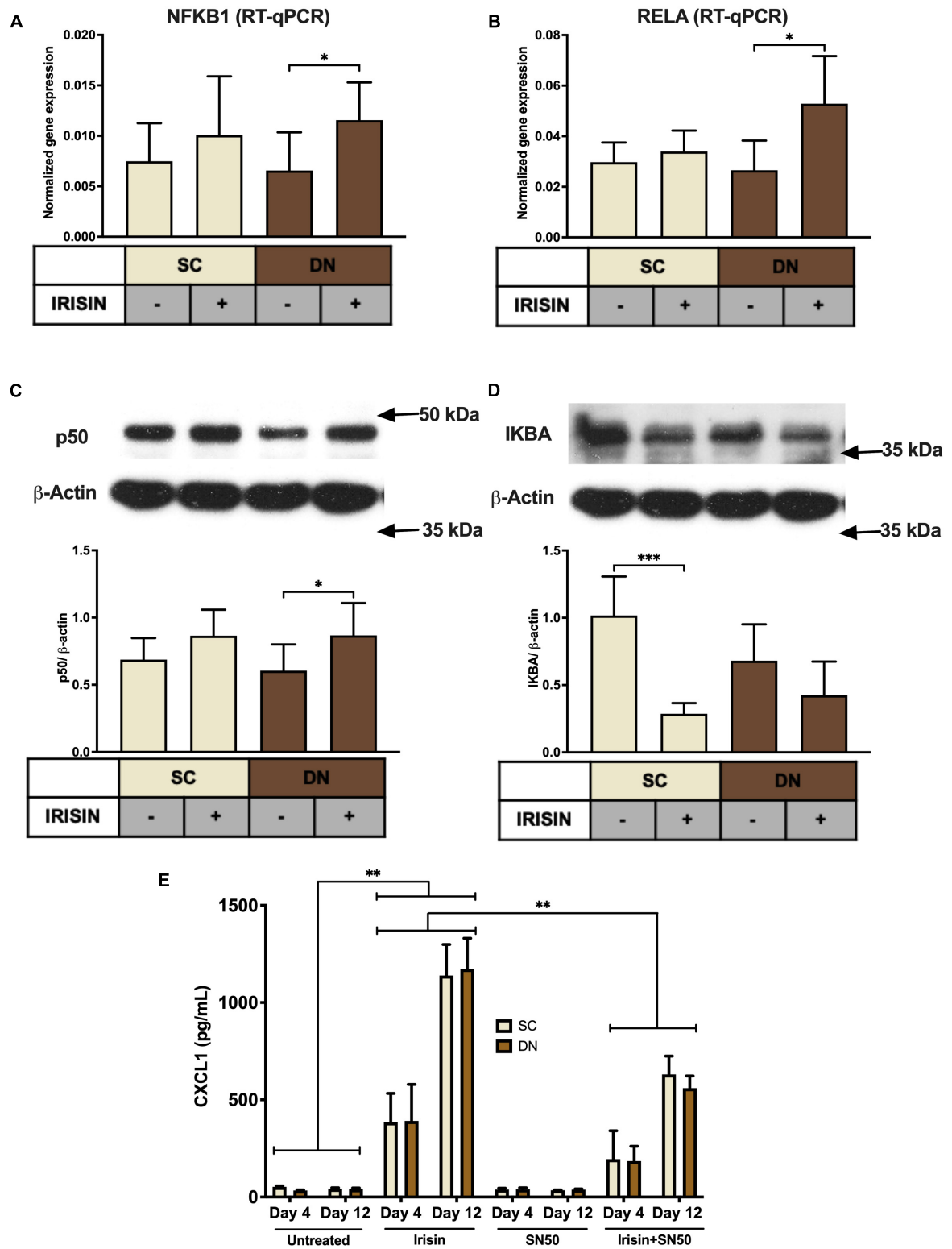

FIGURE 5 | CXCL1 release is stimulated *via* the NFκB pathway during the differentiation of subcutaneous (SC) and deep-neck (DN) area adipocytes. SC and DN preadipocytes were differentiated and treated as in **Figures 1–4**. Quantification of gene expression for *NFKB1* **(A)** and *RELA* **(B)**, normalized to *GAPDH* by RT-qPCR ($n = 5$), **(C)** p50 and IKBA **(D)** protein expression, normalized to β-actin ($n = 6$), **(E)** CXCL1 release from differentiating adipocytes with or without irisin treatment, in the presence or absence of 50 μg/ml SN50 ($n = 4$); comparisons are for the respective days. Data presented as Mean ± SD. $^{*}p < 0.05$, $^{**}p < 0.01$, and $^{***}p < 0.001$. Statistics: One-way ANOVA with Tukey's post-test **(A–D)** and Two-way ANOVA with Tukey's post-test **(E)**.

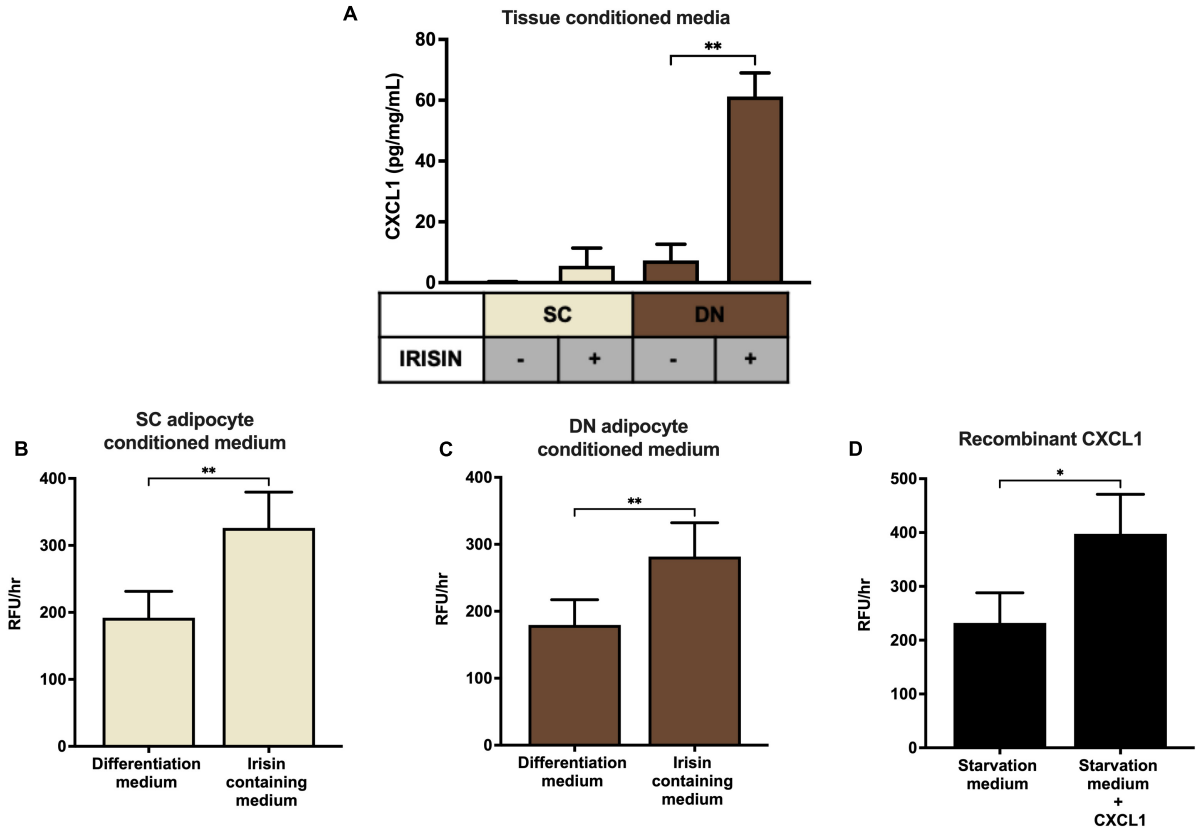

FIGURE 6 | Irisin stimulated the release of CXCL1 from deep-neck (DN) tissue biopsies, which improves the adhesion property of endothelial cells. **(A)** CXCL1 released into the conditioned media of paired subcutaneous (SC) and DN biopsies after 24 h incubation in the presence or absence of irisin (n = 4), Quantification of adhesion of endothelial cells upon incubation with the conditioned media (with or without irisin treatment) from *ex vivo* differentiated (incubation period from day 8–12 of differentiation) SC **(B)** and DN **(C)** area adipocytes (n = 5), **(D)** Quantification of endothelial cell adhesion upon incubation with recombinant CXCL1 in starvation medium (n = 3). Data presented as Mean ± SD. *$p < 0.05$, **$p < 0.01$. Statistics: One-way ANOVA with Tukey's post-test **(A)** and Welch's t-test **(B–D)**.

has been intensively studied in various cellular models before any measurement of the hormone level in a physiological context was successfully carried out. In several studies, the recombinant peptide was applied at higher concentrations than its reported range in human plasma (Jedrychowski et al., 2015). Of note, the biological activity of commercially available recombinant peptides might be less than the endogenous hormone, as a result of folding deficiency, partial denaturation or lack of possible post-translational modifications. Irisin significantly increased UCP1 gene and protein expression of rat primary adipocytes at concentrations from 2 to 100 nM that corresponds to 25–1,250 ng/mL (Zhang et al., 2014). The expression of BAT marker proteins (PGC1α, PRDM16, and UCP1) was increased when the peptide was applied at 20 nM (250 ng/mL) on 3T3L1 adipocytes (Tsai et al., 2020). Irisin also protected murine osteocyte-like cells from hydrogen peroxide induced apoptotic cell death at concentrations up to 500 ng/mL (Kim et al., 2018). Irisin elevated mitochondrial respiration of human visceral and subcutaneous WAT-derived and perirenal BAT-derived adipocytes when applied at 50 nM (625 ng/mL) (Li et al., 2019). Another study reported that irisin treatment induced UCP1 protein expression in subcutaneous human adipocytes when the peptide was applied at 50 nM (Huh et al., 2014). Mediastinal brown hASCs that were directionally differentiated in the presence of FNDC5 at 20 nM (800 ng/mL) exhibited a higher gene expression profile of brown marker genes as compared to the untreated cells (Silva et al., 2014). We reported that recombinant irisin at above 50 ng/mL induced a beige phenotype of human primary abdominal subcutaneous and Simpson-Golabi-Behmel syndrome (SGBS) adipocytes when they were treated on top the white adipogenic protocol that was used in this study (Kristóf et al., 2015; Klusóczki et al., 2019). In our previous experiments, irisin administration at 250 ng/mL also facilitated the secretion of batokines, such as IL-6 and MCP1, by abdominal subcutaneous and neck area adipocytes (Kristóf et al., 2019).

Adipocytes from the neck, especially the DN, area play a significant role in maintaining whole body energy homeostasis by performing continuous non-shivering thermogenesis (Svensson et al., 2011; Wu et al., 2012; Cypess et al., 2013; Jespersen et al., 2013). However, the effect of irisin during the differentiation of SC and DN area adipocytes has not yet been elucidated. Recent publications pointed out that irisin may induce a different degree of browning response based on the origin of the human adipose

tissue (Buscemi et al., 2018; Li et al., 2019). According to our RNA-sequencing results presented here, irisin did not directly influence the expression of thermogenesis-related genes in the SC and DN area adipocytes. However, it induced components of a secretory pathway leading to the release of *CXCL1*.

The targeted genetic impairment of the thermogenic capacity of BAT in mice (e.g., Ucp1$^{-/-}$ mice) results in a less pronounced phenotype than the ablation of BAT (Villarroya et al., 2019). Transplantation of small amounts of BAT or activated beige adipocytes leads to significant effects on systemic metabolism, including increased glucose tolerance or attenuated fat accumulation in the liver in response to an obesogenic diet (Min et al., 2016). Further studies highlighted the important secretory role of BAT, leading to an increased interest in identifying batokines in rodents that can exert autocrine, paracrine, or endocrine effects. Several recently discovered batokines, such as FGF21, NRG4, BMP8b, CXCL14, or adiponectin have been shown to exert a protective role against obesity by enhancing beiging of WAT, lipolysis, sympathetic innervation, or polarization of M2 macrophages (Ahmad et al., 2021). We found that IL-6, released as a batokine, directly improves browning of human abdominal subcutaneous adipocytes (Kristóf et al., 2019). Our findings suggest that CXCL1 is a novel adipokine, which can be secreted in response to specific cues. This is further supported by gene expression data from single cell analysis of human subcutaneous adipocytes; in thermogenic cells, genes of *CXCL1*, and other secreted factors, such as *CXCL2*, *CXCL3*, *CXCL5*, *CCL2*, and *IL6*, were significantly upregulated in response to forskolin that models adrenergic stimulation of heat production (Min et al., 2019).

CXCL1 is a small peptide belonging to the CXC chemokine family. Upon binding to its receptor, CXCR2 (Silva et al., 2017), it acts as a chemoattractant of several immune cells, especially neutrophils (Schumacher et al., 1992). CXCL1 initiates the migration of immune and endothelial cells upon injury-mediated tissue repair (Gillitzer and Goebeler, 2001). Conditioned medium containing CXCL1, collected during differentiation of SC and DN adipocytes in the presence of irisin, significantly improved the adhesion property of HUVECs. We observed the similar response when they were directly treated with the recombinant chemokine (**Figure 6D**). Together this raised a possible beneficial paracrine role of the released CXCL1 from differentiating adipocytes upon irisin treatment, which can be further proven by applying a neutralizing antibody against the chemokine or its receptor. Of note, significant involvement of other released factors cannot be excluded.

Our study shed light on an important role of irisin, as a regulator of cytokine release from differentiating adipocytes of the neck area. The study also indicated the upregulation of various other cytokines, such as *CX3CL1*, *IL32*, *CXCL2*, *IL34*, *CXCL5*, and *CXCL3*. Release of IL-6 and MCP1, encoded by *CCL2*, was detected from media collected during differentiation and was found to be specifically released by differentiated lipid laden adipocytes as described in our previous publication (Kristóf et al., 2019). Further studies are required to reveal the impact of irisin stimulated release of other cytokines, which may have beneficial effects on local tissue homeostasis or metabolic parameters of the entire body.

Irisin can exert non-thermogenic effects on several tissues, including the liver (Tang et al., 2016), central nervous system (Ferrante et al., 2016; Zsuga et al., 2018), blood vessels (Han et al., 2015), or the heart (Xie et al., 2015). In mouse osteocytes, irisin acts *via* a subset of integrin receptor complexes, which are assembled from ITGAV and either ITGB1, ITGB3, or ITGB5 (Kim et al., 2018). These integrins transmit the effect of irisin in inguinal fat and osteoclasts *in vivo* (Kim et al., 2018; Estell et al., 2020). In our experiments, RT-qPCR analysis of *ITGAV* expression has revealed its high expression in both preadipocytes and differentiated adipocytes, which was further upregulated upon irisin treatment in DN adipocytes (**Figure 1D**). RNA Sequencing also proved that the β-integrin subunits were abundantly expressed in both preadipocytes and differentiated adipocytes (**Supplementary Figure 1**). However, RGDS peptide exerted only a moderate effect on the irisin-stimulated CXCL1 secretion by DN adipocytes. This suggests that irisin initiates some of its biological effects *via* other, currently unknown receptor(s) as well. The canonical integrin signaling includes the phosphorylation of FAK and Zyxin, followed by phosphorylation of AKT (at T308) and CREB (Kim et al., 2018). However, other studies proposed positive effects of irisin on cAMP-PKA-HSL (Xiong et al., 2015), AMPK (So and Leung, 2016; Xin et al., 2016), or p38 MAPK (Zhang et al., 2014) pathways. Of note, RGDS peptide was applied at a relatively low concentration, in which anoikis was not observed. It is still possible that some of the administered irisin still access their integrin receptors at this condition.

It has already been reported that *CXCL1* gene expression is directly controlled by NFκB (Burke et al., 2014). NFκB-signaling might be induced in *ex vivo* differentiated adipocytes by released saturated fatty acids that can activate toll-like receptor (TLR) 4, which is abundantly expressed at mRNA level in hASCs and adipocytes of human neck (data not shown) (Lee et al., 2003; Suganami et al., 2007). Our data indicate that genes of canonical NFκB-signaling, which are abundantly expressed in neck area adipocytes, are upregulated when differentiated in the presence of irisin (**Figures 5A,B**). The induced expression of inflammation-related genes might explain why thermogenic genes were not upregulated further when adipocytes were differentiated in the presence of irisin (Chung et al., 2017). The absence of TNFα or IL-1β-upregulation and release during the differentiation in the presence of irisin excluded the possibility of endotoxin contamination of the recombinant hormone. Although irisin was reported previously to inhibit LPS-induced NFκB activation (Mazur-Bialy et al., 2017; Jiang et al., 2020), adipocytes differentiated in the presence of both SN50 and irisin released less CXCL1 than those of treated with irisin alone (**Figure 5E**). Further research is needed to explore the irisin-induced molecular events in the distinct human adipocyte subsets.

In this study, we have shown that irisin applied in a higher concentration than that reported in human blood plasma upregulated the expression of several genes with respect to

cytokine signaling in human adipocytes derived from the neck. CXCL1 was upregulated at the greatest extent, at least partially by upregulation of the NFκB pathway, and was proved to be secreted mainly by differentiated adipocytes. Of note, the expression of thermogenesis-related genes were not induced that might be explained by the desensitization of irisin receptors by the high concentration of the hormone. On the other hand, results of *in vitro* endothelial adhesion assay suggested a positive effect of the released chemokine on angiogenesis. Further studies are required to assess how irisin at physiological levels affects thermogenesis and cytokine release of human adipocytes.

DATA AVAILABILITY STATEMENT

The datasets presented in this study can be found in online repositories. The names of the repository/repositories and accession number(s) can be found below: https://www.ncbi.nlm.nih.gov/, PRJNA607438.

ETHICS STATEMENT

The studies involving human participants were reviewed and approved by Medical Research Council of Hungary (20571-476 2/2017/EKU). The patients/participants provided their written informed consent to participate in this study.

AUTHOR CONTRIBUTIONS

LF, EK, AS, and RK conceived and designed the experiments. AS, EK, SP, RK, and AV performed the experiments. EK, AS, and AV generated primary cell cultures for the experiments. BT analyzed the RNAseq data. RA analyzed and visualized gene interaction networks. IC, AS, AV, and ZB performed microscopy and image analysis. FG provided tissue samples, IK-S provided HUVEC cells. AS and EK wrote the manuscript with inputs from BT. LF mentored the writing and revised the draft. LF, EK, and IK-S acquired funding. All authors approved the submitted version.

FUNDING

This research was funded by the European Union and the European Regional Development Fund (GINOP-2.3.2-15-2016-00006) and the National Research, Development and Innovation Office (NKFIH-FK131424, K129139, and K120392) of Hungary. EK was supported by the János Bolyai Fellowship of the Hungarian Academy of Sciences and the ÚNKP-20-5 New National Excellence Program of the Ministry for Innovation and Technology from the source of the National Research, Development and Innovation Fund.

ACKNOWLEDGMENTS

We would like to thank Jennifer Nagy for technical assistance and Zsuzsa Szondy for reviewing the manuscript.

SUPPLEMENTARY MATERIAL

The Supplementary Material for this article can be found online at: https://www.frontiersin.org/articles/10.3389/fcell.2021.737872/full#supplementary-material

REFERENCES

Ahmad, B., Vohra, M. S., Saleemi, M. A., Serpell, C. J., Fong, I. L., and Wong, E. H. (2021). Brown/Beige adipose tissues and the emerging role of their secretory factors in improving metabolic health: the batokines. *Biochimie* 184, 26–39. doi: 10.1016/j.biochi.2021.01.015

Aydin, S., Kuloglu, T., Eren, M. N., Celik, A., Yilmaz, M., Kalayci, M., et al. (2014). Cardiac, skeletal muscle and serum irisin responses to with or without water exercise in young and old male rats: cardiac muscle produces more irisin than skeletal muscle. *Peptides* 52, 68–73. doi: 10.1016/j.peptides.2013.11.024

Ballak, D. B., Stienstra, R., Hijmans, A., Joosten, L. A., Netea, M. G., and Tack, C. J. (2013). Combined B- and T-cell deficiency does not protect against obesity-induced glucose intolerance and inflammation. *Cytokine* 62, 96–103. doi: 10.1016/j.cyto.2013.02.009

Boström, P., Wu, J., Jedrychowski, M. P., Korde, A., Ye, L., Lo, J. C., et al. (2012). A PGC1-α-dependent myokine that drives brown-fat-like development of white fat and thermogenesis. *Nature* 481, 463–468. doi: 10.1038/nature10777

Burke, S. J., Lu, D., Sparer, T. E., Masi, T., Goff, M. R., Karlstad, M. D., et al. (2014). NF-κB and STAT1 control CXCL1 and CXCL2 gene transcription. *Am. J. Physiol. Endocrinol. Metab.* 306, E131–E149. doi: 10.1152/ajpendo.00347.2013

Buscemi, S., Corleo, D., Buscemi, C., and Giordano, C. (2018). Does iris(in) bring bad news or good news? *Eat. Weight Disord.* 23, 431–442. doi: 10.1007/s40519-017-0431-8

Cannon, B., and Nedergaard, J. (2004). Brown adipose tissue: function and physiological significance. *Physiol. Rev.* 84, 277–359. doi: 10.1152/physrev.00015.2003

Cereijo, R., Gavaldà-Navarro, A., Cairó, M., Quesada-López, T., Villarroya, J., Morón-Ros, S., et al. (2018). CXCL14, a brown adipokine that mediates brown-fat-to-macrophage communication in thermogenic adaptation. *Cell Metab.* 28, 750–763.e6. doi: 10.1016/j.cmet.2018.07.015

Chung, K. J., Chatzigeorgiou, A., Economopoulou, M., Garcia-Martin, R., Alexaki, V. I., Mitroulis, I., et al. (2017). A self-sustained loop of inflammation-driven inhibition of beige adipogenesis in obesity. *Nat. Immunol.* 18, 654–664. doi: 10.1038/ni.3728

Counter, C. M., Hahn, W. C., Wei, W., Caddle, S. D., Beijersbergen, R. L., Lansdorp, P. M., et al. (1998). Dissociation among in vitro telomerase activity, telomere maintenance, and cellular immortalization. *Proc. Natl. Acad. Sci. U.S.A.* 95, 14723–14728. doi: 10.1073/pnas.95.25.14723

Cuevas-Ramos, D., Mehta, R., and Aguilar-Salinas, C. A. (2019). Fibroblast growth factor 21 and browning of white adipose tissue. *Front. Physiol.* 10:37. doi: 10.3389/fphys.2019.00037

Cypess, A. M., Lehman, S., Williams, G., Tal, I., Rodman, D., Goldfine, A. B., et al. (2009). Identification and importance of brown adipose tissue in adult humans. *N. Engl. J. Med.* 360, 1509–1517. doi: 10.1056/NEJMoa0810780

Cypess, A. M., White, A. P., Vernochet, C., Schulz, T. J., Xue, R., Sass, C. A., et al. (2013). Anatomical localization, gene expression profiling and functional characterization of adult human neck brown fat. *Nat. Med.* 19, 635–639. doi: 10.1038/nm.3112

Doan-Xuan, Q. M., Sarvari, A. K., Fischer-Posovszky, P., Wabitsch, M., Balajthy, Z., Fesus, L., et al. (2013). High content analysis of differentiation and cell death in human adipocytes. *Cytometry A* 83, 933–943. doi: 10.1002/cyto.a.22333

Dobin, A., Davis, C. A., Schlesinger, F., Drenkow, J., Zaleski, C., Jha, S., et al. (2013). STAR: ultrafast universal RNA-seq aligner. *Bioinformatics* 29, 15–21. doi: 10.1093/bioinformatics/bts635

Estell, E. G., Le, P. T., Vegting, Y., Kim, H., Wrann, C., Bouxsein, M. L., et al. (2020). Irisin directly stimulates osteoclastogenesis and bone resorption in vitro and in vivo. *Elife* 9:e58172. doi: 10.7554/eLife.58172.sa2

Ferrante, C., Orlando, G., Recinella, L., Leone, S., Chiavaroli, A., Di Nisio, C., et al. (2016). Central inhibitory effects on feeding induced by the adipo-myokine irisin. *Eur. J. Pharmacol.* 791, 389–394. doi: 10.1016/j.ejphar.2016.09.011

Fischer-Posovszky, P., Newell, F. S., Wabitsch, M., and Tornqvist, H. E. (2008). Human SGBS cells a unique tool for studies of human fat cell biology. *Obes. Facts* 1, 184–189. doi: 10.1159/000145784

Frühbeck, G., Fernández-Quintana, B., Paniagua, M., Hernández-Pardos, A. W., Valentí, V., Moncada, R., et al. (2020). FNDC4, a novel adipokine that reduces lipogenesis and promotes fat browning in human visceral adipocytes. *Metabolism* 108:154261. doi: 10.1016/j.metabol.2020.154261

Gillitzer, R., and Goebeler, M. (2001). Chemokines in cutaneous wound healing. *J. Leukoc. Biol.* 69, 513–521.

Han, F., Zhang, S., Hou, N., Wang, D., and Sun, X. (2015). Irisin improves endothelial function in obese mice through the AMPK-eNOS pathway. *Am. J. Physiol. Heart Circ. Physiol.* 309, H1501–H1508. doi: 10.1152/ajpheart.00443.2015

Hondares, E., Iglesias, R., Giralt, A., Gonzalez, F. J., Giralt, M., Mampel, T., et al. (2011). Thermogenic activation induces FGF21 expression and release in brown adipose tissue. *J. Biol. Chem.* 286, 12983–12990. doi: 10.1074/jbc.M110.215889

Huh, J. Y., Dincer, F., Mesfum, E., and Mantzoros, C. S. (2014). Irisin stimulates muscle growth-related genes and regulates adipocyte differentiation and metabolism in humans. *Int. J. Obes.* 38, 1538–1544. doi: 10.1038/ijo.2014.42

Jedrychowski, M. P., Wrann, C. D., Paulo, J. A., Gerber, K. K., Szpyt, J., Robinson, M. M., et al. (2015). Detection and quantitation of circulating human irisin by tandem mass spectrometry. *Cell Metab.* 22, 734–740. doi: 10.1016/j.cmet.2015.08.001

Jespersen, N. Z., Larsen, T. J., Peijs, L., Daugaard, S., Homøe, P., Loft, A., et al. (2013). A classical brown adipose tissue mRNA signature partly overlaps with brite in the supraclavicular region of adult humans. *Cell Metab.* 17, 798–805. doi: 10.1016/j.cmet.2013.04.011

Jiang, X., Shen, Z., Chen, J., Wang, C., Gao, Z., Yu, S., et al. (2020). Irisin protects against motor dysfunction of rats with spinal cord injury via adenosine 5'-monophosphate (AMP)-activated protein kinase-nuclear factor kappa-B pathway. *Front. Pharmacol.* 11:582484. doi: 10.3389/fphar.2020.582484

Kajimura, S., Spiegelman, B. M., and Seale, P. (2015). Brown and beige fat: physiological roles beyond heat generation. *Cell Metab.* 22, 546–559. doi: 10.1016/j.cmet.2015.09.007

Kim, H., Wrann, C. D., Jedrychowski, M., Vidoni, S., Kitase, Y., Nagano, K., et al. (2018). Irisin mediates effects on bone and fat via αV integrin receptors. *Cell* 175, 1756–1768.e17. doi: 10.1016/j.cell.2018.10.025

Klusóczki, Á, Veréb, Z., Vámos, A., Fischer-Posovszky, P., Wabitsch, M., Bacso, Z., et al. (2019). Differentiating SGBS adipocytes respond to PPARγ stimulation, irisin and BMP7 by functional browning and beige characteristics. *Sci. Rep.* 9:5823. doi: 10.1038/s41598-019-42256-0

Kristóf, E., Doan-Xuan, Q. M., Bai, P., Bacso, Z., and Fésüs, L. (2015). Laser-scanning cytometry can quantify human adipocyte browning and proves effectiveness of irisin. *Sci. Rep.* 5:12540. doi: 10.1038/srep12540

Kristóf, E., Klusóczki, Á, Veress, R., Shaw, A., Combi, Z. S., Varga, K., et al. (2019). Interleukin-6 released from differentiating human beige adipocytes improves browning. *Exp. Cell Res.* 377, 47–55. doi: 10.1016/j.yexcr.2019.02.015

Lee, J. Y., Ye, J., Gao, Z., Youn, H. S., Lee, W. H., Zhao, L., et al. (2003). Reciprocal modulation of Toll-like receptor-4 signaling pathways involving MyD88 and phosphatidylinositol 3-kinase/AKT by saturated and polyunsaturated fatty acids. *J. Biol. Chem.* 278, 37041–37051. doi: 10.1074/jbc.M305213200

Lee, P., Linderman, J. D., Smith, S., Brychta, R. J., Wang, J., Idelson, C., et al. (2014). Irisin and FGF21 are cold-induced endocrine activators of brown fat function in humans. *Cell Metab.* 19, 302–309. doi: 10.1016/j.cmet.2013.12.017

Leitner, B. P., Huang, S., Brychta, R. J., Duckworth, C. J., Baskin, A. S., McGehee, S., et al. (2017). Mapping of human brown adipose tissue in lean and obese young men. *Proc. Natl. Acad. Sci. U.S.A.* 114, 8649–8654. doi: 10.1073/pnas.1705287114

Li, H., Zhang, Y., Wang, F., Donelan, W., Zona, M. C., Li, S., et al. (2019). Effects of irisin on the differentiation and browning of human visceral white adipocytes. *Am. J. Transl. Res.* 11, 7410–7421.

Liao, Y., Smyth, G. K., and Shi, W. (2014). featureCounts: an efficient general purpose program for assigning sequence reads to genomic features. *Bioinformatics* 30, 923–930. doi: 10.1093/bioinformatics/btt656

Maak, S., Norheim, F., Drevon, C. A., and Erickson, H. P. (2021). Progress and challenges in the biology of FNDC5 and irisin. *Endocr. Rev.* 42, 436–456. doi: 10.1210/endrev/bnab003

Mahdaviani, K., Chess, D., Wu, Y., Shirihai, O., and Aprahamian, T. R. (2016). Autocrine effect of vascular endothelial growth factor-A is essential for mitochondrial function in brown adipocytes. *Metabolism* 65, 26–35. doi: 10.1016/j.metabol.2015.09.012

Mahgoub, M. O., D'Souza, C., Al Darmaki, R. S. M. H., Baniyas, M. M. Y. H., and Adeghate, E. (2018). An update on the role of irisin in the regulation of endocrine and metabolic functions. *Peptides* 104, 15–23. doi: 10.1016/j.peptides.2018.03.018

Mazur-Bialy, A. I., Bilski, J., Pochec, E., and Brzozowski, T. (2017). New insight into the direct anti-inflammatory activity of a myokine irisin against proinflammatory activation of adipocytes. Implication for exercise in obesity. *J. Physiol. Pharmacol.* 68, 243–251.

Min, S. Y., Desai, A., Yang, Z., Sharma, A., DeSouza, T., Genga, R. M. J., et al. (2019). Diverse repertoire of human adipocyte subtypes develops from transcriptionally distinct mesenchymal progenitor cells. *Proc. Natl. Acad. Sci. U.S.A.* 116, 17970–17979. doi: 10.1073/pnas.1906512116

Min, S. Y., Kady, J., Nam, M., Rojas-Rodriguez, R., Berkenwald, A., Kim, J. H., et al. (2016). Human 'brite/beige' adipocytes develop from capillary networks, and their implantation improves metabolic homeostasis in mice. *Nat. Med.* 22, 312–318. doi: 10.1038/nm.4031

Palatka, K., Serfozo, Z., Veréb, Z., Bátori, R., Lontay, B., Hargitay, Z., et al. (2006). Effect of IBD sera on expression of inducible and endothelial nitric oxide synthase in human umbilical vein endothelial cells. *World J. Gastroenterol.* 12, 1730–1738. doi: 10.3748/wjg.v12.i11.1730

Polyzos, S. A., Anastasilakis, A. D., Efstathiadou, Z. A., Makras, P., Perakakis, N., Kountouras, J., et al. (2018). Irisin in metabolic diseases. *Endocrine* 59, 260–274. doi: 10.1007/s12020-017-1476-1

Raschke, S., Elsen, M., Gassenhuber, H., Sommerfeld, M., Schwahn, U., Brockmann, B., et al. (2013). Evidence against a beneficial effect of irisin in humans. *PLoS One* 8:e73680. doi: 10.1371/journal.pone.0073680

Rosen, E. D., and Spiegelman, B. M. (2014). What we talk about when we talk about fat. *Cell* 156, 20–44. doi: 10.1016/j.cell.2013.12.012

Ruan, C. C., Kong, L. R., Chen, X. H., Ma, Y., Pan, X. X., Zhang, Z. B., et al. (2018). A2A receptor activation attenuates hypertensive cardiac remodeling via promoting brown adipose tissue-derived FGF21. *Cell Metab.* 28, 476–489.e5. doi: 10.1016/j.cmet.2018.06.013

Saito, M., Okamatsu-Ogura, Y., Matsushita, M., Watanabe, K., Yoneshiro, T., Nio-Kobayashi, J., et al. (2009). High incidence of metabolically active brown adipose tissue in healthy adult humans: effects of cold exposure and adiposity. *Diabetes* 58, 1526–1531. doi: 10.2337/db09-0530

Sárvári, A. K., Doan-Xuan, Q. M., Bacsó, Z., Csomós, I., Balajthy, Z., and Fésüs, L. (2015). Interaction of differentiated human adipocytes with macrophages leads to trogocytosis and selective IL-6 secretion. *Cell Death Dis.* 6:e1613. doi: 10.1038/cddis.2014.579

Schumacher, C., Clark-Lewis, I., Baggiolini, M., and Moser, B. (1992). High- and low-affinity binding of GRO alpha and neutrophil-activating peptide 2 to interleukin 8 receptors on human neutrophils. *Proc. Natl. Acad. Sci. U.S.A.* 89, 10542–10546. doi: 10.1073/pnas.89.21.10542

Silva, F. J., Holt, D. J., Vargas, V., Yockman, J., Boudina, S., Atkinson, D., et al. (2014). Metabolically active human brown adipose tissue derived stem cells. *Stem Cells* 32, 572–581. doi: 10.1002/stem.1595

Silva, R. L., Lopes, A. H., Guimarães, R. M., and Cunha, T. M. (2017). CXCL1/CXCR2 signaling in pathological pain: role in peripheral and central sensitization. *Neurobiol. Dis.* 105, 109–116. doi: 10.1016/j.nbd.2017.06.001

So, W. Y., and Leung, P. S. (2016). Irisin ameliorates hepatic glucose/lipid metabolism and enhances cell survival in insulin-resistant human HepG2 cells through adenosine monophosphate-activated protein kinase signaling. *Int. J. Biochem. Cell Biol.* 78, 237–247. doi: 10.1016/j.biocel.2016.07.022

Stewart, S. A., Dykxhoorn, D. M., Palliser, D., Mizuno, H., Yu, E. Y., An, D. S., et al. (2003). Lentivirus-delivered stable gene silencing by RNAi in primary cells. *RNA* 9, 493–501. doi: 10.1261/rna.2192803

Suganami, T., Tanimoto-Koyama, K., Nishida, J., Itoh, M., Yuan, X., Mizuarai, S., et al. (2007). Role of the Toll-like receptor 4/NF-kappaB pathway in saturated fatty acid-induced inflammatory changes in the interaction between adipocytes and macrophages. *Arterioscler. Thromb. Vasc. Biol.* 27, 84–91. doi: 10.1161/01.ATV.0000251608.09329.9a

Sun, K., Kusminski, C. M., Luby-Phelps, K., Spurgin, S. B., An, Y. A., Wang, Q. A., et al. (2014). Brown adipose tissue derived VEGF-A modulates cold tolerance and energy expenditure. *Mol. Metab.* 3, 474–483. doi: 10.1016/j.molmet.2014.03.010

Svensson, P. A., Jernås, M., Sjöholm, K., Hoffmann, J. M., Nilsson, B. E., Hansson, M., et al. (2011). Gene expression in human brown adipose tissue. *Int. J. Mol. Med.* 27, 227–232. doi: 10.3892/ijmm.2010.566

Szatmári-Tóth, M., Shaw, A., Csomós, I., Mocsár, G., Fischer-Posovszky, P., Wabitsch, M., et al. (2020). Thermogenic activation downregulates high mitophagy rate in human masked and mature beige adipocytes. *Int. J. Mol. Sci.* 21:6640. doi: 10.3390/ijms21186640

Tang, H., Yu, R., Liu, S., Huwatibieke, B., Li, Z., and Zhang, W. (2016). Irisin inhibits hepatic cholesterol synthesis via AMPK-SREBP2 signaling. *EBioMedicine* 6, 139–148. doi: 10.1016/j.ebiom.2016.02.041

Tóth, B. B., Arianti, R., Shaw, A., Vámos, A., Veréb, Z., Póliska, S., et al. (2020). FTO intronic SNP strongly influences human neck adipocyte browning determined by tissue and PPARγ specific regulation: a transcriptome analysis. *Cells* 9:987. doi: 10.3390/cells9040987

Tsai, Y. C., Wang, C. W., Wen, B. Y., Hsieh, P. S., Lee, Y. M., Yen, M. H., et al. (2020). Involvement of the p62/Nrf2/HO-1 pathway in the browning effect of irisin in 3T3-L1 adipocytes. *Mol. Cell. Endocrinol.* 514:110915. doi: 10.1016/j.mce.2020.110915

van Marken Lichtenbelt, W. D., and Schrauwen, P. (2011). Implications of nonshivering thermogenesis for energy balance regulation in humans. *Am. J. Physiol. Regul. Integr. Comp. Physiol.* 301, R285–R296. doi: 10.1152/ajpregu.00652.2010

van Marken Lichtenbelt, W. D., Vanhommerig, J. W., Smulders, N. M., Drossaerts, J. M., Kemerink, G. J., Bouvy, N. D., et al. (2009). Cold-activated brown adipose tissue in healthy men. *N. Engl. J. Med.* 360, 1500–1508. doi: 10.1056/NEJMoa0808718

Villarroya, F., Cereijo, R., Villarroya, J., and Giralt, M. (2017). Brown adipose tissue as a secretory organ. *Nat. Rev. Endocrinol.* 13, 26–35. doi: 10.1038/nrendo.2016.136

Villarroya, J., Cereijo, R., Gavaldà-Navarro, A., Peyrou, M., Giralt, M., and Villarroya, F. (2019). New insights into the secretory functions of brown adipose tissue. *J. Endocrinol.* 243, R19–R27. doi: 10.1530/JOE-19-0295

Virtanen, K. A., Lidell, M. E., Orava, J., Heglind, M., Westergren, R., Niemi, T., et al. (2009). Functional brown adipose tissue in healthy adults. *N. Engl. J. Med.* 360, 1518–1525. doi: 10.1056/NEJMoa0808949

Wang, Q. A., Tao, C., Jiang, L., Shao, M., Ye, R., Zhu, Y., et al. (2015). Distinct regulatory mechanisms governing embryonic versus adult adipocyte maturation. *Nat. Cell Biol.* 17, 1099–1111. doi: 10.1038/ncb3217

Wu, J., Boström, P., Sparks, L. M., Ye, L., Choi, J. H., Giang, A. H., et al. (2012). Beige adipocytes are a distinct type of thermogenic fat cell in mouse and human. *Cell* 150, 366–376. doi: 10.1016/j.cell.2012.05.016

Xie, C., Zhang, Y., Tran, T. D., Wang, H., Li, S., George, E. V., et al. (2015). Irisin controls growth, intracellular Ca2+ signals, and mitochondrial thermogenesis in cardiomyoblasts. *PLoS One* 10:e0136816. doi: 10.1371/journal.pone.0136816

Xin, C., Liu, J., Zhang, J., Zhu, D., Wang, H., Xiong, L., et al. (2016). Irisin improves fatty acid oxidation and glucose utilization in type 2 diabetes by regulating the AMPK signaling pathway. *Int. J. Obes.* 40, 443–451. doi: 10.1038/ijo.2015.199

Xiong, X. Q., Chen, D., Sun, H. J., Ding, L., Wang, J. J., Chen, Q., et al. (2015). FNDC5 overexpression and irisin ameliorate glucose/lipid metabolic derangements and enhance lipolysis in obesity. *Biochim. Biophys. Acta* 1852, 1867–1875. doi: 10.1016/j.bbadis.2015.06.017

Xue, Y., Petrovic, N., Cao, R., Larsson, O., Lim, S., Chen, S., et al. (2009). Hypoxia-independent angiogenesis in adipose tissues during cold acclimation. *Cell Metab.* 9, 99–109. doi: 10.1016/j.cmet.2008.11.009

Yu, Q., Kou, W., Xu, X., Zhou, S., Luan, P., Li, H., et al. (2019). FNDC5/Irisin inhibits pathological cardiac hypertrophy. *Clin. Sci.* 133, 611–627. doi: 10.1042/CS20190016

Zhang, Y., Li, R., Meng, Y., Li, S., Donelan, W., Zhao, Y., et al. (2014). Irisin stimulates browning of white adipocytes through mitogen-activated protein kinase p38 MAP kinase and ERK MAP kinase signaling. *Diabetes* 63, 514–525. doi: 10.2337/db13-1106

Zsuga, J., More, C. E., Erdei, T., Papp, C., Harsanyi, S., and Gesztelyi, R. (2018). Blind spot for sedentarism: redefining the diseasome of physical inactivity in view of circadian system and the irisin/BDNF axis. *Front. Neurol.* 9:818. doi: 10.3389/fneur.2018.00818

Conflict of Interest: The authors declare that the research was conducted in the absence of any commercial or financial relationships that could be construed as a potential conflict of interest.

Publisher's Note: All claims expressed in this article are solely those of the authors and do not necessarily represent those of their affiliated organizations, or those of the publisher, the editors and the reviewers. Any product that may be evaluated in this article, or claim that may be made by its manufacturer, is not guaranteed or endorsed by the publisher.

frontiers in Cell and Developmental Biology

REVIEW
published: 19 January 2022
doi: 10.3389/fcell.2021.816301

Role of Ceramides in the Molecular Pathogenesis and Potential Therapeutic Strategies of Cardiometabolic Diseases: What we Know so Far

Youssef M. Shalaby[1,2], *Anas Al Aidaros*[1], *Anjana Valappil*[1], *Bassam R. Ali*[1,3] *and Nadia Akawi*[1,4]*

[1]Department of Genetics and Genomics, College of Medicine and Health Sciences, United Arab Emirates University, Al-Ain, United Arab Emirates, [2]Department of Pharmacology and Toxicology, Faculty of Pharmacy, Ahram Canadian University, Egypt, [3]Zayed Centre for Health Sciences, United Arab Emirates University, Al-Ain, United Arab Emirates, [4]Division of Cardiovascular Medicine, Radcliffe Department of Medicine, University of Oxford, Oxford, United Kingdom

OPEN ACCESS

Edited by:
Jun Ren,
University of Washington,
United States

Reviewed by:
Francesco Spallotta,
National Research Council (CNR), Italy
Ne Natalie Wu,
Fudan University, China
Qiurong Wang,
University of Wyoming, United States

***Correspondence:**
Nadia Akawi
nadia.akawi@uaeu.ac.ae

Specialty section:
This article was submitted to Cellular Biochemistry, a section of the journal Frontiers in Cell and Developmental Biology

Received: 16 November 2021
Accepted: 29 December 2021
Published: 19 January 2022

Citation:
Shalaby YM, Al Aidaros A, Valappil A, Ali BR and Akawi N (2022) Role of Ceramides in the Molecular Pathogenesis and Potential Therapeutic Strategies of Cardiometabolic Diseases: What we Know so Far. Front. Cell Dev. Biol. 9:816301. doi: 10.3389/fcell.2021.816301

Ceramides represent a class of biologically active lipids that are involved in orchestrating vital signal transduction pathways responsible for regulating cellular differentiation and proliferation. However, accumulating clinical evidence have shown that ceramides are playing a detrimental role in the pathogenesis of several diseases including cardiovascular disease, type II diabetes and obesity, collectively referred to as cardiometabolic disease. Therefore, it has become necessary to study in depth the role of ceramides in the pathophysiology of such diseases, aiming to tailor more efficient treatment regimens. Furthermore, understanding the contribution of ceramides to the pathological molecular mechanisms of those interrelated conditions may improve not only the therapeutic but also the diagnostic and preventive approaches of the preceding hazardous events. Hence, the purpose of this article is to review currently available evidence on the role of ceramides as a common factor in the pathological mechanisms of cardiometabolic diseases as well as the mechanism of action of the latest ceramides-targeted therapies.

Keywords: ceramides, cardiometabolic diseases, ROS, cytokines, apoptosis

INTRODUCTION

Cardiometabolic disorders is an umbrella term for a group of interrelated diseases and risk factors including cardiovascular diseases (CVDs), type II diabetes, hypercholesterolemia, and their underlying risk events such as insulin resistance, endothelial dysfunction, and atherosclerosis (Zhang et al., 2018; Miranda et al., 2019; Yang et al., 2021). Researchers are constantly searching for new biomarkers to help in the early diagnosis of such diseases and ways for addressing the increasing levels of their prevalence across the world (Roberts and Gerszten, 2013). Out of these diseases, CVDs remain one of the world's biggest killers to mankind, despite the significant advancements in related therapies (Goradel et al., 2018). CVDs impose a devastating and crippling economic impact on health care systems globally as the direct costs of CVDs surpass medical costs for any other chronic condition (Go et al., 2014). Therefore, it is generally accepted that

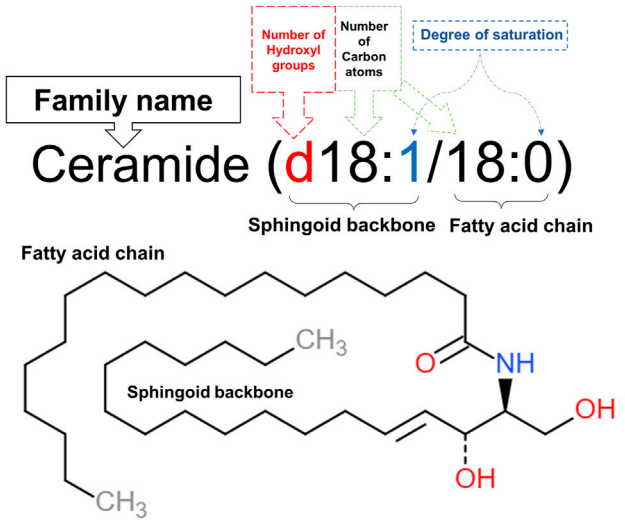

FIGURE 1 | Nomenclature of C18:0 ceramide (d18:1/18:0). The first part of the name (d18:1) denotes the 18 carbon atoms, having one double bond in its sphingoid backbone along with two hydroxyl groups. This sphingosine chain is attached to a saturated fatty acid chain, represented by the second part of the name (18:0), through an amide bond. This illustration was adapted from caymanchem.com.

new therapeutic solutions and prognostic biomarkers are urgently needed to reduce the suffering of patients with CVDs and health care costs (Deng et al., 2020).

Excitement and hopes flared when researchers found a correlation between ceramides levels and prevention of metabolic CVDs in animal models (Bikman and Summers, 2011a; Raichur et al., 2014). Later, researchers found that increased levels of circulatory ceramides in humans resulted in their accumulation in various types of tissues, particularly adipose tissue, which may have beneficial or pathological consequences on their health depending on the type of ceramide (Summers et al., 2019). For example, the length of either sphingoid or N-acyl chain has been found to be a determinant factor for ceramides physiological and pathological properties as well as their synthesis (Alonso and Goñi, 2018). Indeed, although ceramides at normal levels have useful physiological and biological functions, such as reducing the concentration of free fatty acids through facilitating fat storage, their abnormal levels can impair the cardiovascular system in addition to the induction of obesity-related metabolic complications such as insulin resistance, atherosclerosis, and liver diseases (Summers, 2006). Given the fact that a variety of human diseases such as CVDs, diabetes and neurological diseases have become coupled with the circulating levels of ceramide, it has been proposed to use ceramides as reliable biomarkers for the prediction of such pathological conditions (Kurz et al., 2019). Using Liquid chromatography-tandem mass spectrometry (LC-MS/MS) has enabled researchers to measure the normal plasma levels of ceramides in adult populations and reference ranges were determined to be 0.26–0.34 μmol/L for C16:0 ceramide, 0.09–0.14 μmol/L for C18:0 ceramide, and 0.96–1.35 μmol/L for C24:1 ceramide (Meeusen et al., 2018). Based on the plasma concentration of ceramides (C16:0, C18:0, C24:1) and their ratios to C24:0 ceramide, a risk of developing CVDs can be categorized according to standardized risk scores (e.g., CERT1 score) into low, moderate, increased and high risk (Carrard et al., 2021). However, numerous limitations of using LC-MS/MS to measure ceramides still exist particularly regarding its specificity in detecting the broad spectrum of ceramides species and derivatives, in addition to the substantial variation of these lipids among individuals depending on many factors such as age, sex, and diet (Gaggini et al., 2021).

CERAMIDES STRUCTURE AND PHYSIOLOGICAL FUNCTION

Structurally, ceramides belong to sphingolipids as they individually have a long-chain fatty acid (non-hydroxy acids, α-hydroxy acids and ω-hydroxy acids), that is amide-linked to a sphingoid base (**Figure 1**), namely sphingosine, phytosphingosine, dihydrosphingosine or 6-hydroxysphingosine. In human skin, over a hundred ceramide subclasses have been identified so far (Wartewig and Neubert, 2007; Alonso and Goñi, 2018). Ceramides exist mainly as structural elements in cell membranes since they are derived from sphingolipids that make up sphingomyelin, a major component of the phospholipid bilayer. Besides their structural function, ceramides play significant roles in cell signaling as they act as second messengers modulating several metabolic pathways depending on their chain length (Grösch et al., 2012). Furthermore, ceramides possess a central role in cell biological activities, including proliferation, differentiation, senescence, as well as inflammation, and apoptosis (Rivera et al., 2015). The nomenclature of ceramides relies on the number of carbon atoms in the sphingoid backbone, fatty acid chain, and saturation level (McGurk et al., 2021) as shown in **Figure 1**, naming C18:0 ceramide (d18:1/18:0) as an example.

CERAMIDES BIOSYNTHESIS

Many studies have revealed some of the pivotal triggers for ceramide *de novo* synthesis. For instance, exogenous lipid overload, ultraviolet B rays (UVB), and cytokines can increase the expression of serine palmitoyltransferase (SPT), which in turn increases ceramide production. It is worth mentioning that these studies have found that TNF-α, Fas ligand, toll-like receptor-4 activation, or oxidative stress may increase the breakdown of sphingomyelin into ceramides, which has been described as a stress-activated pathway (Summers, 2006;Sokolowska and Blachnio-Zabielska, 2019; Chaurasia and Summers, 2020).

In addition to the *de novo* synthesis pathway which is initiated by condensation of serine with palmitoyl-CoA via SPT, ceramides can be synthesized via two more different pathways as illustrated in **Figure 2**. These include the sphingomyelin pathway where hydrolysis of sphingomyelin to ceramide occurs using neutral or acid sphingomyelinase (nSMase or aSMase, respectively), and the salvage pathway, in which ceramides are recycled and generated

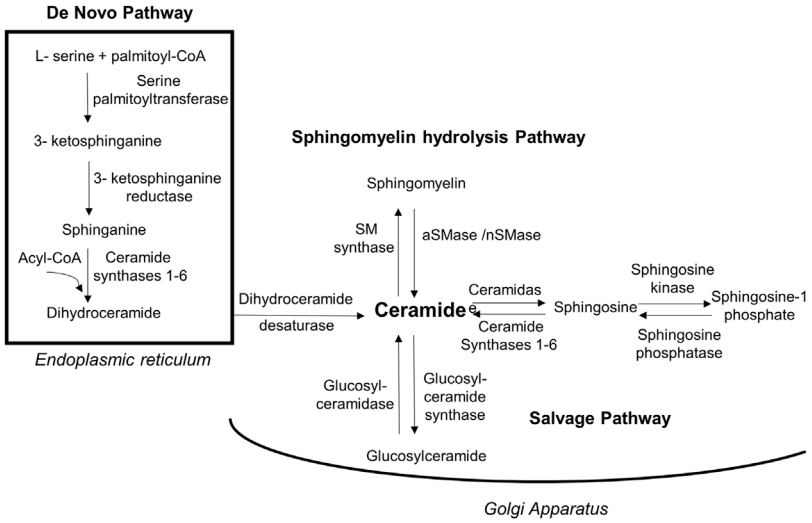

FIGURE 2 | Biosynthesis routes of ceramides. Ceramides are synthesized via 3 pathways. Firstly, *de novo* synthesis of ceramides starts in endoplasmic reticulum by coupling amino acid serine to palmityl-CoA using palmitoyltransferase in a multi-step process and yielding dihydroceramide that will be activated into ceramide by dihydroceramide desaturase. Secondly, in Golgi apparatus ceramides can be generated by sphingomyelin hydrolysis via acidic/neutral sphingomyelinase. The third biosynthesis method is through salvage pathway in which glucosylceramide is converted into ceramides via glucosylceramidase. Moreover, ceramides can be metabolized into less toxic sphingosine that get phosphorylated to sphingosine-1phosphate via sphingosine kinase. [aSMase, acid sphingomyelinase; nSMase, neutral sphingomyelinase; SM, sphingomyelin].

TABLE 1 | Ceramide synthases tissue distribution and their inhibitors as therapeutic targets.

Ceramide synthase (CerS)	Tissue distribution	Derived-ceramide	Physiological impact	Pathological alteration	Inhibitors	References
CerS1	C.N.S, skeletal muscle	C18:0	Brain development and neuronal signaling	Neurodegeneration (Parkinsonism), Insulin resistance	Myriocin	Levy and Futerman (2010); Abbott et al. (2014); Wegner et al. (2016); Choi et al. (2021)
CerS2	Brain, heart, Liver, kidney	C20:0-C26:0	Maintains healthy functions of lungs, brain, heart, and kidney tissues	Alzheimer disease, breast cancer, obesity, cardiomyopathy	S1P	Laviad et al. (2008); Wegner et al. (2016); Choi et al. (2021)
CerS3	Skin, testes	C22-C26	Spermatogenesis, normal keratinization	Disruption of skin barrier function	Not known	Park et al. (2014); Fucho et al. (2017)
CerS4	Heart, liver, skin	C18:0, C20:0	Stem cell homeostasis and hair growth	Obesity (m), diabetes(m), heart failure	ST1072	Laviad et al. (2008); Schiffmann et al. (2012); Abbott et al. (2014); Peters et al. (2015); Fucho et al. (2017); Choi et al. (2021)
CerS5	Heart, lungs, kidney, ubiquitous	C16:0	Brain development	Heart failure, apoptosis	Fingolimod (FTY720)	
CerS6	Heart, brain, other tissues	C14, C16:0	Brain development, immunity, tumor suppressor effects	Heart failure, obesity, multiple sclerosis	ST1072	Schiffmann et al. (2012); Park et al. (2014); Fucho et al. (2017); Choi et al. (2021)

C.N.S, central nervous system; m, mouse model; S1P, sphingosine 1 phosphate.

from their metabolites sphingosine and glucosylceramide by ceramide synthase and glucosylceramide synthase, respectively (Sokolowska and Blachnio-Zabielska, 2019). The identification of many types of ceramides with various lengths of fatty acid side chains that exhibit different levels of saturation in human tissues facilitated our improved understanding of their chemistry, functions and pathophysiology (Moore and Rawlings, 2017). It has been stated that each of these types is initially produced as an intermediate dihydroceramide from sphinganine and C14-C30 acyl chain via dihydroceramide synthases, which include six protein isoforms family members (CerS 1-6). Thereafter, the intermediate is converted into a fully developed ceramide by dihydroceramide desaturase (**Figure 2**) (Cowart, 2009; Turpin et al., 2014).

The distribution of CerS enzymes among body tissues is variable (**Table 1**), where they catalyze the production of

ceramides with different acyl chain lengths, and therefore with different functions. For instance, CerS1, CerS5, and CerS6 are widely distributed in skeletal muscle and brain tissues, and they are responsible for the generation of C16:0 and C18:0 long-chain ceramides (Grösch et al., 2012). In contrast, CerS2 which catalyzes the production of C20-C26 is abundant in many tissues, including heart, liver, and kidney tissues. It was reported that CerS enzymes are implicated in the regulation of various biological and metabolic functions through ceramide production in the human body. A prime example of those functions is that of CerS1-derived C18;0 ceramide, which is critical for brain development, while CerS2 resulting ceramides are essential for normal liver functions. However, it has been shown that dysregulation of CerS can lead to metabolic and CVDs (Raichur et al., 2014; Turpin et al., 2014).

THE INTERRELATED ROLE OF CERAMIDES IN THE MOLECULAR PATHOGENESIS OF CARDIOMETABOLIC DISORDERS

Recently, compelling evidence has been established regarding the contribution of ceramides to the molecular pathogenesis of CVDs along with the associated comorbidities through an interconnected mechanism (Ormazabal et al., 2018). Indeed, in addition to confirming the correlation between ceramides levels in the plasma and the risk of CVD, several large cardiac-cohort studies suggested ceramides as powerful prognostic biomarkers of CVDs progression in humans (Yu et al., 2015; Cao et al., 2020; Li et al., 2020; Akawi et al., 2021). Indeed, several studies specified three particular ceramides (C16:0, C18:0, C24:1) to be strongly associated with CVDs major adverse outcomes including cardiac related mortality (Fabbri et al., 2016; Li et al., 2020). For instance, in their comprehensive review, Cogolludo et al searched for human studies that evaluated the association of plasma levels of ceramides with adverse cardiovascular events and found 8 studies within their search scope. In 6 out of 8 reviewed studies, C16:0, C18:0, and C24:1 ceramides were found to be significantly linked to an increased risk of adverse cardiovascular outcomes and therefore considered to be the strongest predictive markers, among ceramides, for CVD (Cogolludo et al., 2019).

Cardiac: Dilation and Contractility

In animal models, it has been suggested that alteration of ceramide signaling may contribute to the pathophysiology of diabetic cardiomyopathy (Colligan et al., 2002). In another *in vitro* study, ceramide (C2:0) has been shown to reduce high glucose-induced myocyte dysfunction, increase calcium influx, and improve smooth muscle contraction (Relling et al., 2003). On the other hand, ceramide analog dihydroceramide (C2:0) was reported to potentiate cardiac depressive effects of leptin, leading to cardiac dysfunction (Ren and Relling, 2006). Likewise, Javaheri et al have noted that elevated concentrations of circulating C16:0 and C18:0 ceramides were very much associated with the incidence of heart failure and that was attributed to CerS regardless of food intake (Javaheri et al., 2020). Prior to that, Bielawska et al. reported that a synthetic analogue of C16:0 ceramide induced apoptosis in cardiomyocytes of an ischemia-reperfusion rodent model (Bielawska et al., 1997). Furthermore, in animal models of obesity, ceramides were considered cardiotoxic molecules as they have contributed to the development of dilated cardiomyopathy as well as inhibition of cardiac contractility (Simon et al., 2014), which is consistent with previous observations of ceramide accumulation in CVD (Alewijnse et al., 2004). In humans, it was found that levels of long-chain ceramides and their metabolites, lactosylceramides, rise extensively in the plasma of children with chronic kidney disease, and this was associated with abnormal cardiac structure and function, suggesting an extensive role of cardiac lipotoxicity in the pathogenesis of cardiac dysfunction in the presence of kidney disease (Mitsnefes et al., 2014). Several mechanisms have been proposed for ceramides-induced cardiovascular toxicity, yet the full mechanism of action is incompletely understood. One of the suggested mechanisms is via accumulation of ceramides in myocardial cells and lead to cellular apoptosis (Parra et al., 2013). Ceramides accumulation may be attributed to an increase in nSMase without a corresponding increase in ceramidase activity (Reidy et al., 2020), or due to increased fat intake that stimulate ceramide biosynthesis (de la Maza et al., 2015). Additional evidence for the detrimental CVD outcomes associated with increased levels of circulating ceramides was provided by blocking the *de novo* pathway of ceramide synthesis in mice treated with Myriocin which showed enhanced cardiac dilation and improved cardiac contractility (Park et al., 2008).

Vascular: Atherosclerosis and Inflammation

One of the speculated mechanisms for ceramides induced cardiovascular manifestations is that sphingomyelin, a precursor of ceramides (**Figure 2**), could aggregate at higher concentrations with low-density lipoproteins in atherosclerotic lesions where sphingomyelinase can also be found, suggesting a role for SMase along with ceramides in the development of atherosclerosis and coronary artery disease (Iqbal et al., 2017; Seah et al., 2020). In their observational study, De Mello et al. have found a positive rapport between plasma ceramides (C23:0 and C24:1) and inflammatory marker IL-6 (De Mello et al., 2009). Also, ceramides were reported to have stimulatory effects on TNF-α and NF-κB pathways which may work sequentially, initiating an inflammation cascade (Osorio et al., 2016; Al-Rashed et al., 2021). Eventually, those inflammatory mediators will increase the risk of developing atherosclerosis, contributing to vascular diseases (Okazaki et al., 2014; Zhang et al., 2014; Pan, 2017).

Vascular: Oxidative Stress and Endothelial Dysfunction

Both animal and human studies have demonstrated a positive correlation between plasma ceramide endothelium-dependent vasoconstriction being most likely the reason behind it (McGurk et al., 2021). Although it is still controversial whether ceramides produce vasodilation or vasoconstriction

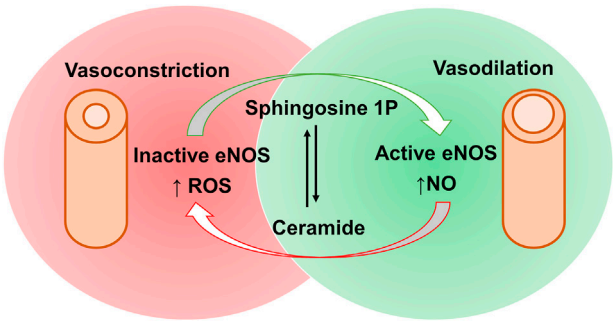

FIGURE 3 | Contradictory effects of sphingosine-1 phosphate and ceramides via activation and inactivation of eNOS and the subsequent impacts on blood vessels. Sphingosine-1 phosphate causes eNOS activation, increasing nitric acid (NO) production and subsequent vasodilation. This can be opposed by ceramides mediated eNOS inactivation, increasing reactive oxygen species (ROS) production leading to vasoconstrictive effects. [eNOS, endothelial nitric oxide synthase; S1P, sphingosine-1 phosphate].

effects, there is a postulated mechanism for C16:0 ceramide mediated vasoconstriction through protein kinase C activation. This, in turn, increases calcium entry into vascular smooth muscles, thereby resulting in vascular contraction (Zheng et al., 2000). On the other hand, it is worthy to mention the contradictory vasodilation effects of sphingosine-1 phosphate (S1P) at low concentrations on rat aorta and mesenteric artery, which are mediated through $S1P_1$ or $S1P_3$ activation of endothelial nitric synthase (eNOS) and consequent release of endothelium-derived nitric oxide (NO) (Kennedy et al., 2009). Thus, the vascular tone is maintained by a balance between ceramide and S1P (**Figure 3**) (Van Brocklyn and Williams, 2012), which may open new routes of research for the treatment of hypertension.

Another postulated pathological mechanism for ceramides on the cardiovascular system has involved an oxidative stress pathway through the generation of reactive oxygen species (ROS). In agreement with that context, an *in-vitro* study conducted by Akawi et al. has demonstrated that elevated levels of C16:0 ceramide not only triggers uncoupling of eNOS, but also generates ROS such as superoxide radical ($O_2^{\cdot-}$) (Akawi et al., 2021). Consequently, a reduction of NO availability in blood vessels occurs, which can be partially explained by an increase in the activity of protein phosphatase 2A (PP2A) in vascular endothelial cells, and this may result in vasoconstrictive effects, atherogenesis, and/or oxidative stress as depicted in **Figure 4**.

Additionally, there has been a growing amount of evidence over the last decades that points towards a mutual synergistic relationship between ROS production and ceramide accumulation, sometimes referred to as "Feedforward Amplifying Mechanism" (Cogolludo et al., 2019). ROS involving superoxide radical, a precursor of many other free radicals, exhibit a wide range of deleterious effects on mammalian cells as they can be generated in various types of cells, including endothelial cells, aorta, and macrophages (Bhunia et al., 1997; Zhang et al., 2008). The effects of ceramides on ROS production are not limited to the activation of ROS-generating enzymes, such as NADPH oxidase and NOS; ceramides also interact with the respiratory electron transport chain and thereby increase the production of ROS as by-products (Li et al., 2010). Most notably, NADPH oxidase activity is responsible for the generation of highly reactive $O_2^{\cdot-}$ which is unstable. Thus, it is rapidly reduced by superoxide dismutase into H_2O_2 that can be further reduced into another highly toxic hydroxyl radical (Das and Roychoudhury, 2014). In addition, many studies have confirmed that ceramides have the ability to induce endothelial dysfunction in small coronary arteries based on the activation of NADPH oxidase, and the consequent increase of ROS production as well as diminishing NO availability (Zhang et al., 2003; Zhang et al., 2007; Li and Zhang, 2013), As a result, this may contribute to a malfunction of coronary circulation and lead to CVDs (**Figure 4**). Moreover, several studies have addressed ceramides' negative impacts on cardiac function in terms of altering signal transduction, modulation of intracellular ion channels and stimulation of apoptosis (Alewijnse et al., 2004) (**Table 2**).

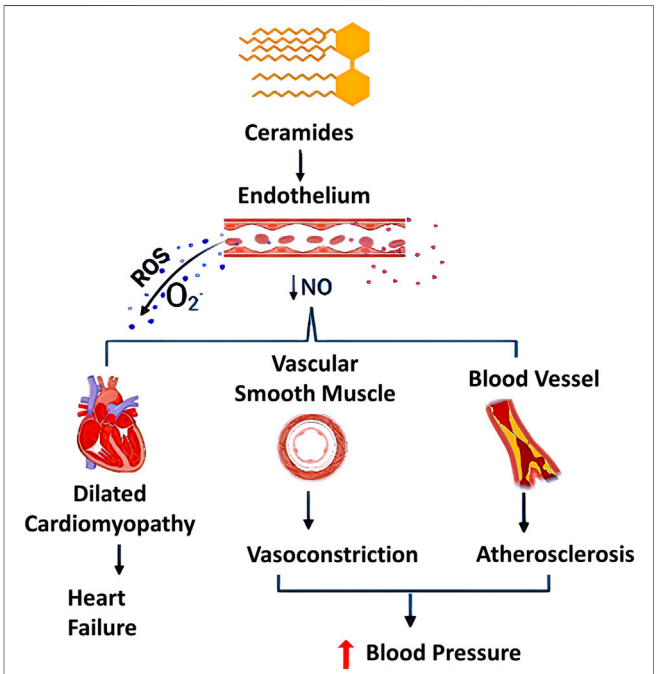

FIGURE 4 | Different pathological effects of ceramides (C16:0, C18:0, and C24:1). Effects of ceramides include generation of reactive oxygen species (ROS) and decrease in nitric oxide (NO) production, adversely affecting the human body. Ceramides showed dual effect on vascular system through uncoupling endothelial nitric oxide synthase, decreasing NO availability and sustainable stimulation of ROS production especially superoxide free radicals ($O_2^{\cdot-}$). This may contribute to multiple dysfunctions in the cardiovascular system including oxidative stress, atherosclerosis and it can be promoted to a dilated cardiomyopathy [NO, nitric oxide synthase; ROS, reactive oxygen species]. This figure was created using Biorender.com.

TABLE 2 | Summary of ceramides impacts on cardiovascular outcomes in humans.

Observed markers	Associated cardiovascular outcomes	Number of participants	References
Ceramide ratios C16:0/C24:0 C24:1/C22:0	Major adverse cardiovascular incidents that involve acute coronary syndrome, heart failure, stroke, and CV death	N = 920 HTN patients	Yin et al. (2021)
C16:0, C18:0, C24:1 and Ceramide ratios: C16:0/C24:0, C18:0/C24:0, C24:1/C24:0	Cardiovascular mortality	N = 1704 CAD patients	Li et al. (2020)
C16:0, C18:0, C24:1	Cardiovascular mortality	N = 400	Targher et al. (2020)
C16:0, C18:0, C18:1	Heart failure	N = 433	Javaheri et al. (2020)
C16:0	Heart failure	N = 4,249	Lemaitre et al. (2019)
C16:0, C18:0 C20:0, C22:0, C24:0	Hyperinsulinemia and insulin resistance	N = 2086	Lemaitre et al. (2018)
C18:0	Hyperinsulinemia and insulin resistance	N = 962	Wigger et al. (2017)
C16:0, C18:0, C24:1 and Ceramide ratios: C16:0/C24:0, C18:0/C24:0, C24:1/C24:0	Myocardial infarction, stroke, revascularization, and death	N = 495	Meeusen et al. (2018)

CAD, coronary artery disease; HTN, hypertension.

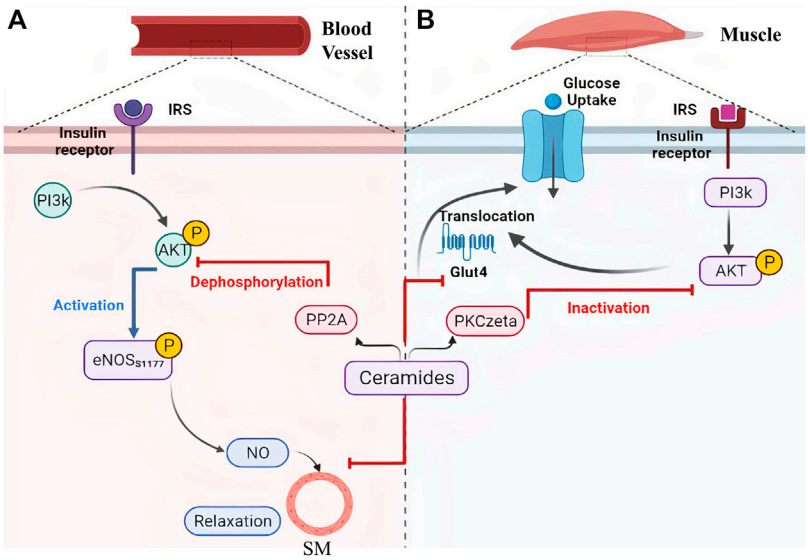

FIGURE 5 | Ceramides contribute to metabolic disorders via inhibition of PI3k/Akt as a common pathway between vasoconstriction and insulin resistance. Ceramides can facilitate the inactivation of protein kinase B (AKT) through **(A)** its dephosphorylation by protein phosphatase 2A or **(B)** binding to the inhibitor PKCzeta protein which leads to narrowing of blood vessels and inhibition of glucose transporter 4 translocation (glucose intolerance), respectively. [eNOS, Endothelial Nitric Oxide Synthase; Glut 4, Glucose Transporter 4; IRS, Insulin Receptor Substrate; NO, Nitric Oxide; PI3k, Phosphoinositide-3-kinase; PKCzeta, Protein kinase C zeta; PP2A, Protein Phosphatase 2A; SM, Smooth Muscles]. This illustration was created with Biorender.com.

Metabolic: Insulin Resistance and Obesity

High saturated fat diet promote obesity, and this has been coupled with an increased risk of developing cardiomyopathy in mice models. The underlying mechanism for that was attributed to increased ceramides levels that mediated disruption of caveolae, specialized membrane invaginations important for cellular signaling, in mice heart cells (Knowles et al., 2013). It has also been shown that ceramides restrain glucose uptake by mammalian cells as a part of their role in enhancing the entry of fatty acids in adipose and non-adipose tissues (Summers, 2020). This, indeed, causes impaired glucose utilization and contributes to insulin resistance, which could be explained by two molecular mechanisms as exhibited in **Figure 5**. Firstly, ceramides restrict glucose transporter (GLUT-4) translocation and prevent its binding to the cell membrane. Secondly, they inactivate protein kinase B, also known as PKB/Akt, by facilitating its binding to an inhibitory protein called PKCzeta. Similarly, ceramides are also involved in the

TABLE 3 | Medications that target ceramides biosynthesis pathways.

Target	Drug class	Example	References
Ceramide's precursors	GLP-1 agonists	Liraglutide	Meikle et al. (2015); Somm et al. (2021)
	Cholesterol lowering agents	Statins	
De Novo Pathway	SPT inhibitors	Myriocin	Park et al. (2008); Berdyshev et al. (2009); Riley and Merrill (2019)
	CerS inhibitors	Fumonisin B1, Fingolimod	
Sphingomyelin hydrolysis	Functional inhibitor of acid sphingomyelinase (FIASMAs)	Antidepressant drugs GW4869	Kornhuber et al. (2014)
Salvage Pathway	CerS inhibitors	Fumonisin B1, Fingolimod	Berdyshev et al. (2009); Tada et al. (2010); Riley and Merrill (2019)
	Ceramidase stimulators	Vanadate	

CerS, ceramide synthase; SPT, serine palmitoyltransferase.

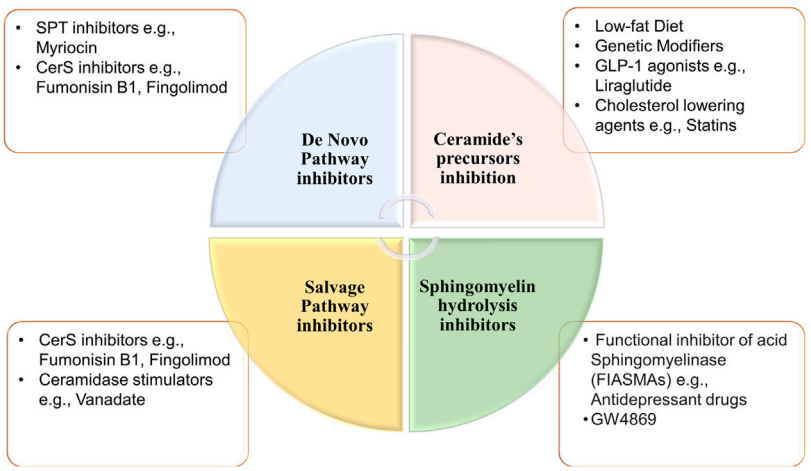

FIGURE 6 | Potential inhibitors of ceramides synthesis pathways. Ceramides can be synthesized through three different pathways. First, *de novo* synthesis pathway which can be repressed by inhibiting ceramide synthases or SPT. Second sphingomyelin hydrolysis pathway that can be inhibited via functional inhibitor of acid or neutral sphingomyelinase or Ceramides can be synthesized through three different pathways. First, De novo synthesis pathway which can be repressed by inhibiting ceramide synthases or Serine palmitoyl-transferase. Second, sphingomyelin hydrolysis pathway that can be inhibited via functional inhibitor of acid or neutral sphingomyelinase. Lastly, inhibition of salvage pathway through depletion of ceramide precursors (ceramide synthases inhibition), or via increasing ceramide metabolism by ceramidases. [CerS, ceramide synthases; SPT, serine palmitoyl-transferase].

activation of PP2A, which leads to dephosphorylation of PKB/Akt (**Figure 5A**), and consequently suppression of its action needed for insulin signaling pathway and GLUT-4 translocation (**Figure 5B**) (Larsen and Tennagels, 2014). As it is known, insulin resistance is an important mechanism that is promoted by obesity and contribute not only to the development of type II diabetes but also to the increased risk of CVD related complications impacting other CVD underlying pathological mechanisms including endothelium dysfunction, constriction of blood vessels, atherosclerosis, and inflammation. To elaborate, insulin resistance alters PI3k/Akt pathway that can inhibit Akt kinase and develop an inactivated form of eNOS, in response to dephosphorylation of its serine 1177. As a result, less NO would be released from vascular endothelium, contracting vascular smooth muscles and negating insulin-mediated vasodilation effects (Huang, 2009), as shown in **Figure 5A**. On the contrary, defects in vascular endothelium and low NO liberation induce vasoconstrictive effects which may lead to glucose intolerance and further insulin resistance due to insufficient insulin delivery to peripheral tissues (Janus et al., 2016).

CERAMIDES TARGETED THERAPIES

Modulation of ceramides levels and limiting their accumulation have attracted much attention recently from researchers worldwide, aiming to tackle their pathological implications and identify new therapeutic targets, especially for cardiac impairment (Mikłosz et al., 2015; Klevstig et al., 2016). Despite lacking evidence of direct cause-effect rapport between CVDs and ceramides, traditional therapies such as lipid-lowering medicines and lifestyle modifications such as low-fat diet may be employed to minimize overall risk while ceramide-specific drugs are being developed (Hilvo et al., 2020). It was shown that the HMG-CoA reductase inhibitors, or statins reduce sphingolipids

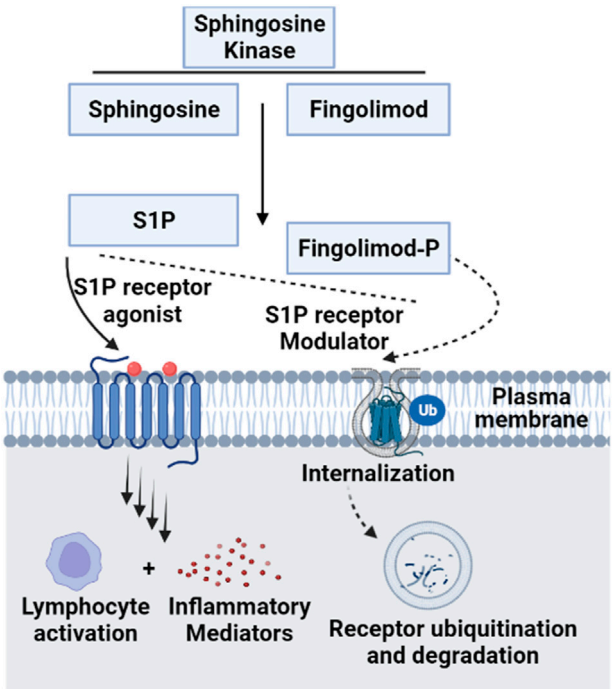

FIGURE 7 | Molecular mechanism of Fingolimod as a functional antagonist for S1P receptors. Since Fingolimod structurally resembles S1P, the former can compete with Sphingosine for Sphingosine kinase and get activated by phosphorylation into Fingolimod phosphate. This active form modulates S1P receptors via internalization and ubiquitination, acting as a functional antagonist for S1P ligand on its receptors. This contributes to the regulatory functions of Fingolimod as an inhibitory of inflammatory cytokines production, which is upregulated by the disruption of S1P signaling (Van Doorn et al., 2010) [S1P, sphingosine 1 phosphate; Ub, ubiquitination]. This figure was generated using Biorender.com.

concentrations such as pitavastatin treatment that lowered significantly the levels of most sphingolipids in treated cardiac patients including ceramides independently of reduction in plasma cholesterol (Meikle et al., 2015). The same effect was observed for non-statin drugs such as proprotein convertase subtilisin/kexin type 9 (PCSK9) inhibitors (Ye et al., 2020). On the other hand, activation of glucagon-like peptide 1 (GLP-1) receptor, a non-cholesterol-lowering drug, has shown cardioprotective effects against ceramides accumulation in experimental models (Monji et al., 2013). Moreover, the protective mechanism of GLP-1 receptor analogues involved suppression of the JNK signaling pathway and reduction of apoptosis induced by lipotoxicity (Leonardini et al., 2017). A prime example of GLP-1 receptor agonist is Liraglutide which is showing a promising therapeutic role in cardiovascular diseases; however, its exact mechanism is not fully understood (Marso et al., 2016). Besides its major role in controlling blood glucose level via enhancing insulin secretion (Mehta et al., 2017), a recent randomized controlled trial has proved that liraglutide can reduce body mass index, which could be partially explained by its role in reducing appetite and gastric emptying (Kelly et al., 2020). Notably, Somm et al. have inferred that liraglutide can inhibit the accumulation of C16:0 ceramide and C24:0 ceramide in methionine-choline deficient dietary mice liver and prevent subsequent inflammation and fibrosis (Somm et al., 2021). In line with these studies, liraglutide may have a potential role in reversing pathological outcomes of cardiac dysfunctions through inhibition of ceramide levels (Akawi et al., 2021). Intriguingly, various classes of drugs (listed in **Table 3**) were found to have multiple therapeutic effects against different diseases via targeting ceramides biosynthesis pathway as depicted in **Figure 6**. For example, Myriocin, SPT inhibitor, was reported to reduce atherosclerotic lesions, fatty liver progression and fibrosis induced by high ceramides levels in mice (Kasumov et al., 2015). Moreover, it could restore normal endothelium-dependent vasodilation function of blood vessels and decrease fat accumulation in diabetic rats via improving PI3K/PKB/eNOS phosphorylation and NO release which are significantly affected by any increase in ceramide levels (Chun et al., 2011). Similarly, a synthetic derivative of Myriocin called Fingolimod (FTY720) was found to inhibit ceramide biosynthesis via interfering with CerS in endothelial cells isolated from human pulmonary artery (Berdyshev et al., 2009). However, the main mechanism of FTY720 is via modulating four of the five types of S1P receptors ($S1P_1$ and $S1P_{3-5}$) (Chiba, 2020). It has become known that increased levels of S1P can evoke inflammatory outcomes through regulating lymphocyte trafficking and other inflammatory cytokines production such as, TNF-α and IL-6 (see Nagahashi et al., 2018 and references therein). Thus, S1P receptors, particularly S1P1 downregulation that occurs as a consequence of FTY720 phosphorylation may counteract the production of proinflammatory cytokines induced by the increased levels of S1P (Seki et al., 2013) (**Figure 7**). Due to its promising therapeutic value, researchers investigated some derivatives of Fingolimod (ST1058, ST1060 ST1072, ST1074), seeking new treatment approaches through selective ceramide reduction mechanisms. Remarkably, they found that both ST 1058 and ST 1074 could suppress CerS2, also can be inhibited by ST1060, and CerS4, whereas ST1072 selectively inhibits CerS4 and CerS6 (Schiffmann et al., 2012). Later on, Fingolimod has proved its efficacy in reversing insulin resistance via reduction of ceramide levels and enhancement of Akt phosphorylation in mice (Bruce et al., 2013). On the contrary, Fumonisin B1, a mycotoxin, retains its toxicity through inhibition of both *de novo* and salvage pathways as it can block the six isoforms of CerS (Riley and Merrill, 2019). As summarized in **Table 1**, several studies have investigated the role of CerS enzymes (Grösch et al., 2012) and their inhibitors as a distinct therapeutic target in the management of cardiometabolic diseases as well as other common diseases (see Choi et al., 2021 and references therein). It is noteworthy that genetic ablation of genes that encode sphingolipid biosynthesis enzymes (SPT, sphingomyelinase, ceramidases) may alleviate ceramide-associated metabolic disease (Bikman and Summers, 2011b). Ceramide levels can additionally be reduced through inhibition in the sphingomyelin hydrolysis pathway. GW4869 is commonly used as a selective repressor of nSMase, whereas functional inhibitors of aSMase such as antidepressants possess higher clinical tolerability and therefore have wider clinical applications (Kornhuber et al., 2014). Moreover,

TABLE 4 | Various models for ceramide metabolism.

Transgenic model	Effects	Mechanism	Ceramide's targets	References
Mice that overexpress long-chain acyl-CoA synthetase in the heart	Initial cardiac hypertrophy and cardiac dysfunction	Lipid accumulation associated with an increase in ceramide synthesis in cardiac tissues	—	Chiu et al. (2001)
Cardiac overexpression of glycosylphosphatidylinositol -anchored human lipoprotein lipase	Dilated cardiomyopathy	Increase the *de novo* biosynthesis of ceramides and accumulation of ceramide in heart tissues	SPT inhibitors, e.g., Myriocin	Park et al. (2008)
APPL1 overexpression in transgenic mice	Showed protection against cardiac dysfunction induced by high-fat-diet Increased insulin sensitivity	Regulation of adiponectin and insulin signaling Also decreased ceramide in favor of sphingomyelin biosynthesis in cardiac tissues	—	Park et al. (2013)
Mutated (V717I) amyloid β precursor protein (AβPP) transgene in mouse hippocampus	Upregulation of ceramide synthesis in brain tissues that promote Alzheimer disease	Upregulation of ceramide synthases (increase ceramide turnover in the salvage pathway) and downregulation of sphingomyelin synthases	FTY720 counteracts reduction of sphingomyelin synthases and decrease of mRNA expression of ceramide synthases	Jęśko et al. (2020)
Transgenic mice with overexpression acid sphingomyelinase in hippocampus	Upregulation of ceramide production in the hippocampus enhanced depression-like behavior	Reduction in Akt phosphorylation at Ser473, which known to regulate neurogenesis	Functional inhibitor of acid sphingomyelinase (FIASMAs) e.g., Antidepressant drugs GW4869	Park et al. (2008); Kornhuber et al. (2014)

FTY720, fingolimod; SPT, serine palmitoyltransferase.

Vanadate may increase ceramide phosphorylation and metabolism via increasing ceramide kinase and ceramidase activities, respectively which will decrease ceramide concentrations in correspondence to those effects (Tada et al., 2010), **Table 4** summarizes the various transgenic models for ceramide metabolism.

CONCLUSION AND FUTURE PERSPECTIVES

Ceramides are endogenous lipids with various structural and biological functions that are essential to regulate myriad of cellular activities. However, high plasma levels of specific ceramides has been linked with several conditions, including CVDs, type II diabetes, obesity, hypercholesteremia, insulin resistance, and hypertension. . The pathogenesis of ceramides in cardiometabolic diseases may be partially explicated through mutual pathological mechanisms based on their inflammatory, and oxidative stress effects in addition to being the main players in the dysregulation of the PI3k/Akt pathway. Hence, targeted inhibition of ceramides biosynthesis may broaden the scope of non-invasive therapies for these diseases. This, indeed, needs further studies to fully understand the role of ceramides and their pathological mechanism of actions. Additionally, more research is needed to screen the derivatives of available drugs that can modulate ceramide pathways, hoping to discover more selective and efficient treatments.

AUTHOR CONTRIBUTIONS

All authors listed have made a substantial, direct, and intellectual contribution to the work and approved it for publication.

FUNDING

This project is funded by the United Arab Emirates University (grant number 12M012).

REFERENCES

Abbott, S. K., Li, H., Muñoz, S. S., Knoch, B., Batterham, M., Murphy, K. E., et al. (2014). Altered Ceramide Acyl Chain Length and Ceramide Synthase Gene Expression in Parkinson's Disease. *Mov Disord.* 29 (4), 518–526. doi:10.1002/mds.25729

Akawi, N., Checa, A., Antonopoulos, A. S., Akoumianakis, I., Daskalaki, E., Kotanidis, C. P., et al. (2021). Fat-secreted Ceramides Regulate Vascular Redox State and Influence Outcomes in Patients with Cardiovascular Disease. *J. Am. Coll. Cardiol.* 77 (20), 2494–2513. doi:10.1016/j.jacc.2021.03.314

Al-Rashed, F., Ahmad, Z., Snider, A. J., Thomas, R., Kochumon, S., Melhem, M., et al. (2021). Ceramide Kinase Regulates TNF-α-Induced Immune Responses in Human Monocytic Cells. *Scientific Rep.* 11 (1), 1–14. doi:10.1038/s41598-021-87795-7

Alewijnse, A. E., Peters, S. L. M., and Michel, M. C. (2004). Cardiovascular Effects of Sphingosine-1-Phosphate and Other Sphingomyelin Metabolites. *Br. J. Pharmacol.* 143 (6), 666–684. doi:10.1038/sj.bjp.0705934

Alonso, A., and Goñi, F. M. (2018). The Physical Properties of Ceramides in Membranes. *Annu. Rev. Biophys.* 47, 633–654. doi:10.1146/annurev-biophys-070317-033309

Berdyshev, E. V., Gorshkova, I., Skobeleva, A., Bittman, R., Lu, X., Dudek, S. M., et al. (2009). FTY720 Inhibits Ceramide Synthases and Up-Regulates Dihydrosphingosine 1-phosphate Formation in Human Lung Endothelial Cells. *J. Biol. Chem.* 284 (9), 5467–5477. doi:10.1074/jbc.m805186200

Bhunia, A. K., Han, H., Snowden, A., and Chatterjee, S. (1997). Redox-regulated Signaling by Lactosylceramide in the Proliferation of Human Aortic Smooth Muscle Cells. *J. Biol. Chem.* 272 (25), 15642–15649. doi:10.1074/jbc.272.25.15642

Bielawska, A. E., Shapiro, J. P., Jiang, L., Melkonyan, H. S., Piot, C., Wolfe, C. L., et al. (1997). Ceramide Is Involved in Triggering of Cardiomyocyte Apoptosis Induced by Ischemia and Reperfusion. *Am. J. Pathol.* 151 (5), 1257–1263.

Bikman, B. T., and Summers, S. A. (2011a). Ceramides as Modulators of Cellular and Whole-Body Metabolism. *J. Clin. Invest.* 121 (11), 4222–4230. doi:10.1172/jci57144

Bikman, B. T., and Summers, S. A. (2011b). "Sphingolipids and Hepatic Steatosis," in *Sphingolipids and Metabolic Disease*. Editor L.A. Cowart (New York, NY: Springer New York), 87–97. doi:10.1007/978-1-4614-0650-1_6

Bruce, C. R., Risis, S., Babb, J. R., Yang, C., Lee-Young, R. S., Henstridge, D. C., et al. (2013). The Sphingosine-1-Phosphate Analog FTY720 Reduces Muscle Ceramide Content and Improves Glucose Tolerance in High Fat-Fed Male Mice. *Endocrinology* 154 (1), 65–76. doi:10.1210/en.2012-1847

Cao, R., Fang, Z., Li, S., Xu, M., Zhang, J., Han, D., et al. (2020). Circulating Ceramide: a New Cardiometabolic Biomarker in Patients with Comorbid Acute Coronary Syndrome and Type 2 Diabetes Mellitus. *Front. Physiol.* 11, 1104. doi:10.3389/fphys.2020.01104

Carrard, J., Gallart-Ayala, H., Weber, N., Colledge, F., Streese, L., Hanssen, H., et al. (2021). How Ceramides Orchestrate Cardiometabolic Health-An Ode to Physically Active Living. *Metabolites* 11 (10), 675. doi:10.3390/metabo11100675

Chaurasia, B., and Summers, S. A. (2020). Ceramides in Metabolism: Key Lipotoxic Players. *Annu. Rev. Physiol.* 83. doi:10.1146/annurev-physiol-031620-093815

Chiba, K. (2020). Discovery of Fingolimod Based on the Chemical Modification of a Natural Product from the Fungus, Isaria Sinclairii. *J. Antibiot.* 73 (10), 666–678. doi:10.1038/s41429-020-0351-0

Chiu, H.-C., Kovacs, A., Ford, D. A., Hsu, F.-F., Garcia, R., Herrero, P., et al. (2001). A Novel Mouse Model of Lipotoxic Cardiomyopathy. *J. Clin. Invest.* 107 (7), 813–822. doi:10.1172/jci10947

Choi, R. H., Tatum, S. M., Symons, J. D., Summers, S. A., and Holland, W. L. (2021). Ceramides and Other Sphingolipids as Drivers of Cardiovascular Disease. *Nat. Rev. Cardiol.*, 1–11. doi:10.1038/s41569-021-00536-1

Chun, L., Junlin, Z., Aimin, W., Niansheng, L., Benmei, C., Minxiang, L., et al. (2011). Inhibition of Ceramide Synthesis Reverses Endothelial Dysfunction and Atherosclerosis in Streptozotocin-Induced Diabetic Rats. *Diabetes Res. Clin. Pract.* 93 (1), 77–85. doi:10.1016/j.diabres.2011.03.017

Cogolludo, A., Villamor, E., Perez-Vizcaino, F., and Moreno, L. (2019). Ceramide and Regulation of Vascular Tone. *Ijms* 20 (2), 411. doi:10.3390/ijms20020411

Colligan, P. B., Relling, D. P., and Ren, J. (2002). Ceramide Attenuates High Glucose-Induced Cardiac Contractile Abnormalities in Cultured Adult Rat Ventricular Myocytes. *Cel Mol Biol (Noisy-le-grand)* 48 Online Pub, OL251–7.

Cowart, L. A. (2009). Sphingolipids: Players in the Pathology of Metabolic Disease. *Trends Endocrinol. Metab.* 20 (1), 34–42. doi:10.1016/j.tem.2008.09.004

Das, K., and Roychoudhury, A. (2014). Reactive Oxygen Species (ROS) and Response of Antioxidants as ROS-Scavengers during Environmental Stress in Plants. *Front. Environ. Sci.* 2, 53. doi:10.3389/fenvs.2014.00053

de la Maza, M. P., Rodriguez, J., Hirsch, S., Leiva, L., Barrera, G., Bunout, D., et al. (2015). Skeletal Muscle Ceramide Species in Men with Abdominal Obesity. *J. Nutr. Health Aging* 19 (4), 389–396. doi:10.1007/s12603-014-0548-7

De Mello, V. D. F., Lankinen, M., Schwab, U., Kolehmainen, M., Lehto, S., Seppänen-Laakso, T., et al. (2009). Link between Plasma Ceramides, Inflammation and Insulin Resistance: Association with Serum IL-6 Concentration in Patients with Coronary Heart Disease. *Diabetologia* 52 (12), 2612–2615. doi:10.1007/s00125-009-1482-9

Deng, Y., Zhang, X., Shen, H., He, Q., Wu, Z., Liao, W., et al. (2020). Application of the Nano-Drug Delivery System in Treatment of Cardiovascular Diseases. *Front. Bioeng. Biotechnol.* 7, 489. doi:10.3389/fbioe.2019.00489

Fabbri, E., Yang, A., Simonsick, E. M., Chia, C. W., Zoli, M., Haughey, N. J., et al. (2016). Circulating Ceramides Are Inversely Associated with Cardiorespiratory Fitness in Participants Aged 54-96 Years from the Baltimore Longitudinal Study of Aging. *Aging Cell* 15 (5), 825–831. doi:10.1111/acel.12491

Fucho, R., Casals, N., Serra, D., and Herrero, L. (2017). Ceramides and Mitochondrial Fatty Acid Oxidation in Obesity. *FASEB j.* 31 (4), 1263–1272. doi:10.1096/fj.201601156r

Gaggini, M., Pingitore, A., and Vassalle, C. (2021). Plasma Ceramides Pathophysiology, Measurements, Challenges, and Opportunities. *Metabolites* 11 (11), 719. doi:10.3390/metabo11110719

Go, A. S., Mozaffarian, D., Roger, V. L., Benjamin, E. J., Berry, J. D., Blaha, M. J., et al. (2014). Executive Summary: Heart Disease and Stroke Statistics--2014 Update: a Report from the American Heart Association. *circulation* 129 (3), 399–410. doi:10.1161/01.cir.0000442015.53336.12

Goradel, N. H., Hour, F. G., Negahdari, B., Malekshahi, Z. V., Hashemzehi, M., Masoudifar, A., et al. (2018). Stem Cell Therapy: a New Therapeutic Option for Cardiovascular Diseases. *J. Cel. Biochem.* 119 (1), 95–104. doi:10.1002/jcb.26169

Grösch, S., Schiffmann, S., and Geisslinger, G. (2012). Chain Length-specific Properties of Ceramides. *Prog. lipid Res.* 51 (1), 50–62.

Hilvo, M., Vasile, V. C., Donato, L. J., Hurme, R., and Laaksonen, R. (2020). Ceramides and Ceramide Scores: Clinical Applications for Cardiometabolic Risk Stratification. *Front. Endocrinol. (Lausanne)* 11, 570628. doi:10.3389/fendo.2020.570628

Huang, P. L. (2009). eNOS, Metabolic Syndrome and Cardiovascular Disease. *Trends Endocrinol. Metab.* 20 (6), 295–302. doi:10.1016/j.tem.2009.03.005

Iqbal, J., Walsh, M. T., Hammad, S. M., and Hussain, M. M. (2017). Sphingolipids and Lipoproteins in Health and Metabolic Disorders. *Trends Endocrinol. Metab.* 28 (7), 506–518. doi:10.1016/j.tem.2017.03.005

Janus, A., Szahidewicz-Krupska, E., Mazur, G., and Doroszko, A. J. M. o. i. (20162016). Insulin Resistance and Endothelial Dysfunction Constitute a Common Therapeutic Target in Cardiometabolic Disorders. *Mediators Inflamm.* doi:10.1155/2016/3634948

Javaheri, A., Allegood, J. C., Cowart, L. A., and Chirinos, J. A. (2020). Circulating Ceramide 16:0 in Heart Failure with Preserved Ejection Fraction. *J. Am. Coll. Cardiol.* 75 (17), 2273–2275. doi:10.1016/j.jacc.2020.02.062

Jęśko, H., Wencel, P. L., Wójtowicz, S., Strosznajder, J., Lukiw, W. J., and Strosznajder, R. P. (2020). Fingolimod Affects Transcription of Genes Encoding Enzymes of Ceramide Metabolism in Animal Model of Alzheimer's Disease. *Mol. Neurobiol.* 57 (6), 2799–2811. doi:10.1007/s12035-020-01908-3

Kasumov, T., Li, L., Li, M., Gulshan, K., Kirwan, J. P., Liu, X., et al. (2015). Ceramide as a Mediator of Non-alcoholic Fatty Liver Disease and Associated Atherosclerosis. *PloS one* 10 (5), e0126910. doi:10.1371/journal.pone.0126910

Kelly, A. S., Auerbach, P., Barrientos-Perez, M., Gies, I., Hale, P. M., Marcus, C., et al. (2020). A Randomized, Controlled Trial of Liraglutide for Adolescents with Obesity. *N. Engl. J. Med.* 382 (22), 2117–2128. doi:10.1056/nejmoa1916038

Kennedy, S., Kane, K. A., Pyne, N. J., and Pyne, S. (2009). Targeting Sphingosine-1-Phosphate Signalling for Cardioprotection. *Curr. Opin. Pharmacol.* 9 (2), 194–201. doi:10.1016/j.coph.2008.11.002

Klevstig, M., Ståhlman, M., Lundqvist, A., Scharin Täng, M., Fogelstrand, P., Adiels, M., et al. (2016). Targeting Acid Sphingomyelinase Reduces Cardiac Ceramide Accumulation in the post-ischemic Heart. *J. Mol. Cell Cardiol.* 93, 69–72. doi:10.1016/j.yjmcc.2016.02.019

Knowles, C. J., Cebova, M., and Pinz, I. M. (2013). Palmitate Diet-Induced Loss of Cardiac Caveolin-3: a Novel Mechanism for Lipid-Induced Contractile Dysfunction. *PLoS One* 8 (4), e61369. doi:10.1371/journal.pone.0061369

Kornhuber, J., Müller, C. P., Becker, K. A., Reichel, M., and Gulbins, E. (2014). The Ceramide System as a Novel Antidepressant Target. *Trends Pharmacological Sciences* 35 (6), 293–304. doi:10.1016/j.tips.2014.04.003

Kurz, J., Parnham, M. J., Geisslinger, G., and Schiffmann, S. (2019). Ceramides as Novel Disease Biomarkers. *Trends Molecular Medicine* 25 (1), 20–32. doi:10.1016/j.molmed.2018.10.009

Larsen, P. J., and Tennagels, N. (2014). On Ceramides, Other Sphingolipids and Impaired Glucose Homeostasis. *Mol. Metab.* 3 (3), 252–260. doi:10.1016/j.molmet.2014.01.011

Laviad, E. L., Albee, L., Pankova-Kholmyansky, I., Epstein, S., Park, H., Merrill, A. H., et al. (2008). Characterization of Ceramide Synthase 2. *J. Biol. Chem.* 283 (9), 5677–5684. doi:10.1074/jbc.m707386200

Lemaitre, R. N., Jensen, P. N., Hoofnagle, A., McKnight, B., Fretts, A. M., King, I. B., et al. (2019). Plasma Ceramides and Sphingomyelins in Relation to Heart

Failure Risk. *Circ. Heart Fail.* 12 (7), e005708. doi:10.1161/CIRCHEARTFAILURE.118.005708

Lemaitre, R. N., Yu, C., Hoofnagle, A., Hari, N., Jensen, P. N., Fretts, A. M., et al. (2018). Circulating Sphingolipids, Insulin, HOMA-IR, and HOMA-B: the strong Heart Family Study. *Diabetes* 67 (8), 1663–1672. doi:10.2337/db17-1449

Leonardini, A., D'Oria, R., Incalza, M. A., Caccioppoli, C., Andrulli Buccheri, V., Cignarelli, A., et al. (2017). GLP-1 Receptor Activation Inhibits Palmitate-Induced Apoptosis via Ceramide in Human Cardiac Progenitor Cells. *J. Clin. Endocrinol.* 102 (11), 4136–4147. doi:10.1210/jc.2017-00970

Levy, M., and Futerman, A. H. (2010). Mammalian Ceramide Synthases. *IUBMB life* 62 (5), 347–356. doi:10.1002/iub.319

Li, P.-L., and Zhang, Y. (2013). Cross Talk between Ceramide and Redox Signaling: Implications for Endothelial Dysfunction and Renal Disease. *Sphingolipids Dis.*, 171–197. doi:10.1007/978-3-7091-1511-4_9

Li, Q., Wang, X., Pang, J., Zhang, Y., Zhang, H., Xu, Z., et al. (2020). Associations between Plasma Ceramides and Mortality in Patients with Coronary Artery Disease. *Atherosclerosis* 314, 77–83. doi:10.1016/j.atherosclerosis.2020.09.004

Li, X., Becker, K. A., and Zhang, Y. (2010). Ceramide in Redox Signaling and Cardiovascular Diseases. *Cell Physiol Biochem* 26 (1), 41–48. doi:10.1159/000315104

Marso, S. P., Daniels, G. H., Brown-Frandsen, K., Kristensen, P., Mann, J. F. E., Nauck, M. A., et al. (2016). Liraglutide and Cardiovascular Outcomes in Type 2 Diabetes. *N. Engl. J. Med.* 375 (4), 311–322. doi:10.1056/nejmoa1603827

McGurk, K. A., Keavney, B. D., and Nicolaou, A. (2021). *Circulating Ceramides as Biomarkers of Cardiovascular Disease: Evidence from Phenotypic and Genomic Studies*. Amsterdam, The Netherlands: Atherosclerosis.

Meeusen, J. W., Donato, L. J., Bryant, S. C., Baudhuin, L. M., Berger, P. B., Jaffe, A. S., et al. (2018). Plasma Ceramides: A Novel Predictor of Major Adverse Cardiovascular Events After Coronary Angiography. *Arteriosclerosis, thrombosis, and vascular biology* 38 (8), 1933–1939. doi:10.1161/atvbaha.118.311199

Mehta, A., Marso, S. P., Neeland, I. J., and practice (2017). Liraglutide for Weight Management: a Critical Review of the Evidence. *Obes. Sci. Pract.* 3 (1), 3–14. doi:10.1002/osp4.84

Meikle, P. J., Wong, G., Tan, R., Giral, P., Robillard, P., Orsoni, A., et al. (2015). Statin Action Favors Normalization of the Plasma Lipidome in the Atherogenic Mixed Dyslipidemia of MetS: Potential Relevance to Statin-Associated Dysglycemia. *J. lipid Res.* 56 (12), 2381–2392. doi:10.1194/jlr.p061143

Mikłosz, A., Łukaszuk, B., Chabowski, A., Rogowski, F., Kurek, K., Żendzian-Piotrowska, M., et al. (2015). Hyperthyroidism Evokes Myocardial Ceramide Accumulation. *Cel Physiol Biochem* 35 (2), 755–766. doi:10.1159/000369735

Miranda, J. J., Barrientos-Gutiérrez, T., Corvalan, C., Hyder, A. A., Lazo-Porras, M., Oni, T., et al. (2019). Understanding the Rise of Cardiometabolic Diseases in Low- and Middle-Income Countries. *Nat. Med.* 25 (11), 1667–1679. doi:10.1038/s41591-019-0644-7

Mitsnefes, M., Scherer, P. E., Scherer, P. E., Friedman, L. A., Gordillo, R., Furth, S., et al. (2014). Ceramides and Cardiac Function in Children with Chronic Kidney Disease. *Pediatr. Nephrol.* 29 (3), 415–422. doi:10.1007/s00467-013-2642-1

Monji, A., Mitsui, T., Bando, Y. K., Aoyama, M., Shigeta, T., Murohara, T., et al. (2013). Glucagon-like Peptide-1 Receptor Activation Reverses Cardiac Remodeling via Normalizing Cardiac Steatosis and Oxidative Stress in Type 2 Diabetes. *Am. J. Physiology-Heart Circulatory Physiol.* 305 (3), H295–H304. doi:10.1152/ajpheart.00990.2012

Moore, D. J., and Rawlings, A. V. (2017). The Chemistry, Function and (Patho) physiology of Stratum Corneum Barrier Ceramides. *Int. J. Cosmet. Sci.* 39 (4), 366–372. doi:10.1111/ics.12399

Nagahashi, M., Abe, M., Sakimura, K., Takabe, K., and Wakai, T. (2018). The Role of Sphingosine-1-phosphate in Inflammation and Cancer Progression. *Cancer Sci.* 109 (12), 3671–3678. doi:10.1111/cas.13802

Okazaki, S., Sakaguchi, M., Miwa, K., Furukado, S., Yamagami, H., Yagita, Y., et al. (2014). Association of Interleukin-6 with the Progression of Carotid Atherosclerosis. *Stroke* 45 (10), 2924–2929. doi:10.1161/strokeaha.114.005991

Ormazabal, V., Nair, S., Elfeky, O., Aguayo, C., Salomon, C., and Zuñiga, F. A. (2018). Association between Insulin Resistance and the Development of Cardiovascular Disease. *Cardiovasc. Diabetol.* 17 (1), 122–214. doi:10.1186/s12933-018-0762-4

Osorio, F. G., Soria-Valles, C., Santiago-Fernández, O., Freije, J. M. P., and López-Otín, C. (2016). NF-κB Signaling as a Driver of Ageing. *Int. Rev. Cel. Mol. Biol.* 326, 133–174. doi:10.1016/bs.ircmb.2016.04.003

Pan, J. X. (2017). LncRNA H19 Promotes Atherosclerosis by Regulating MAPK and NF-kB Signaling Pathway. *Eur. Rev. Med. Pharmacol. Sci.* 21 (2), 322–328.

Park, J.-W., Park, W.-J., and Futerman, A. H. (2014). Ceramide Synthases as Potential Targets for Therapeutic Intervention in Human Diseases. *Biochim. Biophys. Acta (Bba) - Mol. Cel Biol. Lipids* 1841 (5), 671–681. doi:10.1016/j.bbalip.2013.08.019

Park, M., Wu, D., Park, T., Choi, C.-s., Li, R.-K., Cheng, K. K. Y., et al. (2013). APPL1 Transgenic Mice Are Protected from High-Fat Diet-Induced Cardiac Dysfunction. *Am. J. Physiology-Endocrinology Metab.* 305 (7), E795–E804. doi:10.1152/ajpendo.00257.2013

Park, T.-S., Hu, Y., Noh, H.-L., Drosatos, K., Okajima, K., Buchanan, J., et al. (2008). Ceramide Is a Cardiotoxin in Lipotoxic Cardiomyopathy. *J. lipid Res.* 49(10), 2101–2112. doi:10.1194/jlr.m800147-jlr200

Parra, V., Moraga, F., Kuzmicic, J., López-Crisosto, C., Troncoso, R., Torrealba, N., et al. (2013). Calcium and Mitochondrial Metabolism in Ceramide-Induced Cardiomyocyte Death. *Biochim. Biophys. Acta (Bba) - Mol. Basis Dis.* 1832 (8), 1334–1344. doi:10.1016/j.bbadis.2013.04.009

Peters, F., Vorhagen, S., Brodesser, S., Jakobshagen, K., Brüning, J. C., Niessen, C. M., et al. (2015). Ceramide Synthase 4 Regulates Stem Cell Homeostasis and Hair Follicle Cycling. *J. Invest. Dermatol.* 135 (6), 1501–1509. doi:10.1038/jid.2015.60

Raichur, S., Wang, S. T., Chan, P. W., Li, Y., Ching, J., Chaurasia, B., et al. (2014). CerS2 Haploinsufficiency Inhibits β-Oxidation and Confers Susceptibility to Diet-Induced Steatohepatitis and Insulin Resistance. *Cel Metab.* 20 (4), 687–695. doi:10.1016/j.cmet.2014.09.015

Reidy, P. T., Mahmassani, Z. S., McKenzie, A. I., Petrocelli, J. J., Summers, S. A., and Drummond, M. J. (2020). Influence of Exercise Training on Skeletal Muscle Insulin Resistance in Aging: Spotlight on Muscle Ceramides. *Ijms* 21 (4), 1514. doi:10.3390/ijms21041514

Relling, D. P., Hintz, K. K., and Ren, J. (2003). Acute Exposure of Ceramide Enhances Cardiac Contractile Function in Isolated Ventricular Myocytes. *Br. J. Pharmacol.* 140 (7), 1163–1168. doi:10.1038/sj.bjp.0705510

Ren, J., and Relling, D. P. (2006). Leptin-induced Suppression of Cardiomyocyte Contraction Is Amplified by Ceramide. *peptides* 27 (6), 1415–1419. doi:10.1016/j.peptides.2005.11.022

Riley, R. T., and Merrill, A. H. (2019). Ceramide Synthase Inhibition by Fumonisins: a Perfect Storm of Perturbed Sphingolipid Metabolism, Signaling, and Disease. *J. lipid Res.* 60 (7), 1183–1189. doi:10.1194/jlr.s093815

Rivera, I.-G., Ordoñez, M., Presa, N., Gomez-Larrauri, A., Simón, J., Trueba, M., et al. (2015). Sphingomyelinase D/ceramide 1-phosphate in Cell Survival and Inflammation. *Toxins* 7 (5), 1457–1466. doi:10.3390/toxins7051457

Roberts, L. D., and Gerszten, R. E. (2013). Toward New Biomarkers of Cardiometabolic Diseases. *Cel Metab.* 18 (1), 43–50. doi:10.1016/j.cmet.2013.05.009

Schiffmann, S., Hartmann, D., Fuchs, S., Birod, K., Ferreiròs, N., Schreiber, Y., et al. (2012). Inhibitors of Specific Ceramide Synthases. *Biochimie* 94 (2), 558–565. doi:10.1016/j.biochi.2011.09.007

Seah, J. Y. H., Chew, W. S., Torta, F., Khoo, C. M., Wenk, M. R., Herr, D. R., et al. (2020). Plasma Sphingolipids and Risk of Cardiovascular Diseases: a Large-Scale Lipidomic Analysis. *Metabolomics* 16 (9), 89–12. doi:10.1007/s11306-020-01709-8

Seki, N., Maeda, Y., Kataoka, H., Sugahara, K., Chiba, K., and Pharmacy (2013). Role of Sphingosine 1-Phosphate (S1P) Receptor 1 in Experimental Autoimmune Encephalomyelitis -I. *Pharmacol. Pharm.* 04 (08), 628–637. doi:10.4236/pp.2013.48089

Simon, J. N., Chowdhury, S. A., Warren, C. M., Sadayappan, S., Wieczorek, D. F., Solaro, R. J., et al. (2014). Ceramide-mediated Depression in Cardiomyocyte Contractility through PKC Activation and Modulation of Myofilament Protein Phosphorylation. *Basic Res. Cardiol.* 109 (6), 445–515. doi:10.1007/s00395-014-0445-6

Sokolowska, E, and Blachnio-Zabielska, A. (2019). The Role of Ceramides in Insulin Resistance. *Front. Endocrinol.* 10, 577. doi:10.3389/fendo.2019.00577

Somm, E., Montandon, S. A., Loizides-Mangold, U., Gaïa, N., Lazarevic, V., De Vito, C., et al. (2021). The GLP-1R Agonist Liraglutide Limits Hepatic

Lipotoxicity and Inflammatory Response in Mice Fed a Methionine-Choline Deficient Diet. *Translational Res.* 227, 75–88. doi:10.1016/j.trsl.2020.07.008

Summers, S. A. (2020). Ceramides: Nutrient Signals that Drive Hepatosteatosis. *J. Lipid Atheroscler.* 9 (1), 50–65. doi:10.12997/jla.2020.9.1.50

Summers, S. A., Chaurasia, B., and Holland, W. L. (2019). Metabolic Messengers: Ceramides. *Nat. Metab.* 1 (11), 1051–1058. doi:10.1038/s42255-019-0134-8

Summers, S. (2006). Ceramides in Insulin Resistance and Lipotoxicity. *Prog. lipid Res.* 45 (1), 42–72. doi:10.1016/j.plipres.2005.11.002

Tada, E., Toyomura, K., Nakamura, H., Sasaki, H., Saito, T., Kaneko, M., et al. (2010). Activation of Ceramidase and Ceramide Kinase by Vanadate via a Tyrosine Kinase-Mediated Pathway. *J. Pharmacol. Sci.* 114 (4), 420–432. doi:10.1254/jphs.10181fp

Targher, G., Lunardi, G., Mantovani, A., Meessen, J., Bonapace, S., Temporelli, P. L., et al. (2020). Relation between Plasma Ceramides and Cardiovascular Death in Chronic Heart Failure: A Subset Analysis of the GISSI-HF Trial. *ESC Heart Fail.* 7 (6), 3288–3297. doi:10.1002/ehf2.12885

Turpin, S. M., Nicholls, H. T., Willmes, D. M., Mourier, A., Brodesser, S., Wunderlich, C. M., et al. (2014). Obesity-Induced CerS6-dependent C16:0 Ceramide Production Promotes Weight Gain and Glucose Intolerance. *Cel Metab.* 20 (4), 678–686. doi:10.1016/j.cmet.2014.08.002

Van Brocklyn, J. R., and Williams, J. B. (2012). The Control of the Balance between Ceramide and Sphingosine-1-Phosphate by Sphingosine Kinase: Oxidative Stress and the Seesaw of Cell Survival and Death. *Comp. Biochem. Physiol. B: Biochem. Mol. Biol.* 163 (1), 26–36. doi:10.1016/j.cbpb.2012.05.006

Van Doorn, R., Van Horssen, J., Verzijl, D., Witte, M., Ronken, E., Van Het Hof, B., et al. (2010). Sphingosine 1-phosphate Receptor 1 and 3 Are Upregulated in Multiple Sclerosis Lesions. *Glia* 58 (12), 1465–1476. doi:10.1002/glia.21021

Wartewig, S., and Neubert, R. H. H. (2007). Properties of Ceramides and Their Impact on the Stratum Corneum Structure: a Review. *Skin Pharmacol. Physiol.* 20 (5), 220–229. doi:10.1159/000104420

Wegner, M.-S., Schiffmann, S., Parnham, M. J., Geisslinger, G., and Grösch, S. (2016). The enigma of Ceramide Synthase Regulation in Mammalian Cells. *Prog. lipid Res.* 63, 93–119. doi:10.1016/j.plipres.2016.03.006

Wigger, L., Cruciani-Guglielmacci, C., Nicolas, A., Denom, J., Fernandez, N., Fumeron, F., et al. (2017). Plasma Dihydroceramides Are Diabetes Susceptibility Biomarker Candidates in Mice and Humans. *Cel Rep.* 18 (9), 2269–2279. doi:10.1016/j.celrep.2017.02.019

Yang, F., Liu, C., Liu, X., Pan, X., Li, X., Tian, L., et al. (2021). Effect of Epidemic Intermittent Fasting on Cardiometabolic Risk Factors: A Systematic Review and Meta-Analysis of Randomized Controlled Trials. *Front. Nutr.*, 803. doi:10.3389/fnut.2021.669325

Ye, Q., Svatikova, A., Meeusen, J. W., Kludtke, E. L., and Kopecky, S. L. (2020). Effect of Proprotein Convertase Subtilisin/kexin Type 9 Inhibitors on Plasma Ceramide Levels. *Am. J. Cardiol.* 128, 163–167. doi:10.1016/j.amjcard.2020.04.052

Yin, W., Li, F., Tan, X., Wang, H., Jiang, W., Wang, X., et al. (2021). Plasma Ceramides and Cardiovascular Events in Hypertensive Patients at High Cardiovascular Risk. *Am. J. Hypertens.* doi:10.1093/ajh/hpab105

Yu, J., Pan, W., Shi, R., Yang, T., Li, Y., Yu, G., et al. (2015). Ceramide Is Upregulated and Associated with Mortality in Patients with Chronic Heart Failure. *Can. J. Cardiol.* 31 (3), 357–363. doi:10.1016/j.cjca.2014.12.007

Zhang, A. Y., Yi, F., Jin, S., Xia, M., Chen, Q. Z., Gulbins, E., et al. (2007). Acid Sphingomyelinase and its Redox Amplification in Formation of Lipid Raft Redox Signaling Platforms in Endothelial Cells. *Antioxid. Redox Signaling* 9 (7), 817–828. doi:10.1089/ars.2007.1509

Zhang, D. X., Zou, A.-P., and Li, P.-L. (2003). Ceramide-induced Activation of NADPH Oxidase and Endothelial Dysfunction in Small Coronary Arteries. *Am. J. Physiology-Heart Circulatory Physiol.* 284 (2), H605–H612. doi:10.1152/ajpheart.00697.2002

Zhang, Y., Li, X., Carpinteiro, A., and Gulbins, E. (2008). Acid Sphingomyelinase Amplifies Redox Signaling inPseudomonas Aeruginosa-Induced Macrophage Apoptosis. *J. Immunol.* 181 (6), 4247–4254. doi:10.4049/jimmunol.181.6.4247

Zhang, Y., Whaley-Connell, A. T., Sowers, J. R., and Ren, J. (2018). Autophagy as an Emerging Target in Cardiorenal Metabolic Disease: from Pathophysiology to Management. *Pharmacol. Ther.* 191, 1–22. doi:10.1016/j.pharmthera.2018.06.004

Zhang, Y., Yang, X., Bian, F., Wu, P., Xing, S., Xu, G., et al. (2014). TNF-α Promotes Early Atherosclerosis by Increasing Transcytosis of LDL across Endothelial Cells: Crosstalk between NF-Kb and PPAR-γ. *J. Mol. Cell Cardiol.* 72, 85–94. doi:10.1016/j.yjmcc.2014.02.012

Zheng, T., Li, W., Wang, J., Altura, B. T., and Altura, B. M. (2000). Sphingomyelinase and Ceramide Analogs Induce Contraction and Rises in [Ca2+]i in Canine Cerebral Vascular Muscle. *Am. J. Physiology-Heart Circulatory Physiol.* 278 (5), H1421–H1428. doi:10.1152/ajpheart.2000.278.5.h1421

Conflict of Interest: The authors declare that the research was conducted in the absence of any commercial or financial relationships that could be construed as a potential conflict of interest.

Publisher's Note: All claims expressed in this article are solely those of the authors and do not necessarily represent those of their affiliated organizations, or those of the publisher, the editors and the reviewers. Any product that may be evaluated in this article, or claim that may be made by its manufacturer, is not guaranteed or endorsed by the publisher.

frontiers in Cell and Developmental Biology

ORIGINAL RESEARCH
published: 03 February 2022
doi: 10.3389/fcell.2022.803029

Upregulation of Neogenin-1 by a CREB1-BAF47 Complex in Vascular Endothelial Cells is Implicated in Atherogenesis

Nan Li[1,2], *Hong Liu*[2], *Yujia Xue*[2], *Junliang Chen*[3], *Xiaocen Kong*[4,5]* and *Yuanyuan Zhang*[6]*

[1]Department of Human Anatomy, Nanjing Medical University, Nanjing, China, [2]Key Laboratory of Targeted Intervention of Cardiovascular Disease and Collaborative Innovation Center for Cardiovascular Translational Medicine, Nanjing Medical University, Nanjing, China, [3]Department of Pathophysiology, Wuxi Medical School, Jiangnan University, Wuxi, China, [4]Department of Endocrinology, Nanjing First Hospital, Nanjing Medical University, Nanjing, China, [5]Institute of Biomedical Research, Liaocheng Univeristy, Liaocheng, China, [6]Hainan Provincial Key Laboratory for Tropical Cardiovascular Diseases Research, Key Laboratory of Emergency and Trauma of Ministry of Education, Department of Cardiology, The First Affiliated Hospital of Hainan Medical University, Haikou, China

OPEN ACCESS

Edited by:
Guillaume Laurent Hoareau, University of Utah Medical Center, United States

Reviewed by:
Tzong-Shyuan Lee, National Taiwan University, Taiwan
Sivareddy Kotla, University of Texas MD Anderson Cancer Center, United States

***Correspondence:**
Xiaocen Kong
kongxiaocen2010@163.com
Yuanyuan Zhang
zyy500382@163.com

Specialty section:
This article was submitted to Cellular Biochemistry, a section of the journal Frontiers in Cell and Developmental Biology

Received: 27 October 2021
Accepted: 10 January 2022
Published: 03 February 2022

Citation:
Li N, Liu H, Xue Y, Chen J, Kong X and Zhang Y (2022) Upregulation of Neogenin-1 by a CREB1-BAF47 Complex in Vascular Endothelial Cells is Implicated in Atherogenesis. Front. Cell Dev. Biol. 10:803029. doi: 10.3389/fcell.2022.803029

Atherosclerosis is generally considered a human pathology of chronic inflammation, to which endothelial dysfunction plays an important role. Here we investigated the role of neogenin 1 (Neo-1) in oxidized low-density lipoprotein (oxLDL) induced endothelial dysfunction focusing on its transcriptional regulation. We report that Neo-1 expression was upregulated by oxLDL in both immortalized vascular endothelial cells and primary aortic endothelial cells. Neo-1 knockdown attenuated whereas Neo-1 over-expression enhanced oxLDL-induced leukocyte adhesion to endothelial cells. Neo-1 regulated endothelial-leukocyte interaction by modulating nuclear factor kappa B (NF-κB) activity to alter the expression of adhesion molecules. Neo-1 blockade with a blocking antibody ameliorated atherogenesis in *Apoe*$^{-/-}$ mice fed a Western diet. Ingenuity pathway analysis combined with validation assays confirmed that cAMP response element binding protein 1 (CREB1) and Brg1-associated factor 47 (BAF47) mediated oxLDL induced Neo-1 upregulation. CREB1 interacted with BAF47 and recruited BAF47 to the proximal Neo-1 promoter leading to Neo-1 trans-activation. In conclusion, our data delineate a novel transcriptional mechanism underlying Neo-1 activation in vascular endothelial cells that might contribute to endothelial dysfunction and atherosclerosis.

Keywords: transcriptional regulation, endothelial cell, chromatin remodeling protein, atherosclerosis, transcription factor

INTRODUCTION

Coronary heart disease represents one of the major causes for heart failure, which affects ~30 million patients annually and is the leading cause of deaths worldwide (Savarese and Lund, 2017). Atherosclerosis is characterized by the deposition of fat-laden plaques in the arteries causing progressive narrowing of the blood vessel and subsequently coronary heart disease (Libby, 2021a). Decades of research have led to the consensus that atherosclerosis is a human pathology of chronic vascular inflammation (Libby, 2021b). On the one hand, multiple different populations of immune cells, including macrophages, granulocytes, lymphocytes, and natural killer cells, are present in the

atherosclerotic plaque in a stage-dependent manner (Libby and Hansson, 2015). On the other hand, modulating the inflammatory response in the vessels has been shown to alter the development and progression of atherosclerosis in model animals (Libby et al., 2013). The most convincing piece of evidence to support the long-held view that vascular inflammation is the linchpin of atherogenesis comes from a recently published clinic study that shows the efficacy of a monoclonal antibody targeting the pro-inflammatory cytokine IL-1β (Canakinumab) in the treatment of atherosclerosis (Ridker et al., 2017).

Hyperlipidemia, or the presence of elevated levels of oxidized low-density lipoprotein (oxLDL) in the circulation, is a major risk factor for atherosclerosis (Steinberg and Witztum, 2010). High levels of oxLDL contribute to atherosclerosis by skewing the phenotypes of vascular cells including endothelial cells. Endothelial dysfunction is considered one of the early pathophysiological events during atherogenesis (Gimbrone and Garcia-Cardena, 2016). Under physiological conditions, the circulating leukocytes (e.g., macrophages) are unable for firmly attach to the vessel wall. In the presence of oxLDL, however, endothelial cells upregulate the expression of a plethora of different adhesion molecules including intercellular adhesion molecules (ICAMs), vascular adhesion molecules (VCAMs), and selectins that mediate the rolling, adhesion, and penetration of leukocytes (Blankenberg et al., 2003). Indeed, blocking antibodies that targets either adhesion molecules directly or their receptors expressed on the surface of leukocytes have been shown to reduce atherogenesis with high efficiency in mice (Galkina and Ley, 2007). Transcriptionally, nuclear factor kappa B (NF-κB) is considered a master regulator of adhesion molecules. Conserved NF-κB motifs have been identified on the promoters of adhesion molecule genes (Tak and Firestein, 2001). Consistently, manipulation of NF-κB activity in endothelial cells, through deletion of its upstream activator IKKγ or over-expression of its upstream inhibitor IκB, protects the mice from Western diet feeding induced atherosclerosis with concomitant down-regulation of adhesion molecules and reduced leukocyte adhesion (Gareus et al., 2008).

Neogenin 1 (Neo-1) was originally identified as a receptor for netrins, a group of guidance molecules; engagement of Neo-1 by netrins provides the cue for neurons to expand and form connections (Livesey, 1999). Recent investigations have expanded the realm of pathophysiological events regulated by Neo-1. A string of reports have suggested that Neo-1 may play a role in regulating the inflammatory response in different tissues. Genetic ablation or pharmaceutical inhibition of Neo-1 in mice can lead to attenuation of ischemia-reperfusion induced hepatic inflammation, zymosan A induced peritonitis, and high pressure ventilation induced pulmonary inflammation (Konig et al., 2012; Mirakaj et al., 2012; Schlegel et al., 2014). Based on these prior observations, we hypothesized that Neo-1 might be involved in atherogenesis by regulating vascular inflammation. We report here that oxLDL upregulates Neo-1 in vascular endothelial cells at the transcriptional level via the CREB1-BAF47 complex. Neo-1 promotes leukocyte adhesion to endothelial cells by modulating NF-κB dependent trans-activation of adhesion molecules. Importantly, Neo-1 inhibition in *Apoe*$^{-/-}$ mice dampens atherosclerosis.

METHODS

Animals

All animal protocols were reviewed and approved by the intramural Ethics Committee on Humane Treatment of Laboratory Animals of Nanjing Medical University. The mice were maintained in an SPF environment with 12 h light/dark cycles and *ad libitum* access to food and water. To induce atherosclerosis, 8-wk male *Apoe*$^{-/-}$ mice were fed a Western diet (D12109, Research Diets, New Brunswick, NJ, United States) for 8 weeks as previously described (Zhang et al., 2020). An anti-Neo1 antibody (5 μg per injection, R&D, AF 1079) or isotype IgG was injected intravenously every day from week 5 of Western diet feeding till the mice were sacrificed. The animals were euthanized by pentobarbital sodium (100–120 mg/kg) to obtain their samples. Atherosclerotic lesions were gauged by en face analysis of the whole aorta and by cross-sectional analysis of the proximal aorta essentially described previously (Liao et al., 2020; Huangfu et al., 2021).

Cell Culture, Plasmids, Transient Transfection, and Reporter Assay

Human immortalized umbilical vein endothelial cells (HUVEC/EAhy926, ATCC), human monocytic/macrophage cells (THP-1, ATCC), and human embryonic kidney cells (HEK293, Invitrogen) were maintained in DMEM (Invitrogen) supplemented with 10% fetal bovine serum (FBS, Hyclone) as previously described (Chen et al., 2020; Yang et al., 2021). Human primary aortic endothelial cells (HAEC, Cambrex/Lonza) were maintained in EGM-2 media with supplements supplied by the vendor; experiments were performed in primary cells between 3rd and 6th passages as previously described (Li et al., 2020). FLAG-tagged CREB1 (Mayr et al., 2005) and GFP-tagged BAF47 (Kadoch and Crabtree, 2013) have been described previously. Neo-1 promoter-luciferase construct was made by amplifying genomic DNA spanning the proximal promoter and the first exon of Neo-1 gene (−1274/+101) and ligating into a pGL3-basic vector (Promega). Truncation mutants were made using a QuikChange kit (Thermo Fisher Scientific, Waltham, MA, United States) and verified by direct sequencing. Small interfering RNAs were purchased from Dharmacon. Transient transfection was performed with Lipofectamine 2000. Cells were harvested 48 h after transfection and reporter activity was measured using a luciferase reporter assay system (Promega) as previously described (Liu et al., 2021).

Protein Extraction, Immunoprecipitation and Western Blot

Whole cell lysates were obtained by re-suspending cell pellets in RIPA buffer (50 mM Tris pH7.4, 150 mM NaCl, 1% Triton X-100) with freshly added protease inhibitor (Roche) as previously described (Lv et al., 2021). Specific antibodies or pre-immune

IgGs were added to and incubated with cell lysates overnight before being absorbed by Protein A/G-plus Agarose beads (Santa Cruz). Precipitated immune complex was released by boiling with 1X SDS electrophoresis sample buffer. Western blot analyses were performed with anti-Neo1 (Abcam, ab183511, 1:1000), anti-CREB1 (Proteintech, 12208-1, 1:1000), anti-BAF47 (Proteintech, 20654-1, 1:1000), anti-FLAG (Sigma, F1804, 1: 5000), anti-GFP (Proteintech, 50430-2, 1:1000), and anti-β-actin (Sigma, A2228, 1:4000) antibodies.

Chromatin Immunoprecipitation

Chromatin Immunoprecipitation (ChIP) assays were performed essentially as described before (Coarfa et al., 2020; Maity et al., 2020; Wang J.-N. et al., 2020; Wang S. et al., 2020; Marti et al., 2021). In brief, chromatin in control and treated cells were cross-linked with 1% formaldehyde. Cells were incubated in lysis buffer (150 mM NaCl, 25 mM Tris pH 7.5, 1% Triton X-100, 0.1% SDS, 0.5% deoxycholate) supplemented with protease inhibitor tablet and PMSF. DNA was fragmented into ~200 bp pieces using a Branson 250 sonicator. Aliquots of lysates containing 200 μg of protein were used for each immunoprecipitation reaction with anti-NF-κB/p65 (Santa Cruz, sc-372), anti-CREB1 (Millipore, 17-600), anti-BAF47 (Cell Signaling Tech, 91735), or pre-immune IgG. For re-ChIP, immune complexes were eluted with the elution buffer (1% SDS, 100 mM $NaCO_3$), diluted with the re-ChIP buffer (1% Triton X-100, 2 mM EDTA, 150 mM NaCl, 20 mM Tris pH 8.1), and subject to immunoprecipitation with a second antibody of interest.

RNA Isolation and Real-Time PCR

RNA was extracted with the RNeasy RNA isolation kit (Qiagen). Reverse transcriptase reactions were performed using a SuperScript First-strand Synthesis System (Invitrogen) as previously described (Hong et al., 2020). Real-time PCR reactions were performed on an ABI Prism 7500 system with the following primers: human *NEO1*, 5′-GGAGCCGGTGGATACACTCT-3′ and 5′-TGGCGTCGATCA TCTGATACTA-3′; human *ICAM1*, 5′-ATGCCCAGACATCTG TGTCC-3′ and 5′-GGGGTCTCTATGCCCAACAA-3′; human *VCAM1*, 5′-GGGAAGATGGTCGTGATCCTT-3′ and 5′-TCT GGGGTGGTCTCGATTTTA-3′; mouse *Icam1*, 5′-GTGATGCTC AGGTATCCATCCA-3′ and 5′-CACAGTTCTCAAAGCACA GCG-3'; mouse *Icam2*, 5′-ATGGTCCGAGAAGCAGATAGT-3′ and 5′-TGCTGTTGAACGTGGCTGT-3'; mouse *Vcam1*, 5′-TTG GGAGCCTCAACGGTACT-3′ and 5′-GCAATCGTTTTGTAT TCAGGGGA-3'; mouse *Il1b*, 5′-GAAATGCCACCTTTTGAC AGTG-3′ and 5′-TGGATGCTCTCATCAGGACAG-3'; mouse *Il6*, 5′-TGGGGCTCTTCAAAAGCTCC-3′ and 5′-AGGAACTAT CACCGGATCTTCAA-3'; mouse *Tnfa*, 5′-CTGGATGTCAAT CAACAATGGGA-3′ and 5′-ACTAGGGTGTGAGTGTTTTCT GT-3′; mouse *Infg*, 5′-TCCTCGCCAGACTCGTTTTC-3′ and 5′-ACGGCTCCCAAGTTAGAATCT-3'; mouse *Mcp1*, 5′-AAAACA CGGGACGAGAAACCC-3′ and 5′-ACGGGAACCTTTATTAAC CCCT-3'; mouse *Rantes*, 5′-GCTGCTTTGCCTACCTCTCC-3′ and 5′-TCGAGTGACAAACACGACTGC-3'. Ct values of target genes were normalized to the Ct values of housekeeping control gene (18s rRNA, 5′-CGCGGTTCTATTTTGTTGGT-3′ and 5′-TCGTCT TCGAAACTCCGACT-3′ for both human and mouse genes) using the ΔΔCT method and expressed as relative mRNA expression levels compared to the control group which is arbitrarily set as 1.

Leukocyte Adhesion Assay

Leukocyte adhesion assay was performed as previously described. Briefly, THP-1 cells were stained with a fluorescent die (2′,7′-Bis-(2-carboxyethyl)-5(6)-carboxyfluorescein tetrakis (acetoxymethyl) ester) (Sigma) for 30 min at 37°C. After several washes with PBS, THP-1 cells were co-incubated for 30 min with endothelial cells. Unbound leukocytes were removed by washing and the number of adhered cells was visualized by fluorescence microscopy and analyzed with Image-Pro Plus (Media Cybernetics). For each group, at least six different fields were randomly chosen and the positively stained cells were counted and divided by the number of total cells. The data are expressed as relative EdU staining compared to the control group arbitrarily set as 1.

Statistical Analysis

One-way ANOVA with post-hoc Scheff´e analyses were performed by SPSS software (IBM SPSS v18.0, Chicago, IL, United States). Unless otherwise specified, values of $p < .05$ were considered statistically significant.

RESULTS

Neogenin 1 Expression is Upregulated by Oxidized Low-Density Lipoprotein in Endothelial Cells

In order to determine the effect of pro-atherosclerotic stimuli on Neo-1 expression, immortalized human vascular endothelial cells (EAhy926) and primary human aortic endothelial cells (HAECs) were treated with different doses of oxidized low-density lipoprotein (oxLDL). As shown in **Figure 1A**, oxLDL at 20 μg/ml upregulated Neo-1 message RNA levels by ~2xfold in both EAhy926 and HAECs as measured by quantitative PCR whereas oxLDL at 50 μg/ml and 100 μg/ml comparably increased Neo-1 mRNA levels by more than 3xfold. Western blotting confirmed that Neo-1 protein levels were similarly upregulated by oxLDL treatment in a dose-dependent manner (**Figure 1B**). Next, a time course experiment was performed in which the cells were treated with 50 μg/ml oxLDL for different periods of time. QPCR analysis showed that Neo-1 mRNA peaked at 24 h but declined at 48 h followed oxLDL stimulation whereas Western blotting showed that changes of Neo-1 protein levels lagged those of Neo-1 mRNA levels (**Figures 1C,D**). Of note, Western blotting showed that Neo-1 was exclusively located to the cell membrane and that oxLDL stimulation did not appear to influence its sub-cellular localization (**Supplementary Figure S1**).

Neogenin 1 Regulates Leukocyte Adhesion

One of the major mechanisms whereby oxLDL contributes to endothelial dysfunction and atherosclerosis is the trans-activation of adhesion molecules, which mediate leukocyte adhesion to endothelial cells (Khan et al., 1995; Cominacini et al., 1997; Takei et al., 2001). Because it was observed that Neo-1 could be

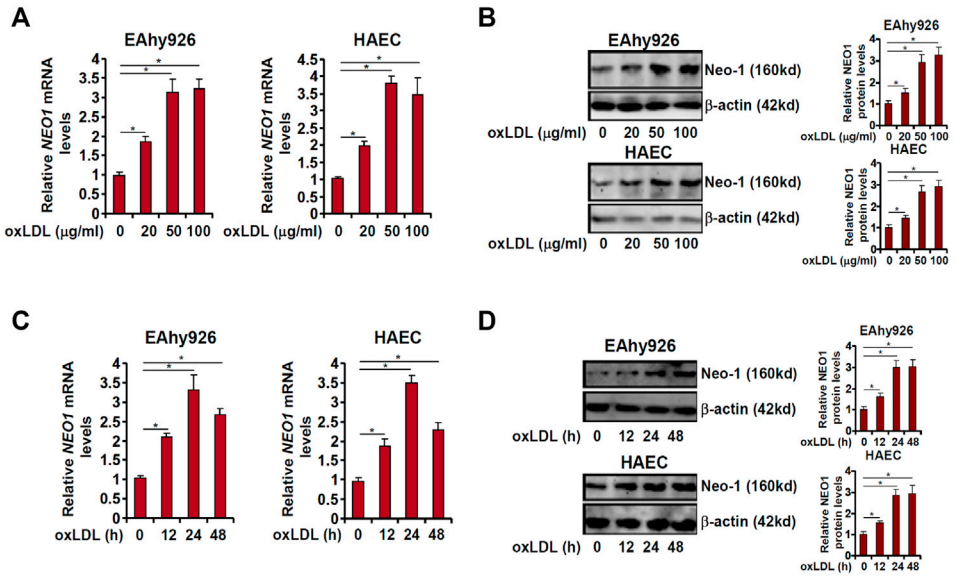

FIGURE 1 | Neo-1 expression is upregulated by oxLDL in endothelial cells. **(A,B)** EAhy926 and HAECs were treated with different concentrations of oxLDL for 24 h. Neo-1 expression was examined by qPCR and Western. **(C,D)** EAhy926 and HAECs were treated with oxLDL (50 μg/ml) and harvested at indicated time points. Neo-1 expression was examined by qPCR and Western.

upregulated by oxLDL in vascular endothelial cells, we asked whether Neo-1 might play a role in leukocyte adhesion. To this end, endogenous Neo-1 was depleted by two independent pairs of siRNAs and knockdown efficiencies were verified by Western blotting (**Figure 2A**). Neo-1 depletion significantly suppressed the leukocyte adhesion to both EAhy926 cells and HAECs (**Figure 2B**). Similarly, the addition of an anti-Neo-1 blocking antibody diminished oxLDL-induced leukocyte adhesion to endothelial cells (**Figure 2C**). In contrast, Neo-1 over-expression, mediated by adenovirus mediated delivery of a Neo-1 vector (**Figure 2A**), did not appreciably influence leukocyte adhesion alone but enhanced leukocyte adhesion in the presence of oxLDL (**Figure 2D**).

The pro-inflammatory transcription factor NF-κB is considered the master regulator for the trans-activation of a slew of adhesion molecules including ICAM1 and VCAM1 (Collins et al., 1995). Both ICAM1 expression and VCAM1 expression were upregulated by oxLDL treatment whereas Neo-1 knockdown attenuated induction of ICAM1 and VCAM1 (**Figures 3A,B**). Consistently, ChIP assay showed that oxLDL treatment strongly promoted the recruitment of NF-κB/p65 to the ICAM1 promoter and the VCAM1 promoter, which was weakened by Neo-1 knockdown (**Figure 3C**). On the contrary, Neo-1 over-expression enhanced the induction of ICAM1 expression and VCAM1 expression by oxLDL treatment (**Figures 3D,E**). The effect of Neo-1 over-expression on the adhesion molecule expression was likely attributable to the stronger association of NF-κB/p65 with target promoters (**Figure 3F**).

Neogenin 1 Inhibition Attenuates Atherosclerosis in Mice

Next, we decided to extrapolate the finding that Neo-1 might be involved in endothelial dysfunction in a classic animal model in which *Apoe*$^{-/-}$ mice were fed a Western diet for 8 weeks to develop atherosclerotic lesions (**Figure 4A**). Blockade of endogenous Neo-1 was achieved by a blocking antibody that has been tested previously (Konig et al., 2012; Mirakaj et al., 2012; Schlegel et al., 2014); this antibody targets the extracellular domain of the Neo-1 protein (a.a.42-1033) thus disrupting the binding of Neo-1 to its ligands. Neo-1 inhibition did not significantly alter plasma triglyceride levels (**Figure 4B**) or plasma cholesterol levels (**Figure 4C**) suggesting that Neo-1 probably does not regulate hyperlipidemia. Oil red O staining of dissected aorta (**Figure 4D**) and aortic sinus (**Figure 4E**) indicated that compared to the isotype IgG injection, anti-Neo-1 injection significantly and markedly reduced atherosclerotic lesions. QPCR profiling showed that Neo-1 inhibition significantly down-regulated the expression of adhesion molecules and pro-inflammatory mediators including interleukin 1 beta (*Il1b*), interleukin 6 (*Il6*), tumor necrosis factor alpha (*Tnfa*), interferon gamma (*Ifng*), macrophage chemoattractive protein 1 (*Mcp1*), and regulated upon activation, normal T cell expressed and secreted (*Rantes*) in the aorta (**Figure 4F**). ELISA assays confirmed that protein levels of pro-inflammatory mediators were decreased by the administration of the Neo1-blocking antibody (**Figure 4G**). In addition, immunofluorescence staining confirmed that fewer leukocytes were detected to be adhered to the endothelium as result of Neo-1 inhibition (**Figure 4H**).

cAMP Response Element Binding Protein 1 and Brg1-Associated Factor 47 are Essential for Transcriptional Activation of Neogenin 1 in Endothelial Cells

The next set of experiments was designed to explore the mechanism underlying upregulation of Neo-1 expression by

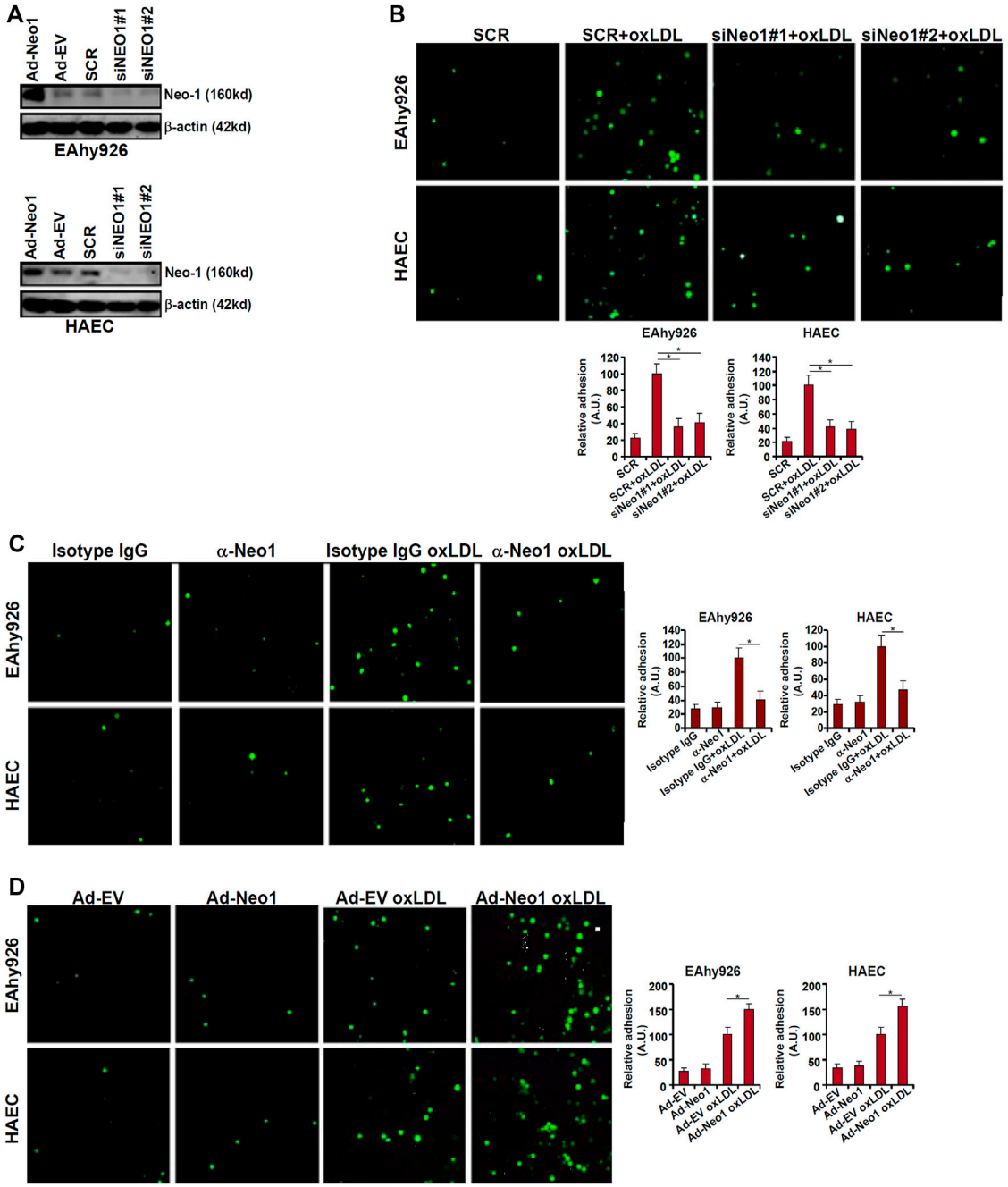

FIGURE 2 | Neo-1 regulates leukocyte adhesion. **(A)** EAhy926 cells and HAECs were transfected with indicated siRNAs. Alternatively, these cells were transduced with adenovirus carrying a Neo-1 vector (Ad-Neo1) or control adenovirus (Ad-EV). Neo-1 protein levels were examined by Western. **(B)** EAhy926 cells and HAECs were transfected with indicated siRNAs followed by treatment with oxLDL (50 μg/ml) for 24 h. Leukocyte adhesion was performed as described in Methods. **(C)** EAhy926 cells and HAECs were treated with oxLDL (50 μg/ml) in the presence or absence of an anti-Neo-1 antibody for 24 h. **(D)** EAhy926 cells and HAECs were transduced with adenovirus carrying a Neo-1 vector (Ad-Neo1) or control adenovirus (Ad-EV) followed by treatment with oxLDL (50 μg/ml) for 24 h. Leukocyte adhesion was performed as described in Methods. SCR, scrambled siRNA.

oxLDL in endothelial cells. First, full-length (−1274/101) and truncated (−783/+101, −409/+101, and −126/+101) Neo-1 promoter-luciferase fusion constructs were transfected into EAhy926 cells followed by oxLDL treatment. As shown in **Figure 5A**, oxLDL treatment robustly augmented the activities of the longer Neo-1 promoters but not the shortest Neo-1 promoter indicating that oxLDL likely regulates Neo-1 expression at the transcriptional level and that a potential response element might reside between −409 and −126 relative to the transcription start site. Ingenuity pathway analysis (IPA)

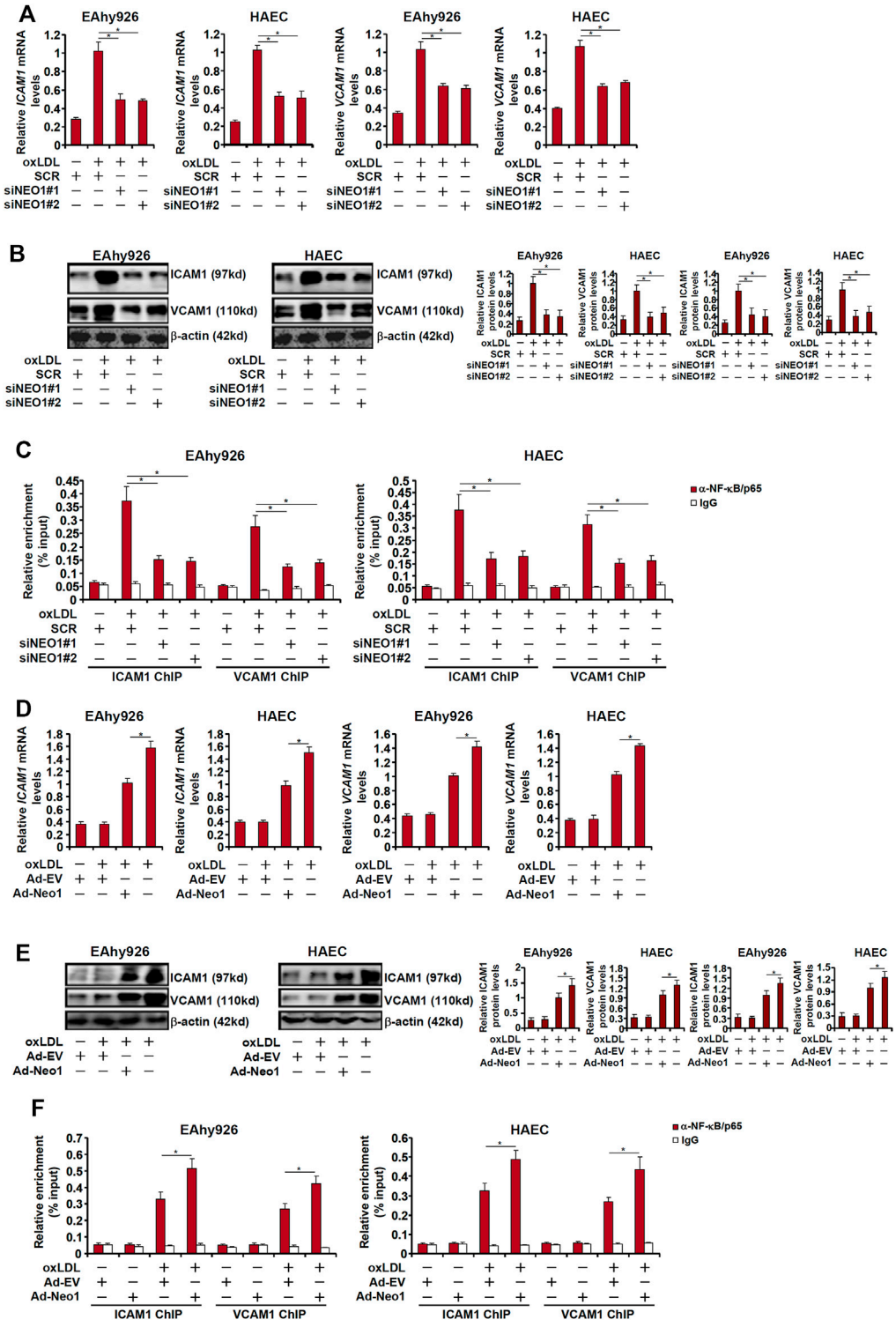

FIGURE 3 | Neo-1 regulates expression of adhesion molecules by modulating *NF-κB* activity. **(A–C)** EAhy926 cells and HAECs were transfected with indicated siRNAs followed by treatment with oxLDL (50 μg/ml) for 24 h. Expression levels of adhesion molecules were examined by qPCR and Western blotting. ChIP assays were performed with anti-NF-κB or IgG. **(D–F)** EAhy926 cells and HAECs were transduced with adenovirus carrying a Neo-1 vector (Ad-Neo1) or control adenovirus (Ad-EV) followed by treatment with oxLDL (50 μg/ml) for 24 h. Expression levels of adhesion molecules were examined by qPCR and Western blotting. ChIP assays were performed with anti-NF-κB or IgG.

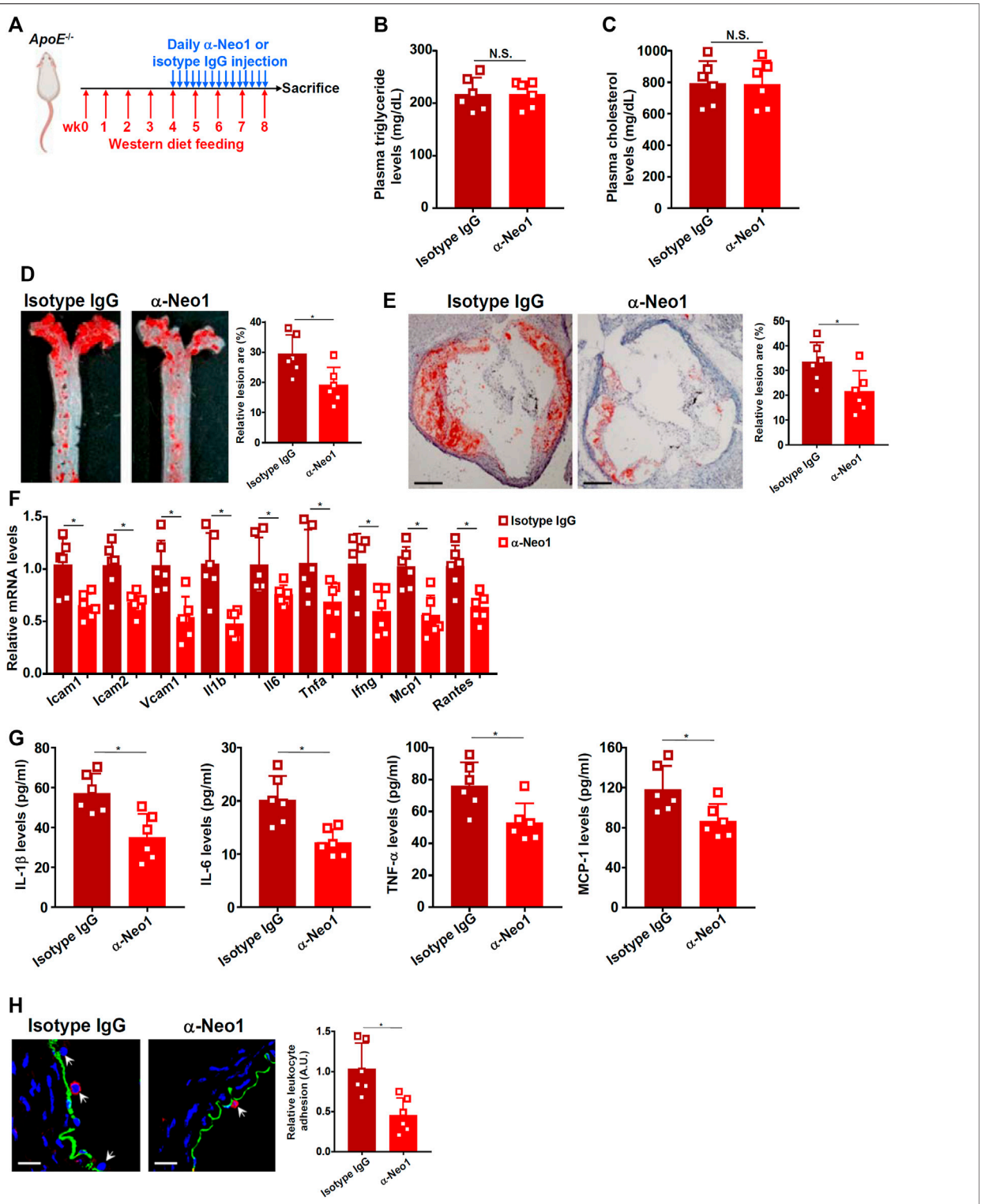

FIGURE 4 | Neo-1 inhibition attenuates atherosclerosis in mice. **(A)** Scheme of animal protocol. **(B)** Plasma triglyceride levels. **(C)** Plasma cholesterol levels. **(D)** Oil red O staining of the thoracic aorta. **(E)** Oil red O staining of the aortic sinus. **(F)** Gene expression in aortic arteries was examined by qPCR. **(G)** Levels of pro-inflammatory mediators were examined by ELISA. **(H)** Infiltration of macrophages was examined by immunofluorescence staining. *N* = 6 mice for each group. Error bars represent SD (*$p < .05$, one-way ANOVA).

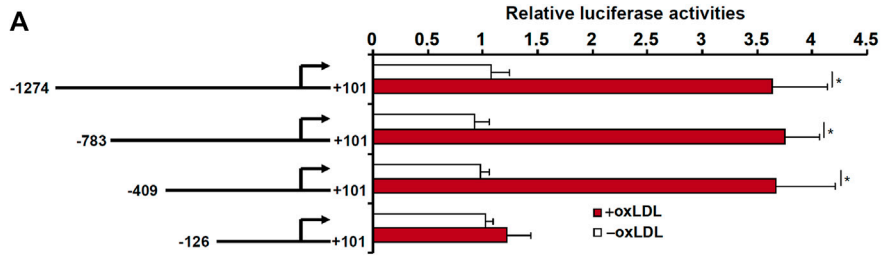

B

Upstream Regulator	Molecule Type	*p*-value	Target Molecules in Dataset
SMARCB1	transcription regulator	0.00799	NEO1
CREB1	transcription regulator	0.0257	NEO1

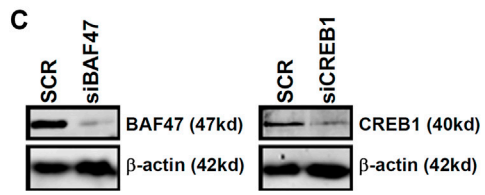

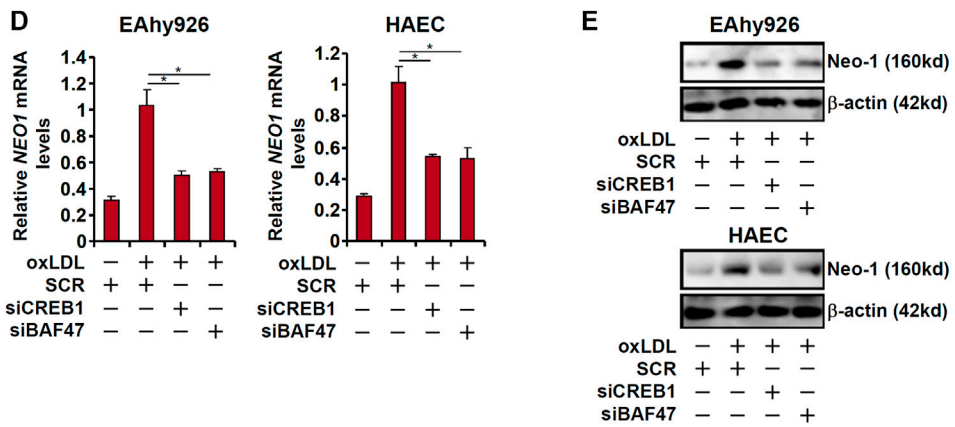

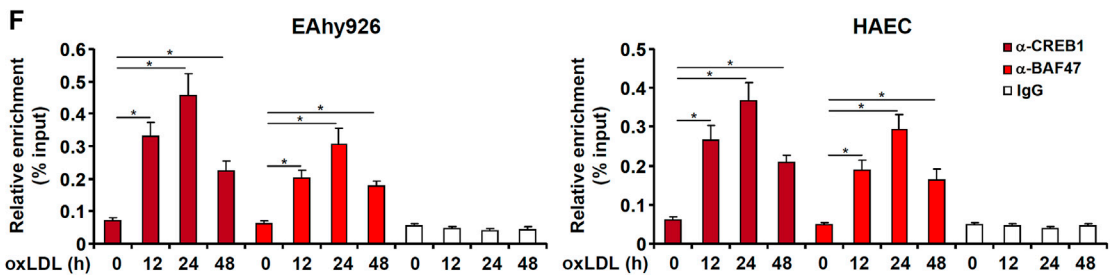

FIGURE 5 | CREB1 and BAF47 are essential for transcriptional activation of Neo-1 in endothelial cells. **(A)** Neo-1 promoter-luciferase constructs were transfected into EAhy926 cells followed by treatment with oxLDL (50 μg/ml) for 24 h. Luciferase activities were normalized by protein concentration and GFP fluorescence. **(B)** Ingenuity pathway analysis. **(C)** EAhy926 cells were transfected with indicated siRNAs. Knockdown efficiencies were examined by Western. **(D,E)** EAhy926 cells and HAECs were transfected with indicated siRNAs followed by treatment with oxLDL (50 μg/ml) for 24 h. Neo-1 expression was examined by qPCR and Western. **(F)** EAhy926 cells and HAECs were treated with oxLDL (50 μg/ml) and harvested at indicated time points. ChIP assays were performed with anti-CREB1, anti-BAF47, or IgG.

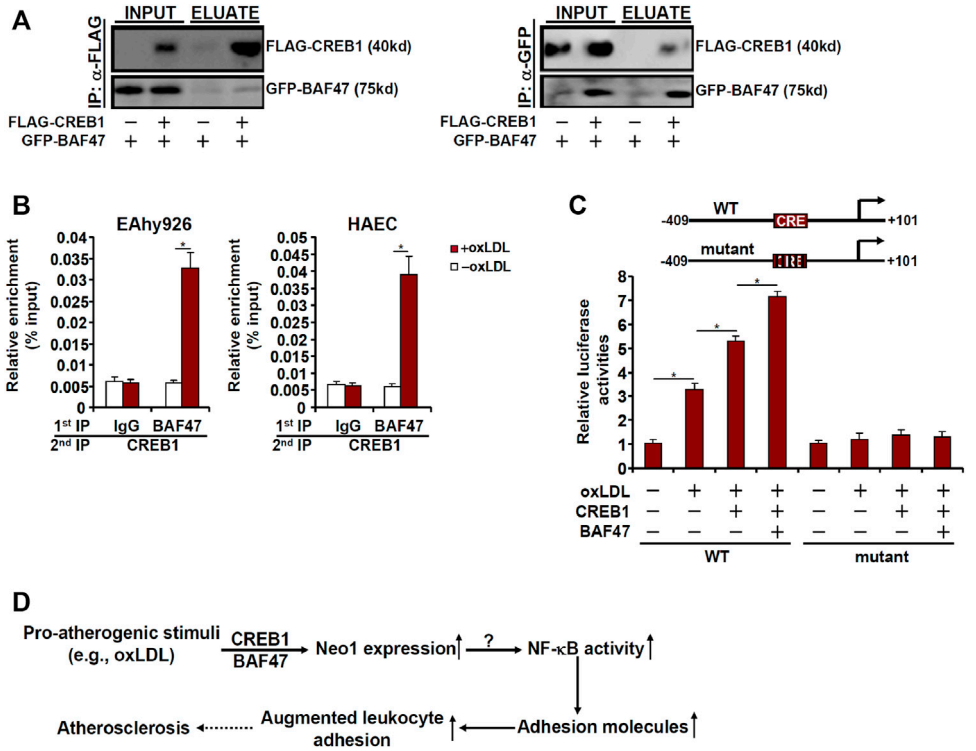

FIGURE 6 | CREB1 interacts with and recruits BAF47 to activate Neo-1 transcription. **(A)** HEK293 cells were transfected with FLAG-tagged CREB1 and GFP-tagged BAF47 as indicated. Immunoprecipitation was performed with anti-FLAG or anti-GFP. **(B)** EAhy926 cells and HAECs were treated with or without with oxLDL (50 μg/ml) for 24 h. Re-ChIP assay was performed with indicated antibodies. **(C)** Wild type or mutant Neo1 promoter-luciferase construct (–409/+101) was transfected into EAhy926 cells with indicated expression constructs followed by treatment with oxLDL (50 μg/ml) for 24 h. Luciferase activities were normalized by protein concentration and GFP fluorescence. **(D)** A schematic model.

revealed cAMP response element binding protein 1 (CREB1) and Brahma-related protein associated factor 47 (BAF47, encoded by *SMARCB1*) as the upstream transcriptional regulators of Neo-1 (**Figure 5B**). Knockdown of endogenous CREB1 and BAF47 with siRNAs (**Figure 5C**) suppressed the upregulation of Neo-1 expression by oxLDL stimulation in both types of endothelial cells (**Figures 5D,E**). More important, ChIP assay showed that oxLDL promoted the recruitment of both CREB1 and BAF47 to the Neo-1 promoter in a kinetics similar to that of Neo-1 induction (**Figure 5F**).

cAMP Response Element Binding Protein 1 Interacts With and Recruits Brg1-Associated Factor 47 to Activate Neogenin 1 Transcription

Because BAF47 is a transcriptional co-factor without a DNA binding domain that recognizes and binds to specific DNA sequences, we speculated that CREB1 might interact with BAF47 to cooperatively regulate Neo-1 transcription. When FLAG-tagged CREB1 and GFP-tagged BAF47 were co-transfected into HEK923 cells, an anti-FLAG antibody immunoprecipitated both CREB1 and BAF47 whereas an anti-GFP antibody simultaneously pulled-down both BAF47 and CREB1 suggesting that these two proteins could interact with each other (**Figure 6A**). Phosphorylation of CREB1 at serine 133 is key to its transcriptional activity (Johannessen et al., 2004). Of note, S133 phosphorylation mutation did not appear to influence the CREB1-BAF47 interaction. Interestingly, treatment with oxLDL enhanced the interaction between CREB1 and BAF47 (**Supplementary Figure S3**). More important, ChIP-on-ChIP (Re-ChIP) experiments demonstrated that oxLDL treatment stimulated the formation of a BAF47-CREB1 complex on the Neo-1 promoter (**Figure 6B**). In addition, reporter assay showed that co-expression of CREB1 and BAF47 enhanced the induction of the Neo-1 promoter activity by oxLDL. The synergistic effect between CREB1 and BAF47 on the Neo-1 promoter was not influenced by CREB1 phosphorylation because the CREB1 S133A mutant was able to cooperate with BAF47 to activate the Neo-1 promoter as potently as the wild type CREB1 (**Supplementary Figure S4**). However, when the putative CREB1 binding site was mutated within the Neo-1 promoter, neither CREB1 alone nor co-expression of CREB1 and BAF47 lost the ability to influence the Neo-1 promoter activity (**Figure 6C**).

DISCUSSION

Vascular inflammation is considered the pathogenic cornerstone of atherosclerosis. Adhesion of circulating leukocytes to the vascular endothelium triggers and perpetuates the inflammatory response. Here we describe a novel

transcriptional pathway that connects Neo-1 activation to leukocyte adhesion in endothelial cells and potentially atherogenesis (**Figure 6D**).

Despite the observation that Neo-1 inhibition by a blocking antibody dampens atherogenesis in mice (**Figure 4**), several lingering issues deserve further attention. First, we focused on the regulation of Neo-1 by oxLDL in vascular endothelial cells. However, the possibility that Neo-1 upregulation by oxLDL in vascular smooth muscle cells (VSMCs) or macrophages may similarly contribute to atherogenesis and thus offer explanation to the observed phenotype cannot be ruled out. Hadi et al. (2018) have recently reported that activation of Neo-1 in VSMCs causes persistent stimulation of metalloproteinase 3 (MMP3) and consequently aberrant degradation of extracellular matrix leading to the pathogenesis of abdominal aortic aneurysm. Because phenotypic switch of VSMCs is a pathophysiological process shared by atherosclerosis and aneurysm (Chakraborty et al., 2021), it is plausible to speculate that Neo-1 might be upregulated by oxLDL in VSMCs and steer VSMCs to switch from a contractile phenotype to a pro-atherogenic phenotype. Alternatively, several reports have suggested that Neo-1 in the myelocytic compartment can potentially drive a pro-inflammatory response in different tissues (Konig et al., 2012; Mirakaj et al., 2012; Schlegel et al., 2014; Schlegel et al., 2019). Gulati et al. (2019) using low-input RNA-seq technique, have shown that Neo-1 positivity in myelocytic cells is associated with a pro-inflammatory signature of gene expression. In addition, motif enrichment analysis reveals that Neo-1 specifically enhances NF-κB activity (Gulati et al., 2019), which is in agreement with our data that Neo-1 critically regulates NF-κB activity in endothelial cells (**Figure 3**). These observations combined appear to suggest that Neo-1 might promote vascular inflammation and hence atherogenesis by skewing the phenotype of macrophages. Second, we relied on the induction of adhesion molecules and leukocyte adhesion as a readout to evaluate the effect of Neo-1 on endothelial dysfunction. Other aspects of endothelial deregulation in the context of atherogenesis should also be considered. For instance, aberrant neovascularization, or formation of new capillaries by endothelial cells, within the atherosclerotic plaque is observed in humans and model animals (Kwon et al., 1998; Moreno et al., 2006). In contrast, inhibition of aberrant angiogenesis can cause regression of atherosclerosis (Moulton et al., 1999; Gossl et al., 2009). Of interest, several independent reports demonstrate that Neo-1 activation elicits strong angiogenic response in endothelial cells (Park et al., 2004; Prieto et al., 2017; Yao et al., 2020). Therefore, attenuation of atherosclerosis by Neo-1 inhibition could be attributed to the suppression of aberrant neovascularization. Third, it is not clear at this point the signaling cascade that mediates the pro-atherogenic effect of Neo-1 in endothelial cells. Typically, Neo-1 signaling can be activated by one of the netrins (e.g., netrin 1). Indeed, netrin 1 deficiency has been shown to attenuate atherosclerosis in $Ldlr^{-/-}$ mice likely through evicting macrophages from the plaque and reining in chronic inflammation (van Gils et al., 2012). Alternatively, the protein structure of Neo-1 shares high degree of resemblance to that of pattern recognition receptors (PRRs); both possess several tandem immunoglobulin (Ig)-like domains and fibronectin type III domains (FnIII) (Wilson and Key, 2007). Because oxLDL can bind to and activate several different types of PRRs, including scavenger receptor (MSR1) and CD36, it is tempting to propose that Neo-1 could be directly bound and activated by oxLDL in endothelial cells to provoke a pro-atherogenic response. These unsolved issues clearly deserve further attention in the future.

We show here that CREB1 is necessary for oxLDL induced trans-activation of Neo-1 in endothelial cells by interacting with and recruiting BAF47. The pathophysiological relevance of this finding, however, remains to be determined. On the one hand, CREB1 down-regulation is observed in the vessels isolated from the atherosclerotic mice compared to the normal mice (Schauer et al., 2010). On the other hand, activation of the pro-inflammatory cytokine IL-17 by CREB1 is directly responsible for macrophages accumulation and the ensuing inflammation in the atherosclerotic plaque in mice (Kotla et al., 2013). Equally ambiguous is the role of CREB1 plays in endothelial homeostasis. A wealth of data seems to suggest that CREB1 deletion in endothelial cells may lead to increased inflammatory response and disrupted barrier function (Chava et al., 2012; Xiong et al., 2020). In contrast, CREB1 can promote leukocyte adhesion by directly binding to and activating the transcription of ICAM1 in human umbilical endothelial cells (Hadad et al., 2011). This apparent discrepancy likely alludes to the cell-type and context specific effects of CREB1 in atherogenesis. Future studies should exploit spatiotemporally controlled CREB1 transgenic animal models to carefully delineate the role of CREB1 in atherosclerosis.

In conclusion, our data unveil a previously unrecognized role for the CREB1-BAF47-Neo1 axis in regulating endothelial dysfunction that might potentially contribute to atherosclerosis. Additional functional and mechanistic studies are warranted to further validate the impact of this axis *in vivo* so that novel therapeutic solutions derived from this study can be devised in the intervention of coronary heart disease.

DATA AVAILABILITY STATEMENT

The original contributions presented in the study are included in the article/**Supplementary Material**, further inquiries can be directed to the corresponding authors.

ETHICS STATEMENT

The animal study was reviewed and approved by the Nanjing Medical University Ethics Committee on Humane Treatment of Experimental Animals.

AUTHOR CONTRIBUTIONS

YZ, NL, and XK conceived project; NL, HL, YX, JC, and YZ designed experiments, performed experiments, collected data,

and analyzed data; All authors wrote the manuscript; YZ, XK, and NL handled funding.

FUNDING

This work was supported by the National Natural Science Foundation of China (81870349), Hainan Key Research and Development Fund (ZDYF2021SHFZ089), Key Laboratory of Emergency and Trauma (KLET-202019), and the Nanjing Medical University Scientific Development Fund.

SUPPLEMENTARY MATERIAL

The Supplementary Material for this article can be found online at: https://www.frontiersin.org/articles/10.3389/fcell.2022.803029/full#supplementary-material

REFERENCES

Blankenberg, S., Barbaux, S., and Tiret, L. (2003). Adhesion Molecules and Atherosclerosis. *Atherosclerosis* 170, 191–203. doi:10.1016/s0021-9150(03)00097-2

Chakraborty, R., Chatterjee, P., Dave, J. M., Ostriker, A. C., Greif, D. M., Rzucidlo, E. M., et al. (2021). Targeting Smooth Muscle Cell Phenotypic Switching in Vascular Disease. *JVS: Vasc. Sci.* 2, 79–94. doi:10.1016/j.jvssci.2021.04.001

Chava, K. R., Tauseef, M., Sharma, T., and Mehta, D. (2012). Cyclic AMP Response Element-Binding Protein Prevents Endothelial Permeability Increase through Transcriptional Controlling p190RhoGAP Expression. *Blood* 119, 308–319. doi:10.1182/blood-2011-02-339473

Chen, B., Zhao, Q., Xu, T., Yu, L., Zhuo, L., Yang, Y., et al. (2020). BRG1 Activates PR65A Transcription to Regulate NO Bioavailability in Vascular Endothelial Cells. *Front. Cel Dev. Biol.* 8, 774. doi:10.3389/fcell.2020.00774

Coarfa, C., Grimm, S. L., Katz, T., Zhang, Y., Jangid, R. K., Walker, C. L., et al. (2020). Epigenetic Response to Hyperoxia in the Neonatal Lung Is Sexually Dimorphic. *Redox Biol.* 37, 101718. doi:10.1016/j.redox.2020.101718

Collins, T., Read, M. A., Neish, A. S., Whitley, M. Z., Thanos, D., and Maniatis, T. (1995). Transcriptional Regulation of Endothelial Cell Adhesion Molecules: NF-κB and Cytokine-inducible Enhancers. *FASEB j.* 9, 899–909. doi:10.1096/fasebj.9.10.7542214

Cominacini, L., Garbin, U., Pasini, A. F., Davoli, A., Campagnola, M., Contessi, G. B., et al. (1997). Antioxidants Inhibit the Expression of Intercellular Cell Adhesion Molecule-1 and Vascular Cell Adhesion Molecule-1 Induced by Oxidized LDL on Human Umbilical Vein Endothelial Cells. *Free Radic. Biol. Med.* 22, 117–127. doi:10.1016/s0891-5849(96)00271-7

Galkina, E., and Ley, K. (2007). Vascular Adhesion Molecules in Atherosclerosis. *Atvb* 27, 2292–2301. doi:10.1161/atvbaha.107.149179

Gareus, R., Kotsaki, E., Xanthoulea, S., Van Der Made, I., Gijbels, M. J. J., Kardakaris, R., et al. (2008). Endothelial Cell-specific NF-Kb Inhibition Protects Mice from Atherosclerosis. *Cel Metab.* 8, 372–383. doi:10.1016/j.cmet.2008.08.016

Gimbrone, M. A., Jr., and García-Cardeña, G. (2016). Endothelial Cell Dysfunction and the Pathobiology of Atherosclerosis. *Circ. Res.* 118, 620–636. doi:10.1161/circresaha.115.306301

Gössl, M., Herrmann, J., Tang, H., Versari, D., Galili, O., Mannheim, D., et al. (2009). Prevention of Vasa Vasorum Neovascularization Attenuates Early Neointima Formation in Experimental Hypercholesterolemia. *Basic Res. Cardiol.* 104, 695–706. doi:10.1007/s00395-009-0036-0

Gulati, G. S., Zukowska, M., Noh, J. J., Zhang, A., Wesche, D. J., Sinha, R., et al. (2019). Neogenin-1 Distinguishes between Myeloid-Biased and Balanced Hoxb5+ Mouse Long-Term Hematopoietic Stem Cells. *Proc. Natl. Acad. Sci. USA* 116, 25115–25125. doi:10.1073/pnas.1911024116

Hadad, N., Tuval, L., Elgazar-Carmom, V., Levy, R., and Levy, R. (2011). Endothelial ICAM-1 Protein Induction Is Regulated by Cytosolic Phospholipase A2α via Both NF-Kb and CREB Transcription Factors. *J.I.* 186, 1816–1827. doi:10.4049/jimmunol.1000193

Hadi, T., Boytard, L., Silvestro, M., Alebrahim, D., Jacob, S., Feinstein, J., et al. (2018). Macrophage-derived Netrin-1 Promotes Abdominal Aortic Aneurysm Formation by Activating MMP3 in Vascular Smooth Muscle Cells. *Nat. Commun.* 9, 5022. doi:10.1038/s41467-018-07495-1

Hong, W., Kong, M., Qi, M., Bai, H., Fan, Z., Zhang, Z., et al. (2020). BRG1 Mediates Nephronectin Activation in Hepatocytes to Promote T Lymphocyte Infiltration in ConA-Induced Hepatitis. *Front Cel Dev Biol* 8, 587502. doi:10.3389/fcell.2020.587502

Huangfu, N., Wang, Y., Xu, Z., Zheng, W., Tao, C., Li, Z., et al. (2021). TDP43 Exacerbates Atherosclerosis Progression by Promoting Inflammation and Lipid Uptake of Macrophages. *Front. Cel Dev. Biol.* 9, 687169. doi:10.3389/fcell.2021.687169

Johannessen, M., Delghandi, M. P., and Moens, U. (2004). What Turns CREB on? *Cell Signal.* 16, 1211–1227. doi:10.1016/j.cellsig.2004.05.001

Kadoch, C., and Crabtree, G. R. (2013). Reversible Disruption of mSWI/SNF (BAF) Complexes by the SS18-SSX Oncogenic Fusion in Synovial Sarcoma. *Cell* 153, 71–85. doi:10.1016/j.cell.2013.02.036

Khan, B. V., Parthasarathy, S. S., Alexander, R. W., and Medford, R. M. (1995). Modified Low Density Lipoprotein and its Constituents Augment Cytokine-Activated Vascular Cell Adhesion Molecule-1 Gene Expression in Human Vascular Endothelial Cells. *J. Clin. Invest.* 95, 1262–1270. doi:10.1172/jci117776

König, K., Gatidou, D., Granja, T., Meier, J., Rosenberger, P., and Mirakaj, V. (2012). The Axonal Guidance Receptor Neogenin Promotes Acute Inflammation. *PLoS One* 7, e32145. doi:10.1371/journal.pone.0032145

Kotla, S., Singh, N. K., Heckle, M. R., Tigyi, G. J., and Rao, G. N. (2013). The Transcription Factor CREB Enhances interleukin-17A Production and Inflammation in a Mouse Model of Atherosclerosis. *Sci. Signal.* 6, ra83. doi:10.1126/scisignal.2004214

Kwon, H. M., Sangiorgi, G., Ritman, E. L., Mckenna, C., Holmes, D. R., Jr., Schwartz, R. S., et al. (1998). Enhanced Coronary Vasa Vasorum Neovascularization in Experimental Hypercholesterolemia. *J. Clin. Invest.* 101, 1551–1556. doi:10.1172/jci1568

Li, N., Liu, S., Zhang, Y., Yu, L., Hu, Y., Wu, T., et al. (2020). Transcriptional Activation of Matricellular Protein Spondin2 (SPON2) by BRG1 in Vascular Endothelial Cells Promotes Macrophage Chemotaxis. *Front. Cel Dev. Biol.* 8, 794. doi:10.3389/fcell.2020.00794

Liao, J., An, X., Yang, X., Lin, Q.-Y., Liu, S., Xie, Y., et al. (2020). Deficiency of LMP10 Attenuates Diet-Induced Atherosclerosis by Inhibiting Macrophage Polarization and Inflammation in Apolipoprotein E Deficient Mice. *Front. Cel Dev. Biol.* 8, 592048. doi:10.3389/fcell.2020.592048

Libby, P., and Hansson, G. K. (2015). Inflammation and Immunity in Diseases of the Arterial Tree. *Circ. Res.* 116, 307–311. doi:10.1161/circresaha.116.301313

Libby, P., Lichtman, A. H., and Hansson, G. K. (2013). Immune Effector Mechanisms Implicated in Atherosclerosis: from Mice to Humans. *Immunity* 38, 1092–1104. doi:10.1016/j.immuni.2013.06.009

Libby, P. (2021a). The Biology of Atherosclerosis Comes Full circle: Lessons for Conquering Cardiovascular Disease. *Nat. Rev. Cardiol.* 18, 683–684. doi:10.1038/s41569-021-00609-1

Libby, P. (2021b). The Changing Landscape of Atherosclerosis. *Nature* 592, 524–533. doi:10.1038/s41586-021-03392-8

Liu, L., Zhao, Q., Kong, M., Mao, L., Yang, Y., and Xu, Y. (2021). Myocardin-related Transcription Factor A (MRTF-A) Regulates Integrin Beta 2 Transcription to Promote Macrophage Infiltration and Cardiac Hypertrophy in Mice. *Cardiovasc. Res.* 22, cvab110. doi:10.1093/cvr/cvab110

Livesey, F. J. (1999). Netrins and Netrin Receptors. *Cell Mol. Life Sci. (Cmls)* 56, 62–68. doi:10.1007/s000180050006

Lv, F., Shao, T., Xue, Y., Miao, X., Guo, Y., Wang, Y., et al. (2021). Dual Regulation of Tank Binding Kinase 1 by BRG1 in Hepatocytes Contributes to Reactive

Oxygen Species Production. *Front. Cel Dev. Biol.* 9, 745985. doi:10.3389/fcell.2021.745985

Maity, J., Deb, M., Greene, C., and Das, H. (2020). KLF2 Regulates Dental Pulp-Derived Stem Cell Differentiation through the Induction of Mitophagy and Altering Mitochondrial Metabolism. *Redox Biol.* 36, 101622. doi:10.1016/j.redox.2020.101622

Martí, J. M., Garcia-Diaz, A., Delgado-Bellido, D., O'valle, F., González-Flores, A., Carlevaris, O., et al. (2021). Selective Modulation by PARP-1 of HIF-1α-Recruitment to Chromatin during Hypoxia Is Required for Tumor Adaptation to Hypoxic Conditions. *Redox Biol.* 41, 101885. doi:10.1016/j.redox.2021.101885

Mayr, B. M., Guzman, E., and Montminy, M. (2005). Glutamine Rich and Basic Region/leucine Zipper (bZIP) Domains Stabilize cAMP-Response Element-Binding Protein (CREB) Binding to Chromatin. *J. Biol. Chem.* 280, 15103–15110. doi:10.1074/jbc.m414144200

Mirakaj, V., Jennewein, C., König, K., Granja, T., and Rosenberger, P. (2012). The Guidance Receptor Neogenin Promotes Pulmonary Inflammation during Lung Injury. *FASEB j.* 26, 1549–1558. doi:10.1096/fj.11-200063

Moreno, P. R., Purushothaman, K.-R., Sirol, M., Levy, A. P., and Fuster, V. (2006). Neovascularization in Human Atherosclerosis. *Circulation* 113, 2245–2252. doi:10.1161/circulationaha.105.578955

Moulton, K. S., Heller, E., Konerding, M. A., Flynn, E., Palinski, W., and Folkman, J. (1999). Angiogenesis Inhibitors Endostatin or TNP-470 Reduce Intimal Neovascularization and Plaque Growth in Apolipoprotein E-Deficient Mice. *Circulation* 99, 1726–1732. doi:10.1161/01.cir.99.13.1726

Park, K. W., Crouse, D., Lee, M., Karnik, S. K., Sorensen, L. K., Murphy, K. J., et al. (2004). The Axonal Attractant Netrin-1 Is an Angiogenic Factor. *Proc. Natl. Acad. Sci.* 101, 16210–16215. doi:10.1073/pnas.0405984101

Prieto, C. P., Ortiz, M. C., Villanueva, A., Villarroel, C., Edwards, S. S., Elliott, M., et al. (2017). Netrin-1 Acts as a Non-canonical Angiogenic Factor Produced by Human Wharton's Jelly Mesenchymal Stem Cells (WJ-MSC). *Stem Cel Res Ther* 8, 43. doi:10.1186/s13287-017-0494-5

Ridker, P. M., Everett, B. M., Thuren, T., Macfadyen, J. G., Chang, W. H., Ballantyne, C., et al. (2017). Antiinflammatory Therapy with Canakinumab for Atherosclerotic Disease. *N. Engl. J. Med.* 377, 1119–1131. doi:10.1056/nejmoa1707914

Savarese, G., and Lund, L. H. (2017). Global Public Health Burden of Heart Failure. *Card. Fail. Rev.* 03, 7–11. doi:10.15420/cfr.2016:25:2

Schauer, I. E., Knaub, L. A., Lloyd, M., Watson, P. A., Gliwa, C., Lewis, K. E., et al. (2010). CREB Downregulation in Vascular Disease. *Atvb* 30, 733–741. doi:10.1161/atvbaha.109.199133

Schlegel, M., Granja, T., Kaiser, S., Körner, A., Henes, J., König, K., et al. (2014). Inhibition of Neogenin Dampens Hepatic Ischemia-Reperfusion Injury. *Crit. Care Med.* 42, e610–e619. doi:10.1097/ccm.0000000000000485

Schlegel, M., Körner, A., Kaussen, T., Knausberg, U., Gerber, C., Hansmann, G., et al. (2019). Inhibition of Neogenin Fosters Resolution of Inflammation and Tissue Regeneration. *J. Clin. Invest.* 129, 2165. doi:10.1172/jci128681

Steinberg, D., and Witztum, J. L. (2010). Oxidized Low-Density Lipoprotein and Atherosclerosis. *Atvb* 30, 2311–2316. doi:10.1161/atvbaha.108.179697

Tak, P. P., and Firestein, G. S. (2001). NF-κB: a Key Role in Inflammatory Diseases. *J. Clin. Invest.* 107, 7–11. doi:10.1172/jci11830

Takei, A., Huang, Y., and Lopes-Virella, M. F. (2001). Expression of Adhesion Molecules by Human Endothelial Cells Exposed to Oxidized Low Density Lipoprotein Influences of Degree of Oxidation and Location of Oxidized LDL. *Atherosclerosis* 154, 79–86. doi:10.1016/s0021-9150(00)00465-2

Van Gils, J. M., Derby, M. C., Fernandes, L. R., Ramkhelawon, B., Ray, T. D., Rayner, K. J., et al. (2012). The Neuroimmune Guidance Cue Netrin-1 Promotes Atherosclerosis by Inhibiting the Emigration of Macrophages from Plaques. *Nat. Immunol.* 13, 136–143. doi:10.1038/ni.2205

Wang, J.-N., Yang, Q., Yang, C., Cai, Y.-T., Xing, T., Gao, L., et al. (2020). Smad3 Promotes AKI Sensitivity in Diabetic Mice via Interaction with P53 and Induction of NOX4-dependent ROS Production. *Redox Biol.* 32, 101479. doi:10.1016/j.redox.2020.101479

Wang, S., Chen, Z., Zhu, S., Lu, H., Peng, D., Soutto, M., et al. (2020). PRDX2 Protects against Oxidative Stress Induced by *H. pylori* and Promotes Resistance to Cisplatin in Gastric Cancer. *Redox Biol.* 28, 101319. doi:10.1016/j.redox.2019.101319

Wilson, N. H., and Key, B. (2007). Neogenin: One Receptor, many Functions. *Int. J. Biochem. Cel Biol.* 39, 874–878. doi:10.1016/j.biocel.2006.10.023

Xiong, S., Hong, Z., Huang, L. S., Tsukasaki, Y., Nepal, S., Di, A., et al. (2020). IL-1β Suppression of VE-Cadherin Transcription Underlies Sepsis-Induced Inflammatory Lung Injury. *J. Clin. Invest.* 130, 3684–3698. doi:10.1172/jci136908

Yang, Y., Wang, H., Zhao, H., Miao, X., Guo, Y., Zhuo, L., et al. (2021). A GSK3-SRF Axis Mediates Angiotensin II Induced Endothelin Transcription in Vascular Endothelial Cells. *Front. Cel Dev. Biol.* 9, 698254. doi:10.3389/fcell.2021.698254

Yao, L.-L., Hu, J.-X., Li, Q., Lee, D., Ren, X., Zhang, J.-S., et al. (2020). Astrocytic Neogenin/netrin-1 Pathway Promotes Blood Vessel Homeostasis and Function in Mouse Cortex. *J. Clin. Invest.* 130, 6490–6509. doi:10.1172/jci132372

Zhang, Y., Wang, H., Song, M., Xu, T., Chen, X., Li, T., et al. (2020). Brahma-Related Gene 1 Deficiency in Endothelial Cells Ameliorates Vascular Inflammatory Responses in Mice. *Front. Cel Dev. Biol.* 8, 578790. doi:10.3389/fcell.2020.578790

Conflict of Interest: The authors declare that the research was conducted in the absence of any commercial or financial relationships that could be construed as a potential conflict of interest.

Publisher's Note: All claims expressed in this article are solely those of the authors and do not necessarily represent those of their affiliated organizations, or those of the publisher, the editors and the reviewers. Any product that may be evaluated in this article, or claim that may be made by its manufacturer, is not guaranteed or endorsed by the publisher.

frontiers in Cell and Developmental Biology

ORIGINAL RESEARCH
published: 03 February 2022
doi: 10.3389/fcell.2022.840866

Associations of Visceral Adipose Tissue, Circulating Protein Biomarkers, and Risk of Cardiovascular Diseases: A Mendelian Randomization Analysis

Yunying Huang[1†], Yaozhong Liu[1†], Yingxu Ma[1], Tao Tu[1], Na Liu[1], Fan Bai[2], Yichao Xiao[1], Chan Liu[3], Zhengang Hu[1], Qiuzhen Lin[1], Mohan Li[1], Zuodong Ning[1], Yong Zhou[1], Xiquan Mao[1] and Qiming Liu[1*]*

[1]Department of Cardiovascular Medicine, Second Xiangya Hospital, Central South University, Changsha, China, [2]Department of Cardiovascular Surgery, Second Xiangya Hospital, Central South University, Changsha, China, [3]Department of International Medicine, Second Xiangya Hospital, Central South University, Changsha, China

Aim: To evaluate the genetic associations of visceral adipose tissue (VAT) mass with metabolic risk factors and cardiovascular disease (CVD) endpoints and to construct a network analysis about the underlying mechanism using Mendelian randomization (MR) analysis.

Methods and Results: Using summary statistics from genome-wide association studies (GWAS), we conducted the two-sample MR to assess the effects of VAT mass on 10 metabolic risk factors and 53 CVD endpoints. Genetically predicted VAT mass was associated with metabolic risk factors, including triglyceride (odds ratio, OR, 1.263 [95% confidence interval, CI, 1.203–1.326]), high-density lipoprotein cholesterol (OR, 0.719 [95% CI, 0.678–0.763]), type 2 diabetes (OR, 2.397 [95% CI, 1.965–2.923]), fasting glucose (OR, 1.079 [95% CI, 1.046–1.113]), fasting insulin (OR, 1.194 [95% CI, 1.16–1.229]), and insulin resistance (OR, 1.204 [95% CI, 1.16–1.25]). Genetically predicted VAT mass was associated with CVD endpoints, including atrial fibrillation (OR, 1.414 [95% CI, 1.332 = 1.5]), coronary artery disease (OR, 1.573 [95% CI, 1.439 = 1.72]), myocardial infarction (OR, 1.633 [95% CI, 1.484 =1.796]), heart failure (OR, 1.711 [95% CI, 1.599–1.832]), any stroke (OR, 1.29 [1.193–1.394]), ischemic stroke (OR, 1.292 [1.189–1.404]), large artery stroke (OR, 1.483 [1.206–1.823]), cardioembolic stroke (OR, 1.261 [1.096–1.452]), and intracranial aneurysm (OR, 1.475 [1.235–1.762]). In the FinnGen study, the relevance of VAT mass to coronary heart disease, stroke, cardiac arrhythmia, vascular diseases, hypertensive heart disease, and cardiac death was found. In network analysis to identify the underlying mechanism between VAT and CVDs, VAT mass was positively associated with 23 cardiovascular-related proteins (e.g., Leptin, Hepatocyte growth factor, interleukin-16), and inversely with 6 proteins (e.g., Galanin peptides, Endothelial cell-specific molecule 1). These proteins were further associated with 32 CVD outcomes.

OPEN ACCESS

Edited by:
Hidekazu Kondo,
Oita University, Japan

Reviewed by:
Ichitaro Abe,
Beth Israel Deaconess Medical Center and Harvard Medical School, United States
Akira Fukui,
Oita University, Japan

***Correspondence:**
Qiming Liu
qimingliu@csu.edu.cn
Xiquan Mao
Xiquan07@csu.edu.cn

[†]These authors have contributed equally to this work

Specialty section:
This article was submitted to Cellular Biochemistry, a section of the journal Frontiers in Cell and Developmental Biology

Received: 21 December 2021
Accepted: 10 January 2022
Published: 03 February 2022

Citation:
Huang Y, Liu Y, Ma Y, Tu T, Liu N, Bai F, Xiao Y, Liu C, Hu Z, Lin Q, Li M, Ning Z, Zhou Y, Mao X and Liu Q (2022) Associations of Visceral Adipose Tissue, Circulating Protein Biomarkers, and Risk of Cardiovascular Diseases: A Mendelian Randomization Analysis. Front. Cell Dev. Biol. 10:840866. doi: 10.3389/fcell.2022.840866

Conclusion: Mendelian randomization analysis has shown that VAT mass was associated with a wide range of CVD outcomes including coronary heart disease, cardiac arrhythmia, vascular diseases, and stroke. A few circulating proteins may be the mediators between VAT and CVDs.

Keywords: obesity, visceral adipose tissue, cardiovascular disease, mendelian randomization, two-sample MR

INTRODUCTION

Obesity is an established risk factor of cardiovascular disease (CVD) (Powell-Wiley et al., 2021). However, some epidemiological studies revealed the protective effect of obesity, classified by body mass index (BMI), on CVD outcomes and questioned the nature of the relationship between obesity and CVDs (Antonopoulos et al., 2016a). This paradoxical phenomenon, also known as the "obesity paradox" or "BMI paradox," indicates that BMI or other general adiposity measurements cannot assess the actual metabolic status and body fat distribution. Central adiposity, especially visceral adipose tissue (VAT)—adiposity accumulated around internal organs—is expected to reflect nature dysmetabolic state in obesity compared with general adiposity. The volume and quality of VAT assessed by computed tomography (CT) were more closely related to metabolic syndrome components than the subcutaneous compartment, regardless of BMI (Shah et al., 2014; Abraham et al., 2015). The associations between VAT area, measured by bioelectrical impedance analysis (BIA), and metabolic risk factors were observed among obese and non-obese participants (Tatsumi et al., 2017).

VAT can be categorized into abdominal adiposity and intrathoracic adiposity. Intrathoracic fat can be further classified as epicardial adipose tissue (EAT), pericardial adipose tissue (PAT), and perivascular adipose tissue (PVAT) according to anatomic location (Oikonomou and Antoniades, 2019). Given the biological heterogeneity of different depots (Hocking et al., 2010; Gaborit et al., 2015), VAT expansion could be both positively or negatively associated with the cardiovascular system (Akoumianakis and Antoniades, 2017). Additionally, CVDs are influenced by VAT and, in turn, influence VAT, especially the adipose depots that anatomical proximity to the cardiovascular system. Epidemiological studies were unable to determine the causal relationship between VAT expansion and CVD outcomes. Together, the relationships between VAT accumulation and the incidence of CVDs are still unclear.

VAT is energy storage and a dynamic endocrine organ that secretes bioactive factors into circulation (Scheja and Heeren, 2019; Ragino et al., 2020). The secretome of VAT includes cytokines (TNF-α, IL-1beta, IL-8), hormones (leptin, adiponectin), growth factors, and others contributing to the pleiotropic effect of VAT. However, the associations of visceral adiposity with a wide range of protein biomarkers of cardiometabolic diseases have not been identified thoroughly. Expanding knowledge of the role of the VAT expansion in cardiometabolic biomarkers leads to the discovery of novel diagnostic biomarkers and therapeutic targets.

It is challenging for observational studies to demonstrate causality between VAT accumulation and CVDs due to confounding and reverse causation bias. We employed Mendelian randomization (MR) analysis to address these issues. MR analysis uses randomly allocated genetic variants as genetic instruments to determine the causal relationship between an exposure and an outcome of interest (Burgess et al., 2019). In the primary study, we implemented the MR approach to evaluate the genetically causal effect of VAT mass on 10 cardiometabolic traits and 53 cardiovascular disease endpoints. In the secondary study, we involved 90 circulating proteins in a network MR analysis to explore the potential mediators engaged in the associations between VAT mass and CVD outcomes. Here, we presented the most comprehensive assessment of the causal relationship between VAT mass and cardiovascular disease to date.

MATERIALS AND METHODS

This study relied on publicly available summary statistics from large-scale GWAS. Ethical approval was obtained for all original studies. The data used in this study were analyzed from 14 June 2021 to 1 October 2021.

Genetic Instruments for Measuring Visceral Adipose Tissue

The genetic association for VAT mass was retrieved from a large GWAS (Karlsson et al., 2019) for predicting VAT mass in 325,153 white British UKB participants. We selected genome-wide significant single nucleotide polymorphisms (SNPs, $p < 5 \times 10^{-8}$) and excluded correlated SNPs using the "clump_data" function in "TwosampleMR" packages (Hemani et al., 2018) in R software (linkage disequilibrium [LD] R^2 = .001, >10,000 kb) and attained 221 independent SNPs as instrument variables for VAT mass (**Supplementary Table S1**).

Summary Data for Cardiovascular Disease Outcomes

Our outcome variables include 10 metabolic risk factors and 10 CVD endpoints in the primary analysis, 43 CVD endpoints in the secondary analysis. Detailed sample source information is available in **Supplementary Table S2**.

For metabolic risk factors, we used publicly available summarized data for genetic associations with high-density lipoprotein cholesterol (HDL-C), low-density lipoprotein cholesterol (LDL-C), total cholesterol (TC), and

triglycerides (TG) from the Global Lipids Genetics Consortium (Willer et al., 2013); systolic blood pressure (SBP) and diastolic blood pressure (DBP) from the International Consortium of Blood Pressure (Evangelou et al., 2018); type 2 diabetes (T2D) from the Diabetes Genetics Replication and Meta-analysis Consortium (Morris et al., 2012); fasting glucose, fasting insulin, and insulin resistance from the Meta-Analyses of Glucose and Insulin related traits Consortium (Dupuis et al., 2010). These consortia do not include any participants from the UKB.

For CVD endpoints, we used publicly available summarized data for genetic associations with atrial fibrillation (AF, n = 1,030,836 individuals of European ancestry) from Nielsen's study (Nielsen et al., 2018); coronary artery disease (CAD, n = 184,305 individuals of mainly European ancestry) and myocardial infarction (MI, n = 171,857 individuals of mainly European ancestry) from the Coronary Artery Disease Genome-wide Replication and Meta-analysis plus The Coronary Artery Disease Genetics Consortium (Nikpay et al., 2015); heart failure (HF, n = 977,323 individuals of European ancestry) from the Heart Failure Molecular Epidemiology for Therapeutic Targets Consortium (Shah et al., 2020); any stroke (AS, with ischemic stroke [IS] and its three subtypes including large artery stroke [LAS], small vessel stroke [SVS], and cardioembolic stroke [CES], n = 150,765 ~ 446,696 of European ancestry) from the International Stroke Genetics Consortium (Malik et al., 2018); and intracranial aneurysm (IA) from the Intracranial Aneurysm Working Group (Bakker et al., 2020). These datasets included primarily or only individuals of European descent, and no dataset included participants from the UKB study except AF and HF. To avoid biases in causal estimates introduced by sample overlap, we chose the maximal sample sizes in GWAS while minimizing sample overlap between exposures and outcomes (Burgess et al., 2016). Therefore, we omitted the Neale Lab UKB GWAS of CVD endpoints. Similarly, more recent and larger GWAS datasets exist that include the UKB participants for CAD; therefore, we did not utilize the UKB CAD dataset in the present study.

We then leveraged FinnGen Datafreeze 5 release (publicly available 14 May 2021) (FinnGen, 2020) to expand the number of CVD endpoints and replicate the associations with AF, CAD, MI, HF, and stroke, which we selected from independent consortia. The FinnGen Datafreeze 5 analysis included only European ancestry, with summary data for 2,803 available endpoints. We included 43 CVD endpoints from FinnGen release 5, and the sample size ranged from 117,755 to 218,792.

Finally, we used publicly available summarized data for genetic associations with 90 cardiovascular-related circulating proteins from the Systematic and Combined Analysis of Olink Proteins Consortium (Folkersen et al., 2020), many of which were established prognostic biomarkers or treatment targets, measured by the Olink proximity extension assay (PEA) cardiovascular I (CVD-I) panel in 30,931 individuals across 15 studies.

Statistical Analysis and Sensitivity Analysis

All analyses were performed using the Two-Sample MR (Hemani et al., 2018) and Mendelian Randomization (Yavorska and Burgess, 2017) packages. Before each MR analysis, if a particular SNP was not present in the outcome dataset, we searched and used the proxy SNP (LD $R^2 \geq 0.8$). Exposure and outcome data were then harmonized to ensure that the effect of an SNP on exposure and the effect of that SNP on the outcome corresponded with the same allele.

In the primary analysis, we analyzed the effect of VAT mass on 10 metabolic risk factors, 10 CVD endpoints from independent consortiums, and 43 CVD endpoints from FinnGen study. We used inverse variance–weighted (IVW) MR as the primary method (Burgess et al., 2013), which provided the highest precision while assuming that all SNPs are valid instrumental variables (Burgess et al., 2017). The IVW method provides an unbiased estimate when no horizontal pleiotropy is present or horizontal pleiotropy is balanced. The horizontal pleiotropy exists when the instrumental variant affects pathways other than those of the exposure, which indicates that the instrument is not independent of the outcome. The unbalanced horizontal pleiotropy would disturb the relationship between exposure and outcome of interest. To account for potential pleiotropy, we applied the MR-Egger analysis, weighted median-based regression method, and contamination mixture method as sensitivity analyses. The MR-Egger analysis has low precision but can correct pleiotropy and provide casual inference, even if all genetic variants have pleiotropic effects (Burgess et al., 2017). The weighted median estimates are almost as precise as IVW estimates but require that at least half of the MR instrument weights on the exposure are valid (Burgess et al., 2017). The contamination mixture method is the latest developed method with the lowest mean squared error across a range of realistic scenarios (Burgess et al., 2020). A consistent effect across all four methods shall guarantee high robustness. The Cochran Q heterogeneity test (Bowden et al., 2019) was used to inspect pleiotropy. The MR-Egger intercept test (Bowden et al., 2017) was used to inspect unbalanced pleiotropy. P values of the Egger intercept test ($P_{\text{Egger intercept}}$) > .05 indicate no directional pleiotropy between the exposure and outcome of interest. The Steiger directionality test was used to test the causal direction between the hypothesized exposures and outcomes (Hemani et al., 2017). We further conducted a reverse-MR analysis to investigate whether the 10 metabolic risk factors and 10 CVD endpoints affect VAT mass. The genetics instrument for CVD endpoints was selected using the same method as VAT.

We further conducted a network MR analysis to demonstrate the potential mechanisms underlying the associations between VAT and CVDs. Firstly, we analyzed the causal effect of VAT on 90 circulating proteins. Secondly, we analyzed the causal effect of circulating proteins on the total 63 CVD endpoints. In the MR analysis of circulating proteins to CVDs, if there was only 1 SNP available, the "Wald Ratio" method was applied. Only those pairs have consistent directions with outcomes between

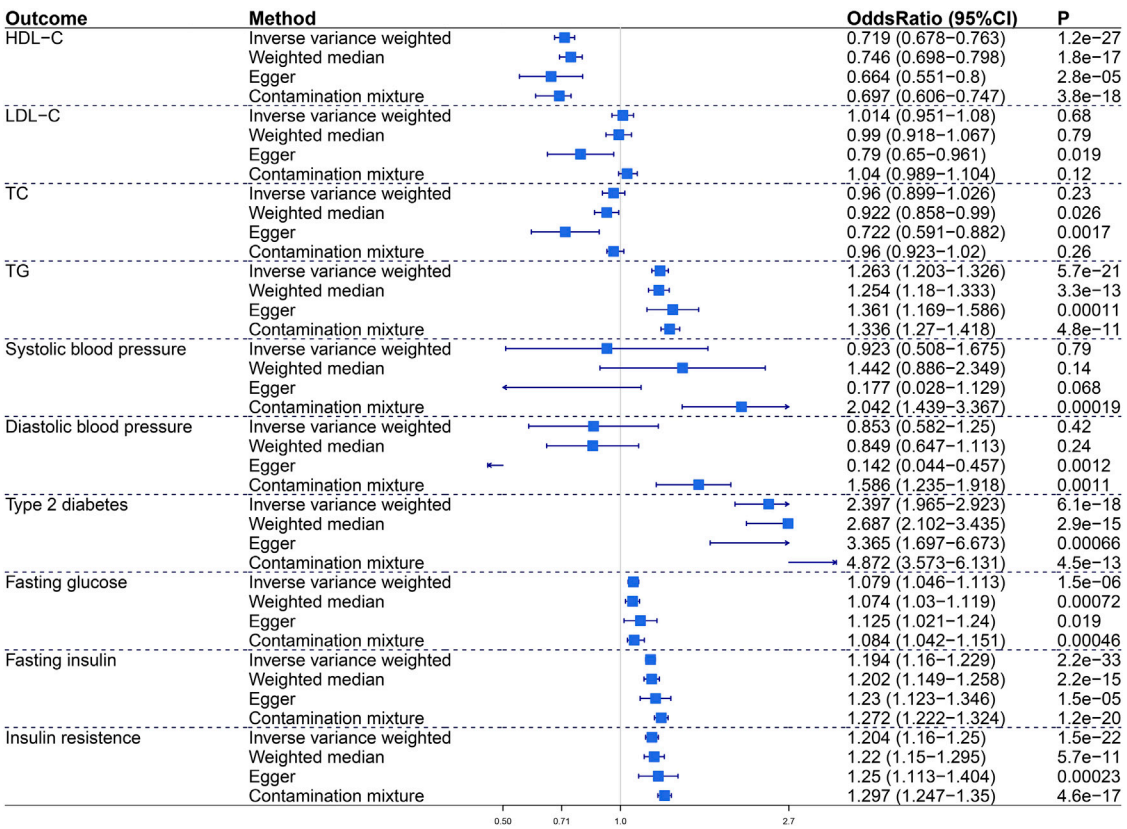

FIGURE 1 | The causal effect of visceral adiposity on 10 metabolic risk factors. Odds ratios are expressed per 1-SD increase in genetically determined VAT mass. CI, confidence interval; HDL-C, high-density lipoprotein cholesterol; LDL-C, low-density lipoprotein cholesterol; TC, total cholesterol; TG, triglycerides.

the associations of VAT with proteins, proteins with CVDs, and VAT with CVDs (beta1*beta2*beta3 > 0, and P1, P2, P3 < .05) were reserved. Finally, 60 VAT-proteins-CVDs axes were identified.

RESULTS

Causal Effect of Visceral Adiposity on Metabolic Risk Factors

We assessed the impact of visceral adiposity on metabolic risk factors including lipid profile (HDL-C, LDL-C, TC, TG), blood pressure (SBP, DBP), glycemic traits (fasting glucose, fasting insulin, insulin resistance), and T2D (**Figure 1**). In primary IVW analysis, genetically predicted increased VAT mass was associated with decreased HDL-C (odds ratio, OR, .719; 95% confidence intercept, CI, .678–0.763; p = 1.2e−27), increased TG (OR, 1.263; 95% CI, 1.203–1.326; p = 5.7e−21), increased T2D (OR, 2.397; 95% CI, 1.965–2.923; p = 6.1e−18), increased fasting glucose (OR, 1.079; 95% CI, 1.046–1.113; p = 1.5e−6), increased fasting insulin (OR, 1.194; 95% CI, 1.16–1.229; p = 2.2e−33), and increased insulin resistance (OR, 1.204; 95% CI, 1.16–1.25; p = 1.5e−22). Sensitivity analyses verified the positive association between VAT mass and metabolic traits. The Egger intercept test indicated no directional pleiotropy in these statistically significant associations.

Causal Effect of Visceral Adiposity on Cardiovascular Disease Endpoints

To characterize the relationship between VAT and CVDs, we conducted MR analyses to investigate the causal effects of VAT on 10 CVD endpoints including AF, CAD, MI, HF, AS, IS, LAS, SVS, CES, and IA (**Figure2**). Genetic predisposition to VAT expansion increased risks of AF (OR, 1.414; 95% CI, 1.332–1.5; p = 5.3e−30), CAD (OR, 1.573; 95% CI, 1.439–1.72; p = 2.6e−23), MI (OR, 1.633; 95% CI, 1.484–1.796; p = 8.2e−24), and HF (OR, 1.711; 95% CI, 1.599–1.832; p = 7.9e−54) in primary IVW analysis. Sensitivity analyses verified the positive association between VAT mass and incident AF, CAD, MI, and HF. Genetically predicted VAT mass presented comparatively small effect on increasing risk of stroke (including AS [OR = 1.29, p = 1.7e−10], IS [OR = 1.292, p = 1.5e−9], LAS [OR = 1.483, p = 0.00018], CES [OR = 1.261, p = 0.0012]) and IA (OR, 1.475; 95% CI, 1.235–1.762; p = 1.8e−5). Consistent results were obtained in all sensitivity estimate except MR-Egger, which had a wide 95% CI including the null. The Egger intercept test indicated that no directional pleiotropy existed in these relationships.

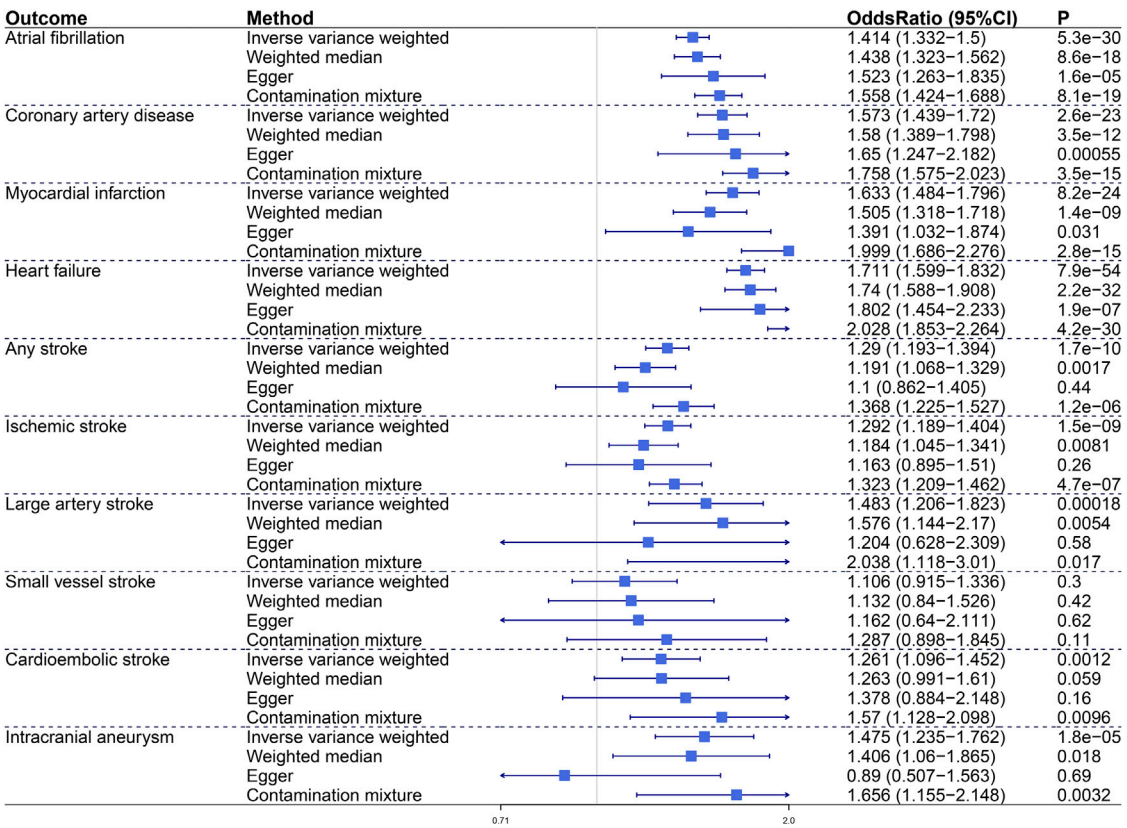

FIGURE 2 | The causal effect of visceral adiposity on 10 independent CVD endpoints. Odds ratios are expressed per 1-SD increase in genetically determined VAT mass. CI, confidence interval.

In the FinnGen study, the proved VAT–CVDs associations were replicated statistically (**Figure 3**). The OR (95% CI) per standard deviation (SD) increase in VAT mass was 1.804 (1.607–2.025) for "Atrial fibrillation and flutter," 1.807 (1.666–1.961) for "All–cause Heart Failure," and 1.212–1.228 for different subtypes of stroke. For subtypes of coronary heart disease, the OR (95% CI) was 1.39 (1.238–1.559) for "Angina pectoris," 1.343 (1.208–1.492) for "Major coronary heart disease event," 1.411 (1.265–1.574) for "Coronary atherosclerosis," 1.386 (1.257–1.529) for "Ischemic heart disease," 1.478 (1.299–1.681) for "Myocardial infarction," and 1.422 (1.224–1.653) for "Unstable angina Pectoris." Expanding to other CVD endpoints of the FinnGen study, we found the relevance of VAT to hypertensive heart disease, cardiac arrhythmia, vascular diseases, and cardiac death. Genetically determined VAT mass increased risk of "Hypertensive Heart Disease" (OR, 2.288; 95% CI, 1.888–2.773; p = 3.2e−17). Besides atrial fibrillation, VAT had impact on other cardiac arrhythmic disease including "AV-block (atrioventricular block)" (OR = 1.45 [1.162–1.808]), "Conduction disorders" (OR = 1.205 [1.023–1.418]), and "Paroxysmal tachycardia" (OR = 1.294 [1.104–1.515]). For diseases of arteries or arterioles including "Aortic aneurysm," "Arterial embolism and thrombosis," "Atherosclerosis, excluding cerebral, coronary and PAD (peripheral artery disease)," and "Peripheral artery disease," the ORs were approximately between 1.406 and 1.693. For diseases of veins including "DVT (deep venous thrombosis) of lower extremities and pulmonary embolism," "Phlebitis and thrombophlebitis (not including DVT)," "DVT of lower extremities," "Varicose veins," and "Venous thromboembolism," the ORs were approximately between 1.446 and 1.668. Genetically predicted VAT mass increased risk of "Death due to cardiac causes" (OR, 1.439; 95% CI, 1.255–1.65; p = 1.9e−7) and "Cardiac arrest" (OR, 1.476; 95% CI, 1.05–2.076; p = 0.025). Detailed information about the associations between VAT mass and CVD outcomes is available in **Supplementary Table S3**.

Potential Mechanism Identification and Network Construction

To explore the potential biological mechanism of the role of VAT to CVDs, we excavated publicly available summarized data for genetic associations with 90 cardiovascular-related circulating proteins from the Systematic and Combined Analysis of Olink Proteins Consortium (Folkersen et al.,

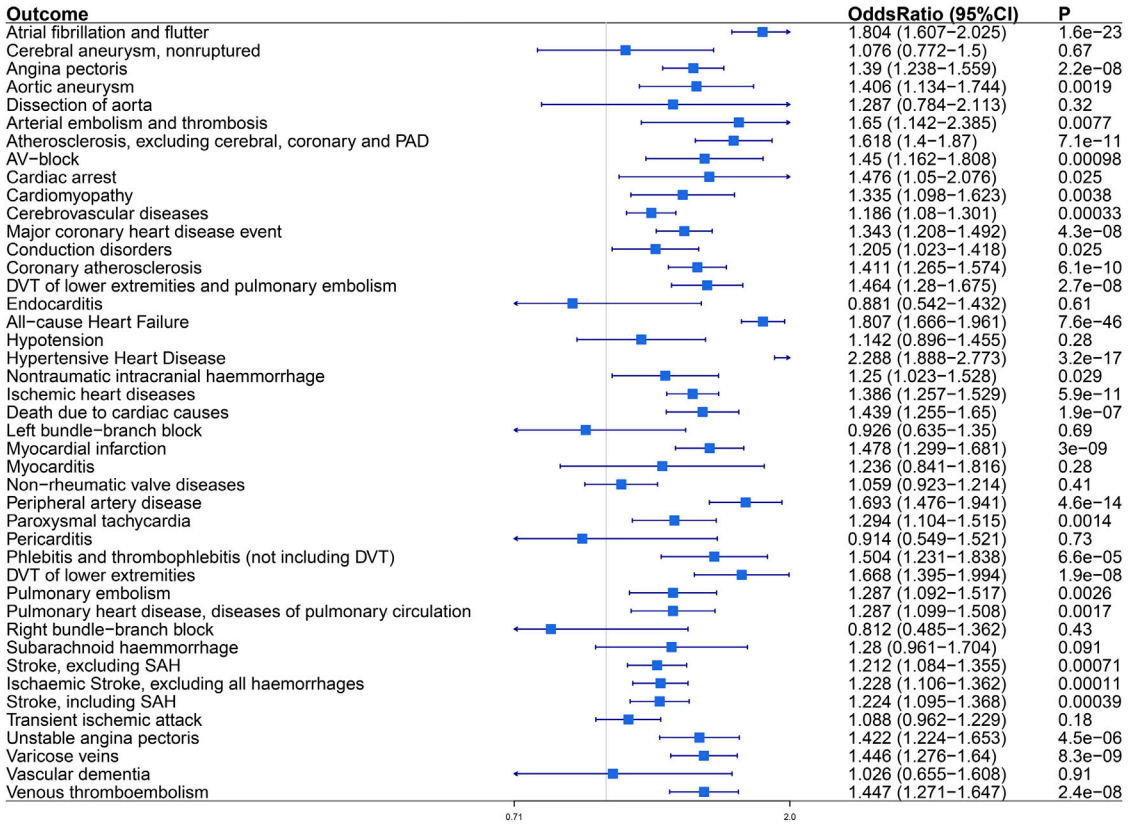

FIGURE 3 | The causal effect of visceral adiposity on 43 CVD endpoints from the FinnGen analysis. Odds ratios are expressed per 1-SD increase in genetically determined VAT mass. CI, confidence interval; PAD, peripheral arterial disease; AV-block, atrioventricular block; DVT, deep vein thrombosis; SAH, subarachnoid haemmorrhage.

2020). Ninety CVD-related circulating proteins were used as either outcomes or exposures in our network MR analysis.

Statistically, 50 of 90 tested proteins were affected by VAT (**Supplementary Table S4**), 85 of 90 proteins were affected by at least one CVD outcome (five proteins were not involved due to the lack of effective instrument variable) (**Supplementary Table S5**). There was consistency in the direction of outcomes between the genetic associations of VAT with proteins, proteins with CVDs, and VAT with CVDs. A network MR analysis was conducted to combine all directionally consistent results. Finally, 60 VAT-proteins-CVDs axes were identified, including 29 proteins and 32 CVD outcomes (**Figure 4**; **Supplementary Table S6**).

Of 29 proteins in the network, a genetically estimated increase of VAT mass was positively associated with 23 proteins, including interleukin and interleukin receptor (IL-1ra, IL16); tumor necrosis factor and tumor necrosis factor receptor (TRANCE, TNFSF14, TNF-R2, TRAIL-R2, FAS); growth factor (VEGF-A, FGF-23, GDF-15, HGF, CSF-1); enzyme (MMP-7, MPO, REN); selectin (PSGL-1, SELE); and others (Gal-3, myoglobin, U-PAR, t-PA, KIM-1, LEP). A genetically estimated increase of VAT mass was negatively associated with six proteins (GAL, ESM-1, RAGE, VEGF-D, KLK6, and AGRP).

The 32 CVD outcomes in the network consisted of four metabolic risk factors (fasting glucose, T2D, HDL-C, TG) and 28 CVD endpoints (due to different database origin, some of them might have overlap), which can be classified into five main categories: coronary heart disease (including diseases of coronary artery and ischemic heart diseases), stroke, cardiac arrhythmia, vascular diseases (including diseases of arteries or arterioles and diseases of veins) and others. Coronary heart disease includes "Coronary artery disease," "Angina pectoris," "Major coronary heart disease event," "Coronary atherosclerosis," "Unstable angina pectoris," and "Myocardial infarction". Stroke includes "Ischemic stroke," "Any stroke," "Cardioembolic stroke," and "Stroke, including SAH." Cardiac arrhythmia includes "Atrial fibrillation," "Atrial fibrillation and flutter," "AV-block," "Conduction disorders," and "Paroxysmal tachycardia." Vascular

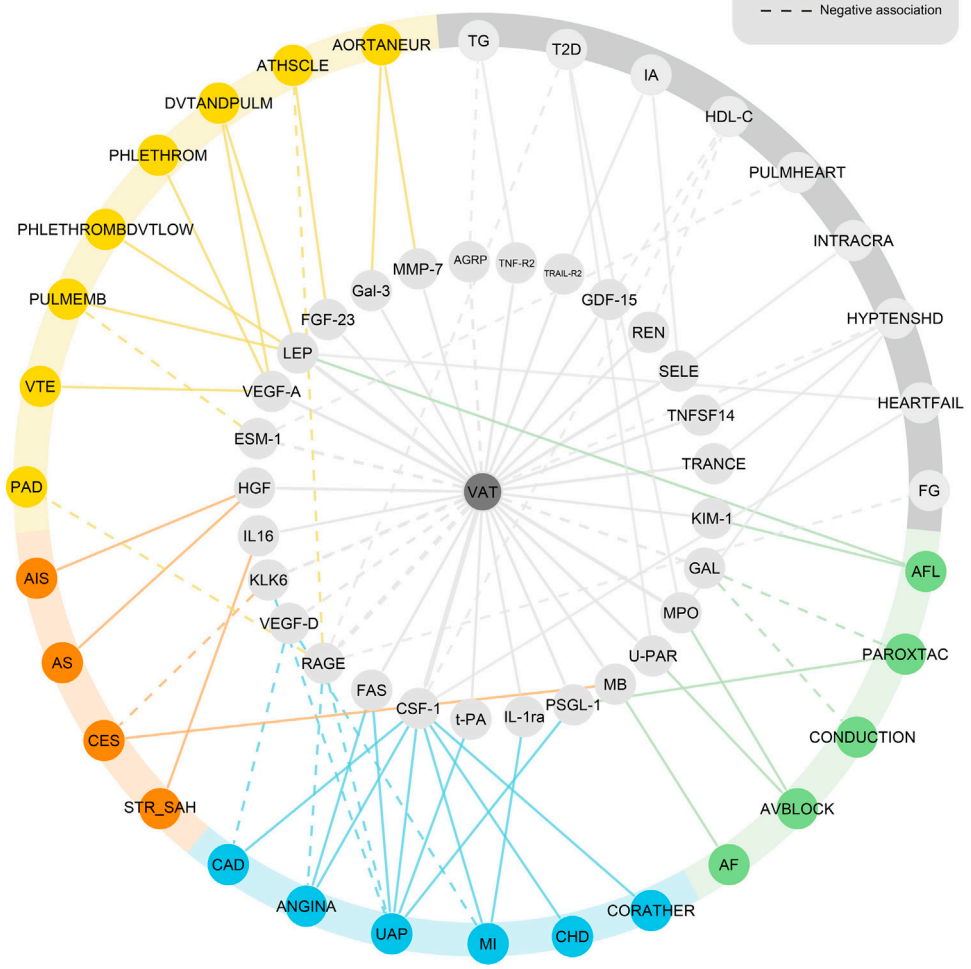

FIGURE 4 | Network analysis of VAT-proteins-CVDs. AGRP, Agouti-related protein; TNF-R2, Tumor necrosis factor receptor 2; TRAIL-R2, TNF-related apoptosis-inducing ligand receptor 2; GDF-15, Growth/differentiation factor 15; REN, Renin; SELE, E-selectin; TNFSF14, Tumor necrosis factor ligand superfamily member 14; TRANCE, TNF-related activation-induced cytokine; KIM-1, Kidney injury molecule 1; GAL, Galanin peptides; MPO, Myeloperoxidase; U-PAR, Urokinase plasminogen activator surface receptor; MB, Myoglobin; PSGL-1, P-selectin glycoprotein ligand 1; IL-1ra, Interleukin-1 receptor antagonist protein; t-PA, Tissue-type plasminogen activator; CSF-1, Macrophage colony-stimulating factor 1; FAS, Tumor necrosis factor receptor superfamily member 6; RAGE, Receptor for advanced glycosylation end products; VEGF-D, Vascular endothelial growth factor D; KLK6, Kallikrein-6; IL16, Pro-interleukin-16; HGF, Hepatocyte growth factor; ESM-1, Endothelial cell-specific molecule 1; VEGF-A, Vascular endothelial growth factor A; LEP, Leptin; FGF-23, Fibroblast growth factor 23; Gal-3, Galectin-3; MMP-7, Matrix metalloproteinase-7; TG, Triglycerides; T2D, Type 2 diabetes; IA, Intracranial aneurysm; HDL-C, High-density lipoprotein cholesterol; PULMHEART, Pulmonary heart disease, diseases of pulmonary circulation; INTRACRA, Nontraumatic intracranial haemmorrhage; HYPTENSHD, Hypertensive Heart Disease; HEARTFAIL, All-cause Heart Failure; FG, fasting glucose; AFL, atrial fibrillation and flutter; PAROXTAC, Paroxysmal tachycardia; CONDUCTION, Conduction disorders; AVBLOCK, AV-block; AF, Atrial fibrillation; CORATHER, Coronary atherosclerosis; CHD, Major coronary heart disease event; MI, myocardial infarction; UAP, Unstable angina pectoris; ANGINA, Angina pectoris; CAD, coronary artery disease; STR_SAH, Stroke, including SAH; CES, Cardioembolic stroke; AS, Any stroke; AIS, Ischemic stroke; PAD, Peripheral artery disease; VTE, Venous thromboembolism; PULMEMB, Pulmonary embolism; PHLETHROMBDVTLOW, DVT of lower extremities; PHLETHROM, Phlebitis and thrombophlebitis (not including DVT); DVTANDPULM, DVT of lower extremities and pulmonary embolism; ATHSCLE, Atherosclerosis, excluding cerebral, coronary and PAD; AORTANEUR, Aortic aneurysm.

diseases include 4 diseases of arteries or arterioles ("Aortic aneurysm," "Atherosclerosis, excluding cerebral, coronary and PAD," "Pulmonary embolism," and "Peripheral artery disease"), 4 diseases of veins ["DVT of lower extremities and pulmonary embolism," "Phlebitis and thrombophlebitis (not including DVT)," "DVT of lower extremities," and "Venous thromboembolism"].

DISCUSSION

Obesity is defined by excessive body fat and is often estimated by BMI or body surface area (BSA) based on weight and height calculation. The value of body mass index and VAT mass are strongly correlated at the population level. Given the heterogeneity of obesity, however, individuals with the same BMI could have distinct body fat distribution and metabolic profiles (Powell-Wiley et al., 2021). Therefore, beyond BMI, it is necessary to quantify different body fat depots to evaluate the metabolic status. The visceral adiposity is the most visible marker of ectopic fat deposition and disturbed hormonal milieu (Després, 2012). Anthropometric measures used to estimate VAT includes the measurement of BMI, waist circumference (WC), waist-to-hip ratio (WHR), and waist-to-height ratio (WHtR). Anthropometric indices are available, but insufficiently reflect actual body fat distribution compared with imaging modalities. Imaging techniques used to estimate VAT, including ultrasonography, CT, magnetic resonance imaging (MRI), positron emission tomography (PET)-CT, and PET-MRI, could depict both quantitative and qualitative features of adipose tissue composition (Oikonomou and Antoniades, 2019). Notably, approaches used to quantify VAT may vary in different populations. In participants of Framingham Heart Study, anthropometric measures, including WC and BMI, captured VAT-associated cardiometabolic risk in men but not in women. In women, abdominal CT–based VAT measures more precisely captured the obesity-associated cardiometabolic risk (Kammerlander et al., 2021).

Studies that quantify the volume or area of VAT by imaging techniques support that excess VAT is an indicator of poor CVD outcomes, independent of BMI. Nevertheless, the relationship between VAT expansion and CVDs is still unclear, as both fewer and more VAT components have been associated with higher risks of CVDs. Two major ideas may account for this phenomenon. The first one is the biological variability of different depots depending on the location and metabolic state. Other than deteriorative effects, VAT components could exert protective effects on the cardiovascular system. Under normal conditions, PVAT had a protective effect on vascular biology by secreting vasorelaxant molecules (Nosalski and Guzik, 2017). Under the pathological condition, the phenotype of PVAT shifted (Gollasch, 2017). Another perspective is that CVDs and other metabolic disorders might affect VAT reversely. For instance, myocardial-derived oxidation products increase the level of adiponectin, a protective protein in regulating metabolism, in the adjacent EAT (Antonopoulos et al., 2016b). In contrast, atrial natriuretic peptide (ANP) secreted by the myocardium contributes to the pro-arrhythmogenic crosstalk between EAT and atrial myocardium (Suffee et al., 2017). Thus, the effect of CVDs on VAT may result in reverse causation bias when determining the effect of VAT on CVDs in observational studies. Besides, observational studies are vulnerable to unmeasured confounding based on available data. A few observational studies have been reported the association between the volume or area of VAT and metabolic risk factors (Fox et al., 2007; Liu et al., 2010; Abraham et al., 2015), hypertension, diabetes (Liu et al., 2010), coronary artery disease (Marques et al., 2010; Ohashi et al., 2010), embolic stroke (Muuronen et al., 2015), and metabolic syndrome (Shah et al., 2014). However, the causal relationship between VAT mass and a wide range of CVD outcomes is still unclear, and the potential mechanism is unknown. Most experimental studies about the relationship between VAT and CVDs focus on the impact of specific depots of VAT on CVDs, like EAT (Wong et al., 2017; Packer, 2018; Ernault et al., 2021) PAT (Al Chekakie et al., 2010; Thanassoulis et al., 2010), and PVAT (Xia and Li, 2017), but not the impact of overall VAT.

To address these issues, we conducted the most comprehensive MR analysis to determine the causality between VAT and CVDs. Consistent with previous observational researches, we confirmed detrimental impacts of VAT on cardiometabolic traits including lipid profiles and glucose profiles (Fox et al., 2007; Liu et al., 2010). We confirmed the adverse effects of VAT accumulation on CAD (Marques et al., 2010; Ohashi et al., 2010; Bachar et al., 2012), vascular disease (Lim and Meigs, 2014; Farb and Gokce, 2015), stroke (Muuronen et al., 2015), and AF (Al Chekakie et al., 2010; Thanassoulis et al., 2010; Shin et al., 2011; Mazurek et al., 2014). Obesity-induced vascular dysfunction could explain the causality of VAT with coronary artery disease and other vascular diseases (Farb and Gokce, 2015). In terms of stroke and its subtypes, the effect of VAT expansion might be partially due to hemodynamic derangements as observed in obese subjects (De Pergola and Pannacciulli, 2002; Darvall et al., 2007). The present study first showed that VAT was the risk factor for atrioventricular-block, conduction disorders, and paroxysmal tachycardia. In summary, our findings demonstrated the extensive deleterious effects of VAT on CVDs. Notably, we did not detect the significant association between VAT mass and systolic/diastolic blood pressure except using the contamination mixture method, which does not align with the evidence that the excess VAT was positively associated with hypertension (Ishikawa et al., 2010; DeMarco et al., 2014; Hall et al., 2015; Lorbeer et al., 2018). Additionally, we found that the genetically determined VAT mass was negatively linked with DBP in the MR-Egger method. This inconsistent result may be attributed to the unbalanced horizontal pleiotropy in the estimates of VAT mass to DBP ($P_{Egger\ intercept}$ = .002).

It is well-documented that the visceral fat, compared with the subcutaneous compartment, is much more metabolically active (Ibrahim, 2010; Alexopoulos et al., 2014). VAT, as an endocrine organ, secrets plenty of adipokines into circulation which contributes to the systematic control of metabolic homeostasis, inflammatory response, and various functions. To explore the

mediate mechanism underlying the association between VAT and CVDs, we introduced 90 circulating proteins from 15 cohorts as potential mediators (Folkersen et al., 2020). Most of the proteins are prognostic biomarkers or drug targets of CVDs. After a strict screening process, we reserved the proteins participating in the adverse effect of VAT on CVDs. We constructed a network involving 29 proteins, 32 CVD outcomes, and 60 pathways. Most VAT-associated proteins increased the incidence of CVDs, and they could be detected in adipose tissue secretome based on the previous study (Hauner, 2005; Dahlman et al., 2012; Lehr et al., 2012; Uhlén et al., 2019). We hence hypothesized that VAT could secret these proteins as circulating adipokines, and then affect the homeostasis of the circulation system. As for the proteins that decreased the incidence of CVDs, VAT expansion could reduce the expressions of which. The underlying mechanism needs further researches. In summary, our profiling provides a comprehensive understanding of linking VAT with the pathogenesis of CVD via these circulating proteins. Most of the proteins in the network were involved in energy metabolism (MB, VEGF-D, CSF-1, RAGE, LEP, FASL, MPO, GAL, VEGF-A, PSGL-1, MMP-7, TNF14, TNF-R2, t-PA, AGRP, REN, GDF-15, and TRAIL-R2), inflammation (HGF, VEGF-D, KLK6, RAGE, LEP, FASL, MPO, VEGF-A, SELE, PSGL-1, ESM-1, TNF14, IL-1ra, IL16, TNF-R2, and REN), or angiogenesis (HGF, VEGF-D, LEP, MPO, VEGF-A, SELE, PSGL-1, and ESM-1).

Among these proteins, genetically estimated VAT mass had the highest OR value for the expression of leptin. The OR per 1-SD increase of VAT mass was 1.742 (95% CI, 1.607–1.888) for the level of leptin. Leptin is one of the most extensively investigated adipokines with an adverse association with CVDs (Sweeney, 2010). Leptin plays a crucial role in metabolism, apoptosis, extracellular matrix remodeling, endothelial dysfunction, and thrombosis. In our network, excessive VAT increased the level of leptin and further increased the incidence of "all-cause heart failure," "atrial fibrillation and flutter," "DVT of lower extremities," "pulmonary embolism," and "DVT of lower extremities and pulmonary embolism." The effect of leptin on extracellular matrix remodeling and cardiac hypertrophy might contribute to the development of HF (Sweeney, 2010). The effect of leptin on endothelial dysfunction might contribute to DVT of lower extremities and pulmonary embolism. Limited studies have reported the effect of leptin on incident AF and provided a discrepant conclusion. An observational study showed that patients with AF had higher serum leptin levels compared with controls (Anaszewicz et al., 2019). Two animal experiments have noted that leptin signaling is essential for developing atrial fibrosis and AF evoked by angiotensinII (Fukui et al., 2013) or high-fat diet (Fukui et al., 2017), while another study reported that leptin attenuates isoproterenol-induced arrhythmogenesis (Lin et al., 2013). The different inducers of the AF model may underlie this discrepancy. Future study to determine the effect of leptin secreted by visceral adiposity on AF is expected.

STRENGTHS AND LIMITATIONS

Our research has multiple strengths. Firstly, we conducted the most comprehensive analysis of the causality between VAT and CVDs. We confirmed the effect of excess VAT on a wide range of cardiometabolic risk factors and CVD endpoints. Our finding indicated that VAT accumulation exacerbated cardiometabolic profiles extensively. Secondly, our MR design reduced confounding and reverse causation bias compared with the observational study. A large sample size of GWAS summary statistics provided a substantial statistical performance to examine the association between VAT and CVD outcomes. Thirdly, we involved cardiovascular-related circulating proteins as potential mediators between VAT and CVDs and conducted a network analysis.

Some limitations need to be noted. Firstly, the results from an MR study can be violated by pleiotropy, which describes a genetic variant associated with multiple traits. However, in most cases, sensitivity analyses using MR-Egger, weighted median, and contamination mixture method provided less precise estimates but consistent direction. Secondly, most participants of the GWASs were of European ancestry, which reduced the generalizability of the conclusion. Thirdly, it should be noted that the function and deposition of adipose tissue differ by sex. Males tend to have more visceral fat that is highly correlated to increased cardiovascular risk; whereas females tend to have more subcutaneous fat (Palmer and Clegg, 2015). It has been reported that the positive associations between VAT and CVD outcomes were stronger in females compared with males (Karlsson et al., 2019; Kammerlander et al., 2021). However, we did not have the GWAS data for solely predicting VAT mass in each gender, so we cannot determine whether the associations between VAT and CVDs vary in gender. Finally, we only included 90 CVD proteins, as they represent the most promising targets. Further studies might include more proteins from large-scale pQTL studies.

Prospective Future

Observational studies demonstrated expanded visceral adiposity as a CVD risk factor. Our MR results added to this body of evidence and presented the causal link between VAT mass and CVDs. However, not only the quantity of VAT but also the quality of VAT is important. Future studies are expected to evaluate the associations between different types of VAT (white adipose tissue and brown adipose tissue) and CVDs. Besides, the external validation and confirmation of our findings in populations of different genders, different races, and different ages may be necessary. The proteins in network analysis provided diagnostic or predictive tools and could be used as therapeutic targets in individuals with excess VAT. Reducing the quantity of VAT (Verheggen et al., 2016; Rao et al., 2019) and targeting the adipokines secreted by VAT might help to prevent or treat CVDs. Future randomized trials are expected to investigate the efficiency.

CONCLUSION

Mendelian randomization analysis showed that VAT mass was associated with a wide range of CVD outcomes including coronary heart disease, cardiac arrhythmia, vascular diseases, and stroke. A few circulating proteins may be the mediators between VAT and CVDs. Future studies are warranted to validate these findings.

DATA AVAILABILITY STATEMENT

The original contributions presented in the study are included in the article/**Supplementary Material**, further inquiries can be directed to the corresponding authors.

AUTHOR CONTRIBUTIONS

YM, TT, NL, FB, YX, and CL designed and drafted the analysis; YH, YL conducted data analysis and wrote the manuscript; ZH, QLin, ML, ZN, and YZ wrote figure legends and revised the manuscript; XM and QLiu provided study guidance and performed quality control of the analysis. All authors have read and approved the final manuscript.

FUNDING

This work was supported by grants from the National Natural Science Foundation of China (grant nos. 82070356 and 81770337) and grants from the Hunan Provincial Health Commission Scientific Research Project (grant no. 20201302).

ACKNOWLEDGMENTS

This study used summary statistics from large genetic consortia. The authors gratefully acknowledge their contributions in making their datasets publicly available, without which this study would not be possible.

SUPPLEMENTARY MATERIAL

The Supplementary Material for this article can be found online at: https://www.frontiersin.org/articles/10.3389/fcell.2022.840866/full#supplementary-material

REFERENCES

Abraham, T. M., Pedley, A., Massaro, J. M., Hoffmann, U., and Fox, C. S. (2015). Association between Visceral and Subcutaneous Adipose Depots and Incident Cardiovascular Disease Risk Factors. *Circulation* 132 (17), 1639–1647. doi:10.1161/circulationaha.114.015000

Akoumianakis, I., and Antoniades, C. (2017). The Interplay between Adipose Tissue and the Cardiovascular System: Is Fat Always Bad? *Cardiovasc. Res.* 113 (9), 999–1008. doi:10.1093/cvr/cvx111

Al Chekakie, M. O., Welles, C. C., Metoyer, R., Ibrahim, A., Shapira, A. R., Cytron, J., et al. (2010). Pericardial Fat Is Independently Associated with Human Atrial Fibrillation. *J. Am. Coll. Cardiol.* 56 (10), 784–788. doi:10.1016/j.jacc.2010.03.071

Alexopoulos, N., Katritsis, D., and Raggi, P. (2014). Visceral Adipose Tissue as a Source of Inflammation and Promoter of Atherosclerosis. *Atherosclerosis* 233 (1), 104–112. doi:10.1016/j.atherosclerosis.2013.12.023

Anaszewicz, M., Wawrzeńczyk, A., Czerniak, B., Banaś, W., Socha, E., Lis, K., et al. (2019). Leptin, Adiponectin, Tumor Necrosis Factor α, and Irisin Concentrations as Factors Linking Obesity with the Risk of Atrial Fibrillation Among Inpatients with Cardiovascular Diseases. *Kardiol Pol.* 77 (11), 1055–1061. doi:10.33963/kp.14989

Antonopoulos, A. S., Margaritis, M., Verheule, S., Recalde, A., Sanna, F., Herdman, L., et al. (2016). Mutual Regulation of Epicardial Adipose Tissue and Myocardial Redox State by PPAR-γ/Adiponectin Signalling. *Circ. Res.* 118 (5), 842–855. doi:10.1161/circresaha.115.307856

Antonopoulos, A. S., Oikonomou, E. K., Antoniades, C., and Tousoulis, D. (2016). From the BMI Paradox to the Obesity Paradox: the Obesity-Mortality Association in Coronary Heart Disease. *Obes. Rev.* 17 (10), 989–1000. doi:10.1111/obr.12440

Bachar, G. N., Dicker, D., Kornowski, R., and Atar, E. (2012). Epicardial Adipose Tissue as a Predictor of Coronary Artery Disease in Asymptomatic Subjects. *Am. J. Cardiol.* 110 (4), 534–538. doi:10.1016/j.amjcard.2012.04.024

Bakker, M. K., van der Spek, R. A. A., van Rheenen, W., Morel, S., Bourcier, R., Hostettler, I. C., et al. (2020). Genome-wide Association Study of Intracranial Aneurysms Identifies 17 Risk Loci and Genetic Overlap with Clinical Risk Factors. *Nat. Genet.* 52 (12), 1303–1313. doi:10.1038/s41588-020-00725-7

Bowden, J., Del Greco M, F., Minelli, C., Zhao, Q., Lawlor, D. A., Sheehan, N. A., et al. (2019). Improving the Accuracy of Two-Sample Summary-Data Mendelian Randomization: Moving beyond the NOME assumption. *Int. J. Epidemiol.* 48 (3), 728–742. doi:10.1093/ije/dyy258

Bowden, J., Del Greco M, F., Minelli, C., Davey Smith, G., Sheehan, N., and Thompson, J. (2017). A Framework for the Investigation of Pleiotropy in Two-Sample Summary Data Mendelian Randomization. *Statist. Med.* 36 (11), 1783–1802. doi:10.1002/sim.7221

Burgess, S., Bowden, J., Fall, T., Ingelsson, E., and Thompson, S. G. (2017). Sensitivity Analyses for Robust Causal Inference from Mendelian Randomization Analyses with Multiple Genetic Variants. *Epidemiology (Cambridge, Mass)* 28 (1), 30–42. doi:10.1097/ede.0000000000000559

Burgess, S., Butterworth, A., and Thompson, S. G. (2013). Mendelian Randomization Analysis with Multiple Genetic Variants Using Summarized Data. *Genet. Epidemiol.* 37 (7), 658–665. doi:10.1002/gepi.21758

Burgess, S., Davey Smith, G., Davies, N. M., Dudbridge, F., Gill, D., Glymour, M. M., et al. (2019). Guidelines for Performing Mendelian Randomization Investigations. *Wellcome Open Res.* 4, 186. doi:10.12688/wellcomeopenres.15555.1

Burgess, S., Davies, N. M., and Thompson, S. G. (2016). Bias Due to Participant Overlap in Two-sample Mendelian Randomization. *Genet. Epidemiol.* 40 (7), 597–608. doi:10.1002/gepi.21998

Burgess, S., Foley, C. N., Allara, E., Staley, J. R., and Howson, J. M. M. (2020). A Robust and Efficient Method for Mendelian Randomization with Hundreds of Genetic Variants. *Nat. Commun.* 11 (1), 376. doi:10.1038/s41467-019-14156-4

Dahlman, I., Elsen, M., Tennagels, N., Korn, M., Brockmann, B., Sell, H., et al. (2012). Functional Annotation of the Human Fat Cell Secretome. *Arch. Physiol. Biochem.* 118 (3), 84–91. doi:10.3109/13813455.2012.685745

Darvall, K. A. L., Sam, R. C., Silverman, S. H., Bradbury, A. W., and Adam, D. J. (2007). Obesity and Thrombosis. *Eur. J. Vasc. Endovascular Surg.* 33 (2), 223–233. doi:10.1016/j.ejvs.2006.10.006

De Pergola, G., and Pannacciulli, N. (2002). Coagulation and Fibrinolysis Abnormalities in Obesity. *J. Endocrinol. Invest.* 25 (10), 899–904. doi:10.1007/bf03344054

DeMarco, V. G., Aroor, A. R., and Sowers, J. R. (2014). The Pathophysiology of Hypertension in Patients with Obesity. *Nat. Rev. Endocrinol.* 10 (6), 364–376. doi:10.1038/nrendo.2014.44

Després, J.-P. (2012). Body Fat Distribution and Risk of Cardiovascular Disease. *Circulation* 126 (10), 1301–1313. doi:10.1161/circulationaha.111.067264

Dupuis, J., Langenberg, C., Prokopenko, I., Saxena, R., Soranzo, N., Jackson, A. U., et al. (2010). New Genetic Loci Implicated in Fasting Glucose Homeostasis and Their Impact on Type 2 Diabetes Risk. *Nat. Genet.* 42 (2), 105–116. doi:10.1038/ng.520

Ernault, A. C., Meijborg, V. M. F., and Coronel, R. (2021). Modulation of Cardiac Arrhythmogenesis by Epicardial Adipose Tissue. *J. Am. Coll. Cardiol.* 78 (17), 1730–1745. doi:10.1016/j.jacc.2021.08.037

Evangelou, E., Warren, H. R., Mosen-Ansorena, D., Mifsud, B., Pazoki, R., Gao, H., et al. (2018). Genetic Analysis of over 1 Million People Identifies 535 New Loci Associated with Blood Pressure Traits. *Nat. Genet.* 50 (10), 1412–1425. doi:10.1038/s41588-018-0205-x

Farb, M. G., and Gokce, N. (2015). Visceral Adiposopathy: a Vascular Perspective. *Horm. Mol. Biol. Clin. Investig.* 21 (2), 125–136. doi:10.1515/hmbci-2014-0047

FinnGen (2020). *FinnGen Documentation of the R4 Release*, 2020.

Folkersen, L., Gustafsson, S., Wang, Q., Hansen, D. H., Hedman, Å. K., Schork, A., et al. (2020). Genomic and Drug Target Evaluation of 90 Cardiovascular Proteins in 30,931 Individuals. *Nat. Metab.* 2 (10), 1135–1148. doi:10.1038/s42255-020-00287-2

Fox, C. S., Massaro, J. M., Hoffmann, U., Pou, K. M., Maurovich-Horvat, P., Liu, C.-Y., et al. (2007). Abdominal Visceral and Subcutaneous Adipose Tissue Compartments. *Circulation* 116 (1), 39–48. doi:10.1161/circulationaha.106.675355

Fukui, A., Ikebe-Ebata, Y., Kondo, H., Saito, S., Aoki, K., Fukunaga, N., et al. (2017). Hyperleptinemia Exacerbates High-Fat Diet-Mediated Atrial Fibrosis and Fibrillation. *J. Cardiovasc. Electrophysiol.* 28 (6), 702–710. doi:10.1111/jce.13200

Fukui, A., Takahashi, N., Nakada, C., Masaki, T., Kume, O., Shinohara, T., et al. (2013). Role of Leptin Signaling in the Pathogenesis of Angiotensin II-Mediated Atrial Fibrosis and Fibrillation. *Circ. Arrhythm Electrophysiol.* 6 (2), 402–409. doi:10.1161/circep.111.000104

Gaborit, B., Venteclef, N., Ancel, P., Pelloux, V., Gariboldi, V., Leprince, P., et al. (2015). Human Epicardial Adipose Tissue Has a Specific Transcriptomic Signature Depending on its Anatomical Peri-Atrial, Peri-Ventricular, or Peri-Coronary Location. *Cardiovasc. Res.* 108 (1), 62–73. doi:10.1093/cvr/cvv208

Gollasch, M. (2017). Adipose-Vascular Coupling and Potential Therapeutics. *Annu. Rev. Pharmacol. Toxicol.* 57, 417–436. doi:10.1146/annurev-pharmtox-010716-104542

Hall, J. E., do Carmo, J. M., da Silva, A. A., Wang, Z., and Hall, M. E. (2015). Obesity-Induced Hypertension. *Circ. Res.* 116 (6), 991–1006. doi:10.1161/circresaha.116.305697

Hauner, H. (2005). Secretory Factors from Human Adipose Tissue and Their Functional Role. *Proc. Nutr. Soc.* 64 (2), 163–169. doi:10.1079/pns2005428

Hemani, G., Zheng, J., Elsworth, B., Wade, K. H., Haberland, V., Baird, D., et al. (2018). The MR-Base Platform Supports Systematic Causal Inference across the Human Phenome. *eLife* 7. doi:10.7554/eLife.34408

Hemani, G., Tilling, K., and Davey Smith, G. (2017). Orienting the Causal Relationship between Imprecisely Measured Traits Using GWAS Summary Data. *Plos Genet.* 13 (11), e1007081. doi:10.1371/journal.pgen.1007081

Hocking, S. L., Wu, L. E., Guilhaus, M., Chisholm, D. J., and James, D. E. (2010). Intrinsic Depot-specific Differences in the Secretome of Adipose Tissue, Preadipocytes, and Adipose Tissue-Derived Microvascular Endothelial Cells. *Diabetes* 59 (12), 3008–3016. doi:10.2337/db10-0483

Ibrahim, M. M. (2010). Subcutaneous and Visceral Adipose Tissue: Structural and Functional Differences. *Obes. Rev.* 11 (1), 11–18. doi:10.1111/j.1467-789x.2009.00623.x

Ishikawa, J., Haimoto, H., Hoshide, S., Eguchi, K., Shimada, K., and Kario, K. (2010). An Increased Visceral-Subcutaneous Adipose Tissue Ratio Is Associated with Difficult-To-Treat Hypertension in Men. *J. Hypertens.* 28 (6), 1340–1346. doi:10.1097/HJH.0b013e328338158b

Kammerlander, A. A., Lyass, A., Mahoney, T. F., Massaro, J. M., Long, M. T., Vasan, R. S., et al. (2021). Sex Differences in the Associations of Visceral Adipose Tissue and Cardiometabolic and Cardiovascular Disease Risk: The Framingham Heart Study. *J. Am. Heart Assoc.* 10 (11), e019968. doi:10.1161/JAHA.120.019968

Karlsson, T., Rask-Andersen, M., Pan, G., Höglund, J., Wadelius, C., Ek, W. E., et al. (2019). Contribution of Genetics to Visceral Adiposity and its Relation to Cardiovascular and Metabolic Disease. *Nat. Med.* 25 (9), 1390–1395. doi:10.1038/s41591-019-0563-7

Lehr, S., Hartwig, S., Lamers, D., Famulla, S., Müller, S., Hanisch, F. G., et al. (2012). Identification and Validation of Novel Adipokines Released from Primary Human Adipocytes. *Mol. Cell Proteomics* 11 (1), M111.010504. doi:10.1074/mcp.M111.010504

Lim, S., and Meigs, J. B. (2014). Links between Ectopic Fat and Vascular Disease in Humans. *Atvb* 34 (9), 1820–1826. doi:10.1161/atvbaha.114.303035

Lin, Y.-K., Chen, Y.-C., Huang, J.-H., Lin, Y.-J., Huang, S.-S., Chen, S.-A., et al. (2013). Leptin Modulates Electrophysiological Characteristics and Isoproterenol-Induced Arrhythmogenesis in Atrial Myocytes. *J. Biomed. Sci.* 20 (1), 94. doi:10.1186/1423-0127-20-94

Liu, J., Fox, C. S., Hickson, D. A., May, W. D., Hairston, K. G., Carr, J. J., et al. (2010). Impact of Abdominal Visceral and Subcutaneous Adipose Tissue on Cardiometabolic Risk Factors: The Jackson Heart Study. *J. Clin. Endocrinol. Metab.* 95 (12), 5419–5426. doi:10.1210/jc.2010-1378

Lorbeer, R., Rospleszcz, S., Schlett, C. L., Heber, S. D., Machann, J., Thorand, B., et al. (2018). Correlation of MRI-Derived Adipose Tissue Measurements and Anthropometric Markers with Prevalent Hypertension in the Community. *J. Hypertens.* 36 (7), 1555–1562. doi:10.1097/hjh.0000000000001741

Malik, R., Chauhan, G., Traylor, M., Sargurupremraj, M., Okada, Y., Mishra, A., et al. (2018). Multiancestry Genome-wide Association Study of 520,000 Subjects Identifies 32 Loci Associated with Stroke and Stroke Subtypes. *Nat. Genet.* 50 (4), 524–537. doi:10.1038/s41588-018-0058-3

Marques, M. D., Santos, R. D., Parga, J. R., Rocha-Filho, J. A., Quaglia, L. A., Miname, M. H., et al. (2010). Relation between Visceral Fat and Coronary Artery Disease Evaluated by Multidetector Computed Tomography. *Atherosclerosis* 209 (2), 481–486. doi:10.1016/j.atherosclerosis.2009.10.023

Mazurek, T., Kiliszek, M., Kobylecka, M., Skubisz-Głuchowska, J., Kochman, J., Filipiak, K., et al. (2014). Relation of Proinflammatory Activity of Epicardial Adipose Tissue to the Occurrence of Atrial Fibrillation. *Am. J. Cardiol.* 113 (9), 1505–1508. doi:10.1016/j.amjcard.2014.02.005

Morris, A. P., Voight, B. F., Teslovich, T. M., Ferreira, T., Segrè, A. V., Steinthorsdottir, V., et al. (2012). Large-scale Association Analysis Provides Insights into the Genetic Architecture and Pathophysiology of Type 2 Diabetes. *Nat. Genet.* 44 (9), 981–990. doi:10.1038/ng.2383

Muuronen, A. T., Taina, M., Hedman, M., Marttila, J., Kuusisto, J., Onatsu, J., et al. (2015). Increased Visceral Adipose Tissue as a Potential Risk Factor in Patients with Embolic Stroke of Undetermined Source (ESUS). *PLoS One* 10 (3), e0120598. doi:10.1371/journal.pone.0120598

Nielsen, J. B., Thorolfsdottir, R. B., Fritsche, L. G., Zhou, W., Skov, M. W., Graham, S. E., et al. (2018). Biobank-driven Genomic Discovery Yields New Insight into Atrial Fibrillation Biology. *Nat. Genet.* 50 (9), 1234–1239. doi:10.1038/s41588-018-0171-3

Nikpay, M., Goel, A., Won, H. H., Hall, L. M., Willenborg, C., Kanoni, S., et al. (2015). A Comprehensive 1,000 Genomes-Based Genome-wide Association Meta-Analysis of Coronary Artery Disease. *Nat. Genet.* 47 (10), 1121–1130. doi:10.1038/ng.3396

Nosalski, R., and Guzik, T. J. (2017). Perivascular Adipose Tissue Inflammation in Vascular Disease. *Br. J. Pharmacol.* 174 (20), 3496–3513. doi:10.1111/bph.13705

Ohashi, N., Yamamoto, H., Horiguchi, J., Kitagawa, T., Kunita, E., Utsunomiya, H., et al. (2010). Association between Visceral Adipose Tissue Area and Coronary Plaque Morphology Assessed by CT Angiography. *JACC: Cardiovasc. Imaging* 3 (9), 908–917. doi:10.1016/j.jcmg.2010.06.014

Oikonomou, E. K., and Antoniades, C. (2019). The Role of Adipose Tissue in Cardiovascular Health and Disease. *Nat. Rev. Cardiol.* 16 (2), 83–99. doi:10.1038/s41569-018-0097-6

Packer, M. (2018). Epicardial Adipose Tissue May Mediate Deleterious Effects of Obesity and Inflammation on the Myocardium. *J. Am. Coll. Cardiol.* 71 (20), 2360–2372. doi:10.1016/j.jacc.2018.03.509

Palmer, B. F., and Clegg, D. J. (2015). The Sexual Dimorphism of Obesity. *Mol. Cell Endocrinol.* 402, 113–119. doi:10.1016/j.mce.2014.11.029

Powell-Wiley, T. M., Poirier, P., Burke, L. E., Després, J. P., Gordon-Larsen, P., Lavie, C. J., et al. (2021). Obesity and Cardiovascular Disease: A Scientific Statement from the American Heart Association. *Circulation* 143 (21), e984–e1010. doi:10.1161/CIR.0000000000000973

Ragino, Y. I., Stakhneva, E. M., Polonskaya, Y. V., and Kashtanova, E. V. (2020). The Role of Secretory Activity Molecules of Visceral Adipocytes in Abdominal Obesity in the Development of Cardiovascular Disease: A Review. *Biomolecules* 10 (3), 374. doi:10.3390/biom10030374

Rao, S., Pandey, A., Garg, S., Park, B., Mayo, H., Després, J.-P., et al. (2019). Effect of Exercise and Pharmacological Interventions on Visceral Adiposity: A Systematic Review and Meta-Analysis of Long-Term Randomized Controlled Trials. *Mayo Clinic Proc.* 94 (2), 211–224. doi:10.1016/j.mayocp.2018.09.019

Scheja, L., and Heeren, J. (2019). The Endocrine Function of Adipose Tissues in Health and Cardiometabolic Disease. *Nat. Rev. Endocrinol.* 15 (9), 507–524. doi:10.1038/s41574-019-0230-6

Shah, R. V., Murthy, V. L., Abbasi, S. A., Blankstein, R., Kwong, R. Y., Goldfine, A. B., et al. (2014). Visceral Adiposity and the Risk of Metabolic Syndrome across Body Mass Index. *JACC: Cardiovasc. Imaging* 7 (12), 1221–1235. doi:10.1016/j.jcmg.2014.07.017

Shah, S., Henry, A., Roselli, C., Lin, H., Sveinbjörnsson, G., Fatemifar, G., et al. (2020). Genome-wide Association and Mendelian Randomisation Analysis Provide Insights into the Pathogenesis of Heart Failure. *Nat. Commun.* 11 (1), 163. doi:10.1038/s41467-019-13690-5

Shin, S. Y., Yong, H. S., Lim, H. E., Na, J. O., Choi, C. U., Choi, J. I., et al. (2011). Total and Interatrial Epicardial Adipose Tissues Are Independently Associated with Left Atrial Remodeling in Patients with Atrial Fibrillation. *J. Cardiovasc. Electrophysiol.* 22 (6), 647–655. doi:10.1111/j.1540-8167.2010.01993.x

Suffee, N., Moore-Morris, T., Farahmand, P., Rücker-Martin, C., Dilanian, G., Fradet, M., et al. (2017). Atrial Natriuretic Peptide Regulates Adipose Tissue Accumulation in Adult Atria. *Proc. Natl. Acad. Sci. USA* 114 (5), E771–E780. doi:10.1073/pnas.1610968114

Sweeney, G. (2010). Cardiovascular Effects of Leptin. *Nat. Rev. Cardiol.* 7 (1), 22–29. doi:10.1038/nrcardio.2009.224

Tatsumi, Y., Nakao, Y. M., Masuda, I., Higashiyama, A., Takegami, M., Nishimura, K., et al. (2017). Risk for Metabolic Diseases in normal Weight Individuals with Visceral Fat Accumulation: a Cross-Sectional Study in Japan. *BMJ Open* 7 (1), e013831. doi:10.1136/bmjopen-2016-013831

Thanassoulis, G., Massaro, J. M., O'Donnell, C. J., Hoffmann, U., Levy, D., Ellinor, P. T., et al. (2010). Pericardial Fat Is Associated with Prevalent Atrial Fibrillation. *Circ. Arrhythmia Electrophysiol.* 3 (4), 345–350. doi:10.1161/circep.109.912055

Uhlén, M., Karlsson, M. J., Hober, A., Svensson, A. S., Scheffel, J., Kotol, D., et al. (2019). The Human Secretome. *Sci. Signal.* 12 (609). doi:10.1126/scisignal.aaz0274

Verheggen, R. J. H. M., Maessen, M. F. H., Green, D. J., Hermus, A. R. M. M., Hopman, M. T. E., and Thijssen, D. H. T. (2016). A Systematic Review and Meta-Analysis on the Effects of Exercise Training versus Hypocaloric Diet: Distinct Effects on Body Weight and Visceral Adipose Tissue. *Obes. Rev.* 17 (8), 664–690. doi:10.1111/obr.12406

Willer, C. J., Schmidt, E. M., Sengupta, S., Peloso, G. M., Gustafsson, S., Kanoni, S., et al. (2013). Discovery and Refinement of Loci Associated with Lipid Levels. *Nat. Genet.* 45 (11), 1274–1283. doi:10.1038/ng.2797

Wong, C. X., Ganesan, A. N., and Selvanayagam, J. B. (2017). Epicardial Fat and Atrial Fibrillation: Current Evidence, Potential Mechanisms, Clinical Implications, and Future Directions. *Eur. Heart J.* 38 (17), 1294–1302. doi:10.1093/eurheartj/ehw045

Xia, N., and Li, H. (2017). The Role of Perivascular Adipose Tissue in Obesity-Induced Vascular Dysfunction. *Br. J. Pharmacol.* 174 (20), 3425–3442. doi:10.1111/bph.13650

Yavorska, O. O., and Burgess, S. (2017). MendelianRandomization: an R Package for Performing Mendelian Randomization Analyses Using Summarized Data. *Int. J. Epidemiol.* 46 (6), 1734–1739. doi:10.1093/ije/dyx034

Conflict of Interest: The authors declare that the research was conducted in the absence of any commercial or financial relationships that could be construed as a potential conflict of interest.

Publisher's Note: All claims expressed in this article are solely those of the authors and do not necessarily represent those of their affiliated organizations, or those of the publisher, the editors and the reviewers. Any product that may be evaluated in this article, or claim that may be made by its manufacturer, is not guaranteed or endorsed by the publisher.

frontiers | Frontiers in Cell and Developmental Biology

ORIGINAL RESEARCH
published: 26 April 2022
doi: 10.3389/fcell.2022.845158

Spontaneous Browning of White Adipose Tissue Improves Angiogenesis and Reduces Macrophage Infiltration After Fat Grafting in Mice

Jiayan Lin†, Shaowei Zhu†, Yunjun Liao†, Zhuokai Liang, Yuping Quan, Yufei He, Junrong Cai and Feng Lu*

Department of Plastic and Cosmetic Surgery, Nanfang Hospital, Southern Medical University, Guangzhou, China

OPEN ACCESS

Edited by:
Nadia Akawi,
United Arab Emirates University,
United Arab Emirates

Reviewed by:
Joseph M. Rutkowski,
Texas A&M University, United States
Petra Kotzbeck,
Medical University of Graz, Austria

***Correspondence:**
Junrong Cai
drjunrongcai@outlook.com

†These authors have contributed equally to this work and share first authorship

Specialty section:
This article was submitted to Cellular Biochemistry, a section of the journal Frontiers in Cell and Developmental Biology

Received: *04 January 2022*
Accepted: *09 March 2022*
Published: *26 April 2022*

Citation:
Lin J, Zhu S, Liao Y, Liang Z, Quan Y, He Y, Cai J and Lu F (2022) Spontaneous Browning of White Adipose Tissue Improves Angiogenesis and Reduces Macrophage Infiltration After Fat Grafting in Mice. Front. Cell Dev. Biol. 10:845158. doi: 10.3389/fcell.2022.845158

Background: Fat grafting is a frequently used technique; however, its survival/regeneration mechanism is not fully understood. The browning of white adipocytes, a process initiated in response to external stimuli, is the conversion of white to beige adipocytes. The physiologic significance of the browning of adipocytes following transplantation is unclear.

Methods: C57BL/6 mice received 150 mg grafts of inguinal adipose tissue, and then the transplanted fat was harvested and analyzed at different time points to assess the browning process. To verify the role of browning of adipocytes in fat grafting, the recipient mice were allocated to three groups, which were administered CL316243 or SR59230A to stimulate or suppress browning, respectively, or a control group after transplantation.

Results: Browning of the grafts was present in the center of each as early as 7 days post-transplantation. The number of beige cells peaked at day 14 and then decreased gradually until they were almost absent at day 90. The activation of browning resulted in superior angiogenesis, higher expression of the pro-angiogenic molecules vascular endothelial growth factor A (VEGF-A) and fibroblast growth factor 21 (FGF21), fewer macrophages, and ultimately better graft survival (Upregulation, 59.17% ± 6.64% vs. Control, 40.33% ± 4.03%, $^*p < 0.05$), whereas the inhibition of browning led to poor angiogenesis, lower expression of VEGF-A, increased inflammatory macrophages, and poor transplant retention at week 10 (Downregulation, 20.67% ± 3.69% vs. Control, 40.33% ± 4.03%, $^*p < 0.05$).

Conclusion: The browning of WAT following transplantation improves the survival of fat grafts by the promotion of angiogenesis and reducing macrophage.

Keywords: fat grafting, browning, beige adipocytes, angiogenesis, inflammation

1 INTRODUCTION

Autologous fat grafting is a procedure for soft-tissue reconstruction and repair (Khouri et al., 2014a; Pu et al., 2015). Although there are a growing number of techniques to optimize the outcome of fat grafting, the quality of the transplanted fat tissue remains unpredictable (Khouri and Khouri 2017). Therefore, the mechanisms by which fat grafts survive following transplantation are under investigation.

Early angiogenesis, immune cells, and activated adipose stem cells (ASCs) have been reported to have effects on the survival of transplanted fat tissue (Chappell et al., 2015; Hong et al., 2018; Cai et al., 2018a). Accumulating evidence suggests that inflammatory cells and ASCs both play important roles during fat grafting, but the behavior of mature adipocytes has been less well studied.

Wu et al. were the first to identify a distinct type of thermogenic adipocyte within subcutaneous white adipose tissue (WAT), which was called a beige adipocyte (Wu et al., 2012). The conversion of white to beige adipocytes in white fat depots is referred to as "browning process." Subsequent studies have shown that WAT undergoes browning after transplantation and that the "browned" area is accompanied by a marked increase in angiogenesis (Qiu et al., 2018). This browning process occurred in human fat grafting as well but the significance of that is unknown (Liu et al., 2021). The administration of either tamoxifen or extracellular vesicles derived from ASCs to stimulate browning of WAT results in an improvement in fat graft survival and retention (Cai et al., 2018a; Zhu et al., 2020). However, both of these promote WAT browning indirectly, instead of by directly targeting the white adipocytes and the thermogenic gene program. Therefore, the direct relationship between the browning of white adipocytes and fat graft survival, and the underlying mechanisms, remain to be identified.

White adipocytes in WAT depots, and especially in subcutaneous depots, are able to be converted to beige adipocytes in response to specific stimuli (Rosenwald et al., 2013). Unlike classical brown adipose tissue (BAT), which expresses uncoupling protein-1 (UCP1) at a high level and has a high capacity for respiratory uncoupling, beige adipocytes demonstrate a lower level of thermogenic gene expression in the basal state (Petrovic et al., 2010). However, differences among adipose tissue types cannot only be attributed to their thermogenic program. In addition to differences in metabolism, the secretome of the various types of adipose tissue significantly varies (Villarroya et al., 2017a). Thermogenic adipose tissue secretes various factors that control the expansion of adipose tissue, whereas the secretome of WAT principally consists of molecules that are not normally released by BAT (Cannon and Nedergaard 2004; Ortega et al., 2011). BAT has been shown to produce vascular endothelial growth factor A (VEGF-A), which promotes local vascularization, particularly during cold exposure (Xue et al., 2009). Moreover, upon thermogenic stimulation, beige adipose tissue secretes fibroblast growth factor 21, a cytokine previously reported to normalize glucose and lipid homeostasis as well as promote angiogenesis (Yaqoob et al., 2014; Huang et al., 2017, Huang et al., 2019; Zhou et al., 2019; Dai et al., 2021). Furthermore, the transplantation of beige precursor cells is associated with the development of larger numbers of blood vessels in a mouse model of delayed repair of rotator cuff tear. This implies that beige adipocytes in transplanted fat might improve gr (Schulz et al., 2011)aft survival by secreting factors that activate angiogenesis (Lee et al., 2020).

Previous studies have shown that various treatments can be used to activate browning in fat tissue and that these significantly improve fat graft survival (Cai et al., 2018b; Zhu et al., 2020). However, the role of the spontaneous browning of WAT following transplantation is poorly understood, as is the mechanism by which beige adipocytes influence fat graft retention. To define the role of adipocyte browning in fat graft retention and study the underlying mechanism by which browning affects fat graft survival, we studied the effects of the β3 adrenoceptor agonist CL316243, which directly tragets the β3 adrenoceptor on white adipocytes and subsequently induces browning (Schulz et al., 2011; Montanari et al., 2017), and those of the β3 adrenoceptor antagonist SR59230A, which inhibits browning (Jiang et al., 2017), on the degree of browning at various time points in a mouse model of fat transplantation.

2 MATERIALS AND METHODS

2.1 Animals and Treatments

The study was approved by the Nanfang Hospital Animal Ethics Committee and was conducted according to the guidelines of the National Health and Medical Research Council of China. Sixty-eight 8-week-old male C57BL/6 mice were obtained from Southern Medical University (Guangzhou, China). For transplantation, the mice were anesthetized by the intraperitoneal injection of pentobarbital sodium (50 mg/kg). One hundred fifty milligrams of fat tissue was harvested from the inguinal fat pad, cut into small pieces, and inserted through a 5 mm-long skin incision into a small dorsal subcutaneous pocket in 32 mice, which was followed by skin closure with 7-0 nylon sutures. After 7, 14, 30, and 90 days, $n = 8$ mice per time point were sacrificed and the transplanted adipose tissue was collected for further analyses. In a second experiment, to investigate the role of browning after transplantation, 36 mice were randomly allocated to three groups ($n = 12$ per group): a browning upregulation group, a browning downregulation group, and a control group. The browning upregulation group was administered CL316243 (APExBIO, Houston, TX, United States) (1 mg/kg body mass) subcutaneously at the site of transplantation for 14 consecutive days following transplantation, the browning downregulation group was administered SR59230A (MedChemExpress, NJ, USA; 1 mg/kg body mass) in the same way, and the control group was administered phosphate-buffered saline (PBS) (5 ml/kg body mass). After 2 or 10 weeks, the mice were killed and the fat grafts were harvested and analyzed.

2.2 Histology and Immunohistochemical Staining

Samples were fixed in 4% paraformaldehyde for 24 h, embedded in paraffin and cut from the middle. Sections were prepared and stained with hematoxylin and eosin, and examined under a light microscope (Olympus BX51, Tokyo, Japan). Paraffin-embedded tissue sections

were incubated with rabbit anti-UCP1 antibody (dilution 1:2,000; Abcam, Cambridge, UK) or rabbit anti-cluster of differentiation (CD)31 (1:1,000; Abcam), followed by secondary antibody and then an avidin-biotin-horseradish peroxidase detection system (ZSGB-BIO, Beijing, China). The slides were then examined using an Olympus BX51 microscope. For immunofluorescence staining, tissue sections were incubated with rabbit anti-mouse macrophage antigen 2 (MAC2) (1:150; Abcam), or guinea pig anti-mouse perilipin (dilution 1:400; Progen Biotechnik, Heidelberg, Germany). For double fluorescence staining, sections were incubated with AlexaFluor 488-conjugated (Thermo Fisher Scientific, Waltham, MA, United States) goat anti-guinea pig immunoglobulin G (1:200; Abcam), and AlexaFluor rhodamine-conjugated chicken anti-rabbit immunoglobulin G (1:200; Invitrogen, Carlsbad, CA, United States). Nuclei were stained with 4′,6-diamidino-2-phenylindole (Sigma, St. Louis, MO, United States). To quantify the degree of browning, at least five microscopic fields per samples of grafts were randomly chosen from the middle to the edge by two of the authors in a double-blinded fashion. To quantify the proinflammatory cells, and angiogenesis in the transplanted fat tissue, the numbers of UCP-1-positive cells, Mac-2-positive cells, and CD31-positive cells were counted in at least five microscopic fields per sample by two of the authors in double-blinded fashion. The percentage of perilipin positive adipose cells area per field was determined with the use of ImageJ (National Institutes of Health, Bethesda, Md.). The diameter of mature adipocytes was determined by analyzing the captured image of mature adipocytes by means of light microscopy with the use of the ImageJ (National Institutes of Health, Bethesda, Md.) program as described previously (Wankhade et al., 2016).

2.3 Quantitative RT-PCR

Adipose tissue was collected, frozen in liquid nitrogen, and stored at −80°C. RNA was extracted from 50 mg tissue samples using RNeasy Lipid Tissue Mini Kits (Qiagen, Hilden, Germany), according to the manufacturer's instructions. cDNA was synthesized and amplified over 40 cycles using a QuantiTect Reverse Transcription Kit (Qiagen) and a Rotor-Gene 3000 Real-Time PCR Detection System (Corbett Research, Sydney, Australia). Expression levels were calculated using the 2−ΔΔCt method. The primer sequences were as follows: Ucp1: forward 5′-CTGATGAAGTCCAGACAGACAG-3′ and reverse 5′-CCAGCATAGAAGCCCAATGA-3′; PRDM16: forward 5′-CAG CACGGTGAAGCCATTC-3′ and reverse 5′-GCGTGCATCCGC TTGTG-3′; PGC1-α: forward 5′-CGACAGCTATGAAGCCTA TGAG-3′ and reverse 5′-CTTCTGCCTCTCTCTCTGTTTG-3′; FGF21: forward: 5′-CTGGGGGTCTACCAAGCATA-3′ and reverse 5′-CACCCAGGATTTGAATGACC-3′; and VEGF-A: forward 5′-GGAGATCCTTCGAGGAGCACTT-3′ and reverse 5′-GGCGATTTAGCAGCAGATATAAGAA-3′HIF1α: forward: 5′-CAAGATCTCGGCGAAGCAA-3′ and reverse 5′-GGTGAG CCTCATAACAGAAGCTTT-3′.

2.4 Energy Expenditure Analysis Using the Comprehensive Lab Animal Monitoring System

Oxygen consumption (VO_2) and carbon dioxide expiration (VCO_2) were collected and measured by indirect calorimetry in a Promethion Metabolic Screening System (Sable systems International, United States) that maintained constant environmental temperature across a 12-h light, 12-h dark cycle. The mice in different groups were individually housed in chambers maintained at 25°C, with free access to food and water. Measurements were made every 15 min for 3 days after the mice had acclimatized to their surroundings for 1 day. Mean values were calculated for all the parameters of interest over the 3 days of monitoring.

2.5 Statistical Analysis

Statistical analyses were performed using SPSS version 22.0 (IBM, Inc., Armonk, NY, United States). The data are expressed as mean ± SEM and were compared among the groups using one-way analysis of variance or the Kruskal-Wallis test. Comparisons between two groups were performed using the least significant difference method or the Mann-Whitney U-test. $P < 0.05$ was considered to represent statistical significance.

3 RESULTS

3.1 Early Accumulation of Beige Adipocytes in the Center of the Grafts

In the present study, to better characterize the timing of the appearance of beige adipocytes, we analyzed the fat grafts at various time points after transplantation. Hematoxylin and eosin staining showed that number of multilocular adipocytes peaked at day 14 while adipocytes in fat graft contained only one single lidpid droplets at day 7, 30 and 90 (**Figure 1A**, above). Immunohistochemistry showed that a large number of UCP-1-positive adipocytes had accumulated by day 14 and that fat grafts harvested on days 7, 30, and 90 mostly comprised large adipocytes with single lipid droplets and few UCP1-positive adipocytes (**Figure 1A**, below). The number of UCP1-positive cells peaked 14 days after surgery, with fewer beige adipocytes being present on days 7, 30, and 90 (Control, 1.0 ± 0.32 vs. Day 7, 24.8 ± 2.41 vs. Day 14, 56.6 ± 10.08 vs. Day 30, 18.6 ± 1.89 vs. Day 90, 3.2 ± 1.16, $^{*}p < 0.05$; $^{**}p < 0.01$; $^{***}p < 0.001$) (**Figure 1B**). Ucp1 gene expression, measured using quantitative reverse transcription polymerase chain reaction, was also highest in fat grafts harvested on day 14 (Control, 1.0 ± 0.26 vs. Day 7, 2.34 ± 0.31 vs. Day 14, 8.38 ± 2.28 vs. Day 30, 2.45 ± 0.56 vs. Day 90, 2.27 ± 0.63, $^{**}p < 0.01$) (**Figure 1C**). Mean adipocyte size was significantly lower on days 14 compared with that at day 7, day 30 and day 90 (Control, 61.05 ± 4.31 vs. Day 7, 60.06 ± 4.58 vs. Day 14, 39.99 ± 3.76 vs. Day 30, 66.91 ± 4.65 vs. Day 90, 74.37 ± 5.61, $^{*}p < 0.05$; $^{**}p < 0.01$; $^{***}p < 0.001$) (**Figure 1D**). Based on the knowledge that depending on the distance from the surface, adipocyte fate after transplantation is categorized into three zones including survival zone, regeneration zone and necrosis zone, we define the zone where most of beige adipocytes accumulated. Immunohistochemistry for UCP1 showed that browning tended to occur in the regeneration zone of the fat grafts, rather than in the survival zone (**Figure 1E**). Counting of the UCP1+ adipocytes indicated that there were significantly more beige adipocytes in the regeneration zone than in the survival zone or necrosis zone (Survival zone, 8.4 ± 2.46 vs. Regeneration zone, 61.6 ± 9.1 vs. Necrosis zone, 30.4 ± 6.15, $^{*}p < 0.05$;$^{***}p < 0.001$) (**Figure 1F**).

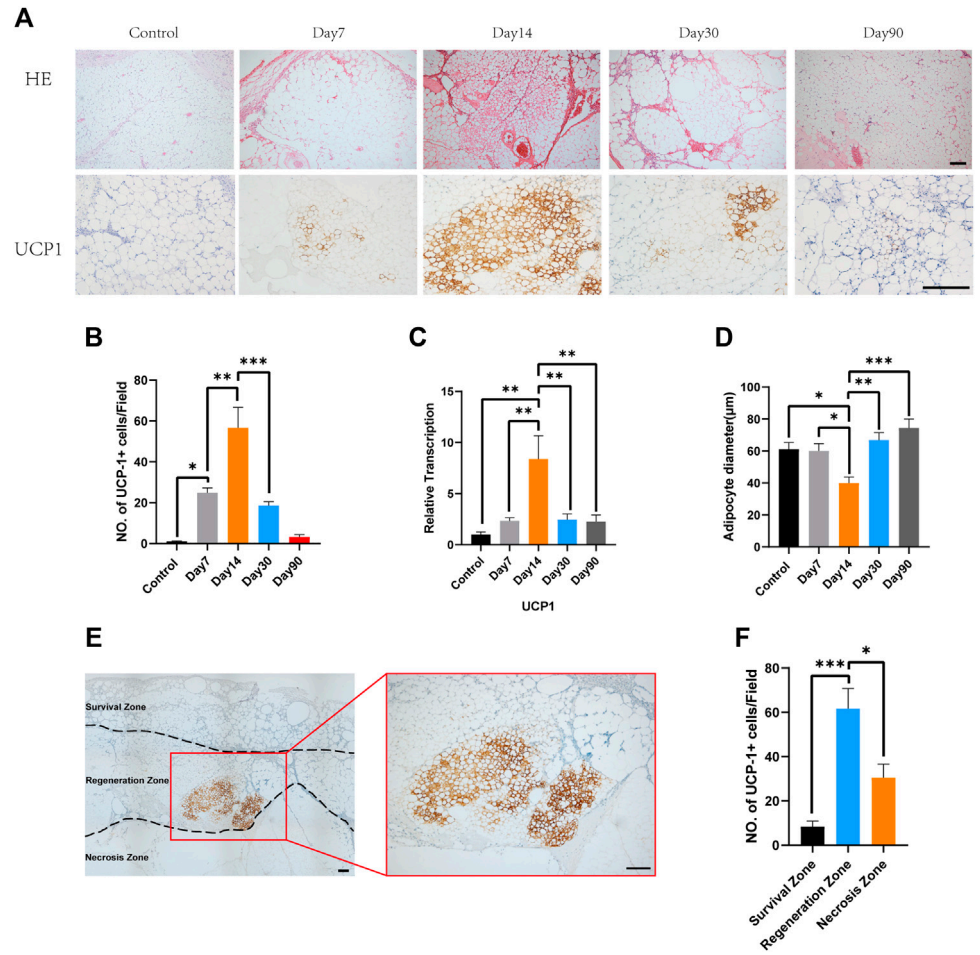

FIGURE 1 | Time course of the accumulation of beige adipocytes in the center of fat grafts. **(A)** Fat grafts on day 14 contain smaller adipocytes and more multilocular adipocytes and show strong immunostaining for uncoupling protein (UCP)-1. On days 7 and 30, there were more unilocular adipocytes and fewer UCP-1-positive fat cells, and still fewer on day 90. Presented figures were from the same zone of each grafts. **(B)** Beige cell counts at the various time points. **(C)** Expression of Ucp1 on days 7, 14, and 30. **(D)** On day 14, mean adipocyte diameter was lower than on day 7, 30 and 90. **(E)** Representative photomicrograph of UCP1 immunostaining, showing beige adipocytes in the "regeneration zone" of a graft. **(F)** Beige cell count in survival zone, regeneration zone and necrosis zone. (*$p < 0.05$; **$p < 0.01$;***$p < 0.001$). Scale bar = 100 μm.

3.2 Pharmacologic Downregulation or Upregulation of Browning Affects Graft Retention and Fat Graft Structure

Two weeks after transplantation, no significant difference was observed among the retention rate of fat grafts from three groups (**Figure 2A**). However, 10 weeks after transplantation, the fat graft volume retention of the browning upregulation group was superior to that of the control group (Upregulation, 59.17% ± 6.64% vs. Control, 40.33% ± 4.03%, *$p < 0.05$) (**Figure 2A**). And the browning downregulation group has worse retention rate than that of the control group (Downregulation, 20.67% ± 3.69% vs. Control, 40.33% ± 4.03%, *$p < 0.05$) (**Figure 2A**). Swelling of the transplanted adipose tissue was found in the upregulation group but not in the control group and downregulation group at week 2; however, the grafts in the downregulation and control groups obviously shrank at week 10 (**Figure 2B**). Hematoxylin and eosin staining showed that 2 weeks after transplantation, no significant difference between upregulation group and control group was observed while some of oil cysts existed in fat grafts in downregulation group (**Figure 2C**, above). 10 weeks following transplantation, there were larger numbers of oil cysts and more severe fibrosis in the downregulation group than in the control group (**Figure 2C**, below). By contrast, the samples from the browning upregulation group had superior adipose structure with less oil cysts or inflammatory cells (**Figure 2C**, below). .

3.3 Pharmacologic Treatment Modifies the Browning of the Fat Grafts

The grafts were harvested from mice in the three groups after treatment with the browning stimulator or inhibitor for 14 consecutive days. Hematoxylin and eosin staining showed that CL316243 treated fat grafts containing multiple, small lipid droplets than the control group and downregulation group

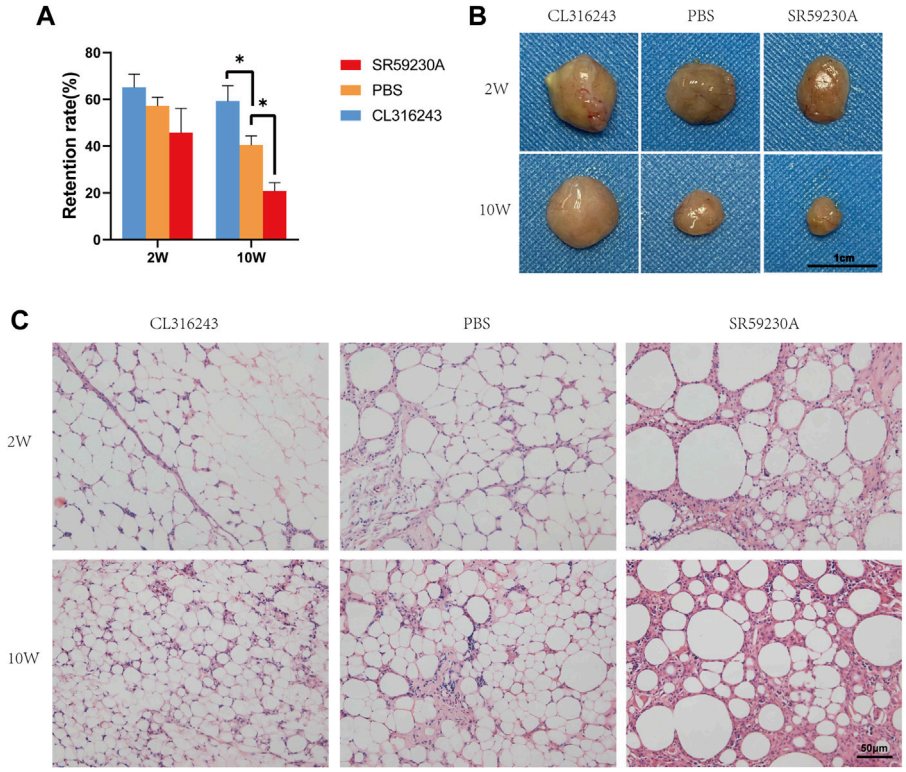

FIGURE 2 | Retention (final mass/initial mass) and adipose structure of the transplanted fat in the three groups. **(A)** After 2 weeks, there was no significant difference, but after 10 weeks, retention was significantly better in the browning upregulation group (CL316243) than in the control group (PBS) and the browning downregulation group (SR59230A) showed significantly poorer retention than the control group. **(B)** Swelling of the transplanted adipose tissue was found in the upregulation group but not in the control group and downregulation group at week 2; however, the grafts in the downregulation and control groups obviously shrank at week 10. **(C)** Histologic analysis showed that fat grafts from the control group had normal adipose structure 10 weeks after transplantation, whereas samples from CL316243-treated mice had superior structure. However, grafts from the browning upregulation group demonstrated small, brown-like adipocyte features, whereas grafts from the browning downregulation group contained more oil cysts, larger adipocytes, and crown-like structures. (*$p < 0.05$)

(**Figure 3A**, above). Immunohistochemistry showed that grafts from the browning upregulation group had larger numbers of UCP1-positive beige cells (**Figure 3A**, below). However, the induction of browning was significantly inhibited in fat grafts from SR59230A-treated mice vs. control mice (**Figure 3A**, below). There was significantly higher expression of Ucp1 and Prdm16 mRNA in the upregulation group than in the control group (**Figure 3B**) and significantly lower expression in the downregulation group than in the control group (**Figure 3B**). No significant difference of PGC1-α mRNA expression was observed among different groups (**Figure 3B**). Two weeks of treatment of both CL316243 and SR59230A had no influence on weight gain and food intake (**Supplementary Figures S1A, B**). Besides, oxygen consumption, CO_2 production, and heat production were not affected by CL316243 and SR59230A (**Supplementary Figures S1C, D and E**). Local administration, but not intraperitoneal injection, of the agonist and the antagonist might explain why there was no significant difference among different groups. Also, lack of sufficient blood vessels in grafts at this early stage could not facilitate the delivery of substances throughout the body.

3.4 Browning is Associated with Higher Expression of VEGF-A and FGF21 and Superior Angiogenesis in the Fat Grafts

To better determine the relationship between browning and angiogenesis, we evaluated angiogenesis of fat grafts at different time points in the non-treated mice. Immunohistochemistry of CD31 showed that formation of vessels occurred as early as 7 days after grafting and that fat grafts harvested on day 14 contained the most newly formed vessels (**Figure 4A**). Quantification of newly formed vessels also suggested the superior angiogenesis on day 14 (Day 7, 58.0 ± 3.16 vs. Day 14, 88.4 ± 10.13 vs. Day 30, 34.0 ± 2.569 vs. Day 90, 10.0 ± 1.761, **$p < 0.01$; ****$p < 0.0001$) when the browning level was the highest (**Figure 4B**). There were significantly higher expressions of gene, VEGF-A, on day 14 compared to that at other time points (**Figure 4C**). However, no significant difference of FGF21 expression was observed between day 7 and day 14 (**Figure 4D**).

Next, we evaluated the angiogenesis level in the fat grafts treated with CL316243, SR59230A and PBS. Immunostaining using an antibody against CD31 showed that CD31-positive,

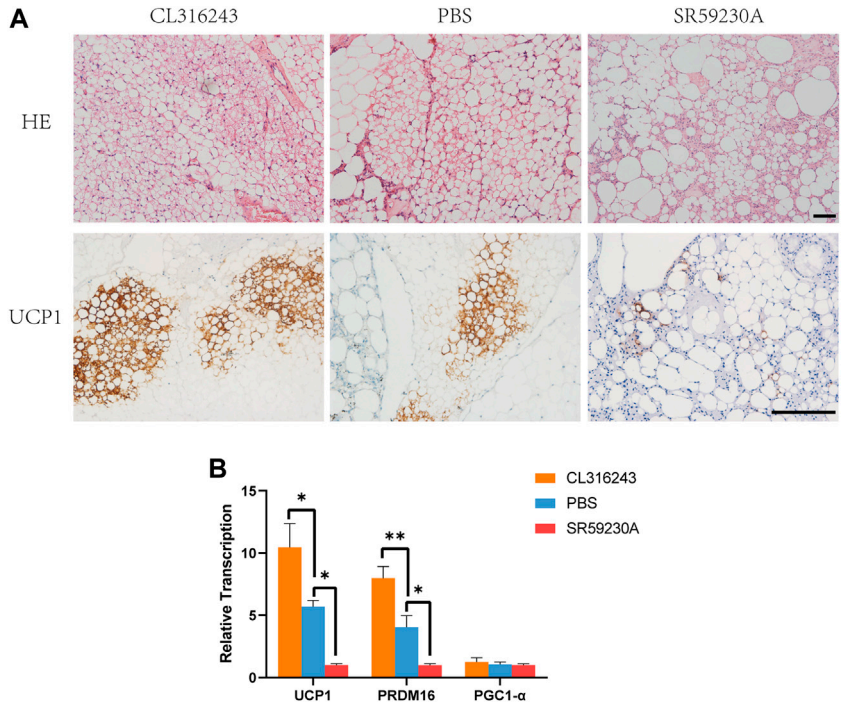

FIGURE 3 | Manipulation of the degree of browning of the grafts using CL316243 and SR59230A. **(A)** Histologic analysis showed that fat grafts from the upregulation group contained smaller and more multilocular adipocytes than the control group and downregulation group 2 weeks after transplantation. (above) Immunohistochemistry for the beige adipocyte marker uncoupling protein (UCP)-1 showed a larger number of UCP1-positive beige adipocytes in the upregulation group and a smaller number in the downregulation group, compared with the control group. (below) **(B)** There was a similar trend for the expression of browning-related genes (Ucp1 and Prdm16). There were no significant differences in the expression of Pgc1a among the groups. (*$p < 0.05$;**$p < 0.01$). Scale bar = 50 μm.

newly formed vessels were more numerous in the browning upregulation group than in the control group, whereas there was less vascularization in the downregulation group at week 2 (**Figure 4E**). The mean number of CD31-positive vessels per field in upregulation group was significantly higher than that in the control and downregulation group at postoperative day 14 (Upregulation, 71.2 ± 10.23 vs. Control, 39.2 ± 6.8 vs. Downregulation, 11.4 ± 3.25, *$p < 0.05$) (**Figure 4F**). However, ten weeks after transplantation, mean number of CD31-positive vessels was significantly higher than that in the control group but there was no difference between control group and downregulation group (Upregulation, 37.6 ± 8.21 vs. Control, 13.0 ± 3.9 vs. Downregulation, 10.2 ± 3.34, *$p < 0.05$) (**Figure 4F**). Furthermore, at week 2, the expression of VEGF-A was significantly higher in the browning upregulation group than in the control group, but significantly lower in the downregulation group (**Figure 4G**). The expression of FGF21 was higher in the upregulation group than the control group, but there was no significant difference in expression between the control and downregulation groups (**Figure 4G**). Compared to the control and downregulation group, lower expression of HIF1-α was observed in the upregulation group at week 2 and week 10, which may reflected that superior angiogenesis stimulated by browning agents CL316243 led to reduced hypoxia (**Figure 4H**).

3.5 Browning is Associated with a Reduction in Inflammatory Cell in Grafts

2 weeks after transplantation, double-staining of sections with antibodies against perilipin (green) and Mac2 (red) to identify tissue macrophages showed that grafts from the browning upregulation group had a superior structure, and contained more smaller, perilipin-positive adipocytes and fewer Mac2-positive cells than the control group (**Figure 5A**, above). 10 weeks after transplantation, fat grafts from downregulation group contained more Mac 2-positive cells and less perilipin-positive adipocytes than the upregulation group and the control group. However, no significant difference was observed between the browning upregulation group and the control group. In grafts from the browning downregulation group, there were fewer perilipin-positive adipocytes and a larger number of Mac 2-positive cells, which can be explained by increased tissue macrophage for the purpose of disposing of the dead cells that accumulate because of insufficient angiogenesis (**Figure 5A**, below). Counting of the Mac2+ cells revealed that they were significantly more numerous in the downregulation group than in the control or upregulation groups at both week 2 (Downregulation, 58.8 ± 7.63 vs. Control, 31.8 ± 4.04 vs. Upregulation, 7.2 ± 2.08, *$p < 0.05$) and week 10 (Downregulation, 34.4 ± 6.08 vs. Control, 11 ± 3.16 vs.

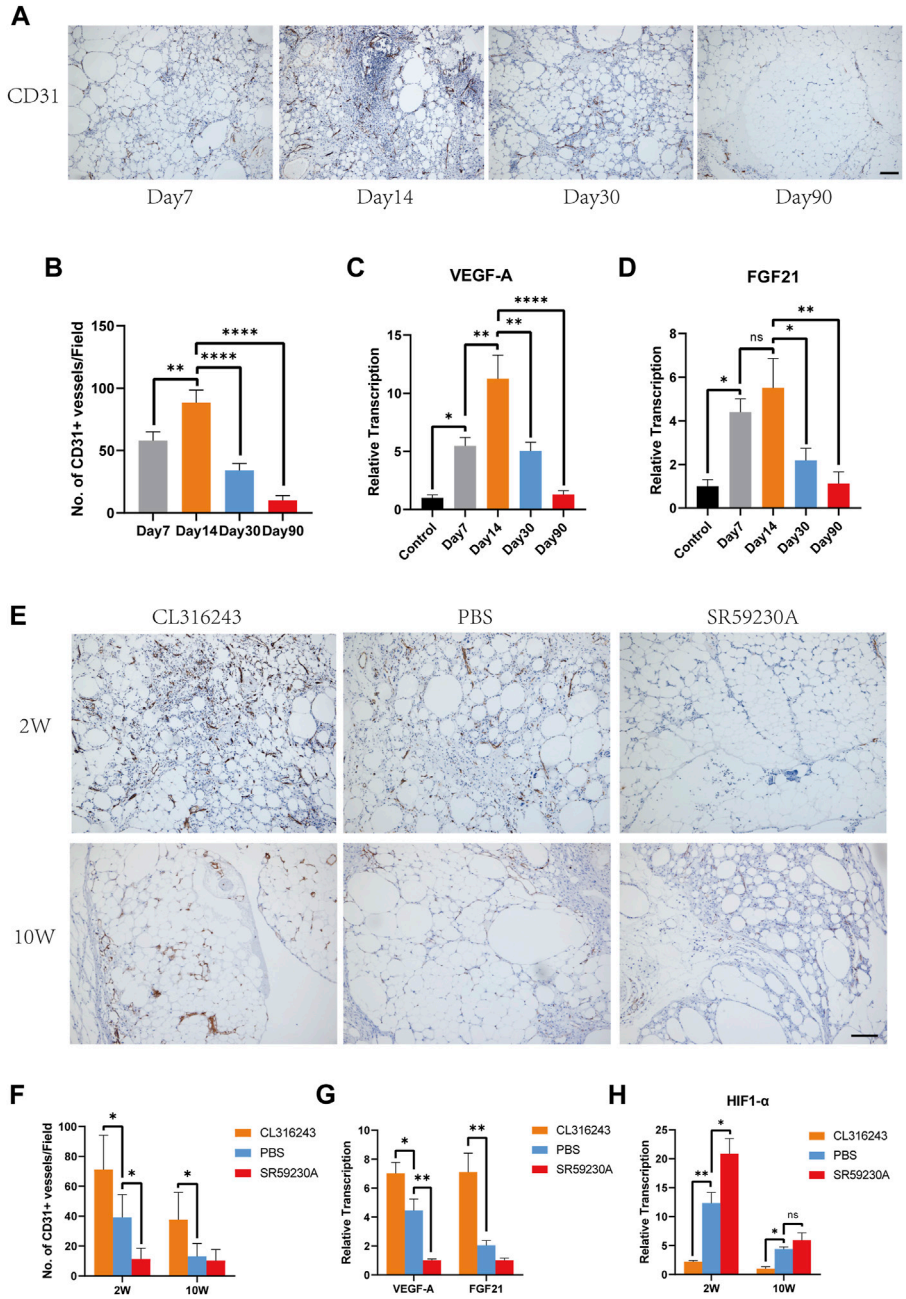

FIGURE 4 | Beige adipocyte formation was associated with early angiogenesis and the production of VEGF-A and FGF21. (A) Angiogenesis of fat grafts was superior at day 14 than day 7, 30 and 90. **(B)** Quantification of CD31-positive cells at different time points. **(C** and **D)** Expression levels of angiogenic genes, VEGF-A and FGF21. **(E)** Angiogenesis in the fat grafts 2 weeks and 10 weeks after transplantation, identified using immunohistochemical staining for CD31. **(F)** Number of $CD31^{+}$ vessels at week 2 and week 10. **(G)** Expression of the Vegfa and Fgf21 genes in the fat grafts at week 2, measured using quantitative RT-PCR. (H) Expression of HIF1-α associated with hypoxia at week 2 and week 10. ($^{*}p < 0.05$;$^{**}p < 0.01$;$^{****}p < 0.0001$). Scale bar = 50 μm.

Upregulation, 8.4 ± 2.98, $^{**}p < 0.01$) but they were significantly less in the browning upregulation groups than in the control group only at week 2 but not week 10 (**Figure 5B**). Quantification of perilipin-positive adipocytes area showed that 2 weeks and ten weeks after transplantation, perilipin-positive adipocytes in fat grafts from upregulation group occupied larger area per field than the control group while perilipin-positive adipocytes in fat grafts from downregulation group occupied smaller area than the control group (Week 2, Upregulation, 80.7 ± 3.03 vs. Control, 63.09 ± 4.25 vs. Downregulation, 16.33 ± 4.69, $^{*}p < 0.05$; $^{****}p < 0.0001$) (Week 10, Upregulation, 89.52 ± 1.27 vs. Control, 74.09 ± 4.42 vs. Downregulation, 34.75 ± 2.77, $^{*}p < 0.05$; $^{****}p < 0.0001$) (**Figure 5C**).

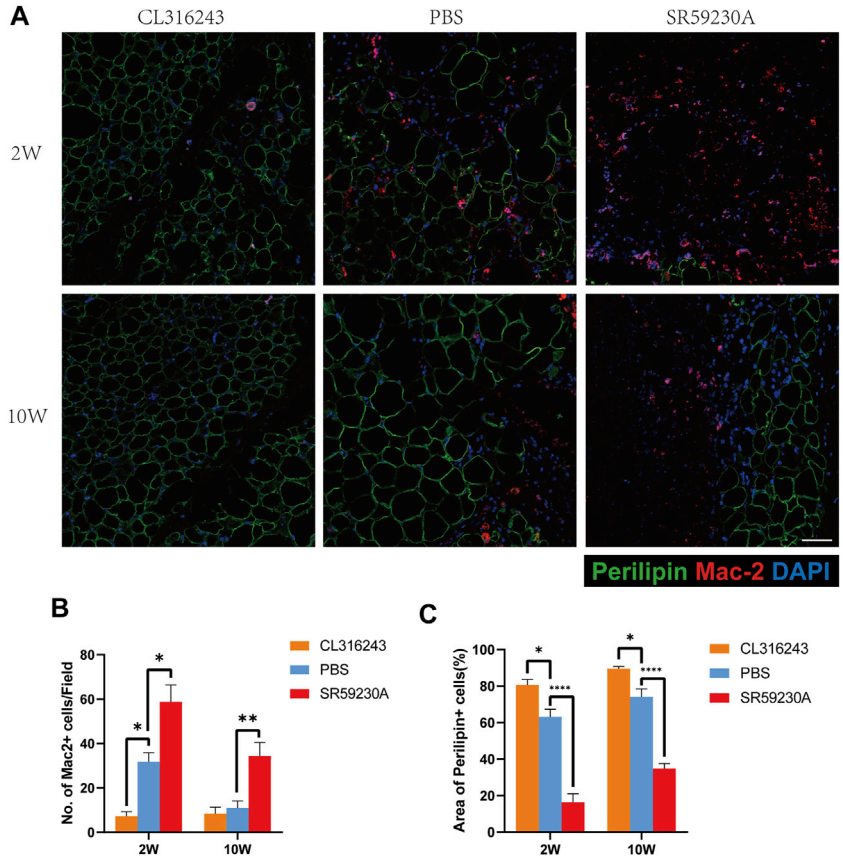

FIGURE 5 | Assessment of adipogenesis and inflammation in fat grafts following transplantation. **(A)** Tissue sections harvested at week 2 and week 10, doubly immunostained for perilipin (green) and Mac2 (red). Fat grafts in the browning upregulation group have the most normal adipose structure, with few macrophages within fat grafts, whereas samples from both the control and browning downregulation groups show severe inflammatory immune cell accumulation at week 2. At week 10, fat grafts in the browning upregulation group and the control group have less inflammatory macrophages in grafts than the downregulation group. Compared with downregulation group, samples in control group and upregulation group have normal adipose structure at week 10. **(B)** Number of Mac2+ cells in each group. **(C)** Area of perilipin positive adipocytes in each group. (*$p < 0.05$;**$p < 0.01$;****$p < 0.0001$) .Scale bar = 50 μm.

4 DISCUSSION

Little is known regarding the mechanism underlying fat graft survival/ regeneration after transplantation. Although the important roles of inflammatory cells and ASCs have been recognized, the role of mature adipocytes themselves has been less well researched (Chappell et al., 2015; Cai et al., 2018b; Hong et al., 2018; Liu et al., 2018). Previously, Qiu et al. demonstrated that beige adipocytes are present at the perriphery at 12 weeks after fat grafting (Qiu et al., 2018). Besides, fat grafting induced browning also occurred in patients, as reported by Liu et al. (Liu et al., 2021). Whereas role of this browning observed in human fat grafting is unclear. Therefore, in the present study, for the first time, we aimed to determine the role of browning after grafting and demonstrated that browning in grafts may improve angiogenesis through greater secretion of VEGF-A and FGF21, leading to superior graft retention.

Firstly, we characterized the kinetics of the browning of WAT grafts. However, this finding raised the question of when the browning program of WAT is turned on and how long this lasts. In the present study, we have shown that the beige phenotype of the fat graft changes with time. Beige adipocytes appeared in fat grafts around the regenerating zone as early as 7 days following surgery, peaked in number on day 14, and then became fewer in number until week 12, when they were almost completely absent. This time course of browning suggests that it is a transient state that develops in response to certain stimuli associated with fat grafting, and that after these stimuli are withdrawn, the beige adipocytes lose this phenotype. Similar results were obtained in our previous study, in which the transplantation of tamoxifen-induced beige adipose tissue was followed by whitening of the graft within 12 weeks (Cai t al., 2018a). Indeed, several previous studies have provided evidence that beige or brown adipocytes require sustained stimuli to maintain their BAT phenotype. It has been shown that the transplantation of BAT away from the interscapular region results in a gradual loss of the BAT phenotype (Ferren 1966). Moreover, the browning of adipocytes induced by cold or pharmacologic agents is reversed once these stimuli are withdrawn (Rosenwald et al., 2013). During the early stage of fat engraftment, adipocytes are exposed to hypoxia and inflammation, and metabolites associated

with hypoxia and transient inflammatory signaling have been reported to contribute to adipocyte browning (Lee et al., 2013; Carriere et al., 2014; Trayhurn and Alomar 2015; Babaei et al., 2018; Sun et al., 2018). During the later stages of engraftment, the hypoxia and inflammation resolve, which reduces the stimulus for browning. However, the particular browning stimulus in fat grafts has yet to be identified.

Next, we evaluated whether the browning level would affect fat graft retention by pharmaceutical up-/ down- regulation of browning. Experiments by Cai et al., which demonstrated that transplantation of tamoxifen-induced beige adipose tissue improves fat graft retention, along with more recent work that showed that the browning of WAT induced by extracellular vesicles improves fat graft survival, indicate a potential role of beige adipocytes within fat grafts (Cai et al., 2018b; Zhu et al., 2020). However, the physiological significance of the spontaneous browning of fat grafts following transplantation has not been investigated. Here, we have shown that the administration of substances that affect the browning of WAT have effects on the survival and volume of fat grafts. Thus, we have shown for the first time that the survival of fat grafts is affected by the spontaneous browning of WAT *in situ*.

β3-adrenoceptor activation is thought to be a key stimulus for the formation of beige adipocytes (Lee et al., 2012). Therefore, in the present study, we pharmacologically activated or inhibited β3-adrenoceptor activation in a mouse model of fat grafting to further evaluate the role of browning in fat graft regeneration. We found that the administration of the β3 adrenoceptor agonist CL316243 or antagonist SR59230A respectively stimulates or suppresses the browning of fat grafts. The more substantial degree of browning was associated with superior angiogenesis and adipose structure. In the present study, CL316243, which represents a browning stimulator, led to superior angiogenesis and fewer tissue macrophages, and ultimately normal adipose structure with higher fat grafts retention rate.

Based on the fact that beige adipocytes contain multiple, small lipid droplets, and that fat grafts exchange nutrients by means of passive diffusion when avascular, Cai et al. suggested that tamoxifen-induced browning is associated with a higher surface area-to-volume ratio, and thus more efficient diffusion of nutrients and an improvement in survival (Khouri et al., 2014b; Cai et al., 2018a). Thus, it is likely that the browning of white adipocytes is initiated to improve tolerance toward an avascular and hypoxic microenvironment, especially during the early stages of engraftment. It is well known that ASCs and adipocytes can survive in the "survival zone," the < 300 μm-thick outer part of the graft, whereas both tend to die in the central part, or "necrosis zone"(Eto et al., 2012; Mashiko and Yoshimura 2015). Thus, the activation of browning may be an important means of improving diffusion of nutrients into the graft and improving survival. Surprisingly, as shown above, only a small cluster of adipocytes around the regenerating zone got spontaneous browning after fat grafting, which implies that the browning of the graft might only improve survival in part through more efficient diffusion resulting from a higher surface area-to-volume ratio of the beige adipocytes, and instead may have its effects through additional, as yet unidentified, mechanisms.

In addition to investigating their differing capacity for energy dissipation as heat, investigators have also focused on the contrasting secretomes of white adipocytes and brown/beige adipocytes (Cannon and Nedergaard 2004; Villarroya et al., 2017a; Villarroya et al., 2017b). Evidence obtained in multiple studies suggests that BAT produces VEGF, which improves angiogenesis , and higher vessel density and capillary permeability facilitate triglyceride uptake from the circulation (Fredriksson et al., 2005; Xue et al., 2009; Sun et al., 2014; Mahdaviani et al., 2016). The activation of BAT improves local angiogenesis through greater production of VEGF, which suggests that a factor secreted by brown-like adipocytes in fat grafts may have a positive impact on their survival. Thus , we hypothesized that inducible beige adipocytes in the regenerating zone of fat grafts would have their beneficial effects on survival through a paracrine mechanism. The fact that the beige adipocytes were located in an intermediate zone of the graft might optimize the paracrine/ endocrine effects of the beige adipocytes.

When thinking about the factors secreted by beige adipose tissue that might have beneficial effects in fat grafts, we reasoned that VEGF-A and FGF21 would be good candidates because VEGF-A is a "BATokine," secreted by BAT, and FGF21 can be released by WAT during thermogenic stimulation (Sun et al., 2014; Huang et al., 2017). To determine whether these beige cells act as a source of such factors, as for BAT, we measured the expression of the Vegfa and Fgf21 genes during the early stages of fat engraftment. Interestingly, the data show a positive association between the degree of browning and the production of the pro-vascularization factors VEGF-A and FGF21. VEGF-A is widely accepted as an regulator of physiological angiogenesis (Ferrara et al., 2003). FGF21, a well recognized batokine released by BAT, also exert an positive effect on angiogenesis (Yaqoob et al., 2014; Huang et al., 2019; Zhou et al., 2019; Dai et al., 2021). FGF21 has been reported to normalize glucose and lipid homeostasis, thus preventing the development of metabolic disorders, such as obesity and diabetes (So et al., 2015; So and Leung 2016). Furthermore, FGF21 is also found to exert cell-protective effects in metabolically active organs, such as the liver and pancreas (Wente et al., 2006; Xu et al., 2016). Moreover, increasing studies showed that FGF21 could promote angiogenesis, inhibit oxidative stress and apoptosis in various disease repair model (Yaqoob et al., 2014; Yan et al., 2018; Huang et al., 2019; Zhang et al., 2019; Zhou et al., 2019; Dai et al., 2021). Of note, during fat grafting, great importance should also be attached to functions of FGF21 associated with metabolism. For example, FGF21 increases translocation of glucose transporter 1 (GLUT1) to membrane of adipocytes, which accounts for the increased glucose uptake (Kharitonenkov et al., 2005; Ge et al., 2011). This process might have great influence on survival of adipocytes at early stage after transplantation because of ischemic environment without complete vascular network. Besides, FGF21 could also regulate lipid metabolism and stimulate lipolysis (Inagaki et al., 2007; Hotta et al., 2009). Therefore, FGF21 induced lipolysis could consume the large lipid droplets in adipocytes and thus increased surface area-to-volume ratio, leading superior diffusion to exchange nutrients, as mentioned above. Together, in this context, FGF21 produced by beige

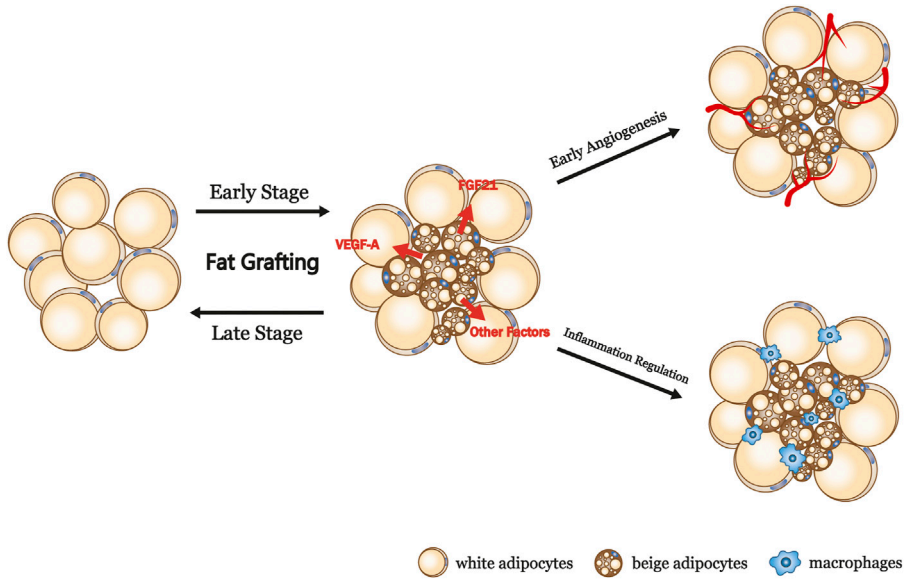

FIGURE 6 | Summary and proposed model of the browning process in fat grafts. VEGF-A, vascular endothelial growth factor A; FGF21, fibroblast growth factor 21.

adipocytes might serves as not only an angiogenesis stimulator but also an powerful metabolic regulator.

The results of the present study suggest that beige adipocytes exist in fat grafts and have beneficial effects, particularly in the early stage of engraftment. We speculate that avascularity and hypoxia during the early stage promote the conversion of white to beige adipocytes, which produce more VEGF-A and FGF21, leading to early revascularization (**Figure 6**). Early revascularization is well known to profoundly affect the long-term outcomes of grafting because a lack of new vessel formation is associated with insufficient nutrient exchange and ultimately cell death (R. J. Khouri et al., 2014a). It is well known that dead cells and cell debris would result in increasing inflammatory macrophages. Conversely, early angiogenesis reduces tissue macrophages which is resulted from improved fat cells survival. The induction of beiging during the early phase of fat engraftment may create a paracrine unit that promotes angiogenesis, leading to a reduction in cell death and relatively moderate inflammation, which contribute to superior graft retention, as shown in **Figure 5**.

Various browning agents have been used clinically. In the present study, we have highlighted the clinical potential for browning agents, such as CL316243, to improve fat engraftment. Even though the present findings were made in an animal model and the clinical validation of CL316243 requires further studies, mirabegron, a β3-adrenoceptor agonist, has been approved for the treatment of overactive bladder symptoms (Blais et al., 2016; Kelleher et al., 2018). Besides, PPAR gamma agonist rosiglitazone and sildenafil that acts via a nitric oxide-cyclic guanosine monophosphate pathway, which are known as drugs for the treatment of diabetes and erectile dysfunction respectively, were reported to promote expression of genes associated with browning of WAT (Mohanty et al., 2004; Lefterova et al., 2008; Johann et al., 2018; Di Maio et al., 2021). Thus, following further investigations, CL316243 or other promising browning inducers mentioned above might be useful for the stimulation of fat graft browning, with the aim of improving early revascularization and long-term fat graft retention and quality.

Because various signaling pathways, besides β3 adrenoceptor signaling pathways, contribute to browning of WAT under different conditions and the exact mechanism underlying the browning process after fat grafting is unknown, CL316243 and SR59230A applied in the present study may manipulate the degree of browning partly. Since transcriptional regulatory protein PRDM16 appears to control development of beige cells,the use of transgenic mice, such as overexpression or deletion of PRDM16 transgenic mice, would provide better understanding of contribution of browning process to remodeling of fat grafts (Ohno et al., 2012; Cohen et al., 2014). Therefore, mechanism of browning occurred after transplantation and the application of compound that could effectively improve browning clinically might be the focus of our work in the future. Another limitation in this study is that only male animals were used in this study; thus, gender bias should be concerned. Because fat grafting always carried out in women and therefore logically female mice should have priority in this research.

5 CONCLUSION

In the present study, we have shown that the local post-transplantation browning of WAT proceeds along a well-defined time course, and is accompanied by early angiogenesis and superior final graft retention. In a mouse model, treatment with CL316243 for 2 weeks promoted beige adipocyte formation and led to superior fat graft survival. The

finding that browning within fat grafts might influence their survival should provoke further research to explore the mechanisms involved in the graft retention and to translate these findings into a clinical means of improving fat graft quality.

DATA AVAILABILITY STATEMENT

The raw data supporting the conclusions of this article will be made available by the authors, without undue reservation.

ETHICS STATEMENT

The animal study was reviewed and approved by Nanfang Hospital Animal Ethics Committee.

AUTHOR CONTRIBUTIONS

JL, SZ, and YL: conception and design, manuscript writing, collection and assembly of data, data analysis and interpretation: ZL, YQ, YH: data analysis, interpretation, and collection data; JC and FL: conception and design, financial support, and final approval of manuscript. All authors reviewed the final manuscript.

FUNDING

This work was supported by the National Nature Science Foundation of China (81971852, 81801932, 81901976), the Natural Science Foundation of Guangdong Province of China (2019A1515010641, 021A1515011721) and the Administrator Foundation of Nanfang Hospital (2018Z010).

SUPPLEMENTARY MATERIAL

The Supplementary Material for this article can be found online at: https://www.frontiersin.org/articles/10.3389/fcell.2022.845158/full#supplementary-material

Supplementary Figure S1 | CL316243 and SR59230A had little effect on body weight and energy expenditure. **(A** and **B)** Both CL316243 and SR59230A did not alter the body weight and food intake of the mice. **(C,D** and **E)** Indirect calorimetry data showing the oxygen consumption, CO_2 production and heat production of each groups.

REFERENCES

Babaei, R., Schuster, M., Meln, I., Lerch, S., Ghandour, R. A., Pisani, D. F., Bayindir-Buchhalter, I., Marx, J., Wu, S., Schoiswohl, G., Billeter, A. T., Krunic, D., Mauer, J., Lee, Y.-H., Granneman, J. G., Fischer, L., Müller-Stich, B. P., Amri, E.-Z., Kershaw, E. E., Heikenwälder, M., Herzig, S., and Vegiopoulos, A. (2018). Jak-TGFβ Cross-Talk Links Transient Adipose Tissue Inflammation to Beige Adipogenesis. *Sci. Signal.* 11 (527), eaai7838. doi:10.1126/scisignal.aai7838

Blais, A.-S., Nadeau, G., Moore, K., Genois, L., and Bolduc, S. (2016). Prospective Pilot Study of Mirabegron in Pediatric Patients with Overactive Bladder. *Eur. Urol.* 70 (1), 9–13. doi:10.1016/j.eururo.2016.02.007

Cai, J., Feng, J., Liu, K., Zhou, S., and Lu, F. (2018a). Early Macrophage Infiltration Improves Fat Graft Survival by Inducing Angiogenesis and Hematopoietic Stem Cell Recruitment. *Plast. Reconstr. Surg.* 141 (2), 376–386. doi:10.1097/PRS.0000000000004028

Cai, J., Li, B., Wang, J., Liu, K., Zhang, Y., Liao, Y., et al. (2018b). Tamoxifen-Prefabricated Beige Adipose Tissue Improves Fat Graft Survival in Mice. *Plast. Reconstr. Surg.* 141 (4), 930–940. doi:10.1097/PRS.0000000000004220

Cannon, B., and Nedergaard, J. (2004). Brown Adipose Tissue: Function and Physiological Significance. *Physiol. Rev.* 84 (1), 277–359. doi:10.1152/physrev.00015.2003

Carrière, A., Jeanson, Y., Berger-Müller, S., André, M., Chenouard, V., Arnaud, E., et al. (2014). Browning of white Adipose Cells by Intermediate Metabolites: An Adaptive Mechanism to Alleviate Redox Pressure. *Diabetes* 63 (10), 3253–3265. doi:10.2337/db13-1885

Chappell, A. G., Lujan-Hernandez, J., Perry, D. J., Corvera, S., and Lalikos, J. F. (2015). Alternatively Activated M2 Macrophages Improve Autologous Fat Graft Survival in a Mouse Model through Induction of Angiogenesis. *Plast. Reconstr. Surg.* 136 (2), 277e. doi:10.1097/PRS.0000000000001435

Cohen, P., Levy, J. D., Zhang, Y., Frontini, A., Kolodin, D. P., Svensson, K. J., et al. (2014). Ablation of PRDM16 and Beige Adipose Causes Metabolic Dysfunction and a Subcutaneous to Visceral Fat Switch. *Cell* 156 (1-2), 304–316. doi:10.1016/j.cell.2013.12.021

Dai, Q., Fan, X., Meng, X., Sun, S., Su, Y., Ling, X., et al. (2021). FGF21 Promotes Ischaemic Angiogenesis and Endothelial Progenitor Cells Function under Diabetic Conditions in an AMPK/NAD+-dependent Manner. *J. Cel. Mol. Med.* 25 (6), 3091–3102. doi:10.1111/jcmm.16369

Di Maio, G., Alessio, N., Demirsoy, I. H., Peluso, G., Perrotta, S., Monda, M., et al. (2021). Evaluation of Browning Agents on the White Adipogenesis of Bone Marrow Mesenchymal Stromal Cells: A Contribution to Fighting Obesity. *Cells* 10 (2), 403. doi:10.3390/cells10020403

Eto, H., Kato, H., Suga, H., Aoi, N., Doi, K., Kuno, S., et al. (2012). The Fate of Adipocytes after Nonvascularized Fat Grafting. *Plast. Reconstr. Surg.* 129 (5), 1081–1092. doi:10.1097/PRS.0b013e31824a2b19

Ferrara, N., Gerber, H.-P., and LeCouter, J. (2003). The Biology of VEGF and its Receptors. *Nat. Med.* 9 (6), 669–676. doi:10.1038/nm0603-669

Ferren, L. (1966). Morphological Differentiation of Implanted Brown and white Fats. *Trans. Kans. Acad. Sci.* 69 (1), 350–353. doi:10.2307/3627430

Fredriksson, J. M., Nikami, H., and Nedergaard, J. (2005). Cold-induced Expression of the VEGF Gene in Brown Adipose Tissue Is Independent of Thermogenic Oxygen Consumption. *FEBS Lett.* 579 (25), 5680–5684. doi:10.1016/j.febslet.2005.09.044

Ge, X., Chen, C., Hui, X., Wang, Y., Lam, K. S. L., and Xu, A. (2011). Fibroblast Growth Factor 21 Induces Glucose Transporter-1 Expression through Activation of the Serum Response factor/Ets-like Protein-1 in Adipocytes. *J. Biol. Chem.* 286 (40), 34533–34541. doi:10.1074/jbc.M111.248591

Hong, K. Y., Yim, S., Kim, H. J., Jin, U. S., Lim, S., Eo, S., et al. (2018). The Fate of the Adipose-Derived Stromal Cells during Angiogenesis and Adipogenesis after Cell-Assisted Lipotransfer. *Plast. Reconstr. Surg.* 141 (2), 365–375. doi:10.1097/PRS.0000000000004021

Hotta, Y., Nakamura, H., Konishi, M., Murata, Y., Takagi, H., Matsumura, S., et al. (2009). Fibroblast Growth Factor 21 Regulates Lipolysis in White Adipose Tissue but Is Not Required for Ketogenesis and Triglyceride Clearance in Liver. *Endocrinology* 150 (10), 4625–4633. doi:10.1210/en.2009-0119

Huang, W., Shao, M., Liu, H., Chen, J., Hu, J., Zhu, L., et al. (2019). Fibroblast Growth Factor 21 Enhances Angiogenesis and Wound Healing of Human Brain Microvascular Endothelial Cells by Activating PPARγ. *J. Pharmacol. Sci.* 140 (2), 120–127. doi:10.1016/j.jphs.2019.03.010

Huang, Z., Zhong, L., Lee, J. T. H., Zhang, J., Wu, D., Geng, L., et al. (2017). The FGF21-CCL11 Axis Mediates Beiging of White Adipose Tissues by Coupling Sympathetic Nervous System to Type 2 Immunity. *Cel Metab.* 26 (3), 493–508. doi:10.1016/j.cmet.2017.08.003

Inagaki, T., Dutchak, P., Zhao, G., Ding, X., Gautron, L., Parameswara, V., et al. (2007). Endocrine Regulation of the Fasting Response by PPARα-Mediated Induction of Fibroblast Growth Factor 21. *Cel Metab.* 5 (6), 415–425. doi:10.1016/j.cmet.2007.05.003

Jiang, Y., Berry, D. C., and Graff, J. M. (2017). Distinct Cellular and Molecular Mechanisms for β3 Adrenergic Receptor-Induced Beige Adipocyte Formation. *eLife* 6, e30329. doi:10.7554/eLife.30329

Johann, K., Reis, M. C., Harder, L., Herrmann, B., Gachkar, S., Mittag, J., et al. (2018). Effects of Sildenafil Treatment on Thermogenesis and Glucose Homeostasis in Diet-Induced Obese Mice. *Nutr. Diabetes* 8 (1), 9. doi:10.1038/s41387-018-0026-0

Kelleher, C., Hakimi, Z., Zur, R., Siddiqui, E., Maman, K., Aballéa, S., et al. (2018). Efficacy and Tolerability of Mirabegron Compared with Antimuscarinic Monotherapy or Combination Therapies for Overactive Bladder: A Systematic Review and Network Meta-Analysis. *Eur. Urol.* 74 (3), 324–333. doi:10.1016/j.eururo.2018.03.020

Kharitonenkov, A., Shiyanova, T. L., Koester, A., Ford, A. M., Micanovic, R., Galbreath, E. J., et al. (2005). FGF-21 as a Novel Metabolic Regulator. *J. Clin. Invest.* 115 (6), 1627–1635. doi:10.1172/JCI23606

Khouri, R. K., Khouri, R.-E. R., Lujan-Hernandez, J. R., Khouri, K. R., Lancerotto, L., and Orgill, D. P. (2014a). Diffusion and Perfusion. *Plast. Reconstr. Surg. Glob. Open* 2 (9), e220. doi:10.1097/GOX.0000000000000183

Khouri, R. K., and Khouri, R. K. (2017). Current Clinical Applications of Fat Grafting. *Plast. Reconstr. Surg.* 140 (3), 466e–486e. doi:10.1097/PRS.0000000000003648

Khouri, R. K., Khouri, R. K., Rigotti, G., Marchi, A., Cardoso, E., Rotemberg, S. C., et al. (2014b). Aesthetic Applications of Brava-Assisted Megavolume Fat Grafting to the Breasts. *Plast. Reconstr. Surg.* 133 (4), 796–807. doi:10.1097/PRS.0000000000000053

Lee, C., Liu, M., Agha, O., Kim, H. T., Liu, X., and Feeley, B. T. (2020). Beige Fibro-Adipogenic Progenitor Transplantation Reduces Muscle Degeneration and Improves Function in a Mouse Model of Delayed Repair of Rotator Cuff Tears. *J. Shoulder Elbow Surg.* 29 (4), 719–727. doi:10.1016/j.jse.2019.09.021

Lee, Y.-H., Petkova, A. P., and Granneman, J. G. (2013). Identification of an Adipogenic Niche for Adipose Tissue Remodeling and Restoration. *Cel Metab.* 18 (3), 355–367. doi:10.1016/j.cmet.2013.08.003

Lee, Y.-H., Petkova, A. P., Mottillo, E. P., and Granneman, J. G. (2012). In Vivo Identification of Bipotential Adipocyte Progenitors Recruited by β3-Adrenoceptor Activation and High-Fat Feeding. *Cel Metab.* 15 (4), 480–491. doi:10.1016/j.cmet.2012.03.009

Lefterova, M. I., Zhang, Y., Steger, D. J., Schupp, M., Schug, J., Cristancho, A., et al. (2008). PPARγ and C/EBP Factors Orchestrate Adipocyte Biology via Adjacent Binding on a Genome-wide Scale. *Genes Dev.* 22 (21), 2941–2952. doi:10.1101/gad.1709008

Liu, K., Cai, J., Li, H., Feng, J., Feng, C., and Lu, F. (2018). The Disturbed Function of Neutrophils at the Early Stage of Fat Grafting Impairs Long-Term Fat Graft Retention. *Plast. Reconstr. Surg.* 142 (5), 1229–1238. doi:10.1097/PRS.0000000000004882

Liu, T., Fu, S., Wang, Q., Cheng, H., Mu, D., and Luan, J. (2021). Evidence of browning of white Adipocytes in Poorly Survived Fat Grafts in Patients. *Aesthet. Surg. J.* 41 (8), P1086–P1091. doi:10.1093/asj/sjab165

Mahdaviani, K., Chess, D., Wu, Y., Shirihai, O., and Aprahamian, T. R. (2016). Autocrine Effect of Vascular Endothelial Growth Factor-A Is Essential for Mitochondrial Function in Brown Adipocytes. *Metabolism* 65 (1), 26–35. doi:10.1016/j.metabol.2015.09.012

Mashiko, T., and Yoshimura, K. (2015). How Does Fat Survive and Remodel after Grafting? *Clin. Plast. Surg.* 42 (2), 181–190. doi:10.1016/j.cps.2014.12.008

Mohanty, P., Aljada, A., Ghanim, H., Hofmeyer, D., Tripathy, D., Syed, T., et al. (2004). Evidence for a Potent Antiinflammatory Effect of Rosiglitazone. *J. Clin. Endocrinol. Metab.* 89 (6), 2728–2735. doi:10.1210/jc.2003-032103

Montanari, T., Pošćić, N., and Colitti, M. (2017). Factors Involved in white-to-brown Adipose Tissue Conversion and in Thermogenesis: A Review. *Obes. Rev.* 18 (5), 495–513. doi:10.1111/obr.12520

Ohno, H., Shinoda, K., Spiegelman, B. M., and Kajimura, S. (2012). PPARγ Agonists Induce a White-to-Brown Fat Conversion through Stabilization of PRDM16 Protein. *Cel Metab.* 15 (3), 395–404. doi:10.1016/j.cmet.2012.01.019

Petrovic, N., Walden, T. B., Shabalina, I. G., Timmons, J. A., Cannon, B., and Nedergaard, J. (2010). Chronic Peroxisome Proliferator-Activated Receptor γ (PPARγ) Activation of Epididymally Derived White Adipocyte Cultures Reveals a Population of Thermogenically Competent, UCP1-Containing Adipocytes Molecularly Distinct from Classic Brown Adipocytes. *J. Biol. Chem.* 285 (10), 7153–7164. doi:10.1074/jbc.M109.053942

Pu, L. L. Q., Yoshimura, K., and Coleman, S. R. (2015). Fat Grafting: Current Concept, Clinical Application, and Regenerative Potential, Part 1. *Clin. Plast. Surg.* 42 (2), ix–x. doi:10.1016/j.cps.2015.02.001

Qiu, L., Zhang, Z., Zheng, H., Xiong, S., Su, Y., Ma, X., et al. (2018). Browning of Human Subcutaneous Adipose Tissue after its Transplantation in Nude Mice. *Plast. Reconstr. Surg.* 142 (2), 392–400. doi:10.1097/PRS.0000000000004603

Rosenwald, M., Perdikari, A., Rülicke, T., and Wolfrum, C. (2013). Bi-directional Interconversion of Brite and white Adipocytes. *Nat. Cel Biol.* 15 (6), 659–667. doi:10.1038/ncb2740

Schulz, T. J., Huang, T. L., Tran, T. T., Zhang, H., Townsend, K. L., Shadrach, J. L., et al. (2011). Identification of Inducible Brown Adipocyte Progenitors Residing in Skeletal Muscle and white Fat. *Proc. Natl. Acad. Sci. U.S.A.* 108 (1), 143–148. doi:10.1073/pnas.1010929108

So, W. Y., Cheng, Q., Xu, A., Lam, K. S. L., and Leung, P. S. (2015). Loss of Fibroblast Growth Factor 21 Action Induces Insulin Resistance, Pancreatic Islet Hyperplasia and Dysfunction in Mice. *Cell Death Dis* 6–e1707. doi:10.1038/cddis.2015.80

So, W. Y., and Leung, P. S. (2016). Fibroblast Growth Factor 21 as an Emerging Therapeutic Target for Type 2 Diabetes Mellitus. *Med. Res. Rev.* 36 (4), 672–704. doi:10.1002/med.21390

Sun, K., Gao, Z., and Kolonin, M. G. (2018). Transient Inflammatory Signaling Promotes Beige Adipogenesis. *Sci. Signal.* 11 (527), eaat3192. doi:10.1126/scisignal.aat3192

Sun, K., Kusminski, C. M., Luby-Phelps, K., Spurgin, S. B., An, Y. A., Wang, Q. A., et al. (2014). Brown Adipose Tissue Derived VEGF-A Modulates Cold Tolerance and Energy Expenditure. *Mol. Metab.* 3 (4), 474–483. doi:10.1016/j.molmet.2014.03.010

Teresa Ortega, M., Xie, L., Mora, S., and Chapes, S. K. (2011). Evaluation of Macrophage Plasticity in Brown and white Adipose Tissue. *Cell Immunol.* 271 (1), 124–133. doi:10.1016/j.cellimm.2011.06.012

Trayhurn, P., and Alomar, S. Y. (2015). Oxygen Deprivation and the Cellular Response to Hypoxia in Adipocytes Â€" Perspectives on White and Brown Adipose Tissues in Obesity. *Front. Endocrinol.* 6, 19. doi:10.3389/fendo.2015.00019

Villarroya, F., Cereijo, R., Villarroya, J., and Giralt, M. (2017a). Brown Adipose Tissue as a Secretory Organ. *Nat. Rev. Endocrinol.* 13 (1), 26–35. doi:10.1038/nrendo.2016.136

Villarroya, F., Gavaldà-Navarro, A., Peyrou, M., Villarroya, J., and Giralt, M. (2017b). The Lives and Times of Brown Adipokines. *Trends Endocrinol. Metab.* 28 (12), 855–867. doi:10.1016/j.tem.2017.10.005

Wankhade, U. D., Shen, M., Yadav, H., and Thakali, K. M. (2016). Novel browning Agents, Mechanisms, and Therapeutic Potentials of Brown Adipose Tissue. *Biomed. Res. Int.* 2016, 1–15. doi:10.1155/2016/2365609

Wente, W., Efanov, A. M., Brenner, M., Kharitonenkov, A., Köster, A., Sandusky, G. E., et al. (2006). Fibroblast Growth Factor-21 Improves Pancreatic β-Cell Function and Survival by Activation of Extracellular Signal-Regulated Kinase 1/2 and Akt Signaling Pathways. *Diabetes* 55 (9), 2470–2478. doi:10.2337/db05-1435

Wu, J., Boström, P., Sparks, L. M., Ye, L., Choi, J. H., Giang, A.-H., et al. (2012). Beige Adipocytes Are a Distinct Type of Thermogenic Fat Cell in Mouse and Human. *Cell* 150 (2), 366–376. doi:10.1016/j.cell.2012.05.016

Xu, P., Zhang, Y., Liu, Y., Yuan, Q., Song, L., Liu, M., et al. (2016). Fibroblast Growth Factor 21 Attenuates Hepatic Fibrogenesis through TGF-B/smad2/3 and NF-Kb Signaling Pathways. *Toxicol. Appl. Pharmacol.* 290, 43–53. doi:10.1016/j.taap.2015.11.012

Xue, Y., Petrovic, N., Cao, R., Larsson, O., Lim, S., Chen, S., et al. (2009). Hypoxia-independent Angiogenesis in Adipose Tissues during Cold Acclimation. *Cel Metab.* 9 (1), 99–109. doi:10.1016/j.cmet.2008.11.009

Yan, X., Gou, Z., Li, Y., Wang, Y., Zhu, J., Xu, G., et al. (2018). Fibroblast Growth Factor 21 Inhibits Atherosclerosis in apoE−/− Mice by Ameliorating Fas-Mediated Apoptosis. *Lipids Health Dis.* 17 (1), 203. doi:10.1186/s12944-018-0846-x

Yaqoob, U., Jagavelu, K., Shergill, U., de Assuncao, T., Cao, S., and Shah, V. H. (2014). FGF21 Promotes Endothelial Cell Angiogenesis through a Dynamin-2 and Rab5 Dependent Pathway. *PLoS One* 9 (5), e98130. doi:10.1371/journal.pone.0098130

Zhang, X., Yang, L., Xu, X., Tang, F., Yi, P., Qiu, B., et al. (2019). A Review of Fibroblast Growth Factor 21 in Diabetic Cardiomyopathy. *Heart Fail. Rev.* 24 (6), 1005–1017. doi:10.1007/s10741-019-09809-x

Zhou, K., Chen, H., Lin, J., Xu, H., Wu, H., Bao, G., et al. (2019). FGF21 Augments Autophagy in Random-Pattern Skin Flaps via AMPK Signaling Pathways and Improves Tissue Survival. *Cel Death Dis.* 10 (12), 872. doi:10.1038/s41419-019-2105-0

Zhu, Y.-z., Zhang, J., Hu, X., Wang, Z.-h., Wu, S., and Yi, Y.-y. (2020). Supplementation with Extracellular Vesicles Derived from Adipose-Derived Stem Cells Increases Fat Graft Survival and browning in Mice: A Cell-free Approach to Construct Beige Fat from white Fat Grafting. *Plast. Reconstr. Surg.* 145 (5), 1183–1195. doi:10.1097/PRS.0000000000006740

Conflict of Interest: The authors declare that the research was conducted in the absence of any commercial or financial relationships that could be construed as a potential conflict of interest.

Publisher's Note: All claims expressed in this article are solely those of the authors and do not necessarily represent those of their affiliated organizations, or those of the publisher, the editors and the reviewers. Any product that may be evaluated in this article, or claim that may be made by its manufacturer, is not guaranteed or endorsed by the publisher.

frontiers | Frontiers in Cell and Developmental Biology

TYPE Correction
PUBLISHED 02 August 2022
DOI 10.3389/fcell.2022.955768

OPEN ACCESS

APPROVED BY
Frontiers in Editorial Office,
Frontiers Media SA, Switzerland

*CORRESPONDENCE
Junrong Cai,
drjunrongcai@outlook.com
Feng Lu,
doctorlufeng@hotmail.com

†These authors have contributed equally to this work and share first authorship
‡These authors have contributed equally to this work and share last authorship

SPECIALTY SECTION
This article was submitted to Cellular Biochemistry,
a section of the journal
Frontiers in Cell and Developmental Biology

RECEIVED 29 May 2022
ACCEPTED 28 June 2022
PUBLISHED 02 August 2022

CITATION
Lin J, Zhu S, Liao Y, Liang Z, Quan Y, He Y, Cai J and Lu F (2022), Corrigendum: Spontaneous browning of white adipose tissue improves angiogenesis and reduces macrophage infiltration after fat grafting in mice. *Front. Cell Dev. Biol.* 10:955768. doi: 10.3389/fcell.2022.955768

Corrigendum: Spontaneous browning of white adipose tissue improves angiogenesis and reduces macrophage infiltration after fat grafting in mice

Jiayan Lin†, Shaowei Zhu†, Yunjun Liao†, Zhuokai Liang, Yuping Quan, Yufei He, Junrong Cai*‡ and Feng Lu*‡

Department of Plastic and Cosmetic Surgery, Nanfang Hospital, Southern Medical University, Guangzhou, China

KEYWORDS

fat grafting, browning, beige adipocytes, angiogenesis, inflammation

A Corrigendum on
Spontaneous Browning of White Adipose Tissue Improves Angiogenesis and Reduces Macrophage Infiltration After Fat Grafting in Mice

by Lin, J, Zhu, S, Liao, Y, Liang, Z, Quan, Y, He, Y, Cai, J and Lu, F (2022). Front. Cell Dev. Biol. 10: 845158. doi: 10.3389/fcell.2022.845158

In the original article, there was an error. The symbols "*" and "‡", indicating correspondence and equal contribution sharing last authorship, were omitted for author Feng Lu.

A correction has been made to the author list:

"Jiayan Lin†, Shaowei Zhu†, Yunjun Liao†, Zhuokai Liang, Yuping Quan, Yufei He, Junrong Cai*‡ and Feng Lu*‡"

*Correspondence:
Junrong Cai,
drjunrongcai@outlook.com
Feng Lu,
doctorlufeng@hotmail.com

The authors apologize for this error and state that this does not change the scientific conclusions of the article in any way. The original article has been updated.

Publisher's note

frontiers | Frontiers in Cell and Developmental Biology

BRIEF RESEARCH REPORT
published: 05 May 2022
doi: 10.3389/fcell.2022.893729

Epicardial Adipose Tissue-Derived IL-1β Triggers Postoperative Atrial Fibrillation

Serena Cabaro[1,2†], Maddalena Conte[1,3†], Donato Moschetta[4,5], Laura Petraglia[1], Vincenza Valerio[4], Serena Romano[1,2], Michele Francesco Di Tolla[1,2], Pasquale Campana[1], Giuseppe Comentale[6], Emanuele Pilato[6], Vittoria D'Esposito[1,2], Annabella Di Mauro[1,7], Monica Cantile[7], Paolo Poggio[4], Valentina Parisi[1]*, Dario Leosco[1‡] and Pietro Formisano[1,2‡]*

[1]Department of Translational Medical Sciences, University of Naples Federico II, Naples, Italy, [2]URT Genomic of Diabetes, Institute of Experimental Endocrinology and Oncology, National Research Council, Naples, Italy, [3]Casa di Cura San Michele, Maddaloni, Italy, [4]Centro Cardiologico Monzino IRCCS, Milan, Italy, [5]Department of Pharmacological and Biomolecular Sciences, University of Milan, Milan, Italy, [6]Department of Advanced Biomedical Sciences, University of Naples Federico II, Naples, Italy, [7]Pathology Unit, INT-IRCCS Fondazione Pascale, Naples, Italy

OPEN ACCESS

Edited by:
Kazuo Miyazawa,
RIKEN Yokohama, Japan

Reviewed by:
Floriana Farina,
LMU Munich University Hospital, Germany
George Nikov Chaldakov,
Medical University of Varna, Bulgaria

***Correspondence:**
Paolo Poggio
paolo.poggio@ccfm.it
Valentina Parisi
parisi.valentina@tiscali.it
valentina.parisi@unina.it

[†]These authors have contributed equally to this work and share first authorship

[‡]These authors have contributed equally to this work and share last authorship

Specialty section:
This article was submitted to Cellular Biochemistry, a section of the journal Frontiers in Cell and Developmental Biology

Received: 10 March 2022
Accepted: 15 April 2022
Published: 05 May 2022

Citation:
Cabaro S, Conte M, Moschetta D, Petraglia L, Valerio V, Romano S, Di Tolla MF, Campana P, Comentale G, Pilato E, D'Esposito V, Di Mauro A, Cantile M, Poggio P, Parisi V, Leosco D and Formisano P (2022) Epicardial Adipose Tissue-Derived IL-1β Triggers Postoperative Atrial Fibrillation. Front. Cell Dev. Biol. 10:893729. doi: 10.3389/fcell.2022.893729

Background and aims: Post-operative atrial fibrillation (POAF), defined as new-onset AF in the immediate period after surgery, is associated with poor adverse cardiovascular events and a higher risk of permanent AF. Mechanisms leading to POAF are not completely understood and epicardial adipose tissue (EAT) inflammation could be a potent trigger. Here, we aim at exploring the link between EAT-secreted interleukin (IL)-1β, atrial remodeling, and POAF in a population of coronary artery disease (CAD) patients.

Methods: We collected EAT and atrial biopsies from 40 CAD patients undergoing cardiac surgery. Serum samples and EAT-conditioned media were screened for IL-1β and IL-1ra. Atrial fibrosis was evaluated at histology. The potential role of NLRP3 inflammasome activation in promoting fibrosis was explored *in vitro* by exposing human atrial fibroblasts to IL-1β and IL-18.

Results: 40% of patients developed POAF. Patients with and without POAF were homogeneous for clinical and echocardiographic parameters, including left atrial volume and EAT thickness. POAF was not associated with atrial fibrosis at histology. No significant difference was observed in serum IL-1β and IL-1ra levels between POAF and no-POAF patients. EAT-mediated IL-1β secretion and expression were significantly higher in the POAF group compared to the no-POAF group. The *in vitro* study showed that both IL-1β and IL-18 increase fibroblasts' proliferation and collagen production. Moreover, the stimulated cells perpetuated inflammation and fibrosis by producing IL-1β and transforming growth factor (TGF)-β.

Conclusion: EAT could exert a relevant role both in POAF occurrence and in atrial fibrotic remodeling.

Keywords: epicardial adipose tissue, cytokines, inflammation, atrial fibrillation, fibrosis, cardiac remodeling

INTRODUCTION

Atrial fibrillation (AF), the most common cardiac arrhythmia, is the result of electrical and structural remodeling of the atria encompassing interactions among cellular and neurohormonal mediators (Hu et al., 2015). Post-operative AF (POAF), defined as new-onset AF in the immediate period after surgery, is associated with hemodynamic instability, increased risk of stroke, an eightfold increase in the risk of subsequent AF (Ahlsson et al., 2010), and cardiovascular death (Ahlsson et al., 2010; Lee et al., 2014; Melduni et al., 2015).

Mechanisms leading to POAF are not completely understood, but it is probably the consequence of both pre-existing factors, related to atrial remodeling, and peri-operative triggers that induce AF when a vulnerable substrate is present. Inflammation could be one of the most potent AF triggers and the NACHT, LRR, and PYD domain-containing protein 3 (NLRP3) inflammasome myocardial activation, through the production of the pro-inflammatory cytokines interleukin (IL)-1β and IL-18, is associated with the pathogenesis of AF by promoting atrial structural and electrical remodeling (Yao et al., 2018). IL-1β increased gene expression levels are associated with atrial remodeling and sustained AF (Matsushita et al., 2019). IL-1β plays an important role in the inflammatory cascade and coordinates the cellular response to tissue injury, promoting the recruitment of inflammatory cells and the increased production of other cytokines (Dinarello, 2011). Animal studies suggest that IL-1β contributes to myocardial electrophysiological remodeling and its inhibition reduces arrhythmogenesis (De Jesus et al., 2017). Epicardial adipose tissue (EAT), the visceral fat depot of the heart, has been proposed as a local source of inflammatory mediators with a potential role in AF (Arai et al., 2011; Wong et al., 2017). Potential arrhythmogenic mechanisms of EAT in AF include structural remodeling of the atria and arrhythmic trigger by infiltrations of adipose tissue, fibrosis modulation, myocardial inflammation, and oxidative stress (Wong et al., 2017). IL-1β stimulates activin A expression (Arai et al., 2011) that has been reported to be produced by epicardial adipose tissue (EAT) of patients evolving POAF after cardiac surgery (de Kretser et al., 2012; Wang et al., 2019). We recently reported an increased inflammatory status of EAT also in POAF (Petraglia et al., 2022). However, further evidence is required to confirm all these hypothetic mechanisms in order to clarify the role of EAT in cardiovascular disease and AF.

In the present manuscript, we aim at exploring the link between EAT-secreted IL-1β, atrial remodeling, and POAF in a population of coronary artery disease (CAD) patients undergoing cardiac surgery.

MATERIALS AND METHODS

Patient Enrollment and Tissue Collection

Forty patients with coronary artery disease (CAD) undergoing elective coronary artery bypass grafting (CABG) were enrolled at the cardiac surgery unit of the University of Naples "Federico II."

Exclusion criteria were the following: chronic inflammatory diseases that could interfere with the systemic or local inflammatory profile, history of AF. Before cardiac surgery, all patients underwent clinical and echocardiographic assessment. Clinical and demographic data were recorded, including cardiovascular risk factors and drug therapies. According to standard techniques, echocardiograms were performed by a Vivid E9 (GE Healthcare) machine. EAT was visualized in a parasternal long-axis view between the free wall of the right ventricle and the anterior surface of the ascending aorta. Once visualized the EAT deposit, the maximum EAT thickness was measured at end-systole, as previously described (Parisi et al., 2020a). The average value from three cardiac cycles was used for the statistical analysis.

Before cardiac surgery, we collected blood samples for serum collection. Intraoperative EAT biopsies (average 0.1–0.5 g) and right atrial appendages were carried out before the initiation of cardiopulmonary bypass. EAT biopsies were taken between the free wall of the right ventricle and the anterior surface of the ascending aorta, just after the opening of the pericardial sac. Each tissue sample was stored at −80°C until analysis. All patients were postoperatively monitored by ECG telemetry and data on POAF occurrence were recorded during the hospital stay.

Informed consent was obtained from every subject before the surgical procedure. Protocols were approved by the ethical committee of the University of Naples (prot. no. 301/19). All procedures performed in the study were in accordance with the ethical standards of the institutional or national research committee and with the 1964 Helsinki declaration and its later amendments or comparable ethical standards and conformed to the Declaration of Helsinki on human research.

Conditioned Media Preparation and Cytokines Assessment

According to tissue weight, serum-free Dulbecco modified Eagle medium (DMEM)-F12 (1:1) containing 0.25% BSA (1 ml medium/0.1 g tissue) was added to the well and incubated at 37°C in a CO2 incubator. After 24 h, the medium was collected, centrifuged at 14,000 × g to remove debris, and then stored as aliquots at −80°C until further use. Serum samples and conditioned media were screened for the concentration of interleukin (IL)-1ra, IL-1b, IL-2, IL-4, IL-5, IL-6, IL-7, IL-8, IL-9, IL-10, IL-12 (p70), IL-13, IL-15, IL-17A, basic fibroblast growth factor (FGF), eotaxin, granulocyte-colony stimulating factor (G-CSF), granulocyte macrophage-colony stimulating factor (GM-CSF), interferon-γ (IFN-γ), interferon-γ inducible protein 10 (IP-10), monocyte chemoattractant protein-1 (MCP-1), macrophage inflammatory protein-1 (MIP-1) α, MIP-1β, C–C motif chemokine ligand 5 (CCL5)/RANTES, TNF-α, platelet-derived growth factor (PDGF-BB) and vascular endothelial growth factor (VEGF) using the Bio-Plex Pro Human Cytokine Grp I Panel 27-Plex kit (cat. no. M500KCAF0Y) according to the supplier's instructions. The magnetic bead-based assay was performed on a Bio-Plex 200 analyzer with Bio-Rad Bio-Plex Manager (Bio-Rad, Hercules, CA, United States).

Atrial Fibrosis Assessment at Histology

Fresh tissue from atrial biopsies was formalin-fixed and paraffin-embedded. For each case 4 μm-thick sections were cut and stained with hematoxylin/eosin and observed on a light microscope to evaluate fibrosis, graded as 0, 1+, 2+ and 3+, respectively when absent or observed in <10%, 10–50% and in >50% of the sample. The volume fraction of collagen (CVF) was analyzed by staining with hematoxylin/eosin. Four separate views were selected (magnification = original ×400) and the CVF was calculated using the following formula: CVF = collagen area/total visual area × 100%, to assess the degree of cardiac fibrosis. Each sample was independently evaluated by two different pathologists.

Cell Culture and Treatments

Human fibroblasts were isolated from the right atrial auricle by mechanical and enzymatic digestion (collagenase type II) of the tissue and cultured in Advanced Dulbecco's modified eagle's medium (Ad DMEM; Life Technologies) with 10% fetal bovine serum (FBS; Microtech, IT), 1% penicillin (Life Technologies), 1% streptomycin (Life Technologies), and 1% L-glutamine (Life Technologies). Primary cells were immortalized by transduction with commercial lentiviral particles carrying out the encoding sequences for SV40 large T antigen and human telomerase reverse transcriptase (hTERT) enzyme, under cytomegalovirus promoter (GeneCopoeia). Interleukin (IL) treatments were performed using human recombinant IL-1β (R&D Systems, Inc., Minneapolis, MN, United States) at 0.1, 1, and 10 ng/ml and IL-18 (R&D Systems, Inc., Minneapolis, MN, United States) at 1, 10, and 100 ng/ml. FBS at 10% was used as a positive control for migration assay.

MTT Assay

To evaluate the proliferation rate, 3000 cells per well were plated in a 96 well plate and followed by Incucyte (Essen BioScience) every 8 h for 5 days. Cells were treated with recombinant ILs (as previously reported) every other day. At the end of the survey, cell viability was assessed by 3-(4, 5-dimethyl thiazolyl-2)-2,5-diphenyltetrazolium bromide (MTT; Sigma-Aldrich). Briefly, MTT solution (0.5 mg/ml) was added into each well and incubated at 37°C, 5% CO2 for 4 h. The supernatant was discarded and dimethylsulfoxide (DMSO; Sigma-Aldrich) was added into each well. The corresponding absorbance value was observed using the microplate reader (TECAN pro infinite M200) at a dual-wavelength of 590 and 620 nm (reference). Cell viability was expressed as a percentage with respect to the mean of untreated, referred to as 100%.

Migration Assay

To evaluate the migration, 5,000 cells per well were plated in a 96 well plate and starved overnight in Ad DMEM without FBS. The day after, a scratch was performed using wound maker 96 (Essen BioScience), treatments with ILs were added and wound healing was evaluated by Incucyte (Essen BioScience) every 2 h for 1 day. Relative wound density was expressed as a percentage referred to the same well at time 0.

RNA Isolation and Expression Analysis

Total RNA was isolated from EAT biopsies and cell culture, using TRIzol solution (Life Technologies, CA, United States), quantified (NanoDrop spectrophotometer, Life Technologies, Carlsbad, CA, United States), and reverse-transcribed using SuperScript III Reverse Transcriptase according to the manufacturer's instructions. qPCR was performed by iTaq Universal SYBR Green Supermix (Biorad). Absolute quantification of gene expression (Arbitrary Units—AU) was measured by using the $2^{-\Delta Ct}$ method (EAT biopsies). Relative quantification (AU) of gene expression was measured by using $2^{-\Delta\Delta Ct}$ method (cell culture). Expression levels of *IL-1β* (*IL-1β* primer pairs: F-5′-ACTGAAAGCTCTCCACCTCC-3'; R-5′-CATCTTTCAACACGCAGGAC-3′), Collagen 1A1 (*COL1A1* primer pairs: F-5′-GGACACAGAGGTTTCAGTGG-3'; R-5′-CCAGTAGCACCATCATTTCC-3′), Collagen 3A1 (*COL3A1* primer pairs: F-5′-CTACTTCTCGCTCTGCTTCATC-3'; R-5′-TTGGCATGGTTCTGGCTT-3′), Transforming Growth Factor β1 (*TGFβ1* primer pairs: F-5′-GTTCAGGTACCGCTTCTCG-3'; R-5′-CCGACTACTACGCCAAGGA-3′) were normalized for the reference sample using Peptidylprolyl Isomerase A (*PPIA*) as housekeeping gene (*PPIA* primer pairs: F-5′-TACGGGTCCTGGCATCTTGT-3'; R-5′-GGTGATCTTCTTGCTGGTC-3′).

Statistical Analysis

Statistical analyses were performed with R statistical platform and with GraphPad Prism 8.0 software (GraphPad Software Inc., La Jolla, CA). D'Agostino-Pearson normality test was used to evaluate whether the continuous data were normally distributed, and according to the results, a Welch's two-tailed *t*-test for independent samples (for normally distributed data) or a Mann-Whitney *U* test (for not normally distributed data) was used. Categorical values were described by the number of occurrences and percentages and compared by the chi-square test. One-way analysis of variance (ANOVA) followed by Tukey's multi comparison test was used for the *in vitro* data.

Receiver-operating characteristics (ROC) curves were used to evaluate IL-1β′s ability to classify POAF and no-POAF patients.

RESULTS

Patient Clinical Characteristics and Atrial Fibrosis

Forty CAD patients were selected for the study (mean age 61 years, male gender 95%). No differences in surgical procedures were noted in the two groups, and in all patients extracorporeal circulation was performed. **Table 1** illustrates the demographic, clinical, and echocardiographic characteristics of overall patients. Sixteen patients out of 40 (40%) developed AF during the 7 days following the cardiac surgery (POAF group), while 60% exhibited constant sinus rhythm in the postoperative period (no-POAF). The two groups were homogeneous concerning age, clinical and echocardiographic parameters, including left atrial volume and EAT thickness (**Table 1**). In a subgroup of 20 patients, we assessed atrial fibrosis at histology. The 60% of patients has grade 0 (no fibrosis), the 5% had grade 1 (<10% fibrosis), the 25% had

TABLE 1 | Patient clinical characteristics in No-POAF and POAF groups.

	No-POAF (*n* = 24)	POAF (*n* = 16)	*p*-value (Test)
Sex (M) (%)	22 (91.67%)	16 (100%)	0.236[a]
Age (years)	61 ± 10.5	62.1 ± 9.51	0.717[b]
BMI (Kg/m^2)	29.4 (27.7; 31.5)	29.4 (27.4; 30.4)	0.445[b]
Diabetes (%)	4 (20%)	6 (37.5%)	0.136[a]
LVEF (%)	55 (51; 60)	55 (48; 59.5)	0.445[c]
E/A	0.72 (0.68; 0.83)	0.805 (0.61; 0.975)	0.712[c]
E/E′	8.8 (6.52; 10)	9.76 (7.22; 11.4)	0.595[b]
EAT thickness (mm)	14.5 (12.3; 16.8)	14.5 (12; 17)	0.904[b]
Left Atrial Volume (ml/m^2)	32.5 (28.5; 45.8)	37 (31.3; 43.8)	0.439[c]
Creatinine (mg/dl)	0.89 (0.80; 1.04)	0.96 (0.78; 1.27)	0.677[c]
GFR (ml/min)	87 (75.25; 99.75)	80 (59; 93)	0.250[b]
Hypertension (%)	21 (87.5%)	16 (100%)	0.141[a]
CRP (mg/L)	1.75 (0.825; 4.85)	1.2 (0.75; 4.1)	0.617[c]
Blood Glucose (mg/dl)	97 (89.25; 115)	107.5 (96; 168.8)	0.068[b]
Sodium (mmol/L)	141 (140; 142)	140 (138; 141)	0.066[b]
Potassium (mmol/L)	4.5 (4.125; 4.7)	4.3 (4.025; 4.7)	0.745[b]
Calcium (mg/dl)	8.95 (8.8; 9.375)	9.2 (8.925; 9.4)	0.367[c]
INR	1.06 (0.96; 1.10)	1.06 (1.02; 1.07)	0.178[b]
aPTT (sec)	29.95 (28.18; 32.65)	30 (28.18; 33.18)	0.736[b]
Serum IL-1β (pg/ml)	3.14 (2.83; 3.53)	3.24 (2.86; 3.34)	0.767[c]
Serum IL-1ra (pg/ml)	1072 (1025; 1176)	1132 (1025; 1191)	0.527[c]
EAT IL-1β (pg/ml)	0.86 (0.76; 0.985)	1.04 (0.873; 1.43)	**0.009**[c]
EAT IL-1ra (pg/ml)	452 (326; 623)	654 (361; 781)	0.121[b]

Results are expressed as median and range (25% percentile; 75% percentile) or as the number of cases (%). Age is expressed as media ±SD. BMI, body mass index; LVEF, left ventricular ejection fraction; EAT, epicardial adipose tissue; IL, interleukine; GFR, glomerular filtration rate; CRP, C-reactive protein; INR, international normalized ratio; aPTT, activated partial thromboplastin time.

Statistically significative values ($p < 0.05$) are reported in bold.

[a]*Chi Squared test.*

[b]*Unpaired t-test.*

[c]*Mann-Whitney U test.*

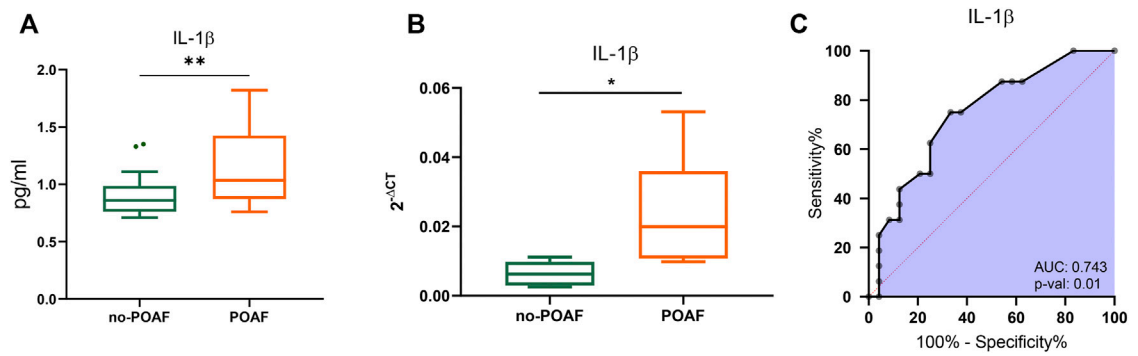

FIGURE 1 | IL-1β in POAF subgroups. **(A)** Boxplots denote IL-1β concentration distributions in conditioned media from EAT biopsies of subjects with the no-POAF outcome ("no-POAF"—green) and with POAF outcome ("POAF"—orange); IL-1β concentration is expressed as pg/ml. Box plots denote median and 25th–75th percentiles (boxes) and tukey whiskers. **(B)** Boxplots denote IL-1β absolute expression in EAT biopsies for 6 subjects with no POAF outcome ("no-POAF"—green) and 6 with POAF outcome ("POAF"—orange). Box plots denote median and 25th–75th percentiles (boxes) and min-to-max whiskers. **(C)** AUC of ROC analysis indicates the performance of IL-1β. *p*-value refers to the significant difference from the AUC basal level of 0.5 (red dotted line). *$p < 0.05$; **$p < 0.01$.

grade 2 (10–50% fibrosis) and 10% had grade 3 (>50%) (**Supplementary Figure S1**). Overall atrial fibrosis was present in eight patients. Of note, no association was observed between POAF and the presence of atrial fibrosis ($p = 0.582$, data not shown).

Circulating and EAT-Derived Interleukins

No significant difference was observed in serum levels of IL-1β, IL-1ra and other cytokines, chemokines, and growth factors between POAF and no-POAF groups [IL-1β: 3.24 pg/ml (2.86; 3.34) *vs.* 3.14 pg/ml (2.83; 3.53); IL-1ra: 1132 pg/ml (1025; 1191) *vs.* 1072 pg/ml (1025; 1176), **Table 1** and **Supplementary Table S1**]. To gain insight into a possible involvement of local inflammation in POAF occurrence, we obtained conditioned media from EAT biopsies and analyzed a panel of inflammatory mediators. IL-1β local levels were significantly higher in the POAF group

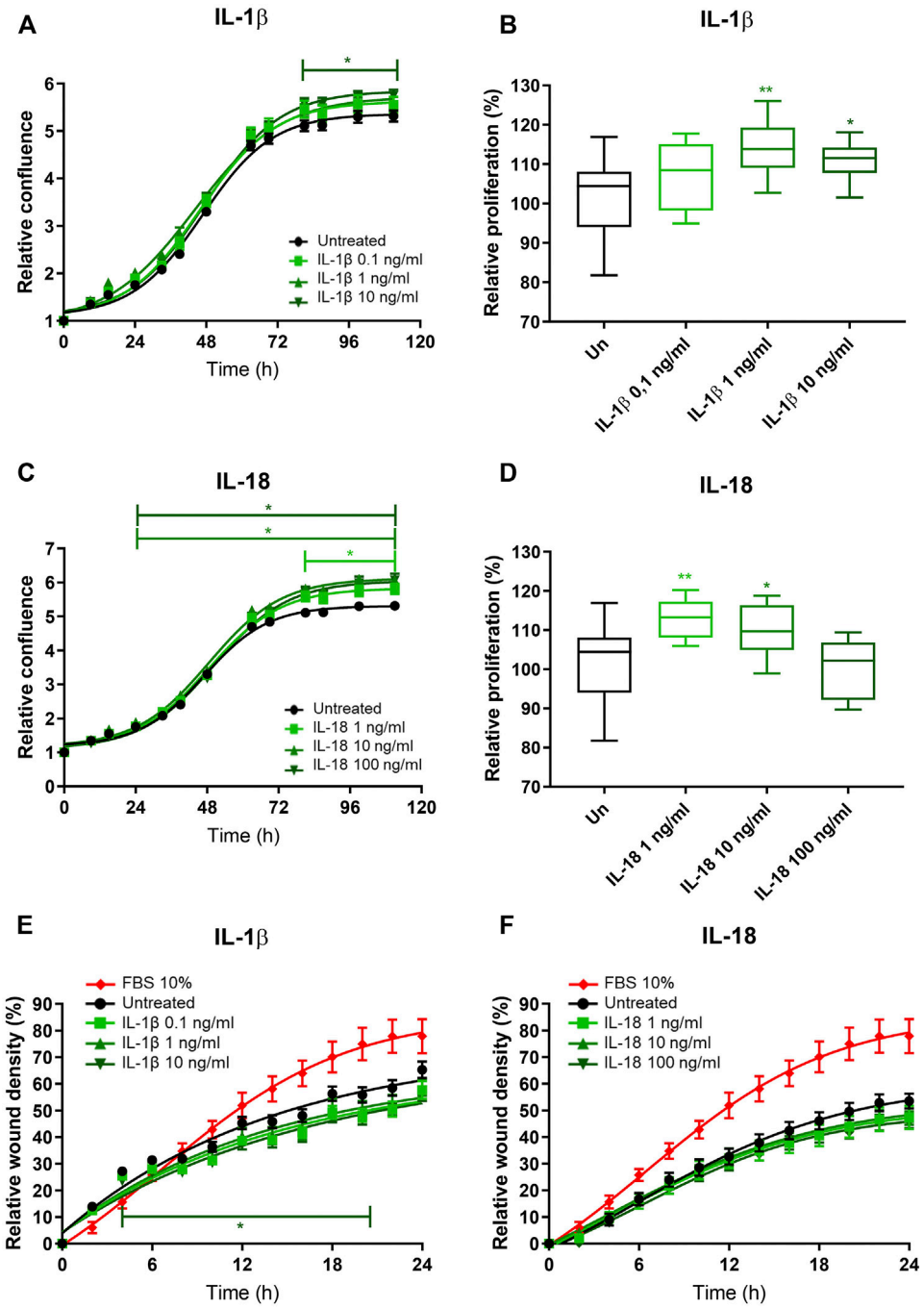

FIGURE 2 | IL-1β and IL-18 effects on cardiac fibroblast proliferation and migration. **(A–C)** Relative confluence normalized on T0 and **(B–D)** relative proliferation with respect to the untreated (setted to 100%) and **(E,F)** relative wound healing density normalized on T0 of human immortalized fibroblasts exposed to different concentrations of **(A,B–E)** IL-1β and **(C,D–F)** IL-18 (n = 8). Data are expressed by mean ± SEM. *p < 0.05; **p < 0.01 vs. untreated.

compared to the no-POAF group (p = 0.009) (**Figure 1A**; **Table 1**). In parallel, no significant differences were observed in EAT-derived IL-1ra between the two groups (**Table 1**). Consistently, EAT-derived IL-2, IL-5, IL-6, IL-8, and IP-10 levels were significantly higher in the POAF group (**Supplementary Table S1**). To note, according to secretion, also *IL-1β* mRNA expression was significantly higher in EAT biopsies from POAF patients compared to no-POAF (p = 0.0308) (**Figure 1B**).

ROC analyses revealed that IL-1β provides valuable discrimination between the two groups (AUC 0.743, 95% CI: 0.588–0.899, p = 0.01) (**Figure 1C**).

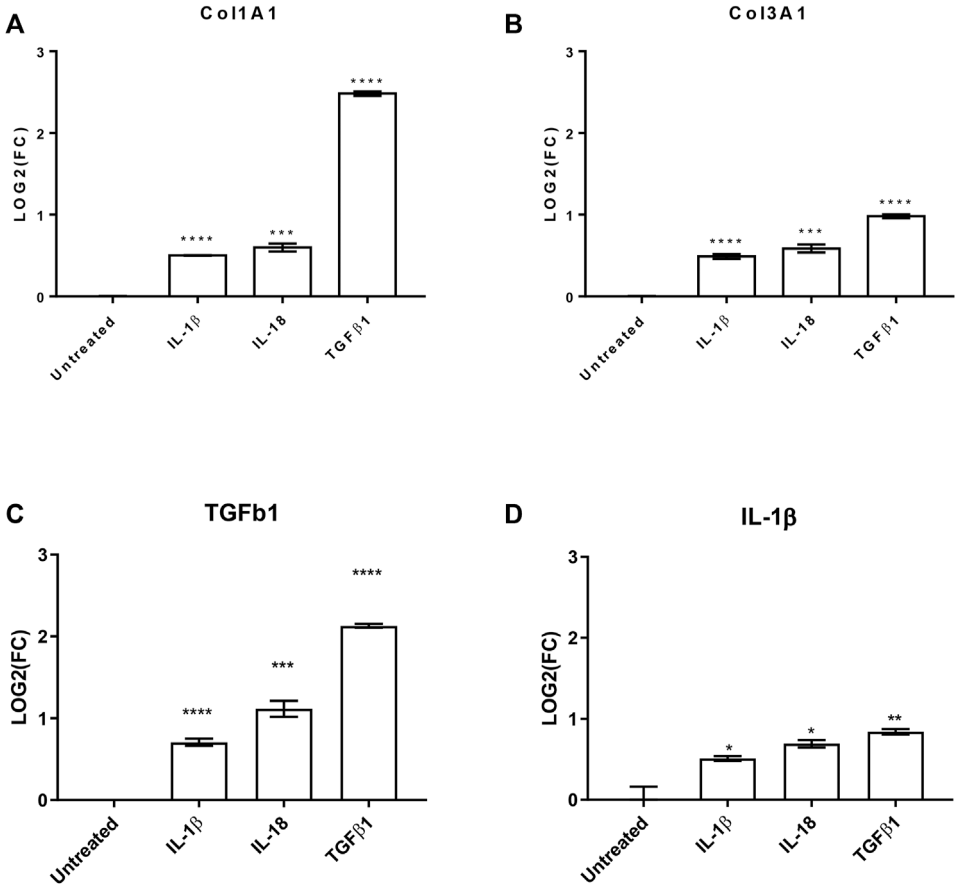

FIGURE 3 | IL-1β and IL-18 effects on pro-fibrotic and pro-inflammatory genes. Bar graphs reporting the relative gene expression of **(A)** collagen 1A1 (Col1A1), **(B)** collagen 3A1 (Col3A1), **(C)** transforming growth factor β1 (TGFβ1), and **(D)** interleukin 1β (IL-1β) of human cardiac fibroblasts under IL-1β, IL-18, and TGFβ1 (as positive control) treatments (n = 3). Data are expressed by mean ± SEM. *p < 0.05; **p < 0.01; ***p < 0.001; ****p < 0.0001 vs. untreated.

Interleukins' Effects on Human Cardiac Fibroblasts

To investigate the potential role of EAT-secreted IL-1β on atrial remodeling and fibrosis, we *in vitro* tested the effects of IL-1β on human immortalized fibroblasts obtained from the right atrium of patients undergoing cardiac surgery. The relative confluence of fibroblasts exposed to increasing concentrations of recombinant IL-1β was higher compared to the untreated, at the highest tested concentration (10 ng/ml) starting from the third day (p < 0.05; **Figure 2A**). MTT assay revealed that the proliferation rate of fibroblasts exposed to IL-1β was higher than the control at the concentration of 1 ng/ml (114.0% ± 7.1% vs. 101.6% ± 9.8%; p = 0.003) and 10 ng/ml (111.0% ± 5.2%; p = 0.03), while the lower tested concentration (0.1 ng/ml) had no effect (107.7% ± 8.7%; p = 0.13; ANOVA p = 0.004; **Figure 2B**). As IL-1β and IL-18 are members of the same structural family and are involved in the NLRP3 inflammasome, we also tested the *in vitro* effects of IL-18 on fibroblasts. IL-18 induced an increased relative confluence than control, even at the lowest tested concentration (1 ng/ml; **Figure 2C**). Indeed, the proliferation rate of cells exposed to IL-18 was higher than control (1 ng/ml 112.9% ± 5.0% vs. 10 ng/ml 109.8% ± 6.8% vs. 100 ng/ml 99.9% ± 7.5% *vs.* control 101.6% ± 9.8%; ANOVA p = 0.003; **Figure 2D**). To better characterize the effects of these ILs on human fibroblasts, we analyzed the migration rate. IL-1β reduced the invasion capacity of fibroblasts at the highest tested concentration (10 ng/ml; p = 0.05; **Figure 2A**), while IL-18 did not have any effects on wound healing capacity at any analyzed concentration (**Figures 2E,F**).

To further evaluate the effects of these interleukins on pro-fibrotic and pro-inflammatory effects on cardiac fibroblast, we investigated by qPCR the production of collagen 1A1 (*COL1A1*), *COL3A1*, and transforming growth factor β 1 (*TGFβ1*) as well as the production of *IL-1β*. All the analyzed transcripts were significantly upregulated by both the used interleukins (**Figure 3**). Interestingly, the treatments increased *TGFβ1* production, which is the most powerful pro-fibrotic inducer, and at the same time potentiate the pro-inflammatory effects.

In conclusion, IL-1β and IL-18 improved the proliferation rate of human cardiac fibroblasts potentiating the fibrosis machinery with a rebound on the inflammation itself.

DISCUSSION

The present study explored the potential role of EAT-secreted IL-1β in atrial remodeling and POAF occurrence in patients undergoing CABG, without a history of AF. We observed: 1) POAF onset is not associated with clinical nor echocardiographic parameters; 2) In patients with and without POAF there are no differences in EAT thickness, atrial dilation, and fibrosis; 3) EAT-IL1β secreted levels, but not circulating IL-1β levels are associated with POAF occurrence; 4) NLRP3 inflammasome cytokines, IL1β and IL-18 could promote atrial fibrosis.

In patients undergoing cardiac surgery, POAF is a frequent complication and occurs approximately in 20–40% of cases (Dobrev et al., 2019). It is a clinically relevant event, being associated with hemodynamic instability, increased risk of stroke, lengthened hospital and intensive care unit stays, and greater hospital costs (Dobrev et al., 2019). POAF is also a predictor of permanent AF. However, the mechanisms underlying AF and POAF are probably different as POAF is mainly driven by periprocedural triggers. Cardiac surgery itself contributes to the pathophysiology of AF, both in the initiation and maintenance of arrhythmia (Hu et al., 2015). In particular, POAF occurs in presence of factors inducing atrial arrhythmogenic remodeling before surgery and is promoted by peri-operative triggers. In some studies, POAF is associated with preoperative structural alterations including interstitial fibrosis (Maesen et al., 2012). However, in the present study neither left atrial volume, evaluated at echocardiography nor atrial fibrosis, evaluated at histology, were associated with POAF occurrence. Similarly, in our population, we didn't observe differences in demographic, clinical, and echocardiographic parameters among patients with and without POAF. Thus, here, we can exclude a possible association of POAF with clear predisposing factors.

Inflammation is considered a major trigger for POAF, even if the association between levels of inflammatory cytokines and the occurrence of POAF is not well defined. Recently, it has been reported a strong association between EAT-derived activin A expression and atrial remodeling (Venteclef et al., 2015; Wang et al., 2019). Of note, it has been shown that there is a direct link between activin A and IL-1β in the contest of inflammation and fibrosis. Moreover, this link is bidirectional since the former is able to stimulate the latter expression and *vice versa* (de Kretser et al., 2012). In this context, our study, focusing on IL-1β, is in accordance with the literature and adds a brick to the wall of knowledge regarding inflammatory cytokines involvement and POAF onset. Of note, in our population, there was no significant differences in circulating levels of cytokines, chemokines and growth factors evaluated. In particular, no variation in circulating levels of IL-1β and IL-1ra between POAF and no-POAF patients, raising the hypothesis of a specific role of EAT and local inflammation in POAF.

EAT is the visceral fat depot of the heart, and it is located between the myocardium and the visceral layer of the pericardium. In physiological conditions, EAT has several protective functions on the heart; however, it is now well established that it can also have undesirable effects on cardiac tissue. In absence of fascial boundaries, EAT directly influences the myocardial electrical and structural remodeling and it is associated with cardiovascular diseases (Mazurek et al., 2003; Chaldakov et al., 2014; Parisi et al., 2015; Ghenev et al., 2016). The release of proinflammatory cytokines by EAT is initiated by the innate inflammatory response through Toll-like receptors (TLRs) located in the macrophages, B cells, dendritic cells, and adipocyte membranes. The receptors recognize antigens such as lipopolysaccharide (LPS) and saturated fatty acids, promoting nuclear factor kappa-beta (NF-$\kappa\beta$) translocation into the nucleus of epicardial adipocytes, with transcription of inflammatory mediators such as IL-1, IL-8, IL-6, and TNF-α, linking innate immunity and chronic inflammatory responses. We previously described that EAT is a source of IL-1β in CAD patients, and the imbalance between levels of IL-1β and its receptor antagonist (IL-1ra) drives cardiovascular events (Parisi et al., 2020b).

Our data indicate that EAT inflammatory profile is increased with POAF occurrence. In particular, EAT-mediated IL-1β secretion and mRNA expression are higher in POAF patients and IL-1ra secretion doesn't differ in the two groups, indicating an increased pro-inflammatory effect of IL-1β in POAF patients. To note, all biopsies were collected at the surgical time, before extracorporeal circulation to avoid possible inflammation of tissues mediated by surgical manipulation. Along with the evidence that local inflammatory status could give rise to abnormal atrial conduction (Mariscalco and Engström, 2008), we have hypothesized that POAF patients may have a pre-existing local inflammatory state characterized by enhanced IL-1β, an essential component of the NLRP3-inflammasome signaling. The NLRP3- inflammasome is a deeply rooted signaling pathway responsible for IL-1β and IL-18 releases from innate immune cells (Heijman et al., 2020).

Patients with POAF are considered to be at higher risk of permanent AF (Dobrev et al., 2019), thus it is plausible that factors that trigger POAF could promote atrial remodeling and fibrosis over time. To verify this hypothesis, we mimicked post-operative inflammation by *in vitro* stimuli of NLRP3-related cytokines, IL-1β and IL-18, on human fibroblasts isolated from atrial myocardium. We observed that both IL-1β and IL-18 promote fibroblasts proliferation. In patients with AF undergoing left atrial appendage excision, EAT-derived IL-1β was associated with the total atrial collagen content (Abe et al., 2018). However, no evidence is available on POAF patients. Animal studies conducted on mice suggested that IL-18 stimulates fibroblast migration and proliferation (Fix et al., 2011). Moreover, recent evidence supports the hypothesis that pre-existing activation of the atrial cardiomyocyte NLRP3-inflammasome contributes to the POAF-predisposing substrate (Heijman et al., 2020). Here, we provide the first evidence that the paracrine release of IL-1β from EAT could promote POAF, even in absence of pre-operative predisposing factors. Furthermore, we observed that inflammatory stimuli on atrial fibroblasts promote the production of collagen and TGFβ1, the most powerful pro-fibrotic inducer, and at the same time potentiate the pro-inflammatory effects. All the way, our observations give convincing proof that IL-1β could be an important mediator of the pro-fibrotic effect of EAT on atrial remodeling as already described for Activin A (Wang et al., 2019) and Galectin-3 (Rhodes et al., 2013; Fashanu et al., 2017).

This intensive crosstalk between EAT-derived molecules and the surrounding myocardium provides novel insights into the potential establishment of a pro-fibrotic milieu and supports promoting changes in the atrial myocardium. These results pay the way for new studies exploring the potential benefits of anti-inflammatory drugs in the perioperative period and suggest that EAT could mediate the antiarrhythmic effects observed by using anti-inflammatory therapies in animal studies (Wu et al., 2020).

Study Limitations

The present study evaluated the predictive value of pre-operative circulating inflammatory markers in POAF occurrence. We didn't explore the predictive value of post-operative inflammatory markers. However, since cardiac intervention is an important inflammatory trigger, a dedicated study should be designed to appropriately identify the impact of post-operative inflammatory markers in POAF occurrence.

We *in vitro* tested the effects of single cytokines on fibroblast proliferation and collagen production. Further studies are required to test the effects of the entire EAT-secretome on cardiac cells and the potential benefits of IL-1β inhibition.

Genetic variation and heritability take part in AF onset (Ellinor et al., 2012; Kolek et al., 2015). Genome-wide association studies have identified several common variant *loci* associated with AF and functionally implicated in cardiac development, electrophysiology, and cardiomyocyte behavior (Roselli et al., 2020). Surely, adding information on AF genetic variability and/or on common risk Single Nucleotide Polymorphisms (SNPs) would improve insight in our population.

DATA AVAILABILITY STATEMENT

The original contributions presented in the study are included in the article/**Supplementary Material**, further inquiries can be directed to the corresponding authors.

ETHICS STATEMENT

The studies involving human participants were reviewed and approved by University of Naples Federico II. The patients/participants provided their written informed consent to participate in this study.

AUTHOR CONTRIBUTIONS

SC and MC designed research, interpreted the data, and wrote the manuscript. LP and PC enrolled patients, collected clinical/anamnestic data, performed echocardiograms. GC and EP performed epicardial adipose tissue and atrial biopsies during cardiac surgery. ADM and MoC performed histology. SR analyzed serum samples and epicardial fat biopsies and analyzed the data. DM and VV carried out *in vitro* experiments. MFDT performed the statistical analysis. VD'E and PP critically reviewed the manuscript. PF, DL, and VP conceived the study, critically reviewed the manuscript, and edited it. The authors had full access to the data and take responsibility for its integrity. All authors have read and agree to the manuscript as written.

ACKNOWLEDGMENTS

We sincerely appreciated the technical help of D. Liguoro and A. D'Andrea.

SUPPLEMENTARY MATERIAL

The Supplementary Material for this article can be found online at: https://www.frontiersin.org/articles/10.3389/fcell.2022.893729/full#supplementary-material

REFERENCES

Abe, I., Teshima, Y., Kondo, H., Kaku, H., Kira, S., Ikebe, Y., et al. (2018). Association of Fibrotic Remodeling and Cytokines/Chemokines Content in Epicardial Adipose Tissue with Atrial Myocardial Fibrosis in Patients with Atrial Fibrillation. *Heart Rhythm* 15 (11), 1717–1727. doi:10.1016/j.hrthm.2018.06.025

Ahlsson, A., Fengsrud, E., Bodin, L., and Englund, A. (2010). Postoperative Atrial Fibrillation in Patients Undergoing Aortocoronary Bypass Surgery Carries an Eightfold Risk of Future Atrial Fibrillation and a Doubled Cardiovascular Mortality. *Eur. J. Cardio-Thoracic Surg.* 37 (6), 1353–1359. doi:10.1016/j.ejcts.2009.12.033

Arai, K. Y., Ono, M., Kudo, C., Fujioka, A., Okamura, R., Nomura, Y., et al. (2011). IL-1β Stimulates Activin βA mRNA Expression in Human Skin Fibroblasts through the MAPK Pathways, the Nuclear Factor-κB Pathway, and Prostaglandin E2. *Endocrinology* 152 (10), 3779–3790. doi:10.1210/en.2011-0255

Chaldakov, G. N., Fiore, M., Ghenev, P. I., Beltowski, J., RanÄ‡iÄ‡, G., TunÃ§el, N., et al. (2014). Triactome: Neuro-Immune-Adipose Interactions. Implication in Vascular Biology. *Front. Immunol.* 5, 130. doi:10.3389/fimmu.2014.00130

De Jesus, N. M., Wang, L., Lai, J., Rigor, R. R., Francis Stuart, S. D., Bers, D. M., et al. (2017). Antiarrhythmic Effects of Interleukin 1 Inhibition after Myocardial Infarction. *Heart Rhythm* 14 (5), 727–736. doi:10.1016/j.hrthm.2017.01.027

de Kretser, D. M., O'Hehir, R. E., Hardy, C. L., and Hedger, M. P. (2012). The Roles of Activin A and its Binding Protein, Follistatin, in Inflammation and Tissue Repair. *Mol. Cell Endocrinol.* 359 (1-2), 101–106. doi:10.1016/j.mce.2011.10.009

Dinarello, C. A. (2011). Interleukin-1 in the Pathogenesis and Treatment of Inflammatory Diseases. *Blood* 117 (14), 3720–3732. doi:10.1182/blood-2010-07-273417

Dobrev, D., Aguilar, M., Heijman, J., Guichard, J.-B., and Nattel, S. (2019). Postoperative Atrial Fibrillation: Mechanisms, Manifestations and Management. *Nat. Rev. Cardiol.* 16 (7), 417–436. doi:10.1038/s41569-019-0166-5

Ellinor, P. T., Lunetta, K. L., Albert, C. M., Glazer, N. L., Ritchie, M. D., Smith, A. V., et al. (2012). Meta-Analysis Identifies Six New Susceptibility Loci for Atrial Fibrillation. *Nat. Genet.* 44 (6), 670–675. doi:10.1038/ng.2261

Fashanu, O. E., Norby, F. L., Aguilar, D., Ballantyne, C. M., Hoogeveen, R. C., Chen, L. Y., et al. (2017). Galectin-3 and Incidence of Atrial Fibrillation: The Atherosclerosis Risk in Communities (ARIC) Study. *Am. Heart J.* 192, 19–25. doi:10.1016/j.ahj.2017.07.001

Fix, C., Bingham, K., and Carver, W. (2011). Effects of Interleukin-18 on Cardiac Fibroblast Function and Gene Expression. *Cytokine* 53 (1), 19–28. doi:10.1016/j.cyto.2010.10.002

Ghenev, P. I., Kitanova, M., Popov, H., Evtimov, N., Stoev, S., Tonchev, A., et al. (2016). Neuroadipobiology of Arrhythmogenic Right Ventricular Dysplasia.

An Immunohistochemical Study of Neurotrophins. *Adipobiology* 8, 55–58. doi:10.14748/adipo.v8.2214

Heijman, J., Muna, A. P., Veleva, T., Molina, C. E., Sutanto, H., Tekook, M., et al. (2020). Atrial Myocyte NLRP3/CaMKII Nexus Forms a Substrate for Postoperative Atrial Fibrillation. *Circ. Res.* 127 (8), 1036–1055. doi:10.1161/CIRCRESAHA.120.316710

Hu, Y.-F., Chen, Y.-J., Lin, Y.-J., and Chen, S.-A. (2015). Inflammation and the Pathogenesis of Atrial Fibrillation. *Nat. Rev. Cardiol.* 12 (4), 230–243. doi:10.1038/nrcardio.2015.2

Kolek, M. J., Muehlschlegel, J. D., Bush, W. S., Parvez, B., Murray, K. T., Stein, C. M., et al. (2015). Genetic and Clinical Risk Prediction Model for Postoperative Atrial Fibrillation. *Circ. Arrhythmia Electrophysiol.* 8 (1), 25–31. doi:10.1161/CIRCEP.114.002300

Lee, S.-H., Kang, D. R., Uhm, J.-S., Shim, J., Sung, J.-H., Kim, J.-Y., et al. (2014). New-Onset Atrial Fibrillation Predicts Long-Term Newly Developed Atrial Fibrillation after Coronary Artery Bypass Graft. *Am. Heart J.* 167 (4), 593–600. doi:10.1016/j.ahj.2013.12.010

Maesen, B., Nijs, J., Maessen, J., Allessie, M., and Schotten, U. (2012). Post-Operative Atrial Fibrillation: A Maze of Mechanisms. *Europace* 14 (2), 159–174. doi:10.1093/europace/eur208

Mariscalco, G., and Engström, K. G. (2008). Atrial Fibrillation after Cardiac Surgery: Risk Factors and Their Temporal Relationship in Prophylactic Drug Strategy Decision. *Int. J. Cardiol.* 129 (3), 354–362. doi:10.1016/j.ijcard.2007.07.123

Matsushita, N., Ishida, N., Ibi, M., Saito, M., Takahashi, M., Taniguchi, S., et al. (2019). IL-1β Plays an Important Role in Pressure Overload-Induced Atrial Fibrillation in Mice. *Biol. Pharm. Bull.* 42 (4), 543–546. doi:10.1248/bpb.b18-00363

Mazurek, T., Zhang, L., Zalewski, A., Mannion, J. D., Diehl, J. T., Arafat, H., et al. (2003). Human Epicardial Adipose Tissue Is a Source of Inflammatory Mediators. *Circulation* 108 (20), 2460–2466. doi:10.1161/01.CIR.0000099542.57313.C5

Melduni, R. M., Schaff, H. V., Bailey, K. R., Cha, S. S., Ammash, N. M., Seward, J. B., et al. (2015). Implications of New-Onset Atrial Fibrillation after Cardiac Surgery on Long-Term Prognosis: A Community-Based Study. *Am. Heart J.* 170 (4), 659–668. doi:10.1016/j.ahj.2015.06.015

Parisi, V., Petraglia, L., Cabaro, S., D'Esposito, V., Bruzzese, D., Ferraro, G., et al. (2020). Imbalance between Interleukin-1β and Interleukin-1 Receptor Antagonist in Epicardial Adipose Tissue is Associated with Non ST-Segment Elevation Acute Coronary Syndrome. *Front. Physiol.* 11, 42. doi:10.3389/fphys.2020.00042

Parisi, V., Petraglia, L., Formisano, R., Caruso, A., Grimaldi, M. G., Bruzzese, D., et al. (2020). Validation of the Echocardiographic Assessment of Epicardial Adipose Tissue Thickness at the Rindfleisch Fold for the Prediction of Coronary Artery Disease. *Nutr. Metab. Cardiovasc. Dis.* 30 (1), 99–105. doi:10.1016/j.numecd.2019.08.007

Parisi, V., Rengo, G., Pagano, G., D'Esposito, V., Passaretti, F., Caruso, A., et al. (2015). Epicardial Adipose Tissue has an Increased Thickness and is a Source of Inflammatory Mediators in Patients with Calcific Aortic Stenosis. *Int. J. Cardiol.* 186, 167–169. doi:10.1016/j.ijcard.2015.03.201

Petraglia, L., Conte, M., Comentale, G., Cabaro, S., Campana, P., Russo, C., et al. (2022). Epicardial Adipose Tissue and Postoperative Atrial Fibrillation. *Front. Cardiovasc. Med.* 9, 810334. doi:10.3389/fcvm.2022.810334

Rhodes, D. H., Pini, M., Castellanos, K. J., Montero-Melendez, T., Cooper, D., Perretti, M., et al. (2013). Adipose Tissue-Specific Modulation of Galectin Expression in Lean and Obese Mice: Evidence for Regulatory Function. *Obesity* 21 (2), 310–319. doi:10.1002/oby.20016

Roselli, C., Rienstra, M., and Ellinor, P. T. (2020). Genetics of Atrial Fibrillation in 2020: GWAS, Genome Sequencing, Polygenic Risk, and Beyond. *Circ. Res.* 127 (1), 21–33. doi:10.1161/CIRCRESAHA.120.316575

Venteclef, N., Guglielmi, V., Balse, E., Gaborit, B., Cotillard, A., Atassi, F., et al. (2015). Human Epicardial Adipose Tissue Induces Fibrosis of the Atrial Myocardium through the Secretion of Adipo-Fibrokines. *Eur. Heart J.* 36 (13), 795–805. doi:10.1093/eurheartj/eht099

Wang, Q., Min, J., Jia, L., Xi, W., Gao, Y., Diao, Z., et al. (2019). Human Epicardial Adipose Tissue Activin A Expression Predicts Occurrence of Postoperative Atrial Fibrillation in Patients Receiving Cardiac Surgery. *Heart Lung Circ.* 28 (11), 1697–1705. doi:10.1016/j.hlc.2018.08.010

Wong, C. X., Ganesan, A. N., and Selvanayagam, J. B. (2017). Epicardial Fat and Atrial Fibrillation: Current Evidence, Potential Mechanisms, Clinical Implications, and Future Directions. *Eur. Heart J.* 38 (17), 1294–1302. doi:10.1093/eurheartj/ehw045

Wu, Q., Liu, H., Liao, J., Zhao, N., Tse, G., Han, B., et al. (2020). Colchicine Prevents Atrial Fibrillation Promotion by Inhibiting IL-1β-induced IL-6 Release and Atrial Fibrosis in the Rat Sterile Pericarditis Model. *Biomed. Pharmacother.* 129, 110384. doi:10.1016/j.biopha.2020.110384

Yao, C., Veleva, T., Scott, L., Cao, S., Li, L., Chen, G., et al. (2018). Enhanced Cardiomyocyte NLRP3 Inflammasome Signaling Promotes Atrial Fibrillation. *Circulation* 138 (20), 2227–2242. doi:10.1161/CIRCULATIONAHA.118.035202

Conflict of Interest: The authors declare that the research was conducted in the absence of any commercial or financial relationships that could be construed as a potential conflict of interest.

Publisher's Note: All claims expressed in this article are solely those of the authors and do not necessarily represent those of their affiliated organizations, or those of the publisher, the editors and the reviewers. Any product that may be evaluated in this article, or claim that may be made by its manufacturer, is not guaranteed or endorsed by the publisher.

frontiers | Frontiers in Cell and Developmental Biology

PERSPECTIVE
published: 25 May 2022
doi: 10.3389/fcell.2022.886086

Trained Immunity in Perivascular Adipose Tissue of Abdominal Aortic Aneurysm—A Novel Concept for a Still Elusive Disease

Luca Piacentini[1,2]*, *Chiara Vavassori*[1,3] *and Gualtiero I. Colombo*[1]*

[1]*Immunology and Functional Genomics Unit, Centro Cardiologico Monzino IRCCS, Milano, Italy,* [2]*Bioinformatics and Artificial Intelligence Facility, Centro Cardiologico Monzino IRCCS, Milano, Italy,* [3]*Department of Clinical Sciences and Community Health, Cardiovascular Section, University of Milano, Milan, Italy*

Abdominal aortic aneurysm (AAA) is a chronic, life-threatening vascular disease whose only therapeutic option is a surgical repair to prevent vessel rupture. The lack of medical therapy results from an inadequate understanding of the etiopathogenesis of AAA. Many studies in animal and human models indicate a 'short-circuiting' of the regulation of the inflammatory-immune response as a major player in the AAA chronic process. In this regard, perivascular adipose tissue (PVAT) has received increasing interest because its dysfunction affects large arteries primarily through immune cell infiltration. Consistently, we have recently produced evidence that innate and adaptive immune cells present in the PVAT of AAAs contribute to sustaining a damaging inflammatory loop. However, it is still unclear how the complex crosstalk between adaptive and innate immunity can be self-sustaining. From our perspective, trained immunity may play a role in this crosstalk. Trained immunity is defined as a form of innate immune memory resulting in enhanced responsiveness to repeated triggers. Specific innate stimuli and epigenetic and metabolic reprogramming events induce and shape trained immunity in myeloid progenitor cells improving host defense, but also contributing to the progression of immune-mediated and chronic inflammatory diseases. Here we present this hypothesis with data from the literature and our observations to support it.

Keywords: abdominal aortic aneurysm, perivascular adipose tissue, immune response, trained immunity, epigenetic markers

OPEN ACCESS

Edited by:
Ileana Badi,
University of Oxford, United Kingdom

Reviewed by:
Donato Santovito,
National Research Council (CNR), Italy

***Correspondence:**
Luca Piacentini
luca.piacentini@cardiologicomonzino.it
Gualtiero I. Colombo
gualtiero.colombo@cardiologicomonzino.it

Specialty section:
This article was submitted to Cellular Biochemistry, a section of the journal Frontiers in Cell and Developmental Biology

Received: *28 February 2022*
Accepted: *25 April 2022*
Published: *25 May 2022*

Citation:
Piacentini L, Vavassori C and Colombo GI (2022) Trained Immunity in Perivascular Adipose Tissue of Abdominal Aortic Aneurysm—A Novel Concept for a Still Elusive Disease. Front. Cell Dev. Biol. 10:886086. doi: 10.3389/fcell.2022.886086

INTRODUCTION

Abdominal aortic aneurysm (AAA) is a chronic and life-threatening vascular disease with a degenerative course leading to rupture of the aorta with fatal consequences in more than 80% of cases. Epidemiologic studies have identified older age, male sex, smoking, family history of AAA, cardiovascular comorbidities (such as ischemic heart disease or peripheral arterial disease), and to lesser extent hypertension and dyslipidemia as the major risk factors associated with the development of AAA (Kent et al., 2010). Patients are mostly asymptomatic and only incidentally are diagnosed for AAA. There are no tests for early diagnosis, nor can the evolution and progression of the disease be predicted. Surgery remains the only treatment option to prevent vessel rupture. The lack of effective noninvasive medical approaches and pharmacological treatments stems substantially from inadequate understanding of the etiopathogenesis of AAA. Despite many

efforts over the past decades to understand AAA, it seems quite clear that we are missing some crucial pieces of an intricate puzzle. Therefore, there is an increasing urgency to identify new lines of research that may shed new light on AAA pathogenesis.

THE PATHOGENESIS OF ABDOMINAL AORTIC ANEURYSM: AN UNRESOLVED TANGLE

Although historically it was believed that the aneurysm was a final stage of an atherosclerotic process, it is now clear that atherosclerosis and AAA are distinct entities with very specific traits (Tilson, 2016). They share many risk factors, but many aspects are distinctive. Male sex and smoking are, for example., much more prominent risk factors for AAA than atherosclerosis. Low-density lipoprotein cholesterol (LDL-C) is a major determinant of atherosclerosis but has no clear association with AAA. Diabetic patients appear to have a much lower risk of developing AAA than nondiabetic subjects; in contrast, diabetes is one of the major predisposing factors to atherosclerosis and markedly increases the risk of myocardial infarction. Furthermore, therapeutic approaches used for atherosclerotic diseases, such as hypolipidemic, antihypertensive, or antiplatelet drugs, are substantially ineffective in treating AAA (Golledge et al., 2020). The atherosclerotic process can be considered, at least for a subgroup of patients, as a concomitant element in the evolution of AAA but certainly not as a pathophysiological determinant.

The Immune Response as a Key Element in the Pathogenesis of Abdominal Aortic Aneurysm

A growing number of studies over the past 2 decades support the idea that immune-mediated inflammation plays an important role in AAA development and progression. A chronic immune-mediated response is followed by the destruction of the aortic media through extracellular matrix (ECM)-mediated degradation by the release of proteolytic enzymes (such as metalloproteinases), production of reactive oxygen species (ROS), cytokine action, and vascular smooth muscle cell death, which are typical hallmarks of AAA (Golledge, 2019). The consistent presence of immune-inflammatory cells in tissues of the abdominal aorta has been robustly demonstrated in both animal models and immunohistochemical analyses of human biopsy specimens, suggesting a key role for both innate and adaptive immune cells in AAA evolution. In particular, perivascular adipose tissue (PVAT) has received increasing interest because it has a relevant role in the regulation of vascular physiology and disease, including atherosclerotic and aneurysmal lesions. This multifaceted role of PVAT can be attributed, at least in part, to the fact that PVAT exhibits regional differences and heterogeneity along the vascular tree, e.g., due to the different nature of adipocytes and cellular infiltrates. The heterogeneity of PVAT depots results in a diversity of effects on vascular structure and function, which may influence vessel pathophysiology and contribute to a different manifestation of vascular disease (Gil-Ortega et al., 2015; Queiroz and Sena, 2020). Importantly, PVAT dysfunction is recognized to affect adjacent structures mainly through immune cell infiltration (Guzik et al., 2017). Consistently, we have recently provided evidence that both innate and adaptive immune responses in AAA PVAT contribute to sustaining a damaging inflammatory loop (Piacentini et al., 2019). The underlying assumption is that the inflammatory mechanism may develop from PVAT dysfunction and propagate from the outside to the inside involving the entire thickness of the vessel (Piacentini et al., 2019; Sagan et al., 2019; Gao and Guo, 2022). The presence of cells of adaptive immunity in each layer of the AAA, from the PVAT to the middle of the aorta, has given rise to the hypothesis that the evolution of the AAA may be linked to an antigen-specific response, putatively an autoimmune response, that would feed the chronic inflammatory circuit responsible for disease progression (Chang et al., 2015; Tilson, 2016; Piacentini et al., 2019). Seemingly in contrast to this hypothesis, immunosuppressive treatment approaches tested to date have not produced positive results on AAA outcome, but at times intense immunosuppression has even demonstrated deleterious effects, promoting AAA progression and rupture (Lindeman et al., 2011). One possible explanation is interference with compensatory protection/repair mechanisms, such as protective regulatory T cells, which are responsible for controlling the immune response and have a clear role in limiting AAA growth (Yodoi et al., 2015; Zhou et al., 2015; Suh et al., 2020), or the actions of other cells involved in tissue repair (stem cell function).

All the above implies the involvement of additional as yet unidentified critical factors that do not respond to immunosuppressive chemotherapy and the need to clarify uncertainties about the precise mechanism by which the complex crosstalk between adaptive and innate immunity can be self-sustaining in AAA progression.

Trained Immunity: a New Concept for Abdominal Aortic Aneurysm

Cells of innate immunity play a key role in AAA because 1) they can perform pathogenically important effector functions on their own, such as responding to stimuli due to tissue damage and secreting soluble factors that degrade the vessel ECM, and 2) they act as mediators of the adaptive response, acting as antigen-presenting cells (exogenous or endogenous) and activating cells of adaptive immunity. Chronic AAA inflammation would thus be a continuous source of stimuli for cells of innate immunity. This would provide the basis for applying a new immunological concept related to innate immunity, so-called 'trained immunity', to AAA pathogenesis.

Trained immunity is a term introduced fairly recently in immunology and defines a form of 'innate immune memory', which produces an enhanced inflammatory response following secondary stimuli. Stimulation of an innate immune cell (or its progenitors) triggers an enhanced nonspecific immunological

reaction as a result of changes in gene transcription caused by modifications in chromatin configuration (Netea et al., 2020). An interplay between epigenetic and metabolic reprogramming events induced by particular innate immune triggers shapes trained immunity in myeloid cells. Among the epigenetic markers that define trained immunity, specific histone modifications have been identified, including histone H3 lysine 4 monomethylation (H3K4me1), trimethylation (H3K4me3), and H3 lysine 27 acetylation (H3K27ac). Furthermore, during the primary challenge, recognition of specific ligands by pattern recognition receptors triggers intracellular cascades that lead to upregulation of metabolic pathways, such as glycolysis, the tricarboxylic acid cycle, and fatty acid metabolism. Several epidemiological and experimental data support the role of trained immunity in the evolution of AAA.

Diet type can positively or negatively influence the development of AAA. Intake of a diet richer in fruits and vegetables is reported to decrease the risk of AAA (Haring et al., 2018) whereas a high-fat diet seems to be associated with an increased risk of AAA rupture, *e.g.,* by accelerating chronic inflammation and altering the physiological functions of PVAT (Hashimoto et al., 2018). Consistently, transcriptomic and epigenomic reprogramming of myeloid progenitor cells that promoted proliferation, skewing of hematopoiesis, and enhanced responses to exogenous and endogenous inflammatory triggers was observed in $Ldlr^{-/-}$ mice fed with the Western diet (Christ et al., 2018).

Long-term changes produced by inflammatory processes that generate alterations in cellular metabolism, epigenome, and transcriptome of bone marrow progenitor cells are known to cause increased myelopoiesis and subsequent expansion of trained innate immune cells (Mitroulis et al., 2018). Consistently, in mouse models of AAA, chronic infusion of angiotensin II caused expansion of hematopoietic progenitors and their differentiation toward proinflammatory $CCR2^{+}$ monocytes (Kim et al., 2016), whereas ablation of the IL-27 receptor protected from aneurysm development by blunting hematopoietic stem cell proliferation and myeloid cell accumulation in the aorta (Peshkova et al., 2019). In the context of AAA, the interaction between activated myeloid cells and a specific T response could be a plausible mechanism to constantly feed the inflammatory loop responsible for the evolution of the dilation process. TLR and NOD signaling pathways could play an important role here both because they have been associated with trained immunity (Owen et al., 2020) and because their involvement in AAA evolution has been extensively documented, including our previous work on the PVAT of AAA (Piacentini et al., 2019; Piacentini et al., 2020).

As mentioned, there is an inverse relationship between diabetes mellitus and AAA. Some studies have suggested that protection is the result of diabetes-induced alterations in the vascular ECM, which make it more resistant to the action of proteolytic enzymes (Dattani et al., 2018). However, important insights have been provided by experimental studies of hypoglycemic drugs in the treatment of AAA. Thiazolidinediones may influence AAA growth by reducing infiltration of innate immune cells (*i.e.*, macrophages) and levels of metalloproteinase and TNFα observed in both the aortic wall and PVAT (Torsney et al., 2013). Of particular interest is the relationship between metformin use and AAA (Raffort et al., 2020). Metformin could exert its anti-inflammatory effect on trained immunity by inhibiting glycolysis through interference with the mTOR/HIF-1α pathway, which is essential for inducing trained immunity (Cheng et al., 2014). The inhibitory effect of metformin on trained immunity provides both an important mechanistic link for a better understanding of AAA pathogenesis and a key clue to its use for the treatment of AAA. Indeed, clinical trials designed to test the efficacy and safety of metformin in preventing the growth of AAA have recently started (Lareyre and Raffort, 2021).

From this complex and varied picture, the possibility arises that the immune response observed in AAAs may have a definite relationship with trained immunity. Therefore, we sought to support this hypothesis by searching for possible associations with epigenetic markers related to trained immunity using the dataset collected on the PVAT of AAAs in our previous study.

EXPERIMENTAL EVIDENCE

Study Population and Gene Expression Data

We relied on data collected in a cohort of patients with infrarenal AAA described in (Piacentini et al., 2019). Briefly, the cohort consisted of 30 patients, who underwent elective surgery for AAA at our Centre between June 2010 and December 2014. Patients presented with either a small (<55.0 mm) or large (≥55.0) diameter AAA. The two subgroups did not differ in demographic, clinical characteristics, risk factors, or medications on admission. At the time of surgery, periaortic fat surrounding the aortic neck proximal to the aneurysm (non-dilated-PVAT) and the aneurysm sac (dilated-PVAT) were collected for each patient. We considered the dilated-PVAT and non-dilated PVAT as the pathological and 'healthy' (non-diseased) segments of the AAA, respectively. Total RNA from these samples was extracted and used to carry out gene expression analysis with microarrays. Performing a pairwise comparison of dilated-PVAT *vs.* non-dilated-PVAT from each subject, we identified several differentially expressed (DE) transcripts, including 84 and 184 unique genes overexpressed in dilated-PVAT of small and large AAAs, respectively (Piacentini et al., 2019). These genes encompass several factors of the immune-inflammatory response, which appeared relevant for the pathogenesis of AAA (see gene annotation in **Supplementary Table S1**).

Bioinformatics Analysis

We used a reverse engineering approach through the *i-cisTarget* software (Imrichova et al., 2015) to analyze the cis-regulatory sequences of genes overexpressed in dilated-PVAT associated with small or large AAAs and predict histone modification signatures. This allowed us to retrieve putative upstream regulators starting from the sets of co-expressed genes and gain insights into functional relationships. The *i-cisTarget* workflow consists of a 'rank-and-recovery' procedure. A set of

TABLE 1 | Predicted histone modifications associated with overexpressed genes in perivascular adipose tissue of small and large abdominal aortic aneurysms.

Feature	Reference	Description	NES
Small AAA			
E124-H3K27ac-broadpeak	**ENCODE**	**H3K27ac in Monocytes-CD14$^+$ RO01746 Primary Cells**	**7.91**
ENCFF001TAS (E124)	ENCODE	H4K20me1 in ChIP-seq on human monocytes CD14$^+$	6.47
E127-H3K36me3-broadpeak	ENCODE	H3K36me3 in NHEK-Epidermal Keratinocyte Primary Cells	6.17
E039-H3K27ac-broadpeak	Roadmap	H3K27ac in Primary T helper naive cells from peripheral blood	5.28
E041-H3K36me3-broadpeak	Roadmap	H3K36me3 in Primary T helper cells PMA-I stimulated	5.03
E025-H3K36me3-broadpeak	Roadmap	H3K36me3 in Adipose-derived Mesenchymal Stem Cell cultured cells	4.85
ENCFF001TBR (E126)	ENCODE	H3K9ac in ChIP-seq on human NHDF-Ad	4.79
E124-H3K9ac-broadpeak	ENCODE	H3K9ac in Monocytes-CD14$^+$ RO01746 Primary Cells	4.58
E126-H3K9ac-broadpeak	ENCODE	H3K9ac in NHDF-Ad Adult Dermal Fibroblast Primary Cells	4.54
E025-H3K9ac-broadpeak	Roadmap	H3K9ac in Adipose-derived Mesenchymal Stem Cell cultured cells	4.52
E119-H3K36me3-broadpeak	ENCODE	H3K36me3 in HMEC Mammary Epithelial Primary Cells	4.33
ENCFF001TAQ (E124)	ENCODE	H3K36me3 in ChIP-seq on human monocytes CD14$^+$	4.31
E124-H3K9ac	ENCODE	H3K9ac in Monocytes-CD14$^+$ RO01746 Primary Cells	4.27
E034-H3K27ac-broadpeak	Roadmap	H3K27ac in Primary T cells from peripheral blood	4.21
E047-H3K9ac-broadpeak	Roadmap	H3K9ac in Primary T CD8$^+$ naive cells from peripheral blood	4.16
E042-H3K36me3-broadpeak	Roadmap	H3K36me3 in Primary T helper 17 cells PMA-I stimulated	4.05
E124-H4K20me1-broadpeak	ENCODE	H4K20me1 in Monocytes-CD14$^+$ RO01746 Primary Cells	4.01
ENCFF001TAL (E124)	**ENCODE**	**H3K4me3 in ChIP-seq on human monocytes CD14$^+$**	**4.00**
Large AAA			
ENCFF001TAS (E124)	ENCODE	H4K20me1 in ChIP-seq on human monocytes CD14$^+$	7.86
E029-H3K36me3-broadpeak	Roadmap	H3K36me3 in Primary monocytes from peripheral blood	7.52
E124-H4K20me1-broadpeak	ENCODE	H4K20me1 in Monocytes-CD14$^+$ RO01746 Primary Cells	7.31
E037-H3K4me1-broadpeak	Roadmap	H3K4me1 in Primary T helper memory cells from peripheral blood 2	6.69
E124-H3K79me2-broadpeak	ENCODE	H3K79me2 in Monocytes-CD14$^+$ RO01746 Primary Cells	6.66
E030-H3K4me1	Roadmap	H3K4me1 in Primary neutrophils from peripheral blood	6.53
E124-H3K4me1-broadpeak	**ENCODE**	**H3K4me1 in Monocytes-CD14$^+$ RO01746 Primary Cells**	**6.42**
E030-H3K4me1-broadpeak	Roadmap	H3K4me1 in Primary neutrophils from peripheral blood	6.37
E124-H3K4me3	**ENCODE**	**H3K4me3 in Monocytes-CD14$^+$ RO01746 Primary Cells**	**6.34**
E030-H3K36me3-broadpeak	Roadmap	H3K36me3 in Primary neutrophils from peripheral blood	6.09
E030-H3K4me3	Roadmap	H3K4me3 in Primary neutrophils from peripheral blood	6.03
ENCFF001TAQ (E124)	ENCODE	H3K36me3 in ChIP-seq on human monocytes CD14$^+$	5.97
E040-H3K4me1-broadpeak	Roadmap	H3K4me1 in Primary T helper memory cells from peripheral blood 1	5.46
E124-H3K27ac-broadpeak	**ENCODE**	**H3K27ac in Monocytes-CD14$^+$ RO01746 Primary Cells**	**5.25**
E124-H3K79me2	ENCODE	H3K79me2 in Monocytes-CD14$^+$ RO01746 Primary Cells	5.24
E046-H3K36me3-broadpeak	Roadmap	H3K36me3 in primary Natural Killer cells from peripheral blood	5.12
E029-H3K27ac	Roadmap	H3K27ac in Primary monocytes from peripheral blood	5.12
E124-H3K9ac	ENCODE	H3K9ac in Monocytes-CD14$^+$ RO01746 Primary Cells	4.83
E043-H3K4me1-broadpeak	Roadmap	H3K4me1 in Primary T helper cells from peripheral blood	4.78
E034-H3K4me1-broadpeak	Roadmap	H3K4me1 in Primary T cells from peripheral blood	4.76
ENCFF001TAR (E124)	ENCODE	H3K79me2 in ChIP-seq on human monocytes CD14$^+$	4.64
E124-H3K27ac	ENCODE	H3K27ac in Monocytes-CD14$^+$ RO01746 Primary Cells	4.62
E030-H3K36me3	Roadmap	H3K36me3 in Primary neutrophils from peripheral blood	4.57
E031-H3K4me1-broadpeak	Roadmap	H3K4me1 in Primary B cells from cord blood	4.44
E050-H3K4me1	Roadmap	H3K4me1 in Primary hematopoietic stem cells G-CSF-mobilized female	4.42
E029-H3K4me1-broadpeak	Roadmap	H3K4me1 in Primary monocytes from peripheral blood	4.38
E031-H3K4me1	Roadmap	H3K4me1 in Primary B cells from cord blood	4.35
E124-H3K4me1	ENCODE	H3K4me1 in Monocytes-CD14$^+$ RO01746 Primary Cells	4.26
E029-H3K36me3	Roadmap	H3K36me3 in Primary monocytes from peripheral blood	4.24

AAA, abdominal aortic aneurysm; ENCODE, Encyclopedia of DNA Elements; Roadmap, NIH Roadmap Epigenomics Consortium.
Histone mark signatures for acute (early) or trained immunity stimulation in small and large AAA, respectively, are highlighted in bold.

candidate regulatory regions (CRRs) has been established based on publicly available data. For histone modification enrichment, CRRs are scored and ranked according to ChIP-seq features from the ENCODE (Encode Project Consortium et al., 2020) and Roadmap Epigenomics (Roadmap Epigenomics Consortium et al., 2015) projects, including 2450 experimental data tracks. We linked and collected all CRRs located in the proximity of all co-expressed genes in our datasets by setting 10 kb upstream and downstream of the transcription start site (TSS) as the regional mapping boundary and 40% (default) as the minimum overlap fraction of CRRs with peaks. The recovery step extracts the features for which the input foreground regions (the input genes mapped to the CRRs) are most enriched. The enrichment is calculated by the Area Under the recovery

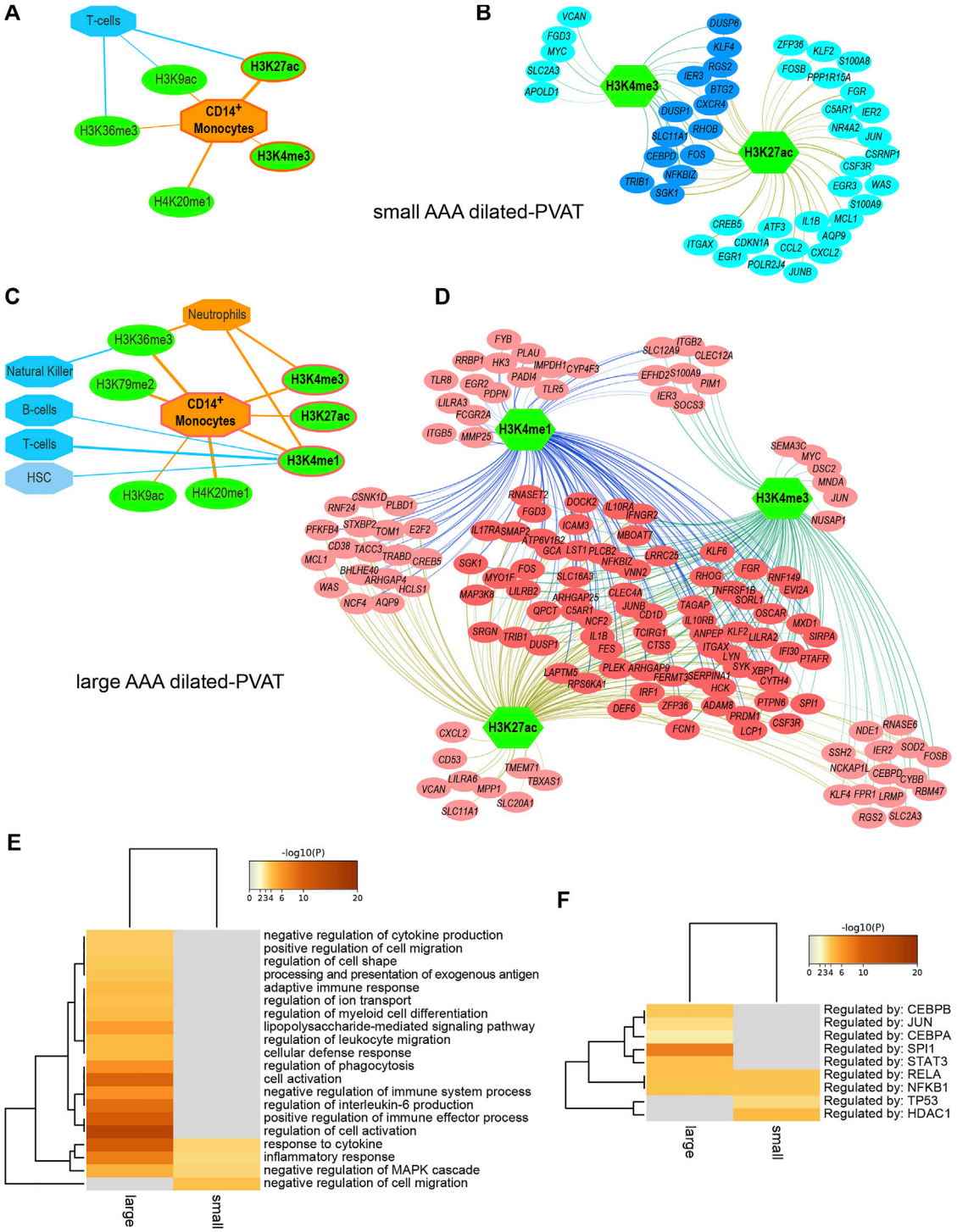

FIGURE 1 | Regulatory networks and functional enrichment analysis of genes overexpressed in AAA dilated-PVAT related to immune cells and functions **(A)** Predicted histone modifications (green ovals) significantly associated with transcriptionally active euchromatin of myeloid or lymphoid immune cells (orange and blue octagons, respectively) in small AAA dilated-PVAT. The histone mark signature recalling immune response after acute stimulation is highlighted with an orange border. In this and panel C, edge thickness is proportional to the normalized enrichment score, which measures the relevance of enrichment **(B)** Regulatory network of histone marks and genes overexpressed in dilated-PVAT linked to acute stimulation in early-stage AAA (small AAA). Green hexagons represent histone marks associated with CD14$^+$ monocytes, blue ovals show associated genes. Overexpressed genes associated with this histone mark signature are highlighted in dark blue **(C)** Predicted histone modifications significantly associated with myeloid or lymphoid immune cells in large AAA dilated-PVAT. The histone mark signature recalling trained immunity is outlined in orange **(D)** Regulatory network of histone marks and genes overexpressed in dilated-PVAT linked to trained immunity in advanced AAA (large AAA). Green

(*Continued*)

FIGURE 1 | hexagons are as in panel B, pink ovals show associated genes. Overexpressed genes associated with this histone signature are highlighted in dark pink **(E)** Functional enrichment of Gene Ontology (GO) biological processes and **(F)** transcription factors relative to overexpressed genes associated with acute stimulation or trained immunity. The ochre to brown color gradient indicates the significance level of the GO terms expressed as -log10 of the adjusted *p*-values; gray color indicates non-significant associations. Significant terms were hierarchically clustered based on the Kappa score.

Curve (AUC) of these regions. To retain the results of only highly ranked regions, we set the AUC threshold parameter to 1%. The AUCs for all features are then normalized using a Normalized Enrichment Score (NES),

$$NES = (AUC - \mu)/\sigma$$

where μ is the mean of all AUC scores across all features and σ is the standard deviation of the AUC scores. We set an NES threshold at ≥4.0 to return more stringent results.

The regulatory networks of predicted histone modifications and overexpressed genes in the dilated-PVAT of large and small AAAs related to immune cells were reconstructed using Cytoscape v3.7.1 software (Shannon et al., 2003).

Functional enrichment analysis was performed through Metascape software (Zhou et al., 2019) on groups of genes associated with relevant histone modification marks in small and large AAAs using predefined parameters. Ontology annotation and enrichment were performed using two databases, the Gene Ontology Biological Processes (GO-BP) (Ashburner et al., 2000) and the reference transcription factor (TF)-target interaction database for humans—Transcriptional Regulatory Relationships Unraveled by Sentence-based Text mining (TTRUST) (Han et al., 2018). Significant terms were hierarchically clustered in a tree based on Kappa-statistical similarities (threshold = 0.3) among gene memberships. Representative terms were then visualized as heatmaps.

Results

Full results and statistics can be accessed and downloaded from the Zenodo repository (Piacentini and Colombo, 2020). The 'report' file for each AAA subtype is an HTML document that can be opened through a browser to explore the analysis parameters and results, including significant features sorted by NES and feature hyperlinks to obtain an overview of significantly high-ranked regions and associated genes. Briefly, reverse engineering analysis allowed us to associate subsets of DE genes with cell type-specific histone modifications. In summary (**Table 1**), we predicted 18 histone modifications associated with regulatory sequences of subsets of genes overexpressed in the dilated-PVAT of small AAAs and 29 associated with genes overexpressed in large AAAs. Most of these histone modifications were related to immune cells. Specifically, 66% of histone marks in small AAAs were associated with $CD14^+$ monocytes, T-helper, and $CD8^+$ lymphocytes, while 100% of histone marks in large AAAs were associated with $CD14^+$ monocytes, neutrophils, natural killers, hematopoietic stem cells, T-helper, and B-lymphocytes. Most of these histone marks (*i.e.*, H4K20me1, H3K36me3, H3K79me2, H3K4me1, H3K4me3, H3K27ac, and H3K9ac) were related to the transcriptionally active euchromatin of myeloid cells (van der Heijden et al., 2018): indeed, myeloid cell-related histone modifications increased in percentage as AAA diameter increased (small = 39% and large = 72%). This suggested greater transcriptional activity linked to innate immune cells in large AAAs. Finally, we observed that the dilated-PVAT of small and large AAAs was associated with H3K27ac/H3K4me3 and H3K27ac/H3K4me3/H3K4me1 signatures in $CD4^+$-monocytes, respectively: the former is suggestive of acute (early) stimulation, the latter is typical of trained immunity (restimulation) (Saeed et al., 2014) (**Figures 1A–D**).

To search for possible biological processes associated with gene signatures of acute (early) or trained immunity, we performed a functional enrichment analysis and identified statistically enriched GO-BP and TF terms. To reduce redundancy, terms were grouped based on similarity and an overview term was used for clustering (**Figure 1E** and **Supplementary Table S2**). Interestingly, the "inflammatory response" and "response to cytokines" processes were enriched in both the small and large dilated-PVAT, but with higher enrichment scores for the large AAA, suggesting a higher inflammatory state for this subtype. Furthermore, large AAA showed significant associations with several immune-related processes, including "positive regulation of immune effector process", "regulation of IL-6", "cellular activation", and "regulation of myeloid cell differentiation", suggesting an increase in the immune-related inflammatory process occurring in later stages of the disease. Consistently, we found enriched TFs that are known to be involved in the innate and inflammatory immune response (**Figure 1F**) such as RELA and NFKB1 in both small and large AAAs and a specific association of large AAAs with CEBPB and SPI1 (PU.1) TFs, which have recently been shown to be associated with trained immunity (de Laval et al., 2020).

DISCUSSION

AAA is still a disease of unknown etiology that requires new ideas to improve our ability to understand its pathogenetic mechanisms so that effective therapeutic approaches can be developed. In this perspective article, we aimed to highlight possible links between the development and progression of AAA and innate immunity. The existence of innate immunological memory has only recently emerged as a new and rapidly growing immunological concept in several areas, including cardiovascular disease, although its association with AAA has not yet been appreciated. We pointed out that trained immunity is an immunological mechanism capable of generating

an excess response when dysregulated, which could contribute to chronic inflammatory disease processes in AAA.

A large number of studies have unequivocally demonstrated that innate and adaptive immunity participate together in the evolution of AAA (Yuan et al., 2020). Furthermore, PVAT has been shown to play a key role in generating the immune-inflammatory response in AAA. Our previous studies corroborate this hypothesis, suggesting that both innate and adaptive immunity in the PVAT of AAAs cooperate to promote an "immunological short circuit" likely responsible for disease progression. Accordingly, through bioinformatics analysis, we previously reconstructed a regulatory network by retrieving transcription factors and upstream regulators (e.g., kinases) of DE genes that characterize dilated AAA PVAT (Piacentini et al., 2020). In the present work, we focused on epigenetic regulators of gene expression, looking for possible histone modifications of pathogenic AAA PVAT genes. Thus, we predicted the histone modification signature associated with trained immunity in the PVAT of large AAAs, which supports the idea that innate immunity may concur with adaptive immunity in consistently feeding the chronic process during later stages of AAA.

Whether elements of innate immunity may be more central than adaptive immunity or *vice versa* is, however, a mere speculative disquisition because both arms of the immune system exert their function through close crosstalk. Consistent with this view, a local environment created by trained innate immune cells during secondary stimulation may indeed influence T-cell responses in AAA, for example by altering the differentiation, polarization, and function of T-cell subtypes, suggesting an important link between trained immunity and an antigen-specific immune response (Murphy et al., 2021).

In this scenario, therefore, it may make sense to test whether trained immunity is a sensitive target that could interrupt this "short circuit" and influence disease evolution. The precise definition of the molecular mechanisms underlying trained immunity in AAA could lead to the identification of possible modulators capable of inhibiting inflammation and vessel wall degeneration, opening new therapeutic solutions for AAA (Arts et al., 2018). To this end, a more thorough investigation using single-cell resolution techniques would be extremely informative in providing insights into the main cell types and their states responsible for the pathophysiology of AAA.

DATA AVAILABILITY STATEMENT

The original gene expression dataset on which this study is based can be found in the NCBI's GEO repository at https://www.ncbi.nlm.nih.gov/geo/query/acc.cgi?acc=GSE119717. Overall results and statistics have been made publicly available on the Zenodo Open Science data repository at https://zenodo.org/record/4139226#.X5rzaVDSJPY.

ETHICS STATEMENT

The studies involving human participants were reviewed and approved by Comitato Etico degli IRCCS IEO e Monzino. The patients/participants provided their written informed consent to participate in this study.

AUTHOR CONTRIBUTIONS

LP and GI.C designed and supervised the experiments and the concept of this work. CV performed the experiments and collected the data. LP analyzed the data and prepared the first draft of the manuscript. GI.C critically reviewed the manuscript. All authors read and approved the final manuscript.

FUNDING

This work was supported by the Italian Ministry of Health (Research Projects RC Nos. 2600658, 2627621, and 2631196) to GIC.

SUPPLEMENTARY MATERIAL

The Supplementary Material for this article can be found online at: https://www.frontiersin.org/articles/10.3389/fcell.2022.886086/full#supplementary-material

Supplementary Table S1 | Annotation of genes significantly overexpressed in dilated-PVAT vs non-dilated-PVAT of large or small abdominal aortic aneurysms or both.

Supplementary Table S2 | Functional enrichment results using Gene Ontology (GO) biological process (BP) terms on genes associated with acute and trained immunity histone modification signatures.

REFERENCES

Arts, R. J. W., Joosten, L. A. B., and Netea, M. G. (2018). The Potential Role of Trained Immunity in Autoimmune and Autoinflammatory Disorders. *Front. Immunol.* 9, 298. doi:10.3389/fimmu.2018.00298

Ashburner, M., Ball, C. A., Blake, J. A., Botstein, D., Butler, H., Cherry, J. M., et al. (2000). Gene Ontology: Tool for the Unification of Biology. The Gene Ontology Consortium. *Nat. Genet.* 25 (1), 25–29. doi:10.1038/75556

Chang, T. W., Gracon, A. S. A., Murphy, M. P., and Wilkes, D. S. (2015). Exploring Autoimmunity in the Pathogenesis of Abdominal Aortic Aneurysms. *Am. J. Physiology-Heart Circulatory Physiology* 309 (5), H719–H727. doi:10.1152/ajpheart.00273.2015

Cheng, S.-C., Quintin, J., Cramer, R. A., Shepardson, K. M., Saeed, S., Kumar, V., et al. (2014). mTOR- and HIF-1α-Mediated Aerobic Glycolysis as Metabolic Basis for Trained Immunity. *Science* 345 (6204), 1250684. doi:10.1126/science.1250684

Christ, A., Günther, P., Lauterbach, M. A. R., Duewell, P., Biswas, D., Pelka, K., et al. (2018). Western Diet Triggers NLRP3-dependent Innate Immune Reprogramming. *Cell* 172 (1-2), 162–175. e114. doi:10.1016/j.cell.2017.12.013

Dattani, N., Sayers, R. D., and Bown, M. J. (2018). Diabetes Mellitus and Abdominal Aortic Aneurysms: A Review of the Mechanisms Underlying the Negative Relationship. *Diabetes Vasc. Dis. Res.* 15 (5), 367–374. doi:10.1177/1479164118780799

de Laval, B., Maurizio, J., Kandalla, P. K., Brisou, G., Simonnet, L., Huber, C., et al. (2020). C/EBPβ-Dependent Epigenetic Memory Induces Trained Immunity in Hematopoietic Stem Cells. *Cell Stem Cell* 26 (5), 657–674. doi:10.1016/j.stem.2020.01.017

Encode Project ConsortiumMoore, J. E., Moore, J. E., Purcaro, M. J., Pratt, H. E., Epstein, C. B., Shoresh, N., et al. (2020). Expanded Encyclopaedias of DNA Elements in the Human and Mouse Genomes. *Nature* 583 (7818), 699–710. doi:10.1038/s41586-020-2493-4

Gao, J.-P., and Guo, W. (2022). Mechanisms of Abdominal Aortic Aneurysm Progression: A Review. *Vasc. Med.* 27 (1), 88–96. doi:10.1177/1358863X211021170

Gil-Ortega, M., Somoza, B., Huang, Y., Gollasch, M., and Fernández-Alfonso, M. S. (2015). Regional Differences in Perivascular Adipose Tissue Impacting Vascular Homeostasis. *Trends Endocrinol. Metabolism* 26 (7), 367–375. doi:10.1016/j.tem.2015.04.003

Golledge, J. (2019). Abdominal Aortic Aneurysm: Update on Pathogenesis and Medical Treatments. *Nat. Rev. Cardiol.* 16 (4), 225–242. doi:10.1038/s41569-018-0114-9

Golledge, J., Moxon, J. V., Singh, T. P., Bown, M. J., Mani, K., and Wanhainen, A. (2020). Lack of an Effective Drug Therapy for Abdominal Aortic Aneurysm. *J. Intern Med.* 288 (1), 6–22. doi:10.1111/joim.12958

Guzik, T. J., Skiba, D. S., Touyz, R. M., and Harrison, D. G. (2017). The Role of Infiltrating Immune Cells in Dysfunctional Adipose Tissue. *Cardiovasc Res.* 113 (9), 1009–1023. doi:10.1093/cvr/cvx108

Han, H., Cho, J.-W., Lee, S., Yun, A., Kim, H., Bae, D., et al. (2018). TRRUST V2: an Expanded Reference Database of Human and Mouse Transcriptional Regulatory Interactions. *Nucleic Acids Res.* 46 (D1), D380–D386. doi:10.1093/nar/gkx1013

Haring, B., Selvin, E., He, X., Coresh, J., Steffen, L. M., Folsom, A. R., et al. (2018). Adherence to the Dietary Approaches to Stop Hypertension Dietary Pattern and Risk of Abdominal Aortic Aneurysm: Results from the ARIC Study. *J. Am. Heart. Assoc* 7 (21), e009340. doi:10.1161/JAHA.118.009340

Hashimoto, K., Kugo, H., Tanaka, H., Iwamoto, K., Miyamoto, C., Urano, T., et al. (2018). The Effect of a High-Fat Diet on the Development of Abdominal Aortic Aneurysm in a Vascular Hypoperfusion-Induced Animal Model. *J. Vasc. Res.* 55 (2), 63–74. doi:10.1159/000481780

Imrichová, H., Hulselmans, G., Kalender Atak, Z., Potier, D., and Aerts, S. (2015). I-cisTarget 2015 Update: Generalized Cis-Regulatory Enrichment Analysis in Human, Mouse and Fly. *Nucleic Acids Res.* 43 (W1), W57–W64. doi:10.1093/nar/gkv395

Kent, K. C., Zwolak, R. M., Egorova, N. N., Riles, T. S., Manganaro, A., Moskowitz, A. J., et al. (2010). Analysis of Risk Factors for Abdominal Aortic Aneurysm in a Cohort of More Than 3 Million Individuals. *J. Vasc. Surg.* 52 (3), 539–548. doi:10.1016/j.jvs.2010.05.090

Kim, S., Zingler, M., Harrison, J. K., Scott, E. W., Cogle, C. R., Luo, D., et al. (2016). Angiotensin II Regulation of Proliferation, Differentiation, and Engraftment of Hematopoietic Stem Cells. *Hypertension* 67 (3), 574–584. doi:10.1161/HYPERTENSIONAHA.115.06474

Lareyre, F., and Raffort, J. (2021). Metformin to Limit Abdominal Aortic Aneurysm Expansion: Time for Clinical Trials. *Eur. J. Vasc. Endovascular Surg.* 61 (6), 1030. doi:10.1016/j.ejvs.2021.02.056

Lindeman, J. H. N., Rabelink, T. J., and van Bockel, J. H. (2011). Immunosuppression and the Abdominal Aortic Aneurysm: Doctor Jekyll or Mister Hyde?. *Circulation* 124 (18), e463–465. doi:10.1161/CIRCULATIONAHA.110.008573

Mitroulis, I., Ruppova, K., Wang, B., Chen, L.-S., Grzybek, M., Grinenko, T., et al. (2018). Modulation of Myelopoiesis Progenitors Is an Integral Component of Trained Immunity. *Cell* 172 (1-2), 147–161. e112. doi:10.1016/j.cell.2017.11.034

Murphy, D. M., Mills, K. H. G., and Basdeo, S. A. (2021). The Effects of Trained Innate Immunity on T Cell Responses; Clinical Implications and Knowledge Gaps for Future Research. *Front. Immunol.* 12, 706583. doi:10.3389/fimmu.2021.706583

Netea, M. G., Domínguez-Andrés, J., Barreiro, L. B., Chavakis, T., Divangahi, M., Fuchs, E., et al. (2020). Defining Trained Immunity and its Role in Health and Disease. *Nat. Rev. Immunol.* 20 (6), 375–388. doi:10.1038/s41577-020-0285-6

Owen, A. M., Fults, J. B., Patil, N. K., Hernandez, A., and Bohannon, J. K. (2020). TLR Agonists as Mediators of Trained Immunity: Mechanistic Insight and Immunotherapeutic Potential to Combat Infection. *Front. Immunol.* 11, 622614. doi:10.3389/fimmu.2020.622614

Peshkova, I. O., Aghayev, T., Fatkhullina, A. R., Makhov, P., Titerina, E. K., Eguchi, S., et al. (2019). IL-27 Receptor-Regulated Stress Myelopoiesis Drives Abdominal Aortic Aneurysm Development. *Nat. Commun.* 10 (1), 5046. doi:10.1038/s41467-019-13017-4

Piacentini, L., Chiesa, M., and Colombo, G. I. (2020). Gene Regulatory Network Analysis of Perivascular Adipose Tissue of Abdominal Aortic Aneurysm Identifies Master Regulators of Key Pathogenetic Pathways. *Biomedicines* 8 (8), 288. doi:10.3390/biomedicines8080288

Piacentini, L., and Colombo, G. I. (2020). Data and Results Related to the Article "Trained Immunity in Perivascular Adipose Tissue of Abdominal Aortic Aneurysm—A Novel Concept for a Still Elusive Disease. v1. Available at: https://zenodo.org/record/4139226#.Yg6XqIiZNhF

Piacentini, L., Werba, J. P., Bono, E., Saccu, C., Tremoli, E., Spirito, R., et al. (2019). Genome-Wide Expression Profiling Unveils Autoimmune Response Signatures in the Perivascular Adipose Tissue of Abdominal Aortic Aneurysm. *Arterioscler. Thromb. Vasc. Biol* 39 (2), 237–249. doi:10.1161/ATVBAHA.118.311803

Queiroz, M., and Sena, C. M. (2020). Perivascular Adipose Tissue in Age-Related Vascular Disease. *Ageing Res. Rev.* 59, 101040. doi:10.1016/j.arr.2020.101040

Raffort, J., Hassen-Khodja, R., Jean-Baptiste, E., and Lareyre, F. (2020). Relationship between Metformin and Abdominal Aortic Aneurysm. *J. Vasc. Surg.* 71 (3), 1056–1062. doi:10.1016/j.jvs.2019.08.270

Roadmap Epigenomics ConsortiumKundaje, A., Kundaje, A., Meuleman, W., Ernst, J., Bilenky, M., and Yen, A. (2015). Integrative Analysis of 111 Reference Human Epigenomes. *Nature* 518 (7539), 317–330. doi:10.1038/nature14248

Saeed, S., Quintin, J., Kerstens, H. H. D., Rao, N. A., Aghajanirefah, A., Matarese, F., et al. (2014). Epigenetic Programming of Monocyte-To-Macrophage Differentiation and Trained Innate Immunity. *Science* 345 (6204), 1251086. doi:10.1126/science.1251086

Sagan, A., Mikolajczyk, T. P., Mrowiecki, W., MacRitchie, N., Daly, K., Meldrum, A., et al. (2019). T Cells Are Dominant Population in Human Abdominal Aortic Aneurysms and Their Infiltration in the Perivascular Tissue Correlates with Disease Severity. *Front. Immunol.* 10, 1979. doi:10.3389/fimmu.2019.01979

Shannon, P., Markiel, A., Ozier, O., Baliga, N. S., Wang, J. T., Ramage, D., et al. (2003). Cytoscape: a Software Environment for Integrated Models of Biomolecular Interaction Networks. *Genome Res.* 13 (11), 2498–2504. doi:10.1101/gr.1239303

Suh, M. K., Batra, R., Carson, J. S., Xiong, W., Dale, M. A., Meisinger, T., et al. (2020). *Ex Vivo* expansion of Regulatory T Cells from Abdominal Aortic Aneurysm Patients Inhibits Aneurysm in Humanized Murine Model. *J. Vasc. Surg.* 72 (3), 1087–1096. e1081. doi:10.1016/j.jvs.2019.08.285

Tilson, M. D. (2016). Decline of the Atherogenic Theory of the Etiology of the Abdominal Aortic Aneurysm and Rise of the Autoimmune Hypothesis. *J. Vasc. Surg.* 64 (5), 1523–1525. doi:10.1016/j.jvs.2016.06.119

Torsney, E., Pirianov, G., and Cockerill, G. W. (2013). Diabetes as a Negative Risk Factor for Abdominal Aortic Aneurysm - Does the Disease Aetiology or the Treatment Provide the Mechanism of Protection? *Curr. Vasc. Pharmacol* 11 (3), 293–298. doi:10.2174/1570161111311030003

van der Heijden, C. D. C. C., Noz, M. P., Joosten, L. A. B., Netea, M. G., Riksen, N. P., and Keating, S. T. (2018). Epigenetics and Trained Immunity. *Antioxidants Redox Signal.* 29 (11), 1023–1040. doi:10.1089/ars.2017.7310

Yodoi, K., Yamashita, T., Sasaki, N., Kasahara, K., Emoto, T., Matsumoto, T., et al. (2015). Foxp3 + Regulatory T Cells Play a Protective Role in Angiotensin II-Induced Aortic Aneurysm Formation in Mice. *Hypertension* 65 (4), 889–895. doi:10.1161/HYPERTENSIONAHA.114.04934

Yuan, Z., Lu, Y., Wei, J., Wu, J., Yang, J., and Cai, Z. (2020). Abdominal Aortic Aneurysm: Roles of Inflammatory Cells. *Front. Immunol.* 11, 609161. doi:10.3389/fimmu.2020.609161

Zhou, Y., Wu, W., Lindholt, J. S., Sukhova, G. K., Libby, P., Yu, X., et al. (2015). Regulatory T Cells in Human and Angiotensin II-Induced Mouse Abdominal Aortic Aneurysms. *Cardiovasc. Res.* 107 (1), 98–107. doi:10.1093/cvr/cvv119

Zhou, Y., Zhou, B., Pache, L., Chang, M., Khodabakhshi, A. H., Tanaseichuk, O., et al. (2019). Metascape Provides a Biologist-Oriented Resource for the Analysis of Systems-Level Datasets. *Nat. Commun.* 10 (1), 1523. doi:10.1038/s41467-019-09234-6

Conflict of Interest: The authors declare that the research was conducted in the absence of any commercial or financial relationships that could be construed as a potential conflict of interest.

Publisher's Note: All claims expressed in this article are solely those of the authors and do not necessarily represent those of their affiliated organizations, or those of the publisher, the editors and the reviewers. Any product that may be evaluated in this article, or claim that may be made by its manufacturer, is not guaranteed or endorsed by the publisher.

frontiers | Frontiers in Cell and Developmental Biology

REVIEW
published: 04 July 2022
doi: 10.3389/fcell.2022.910884

The Epigenetic Role of MiRNAs in Endocrine Crosstalk Between the Cardiovascular System and Adipose Tissue: A Bidirectional View

Ursula Paula Reno Soci[1], *Bruno Raphael Ribeiro Cavalcante*[2,3], *Alex Cleber Improta-Caria*[4,5] *and Leonardo Roever*[4,6,7]*

[1]Biodynamics of the Human Body Movement Department, School of Physical Education and Sports, São Paulo University–USP, São Paulo, Brazil, [2]Gonçalo Moniz Institute, Oswaldo Cruz Foundation (IGM-FIOCRUZ/BA), Salvador, Brazil, [3]Department of Pathology, Faculty of Medicine, Federal University of Bahia, Salvador, Brazil, [4]Post-Graduate Program in Medicine and Health, Faculty of Medicine, Federal University of Bahia, Salvador, Brazil, [5]Physical Education Department, Salvador University (UNIFACS), Salvador, Brazil, [6]Department of Clinical Research, Federal University of Uberlândia, Uberlândia, Brazil, [7]Faculty of Medicine, Sao Paulo University, Sao Paulo, Brazil

OPEN ACCESS

Edited by:
Kazuo Miyazawa,
RIKEN Yokohama, Japan

Reviewed by:
Wei Ying,
University of California, San Diego, United States
Hiroki Takanari,
Tokushima University, Japan
Hiroki Kitakata,
Keio University School of Medicine, Japan

***Correspondence:**
Leonardo Roever
leonardoroever@hotmail.com

Specialty section:
This article was submitted to Cellular Biochemistry, a section of the journal Frontiers in Cell and Developmental Biology

Received: 01 April 2022
Accepted: 24 May 2022
Published: 04 July 2022

Citation:
Soci UPR, Cavalcante BRR, Improta-Caria AC and Roever L (2022) The Epigenetic Role of MiRNAs in Endocrine Crosstalk Between the Cardiovascular System and Adipose Tissue: A Bidirectional View. Front. Cell Dev. Biol. 10:910884. doi: 10.3389/fcell.2022.910884

Overweight and obesity (OBT) is a serious health condition worldwide, and one of the major risk factors for cardiovascular disease (CVD), the main reason for morbidity and mortality worldwide. OBT is the proportional increase of Adipose Tissue (AT) compared with other tissue and fluids, associated with pathological changes in metabolism, hemodynamic overload, cytokine secretion, systemic inflammatory profile, and cardiac metabolism. In turn, AT is heterogeneous in location, and displays secretory capacity, lipolytic activation, insulin sensitivity, and metabolic status, performing anatomic, metabolic, and endocrine functions. Evidence has emerged on the bidirectional crosstalk exerted by miRNAs as regulators between the heart and AT on metabolism and health conditions. Here, we discuss the bidirectional endocrine role of miRNAs between heart and AT, rescuing extracellular vesicles' (EVs) role in cell-to-cell communication, and the most recent results that show the potential of common therapeutic targets through the elucidation of parallel and/or common epigenetic mechanisms.

Keywords: microRNA, adipose tissue, obesity, heart, cardiovascular disease, crosstalk, metabolism

INTRODUCTION

MicroRNAs (miRNAs) are ~22-nt RNAs that posttranscriptionally repress translation of mRNA targets in eukaryotic and prokaryotic lineages, and are transcripts within longer stem-loop RNA. The latest release of miRBase v22 (https://www.mirbase.org/) contains miRNA sequences from 271 organisms: 38,589 hairpin precursors and 48,860 mature miRNAs. As an example, the human genome contains 1,917 annotated hairpin precursors, and 2,654 mature sequences (Bartel, 2018; Kozomara et al., 2019). The miRNAs are highly conserved between species, preferentially conserving interactions with most human mRNAs, regulating a plethora of developmental processes and health states at molecular, cellular, tissue, and physiological levels (Bartel, 2018). Several miRNAs have a role in cardiovascular biology related to disease etiology and progression, revealing potential as cardiovascular disease (CVD) biomarkers and therapeutic targets (Small and Olson, 2011).

Overweight and obesity (OBT) is a serious health condition worldwide, affecting respectively 1.9 billion and 650 million people, and consequently requiring treatment for several secondary diseases,

like CVD, currently the main reason for morbidity and mortality worldwide, which OBT is one of the major risk factors (Hashim, 2017). OBT consists of a body mass index (BMI) > 30 kg/m^2 associated with a proportional increase of adipose tissue (AT) compared with other tissue and fluids. This condition induces pathological changes in metabolism, hemodynamic overload, cytokine secretion, systemic inflammatory profile, and cardiac metabolism. The AT depots are heterogeneous and they differ in location, secretory capacity, lipolytic activation, insulin sensitivity, and metabolic status, performing anatomic, metabolic, and endocrine functions. (Christensen et al., 2020; Zhang et al., 2020).

Recently, a body of evidence postulated that circulating miRNAs act as endocrine factors, performing endocrine and paracrine crosstalk between cells and tissues. Several circulating miRNAs are implicated in physiological and pathological processes related to metabolism (Ji and Guo, 2019). The concept of the heart as an endocrine organ arises from the discovery of the atrial cardiomyocytes expressing polypeptides with natriuretic properties: ANF and BNP, which at present are biomarkers of cardiac stress (Garciá-Arias et al., 2020). Currently, heart-enriched miRNAs are investigated as biomarkers of cardiac diseases and cardiovascular system (CVS) function regulators and some are known as systemic metabolism regulators (van Rooij et al., 2007; Callis et al., 2009; Grueter et al., 2012).

In this review, we discuss the role of miRNAs in the bidirectional endocrine relationship between heart tissue and AT in circulation, within extracellular vesicles (EVs) or not. On the one hand, we summarized some miRNAs already known to be enriched in AT and their regulatory mechanism on cardiac function and morphology. Furthermore, we discuss the epigenetic regulation performed by cardiac miRNAs in crosstalk with AT, showing the latest evidence about common regulation, parallel mechanisms, and the predictive and therapeutic clinical potential of these tiny and powerful molecules.

The Relationship Between Obesity, Cardiovascular Diseases, and MiRNAs

OBT is a multi-causal metabolic disease that is associated with hypertrophy and hyperplasia of white AT (WAT) (Rosen & Spiegelman, 2014). Both AT hypertrophy process and hyperplasia occur mainly due to excess food consumption (calorie consumption) and low caloric expenditure (sedentary lifestyle) (Heindel & Blumberg, 2019). These two processes in the AT promote an increase in the number of immune cells in this tissue, inducing a large production of pro-inflammatory cytokines that are released into the circulation (Han et al., 2020, Maurizi et al., 2018).

In addition to the inflammatory process, obesity configures an inadequate supply of oxygen in the AT, inducing hypoxia in these cells, activating hypoxia-inducible factor 1/(HIF-1), which leads to apoptosis of adipose cells and also attenuates preadipocyte differentiation, favoring the increase of the fibrotic process (Buechler et al., 2015).

The association between inflammation and fibrosis leads to AT dysfunction, insulin resistance, and endothelial dysfunction. This scenario paves the way for the development of cardiovascular and metabolic diseases, like hypertension (Brandes, 2014; Longo et al., 2019; Battineni et al., 2021), type 2 diabetes (Avogaro, 2006), and coronary artery disease (CAD) (Ganz & Hsue, 2013). The increase in AT cells also induces hemodynamic overload, due to the increase of systolic volume of the left ventricle (LV), a condition that in the long term will promote pathological cardiac hypertrophy (CH), and systolic and diastolic dysfunction that may go along with heart failure, which in obese individuals is called OBT cardiomyopathy (Ren et al., 2021).

All these pathological processes in OBT are linked to the deregulation of signaling pathways which activates transcription factors, regulates gene expression, and induces pathological profiles of miRNAs. Several miRNAs have already been described as deregulated in AT, in the differentiation of mesenchymal stem cells to preadipocytes (Improta Caria et al., 2018). Several dysregulated miRNAs in OBT were also associated with the inflammatory (Arner & Kulyté, 2015) and fibrotic processes (Caus et al., 2021). Some of these miRNAs have a common expression pattern with other diseases, such as systemic arterial hypertension (Improta-Caria et al., 2021) and type 2 diabetes (Improta-Caria et al., 2022).

MicroRNAs: Brief History, Biogenesis and Function

MiRNAs were initially discovered during analyzes of the progression from the first larval stage (L1) to L2 of the nematode *Caenorhabditis elegans,* in which the decrease in the expression of the LIN-14 protein was essential for the development of the worms. In addition, the downregulation of LIN-14 occurred due to the progressive transcription of another gene, known as *LIN-4,* short single strand RNAs, which were not translated into protein and adversely transcribed two small RNAs about 22–61 nucleotides in length, and with complementarity in the 3′-untranslated regions (UTR) of the LIN-14 mRNA (Lee et al., 1993). Subsequently, the hybridization in these complementary regions was linked with a decrease in the LIN-14 protein content, without impacting the decrease in the expression of its transcript (Wightman et al., 1993).

Following these findings, other researchers identified another small RNA known as let-7 that promoted the adult larval stage of *C. elegans* (Reinhart et al., 2000). Interestingly, let-7 has also been identified in humans (Pasquinelli et al., 2000), drawing the attention of several researchers around the world. In the following years, several research groups began to further investigate the role of these small RNAs in different organisms, demonstrating their biogenesis and their regulatory function (Lee et al., 2002; Ambros, 2004; Pfeffer et al., 2005; Roush & Slack., 2008; Morlando et al., 2008).

MiRNA biogenesis is a multi-molecular-step process that starts in the nucleus and ends in the cytoplasm with the synthesis of mature miRNA (Kim, 2005). The miRNAs are processed from a precursor molecule, referred to as primary

transcript (pri-miRNA), which is transcribed initially by the RNA polymerase II (Lee et al., 2004; Treiber et al., 2019). This enzyme transcribes the pri-miRNA, which contains one or more sequences that are enveloped in a stem-loop structure. In the nucleus, pri-miRNA receives two cleavages between the lower and upper stems of its structure by Drosha, an RNase III-like enzyme (Davis et al., 2010). It acts together with cofactors including an essential subunit protein, the DiGeorge syndrome chromosomal region 8 (DGCR8). Drosha and DGCR8 processing steps form the microprocessor complex to mature the pri-miRNA into pre-miRNA (Denli et al., 2004; Wang et al., 2007). After processing by Drosha, a long transcript is enveloped in a stem-loop intermediate structure, an ~75 nucleotides called precursor (pre-miRNA) (Krol et al., 2010).

The product of Drosha cleavage is exported to the cytoplasm by Exportin 5, where the next cleavage occurs by Dicer, an RNase III-like endonuclease (Ketting et al., 2001; Yi et al., 2003; Zeng and Cullen, 2004; Okada et al., 2009; Fisher et al., 2011). Dicer cleaves the pre-miRNA hairpin into a miRNA duplex about 25 nucleotides in length (Hutvágner et al., 2001). After the Dicer process, the mature miRNA is incorporated into the RNA-induced silencing complex (RISC), generating the (mi-RISC) complex. This mi-RISC induces downregulation of target genes, modulating gene expression. (Chakravarthy et al., 2010; Horman et al., 2013). Next, the mature miRNA associated with miRISC binds to the 3′-UTR of the target mRNA causing degradation, deadenylation, or inhibition of translation of this gene. Impressively, a single miRNA can have multiple mRNA targets, inducing epigenetic regulation of gene expression at the post-transcriptional level and modulation of several signaling pathways (Samanta et al., 2016; Bartel, 2018).

Adipose Tissue Diversity of Depots and Function

AT is a crucial organ in human anatomy as it plays a key role in regulating body energy and glucose homeostasis. It has effects on physiology and pathophysiology by displaying relevant tasks in lipid handling, energy storage compartment, insulation barrier, and secretion of endocrine mediators such as adipokines or lipokines (Vegiopoulos et al., 2017). Finally, AT is considered a highly active metabolic and endocrine organ (Kershaw and Flier, 2004).

AT is composed of several cells and components, including adipocytes (the most common cell type), lymphocytes, macrophages, fibroblasts, endothelial cells, and extracellular matrix (Corrêa et al., 2019). Morphologically, some types of AT have been identified in humans, namely white, brown, and beige or "brite" (brown-in-white). This classification is based on the colorful diversity and predominant presence of adipocytes: in WAT, there is a significant presence of white adipocytes; in brown AT (BAT), brown adipocytes are mainly present. Considering the plasticity of AT and its ability to proliferate, differentiate, and transdifferentiate, the third type of adipocyte, beige (BeAT) results from white adipocytes that have acquired phenotypic brown features in response to different *stimuli*, in a process called "browning" (Pilkington et al., 2021).

The WAT can also be classified by location, as subcutaneous (under the skin) and visceral/omental (intra-abdominally, adjacent to internal organs). In addition, WAT is confined to defined depots in healthy individuals but in certain conditions like OBT and lipodystrophy, WAT mass can ectopically increase in areas such as the visceral cavity, including intrahepatic fat, epicardial fat (EAT) in the pericardium, perivascular fat (PVAT) surrounding major blood vessels, and visceral fat (VAT), which comprises mesenteric fat, omental fat, and retroperitoneal fat (Chait and den Hartigh, 2020).

AT types can be found in specific anatomical sites throughout the body and each one has displayed distinct characteristics and functions: whereas WAT adipocytes are associated with storage and release of energy during fasting periods (Torres et al., 2015), BAT adipocytes have thermogenic properties, burning glucose and lipids to maintain thermal homeostasis during periods of low temperature and hibernation (Rosen and Spiegelman, 2014). Despite similarities to brown adipocytes, BeAT adipocytes can undergo a thermogenic or storage phenotype depending on environmental conditions (Zoico et al., 2019).

As an endocrine organ, AT responds to physiological cues or metabolic stress, releasing endocrine factors that regulate energy expenditure, appetite control, glucose homeostasis, insulin sensitivity, inflammation, and tissue repair. WAT and thermogenic BAT and BeAT also secrete endocrine molecules, such as adipokines, lipokines, miRNAs, and other noncoding RNAs.

Recent findings emphasize the endocrine role of white versus thermogenic adipocytes in conditions of cardiac health and disease (Scheja and Heeren, 2019). Furthermore, AT secretes molecules, directly or *via* extracellular vesicles (EVs) (including exosomes and nano-sized vesicles generated from late endosomes), containing proteins, lipids, and nucleic acids, such as miRNAs which recently have been investigated as epigenetic mediators of endocrine and paracrine effect between AT and other tissues, like the cardiac (Hartwig et al., 2019; Zhang Y. et al., 2019).

Exosomes and Circulating MiRNAs as Epigenetic Mediators in the Cardiovascular System and Adipose Tissue Crosstalk

The last decade increased understanding of the adipocytes' role in health and disease. There is growing evidence implicating extracellular vesicles miRNAs (EVs-miRNAs) and circulating miRNAs mediating intercellular and inter-organ communication. These miRNAs are classified as extracellular miRNAs, since they are detected in an extracellular environment, as biological fluids and cell culture media.

EVs are systemic messengers that can deliver signaling molecules. Exosomes, microvesicles, and apoptotic bodies are the most important EVs and have distinct biogenesis pathways sizes and types (Mathieu et al., 2019). Adipocytes are a major source of EVs-containing miRNA in circulation. An increasing number of studies have shown that EVs and their cargo play important roles in cellular crosstalk between cells and tissues, and therefore can regulate disease and health conditions.

Nevertheless, the detailed mechanisms in these complex fields are far from being completely elucidated, comprising the interaction between the biogenesis of miRNAs and the biogenesis and maturation of EVs in several tissues and cells related to CVD and AT (Turchinovich et al., 2012; Kranendonk et al., 2014; Fang et al., 2016; Sluijter et al., 2018).

The accurate characterization of EVs is limited by the technical difficulty in isolating and characterizing pure tissue-specific populations and their subtypes since the current methods are mainly based on the co-isolation of EVs of distinct subcellular origins. Many studies use 'exosome' referring to a mixture of small EVs of both exosomal and nonexosomal nature, due to poor specificity of the physical processes for isolation and purification of EVs. Thus, unless the EVs' origin has been clearly stated, it may be preferable to use the generic term 'small EVs' instead of 'exosomes', which range 10–200 nm in diameter (Mathieu et al., 2019). Given the complexity of processes and technical limitations to investigating exosomal miRNAs, it is a promising and challenging field to elucidate tissue crosstalk, including AT and CVD. Furthermore, there is a recent and growing body of evidence that miRNAs content in AT exosomes plays key roles in cardiovascular processes, clinically reinforcing obesity as a CVD risk factor. Similarly, there are established cardiac-enriched miRNAs that can regulate AT depots *via* systemic metabolism and other biological processes, which will be addressed in the last topic.

The Endocrine Function of Adipose Tissue-Enriched MiRNAs on the Cardiovascular System

In OBT, AT increases the size and number of adipocytes, storing more triglycerides. Additionally, AT synthesizes and releases hormones called "adipokines", like leptin and adiponectin, and other factors which affect biological pathways, at autocrine, paracrine, and endocrine levels, including the regulation of whole-body energy homeostasis (Patel et al., 2017). In this condition, AT can become unhealthy as adipocytes lose their ability to store triglycerides adequately, have impaired energy expenditure, and become insulin resistant. Consequently, fatty acids are released into the circulation and accumulate in other organs, causing cellular stress, disturbed metabolism, and altered secretion of endocrine factors, regarded as a hallmark of chronic metabolic and CVD (Reilly, 2017; Scheja and Heeren, 2019).

The evidence postulates that AT-derived circulating miRNAs are currently described as a new form of adipokines (Thomou et al., 2017). Circulating (or extracellular) miRNAs are freely and/or carried within exosomes, lipoproteins, and blood cells, from cells that express them to cells that receive them (Sohel, 2016). Recent evidence shows that AT is the main source of all circulating exosomal miRNAs, in humans and mice. Knockout Dicer-deficient (ADicerKO) mice present lipodystrophic phenotype and AT-deficient miRNA processing, decreasing AT-derived miRNA expression. Similarly, lipodystrophy decreases the levels of circulating exosomal miRNAs compared to healthy people. Among 653 miRNAs in serum EVs, 419 decreased in fat-specific DicerKO mice, 88% by more than four-fold. (Thomou et al., 2017). In summary, 216 miRNAs decreased in patients with lipodystrophy compared to healthy people and 30 common miRNAs decreased between ADicerKO and patients, which shows that AT releases numerous miRNAs *via* exosomes that may be involved in cell-to-cell epigenetic regulation and the regulation between health and CVD (Thomou et al., 2017). Inversely, transplantation of wild-type mice-derived WAT and BAT into ADicerKO mice restored exosomal miRNAs and improved glucose tolerance, showing evidence that AT-miRNAs are also crucial for regulating energy metabolism, and their expression is associated with a proper function of AT (Thomou et al., 2017). The transplantation with BAT and WAT into ADicerKO mice restored miR-325 and miR-743b (predicted to target UCP-1) and miR-98 (predicted to target PGC1α) for BAT and miR-99 for BAT and WAT, suggesting that AT-secreted miRNAs may have both paracrine and endocrine actions. In addition, pediatric obesity presents an increase in 16 circulating miRNAs previously associated with nonalcoholic fatty liver disease, reinforcing that free and exosomal miRNAs are released from AT cells to influence several tissues and biological processes, including cardiovascular health regulation (Thompson et al., 2017).

MEG-3 is a long-noncoding RNA involved in the imprinting of maternal genes that sponges miR-325. Hypoxia-reperfusion in H9c2 cardiomyoblast cells increases MEG-3, decreases miR-325, and increases the protein content of target TRPV4. TRPV4 is a Calmodulin-dependent Ca^{2+} channel that regulates Ca^{2+} concentration in excitable cells and, concomitantly in adipocytes, regulates the expression of chemokines and cytokines related to pro-inflammatory pathways. This entire process denotes not only miRNAs crosstalking but also that it could protect or enhance the response to ischemic injury (Zhou et al., 2021). Furthermore, Hsa-miR-325 is elevated in normal pregnancies and decreases in preeclampsia patients, being implicated in preeclampsia etiology (Lázár et al., 2012). In $ApoE^{-/-}$ mouse with atherosclerosis, miR-325 increases in arterial tissues of atherosclerotic mice, and miR-325 inhibition reduces the contents of total cholesterol, triglyceride, low-density lipoprotein, and CRP, IL-6, IL-1β and TNF-α levels in mouse serum. *In vitro* miR-325 inhibition decreased the lipid content in RAW264.7 macrophage cells *via* KDM1A to reduce SREBF1 expression and activated the PPARγ-LXR-ABCA1 pathway. KDM is a demethylase that regulates lipogenic genes (Pu et al., 2021). LXRs are expressed in the murine heart in the basal state and are activated by myocardial infarction, also associated with an intracardiac accumulation of lipid droplets and protection against myocardial ischemia-reperfusion injury (Lei et al., 2013). PPARγ is a nuclear receptor that stimulates lipid and glucose utilization by increasing mitochondrial function and fatty acid desaturation pathways, being crucial for cardiac function and metabolism (Montaigne et al., 2012). PPARγ also is a regulator of AT signaling and plays a crucial role in insulin sensitivity, making it an important therapeutic target. Moreover, PPARγ activation increases cardiac hypertrophy and oxidative stress in mice. Cocultures of adipocytes and cardiomyocytes showed that stimulation of PPARγ signaling in adipocytes increased miR-200a expression and secretion. Delivery of

miR-200a in adipocyte-derived exosomes to cardiomyocytes inhibits TSC1 and activates the mTOR pathway, leading to CH. Inhibition of miR-200a abrogated the CH, clarifying that the miRNA cargo in EVs can change cardiac phenotypes and showing evidence of endocrine crosstalk between heart and AT performed by EVs (Fang et al., 2016).

In a single study using a rat model in a time course in transverse constriction of the Aorta, cardiac miR-743b acutely increased over 2-fold after 5 days compared with 10, 15, and 20 days of pressure overload. The increase was associated with pathological remodeling and CH; however, additional investigation is needed to assess if EVs circulating AT miR-743b has some additive effect on the cardiac remodeling phenotype (Feng et al., 2014).

In a murine model for cardiac allograft transplantation, miR-98 plays a role in regulating interleukin (IL)-10 expression in B cells (B10 cell) after heart transplantation. The miR-98 inhibition, cortisol inhibition, and transfer with B10 cells enhanced the survival rate and time of transplanted mice (Song et al., 2017). In the first atlas of miRNA profile using internal mammary artery from 192 CAD disease patients, miR-98 was significantly correlated with acute myocardial infarction occurrence, suggesting that this AT-enriched miRNA is also related to the regulation of cardiac function (Neiburga et al., 2021). In addition, miR-98 in human fibroblasts inhibits TGF-β1-induced differentiation and collagen production of cardiac fibroblasts targeting TGFβR1, performing a role in the fibrotic phenotype, present in all cardiac diseases (Cheng et al., 2017). Finally, miR-98 is downregulated in myocardial infarct injury (MII) and neonate primary culture of cardiomyocytes in response to H_2O_2 stress. Additionally, miR-98 overexpression protected cardiomyocytes against apoptosis by its target Fas, inhibiting the Caspase-3 apoptotic pathway (Sun et al., 2017).

Adipocytes-enriched miRNAs play an essential role in regulating gene expression and cell-to-cell communication, through mRNA downregulation, therefore interfering in a multitude of biological processes (Eichhorn et al., 2014; Heyn et al., 2020). OBT changes drastically the profile of the AT-enriched miRNAs, influencing circulating and exosomal miRNAs content. Consequently, aberrant intra- and extracellular miRNAs profiles can induce crosstalk between AT, liver, skeletal muscle, and other organs, which impacts the development of different cancers and metabolic CVD (Muralimanoharan et al., 2015; Sala et al., 2021). There is evidence that OBT and weight loss alter the profile of circulating miRNAs in humans and mice, affecting pathways associated with body mass index (BMI), and others such as percent fat mass, waist-to-height ratio, and plasma adipokine levels. The compared whole profile of circulating miRNAs pre- and post-surgery weight loss in 6 morbidly obese patients showed that the most relevant circulating miRNAs differences were the increased expression of miR-142-3p, miR-140-5p, and miR-222 and the decreased circulating concentrations of miR-221, miR-15a, miR-520c-3p, miR-423-5p, and miR-130b (Ortega et al., 2013; Lörchner et al., 2021). Additionally, the plasma concentrations of all were associated with BMI and most of them with fat mass and waist circumference. Interestingly, the 2 major targets for the *in silico* intersection between miR-142-3p and miR-140-5p (LIFR) and between miR-15a and miR-520c-3p (VEGFA) were significantly associated with the circulating values of their specific transcriptional regulators. The plasma content of LIFR (a cardioprotective IL-6 receptor), was negatively correlated with the circulating concentrations of miR-142-3p, and miR-140-5p, whereas miR-15a and miR-520c-3p were negatively correlated to circulating VEGFA (Ortega et al., 2013; Lörchner et al., 2021). There are several AT-enriched and OBT-related miRNAs with concomitant roles in heart phenotypes. The large-scale mapping of the epigenetic regulations between heart and AT at the systemic level may shed light on corrective post-translational multi-gene therapies.

Another study elucidates the metabolic influence in endocrine crosstalk of miRNAs performed between AT and CVS and delineates a molecular mechanism by which dysfunctional adipocytes could exacerbate myocardial infarct injury (MII) *via* EVs-miRNAs. The transplantation of diabetic epididymal fat or intramyocardial or systemic administration of diabetic adipocyte EVs in MII mice exacerbated the injury in nondiabetic mice. Inversely, the injection of an EVs' biogenesis inhibitor abrogated the additional deleterious effect and improved cardiac function post-MI, increasing dP/dt (max) compared with MII vehicle mice. MiR-130b-3p was implicated in the mechanism due to an increase in diabetic patients' plasma and mice diabetic adipocyte, serum, and EVs. In addition, mimic for miR-130b-3p increased and miR-130b-3p inhibitor decreased MII injury, *via* direct targets such as AMPKα1/α2, BIRC6, and UCP3, showing a direct mechanistic relationship between miRNAs, AT, and cardiac injury (Gan et al., 2020).

Considering the established EAT and PAT bidirectional effects on cardiovascular health *via* the production and secretion of adipokines (Patel et al., 2017), and AT circulating miRNAs emerging as multilevel epigenetic regulators with functional and structural roles in CVS, additional investigation into the miRNAs crosstalk between AT and CV tissue is crucial and has clear clinical potential as therapeutic targets and biomarkers for the assessment of metabolic disorders and obesity-related diseases. In this way, the next topics will show and discuss the bidirectional relationship between AT and CVS miRNAs, rescuing the functional evidence on this issue in an extracellular environment.

Epicardial and Pericardial Adipose Tissue MiRNAs

Epicardial and Pericardial AT (EAT and PAT, respectively) are anatomically and biochemically distinct and have different cellular origins. EAT lies between the outer wall of the myocardium and the visceral layer of the pericardium, while PAT lies between the visceral and parietal pericardium. Since no fascia separates the tissues, EAT is in direct contact and communication with the myocardium, in the atrioventricular and interventricular grooves, and alongside the coronary arteries of the human heart. PAT splits to form the parietal pericardium and the outer thoracic wall. EAT differentiates from

splanchnopleuric mesoderm, whereas PAT arises from the primitive thoracic mesenchyme (Iacobellis, 2009; Zhang et al., 2020).

Translational studies are also interesting approaches to overcome challenges and current limitations to evidence EVs' crosstalk between AT and CVS among species. Microscopic analyses show inflammatory, fibrotic, and apoptotic phenotypes in fresh and cultured EAT tissues from CVD and Atrial Fibrillation (AF) patients. AF-EVs presented a high expression of profibrotic (miR-146b) and low expression of antifibrotic miRNAs respectively (miR-133a, miR-29a). Concomitantly, EVs harvested from AF-EAT patients exacerbated fibrotic phenotype in rats and changed electrophysiological properties facilitating arrhythmias in cardiomyocyte-hiPSC culture, reinforcing the evidence of the paracrine and endocrine effect of AT miRNAs in cardiac cells predisposing to the disease, i.e., showing the crosstalk between EAT and heart phenotypes *via* miRNAs as endocrine effectors (Shaihov-Teper et al., 2021). The role of miR-29a, -133a and -133b, and -146 on cardiac fibrosis, function, and remodeling is well established and does not require additional comments (Carè et al., 2007; Van Rooij et al., 2008; Li et al., 2012; Feng et al., 2017).

In humans, the evidence that the EAT is an active endocrine organ is robust. EAT is metabolically active and a source of several adipokines, potential interactions through paracrine or autocrine mechanisms between epicardial fat and the myocardium regulating between healthy and disease state. The PAT as a source of adipokines is still partially unknown, being more related to atherosclerosis and CAD. However, it is possible that PAT interacts paracrinally with the pericardium tissue and EAT. EAT is very metabolically active, therefore, lipolysis and fatty acid synthesis are greater in EAT compared to visceral fat, and PAT, and EAT adipocytes are smaller than other AT cells (Christensen et al., 2020).

Considering that PAT has more potential to release inflammatory cytokines than subcutaneous fat, it is interesting to investigate its interaction with EAT to explain gene etiology and CAD regulation (Ding et al., 2008; Iacobellis, 2009; Hassan et al., 2020; Zhang et al., 2020). An increased EAT thickness has become a new risk factor for CAD. A study already aimed at identifying the miRNA profile role of EAT dysfunction as a CAD marker. EAT miRNA array profiles from 150 CAD sudden cardiac death victims and 84 non-CAD-sudden death controls were prospectively enrolled at autopsy and showed the following EAT miRNA profile candidates for dysregulation: miR-34a-3p, miR-34a-5p, miR-124-3p, miR-125a-5p, miR-628-5p, miR-1303, miR-4286 related to atherosclerosis and plaque destabilization pathways. MiR-34a-3p and miR-34a-5p were higher in CAD, were positively correlated with age, and were validated as biomarkers of CAD, independently of thickness and plaque formation (Marí-Alexandre et al., 2019).

MiR-34a is regarded as an effector for endocrine AT-CVS crosstalk. The evidence shows it as reinforcing loss of function in CVS by several pathways. MiR-34 levels are relatively low in the CVS, but recently they have been reported to be increased in cardiovascular disorders. MiR-34a is a predictive biomarker in mice after myocardial infarct injury (MII) and presents low expression in healthy hearts (Li et al., 2015; Qipshidze Kelm et al., 2018). The inhibition miR-34 family has been investigated as therapeutic for CVD by regulating apoptosis, telomere waste, DNA damage (targeting PNUTS), inflammatory response (KLF4, SEMA4b, BCL6), inotropic and excitability (Vinculin), and cardiac fibrosis (ALDH2) (Bernardo et al., 2012; Boon et al., 2013; Li et al., 2015; Qipshidze Kelm et al., 2018). In mice, they have the same seed sequence, suggesting their common target mRNAs. In human beings, miR-34a and miR-34c have the same seed sequence, and miR-34b has three short nucleotide sequences identical to miR-34a and miR-34c, showing that the target mRNAs may change between species and miRNAs (Li et al., 2015). The circulating miR-34a expression in AT progressively enhances with the development of diet-induced OBT. Inversely, adipocyte-specific miR-34a-KO mice are resistant to OBT-induced glucose intolerance, insulin resistance, and systemic inflammation, related to a significant shift in the polarization of adipose-resident macrophages from pro-inflammatory M1 to anti-inflammatory M2 phenotype (Pan et al., 2019). Finally, miR-34a can inhibit fat browning by suppressing the browning activators FGF2 and SIRT1 in mice, showing a dual role as a therapeutic target for CVD and OBT (Fu et al., 2014).

MiR-99 family comprises miR-99a, miR-99b and miR-100. They show very similar sequences and identical seeds. MiR-100 has one different nucleotide compared to miR-99a, and four compared to miR-99b. MiR-99a, in turn, differs from four nucleotides compared to miR-99b. This family, in addition to being enriched in AT, also concomitantly shows a regulatory role between physiological and pathological CH, with apoptosis and growth processes in both *in vitro* and *in vivo* settings. (Ramasamy et al., 2015, 2018). Swimming exercise training showed a miRNA profile by RNAseq in which miR-99b and miR-100 were downregulated (Ramasamy et al., 2015). In addition, physiological and pathological CH was induced in H9c2 cells by treatment with α2-macroglobulin and Isoproterenol, respectively. The miR-99b and miR-100 were downregulated in physiological CH and upregulated in pathological CH targeting AKT-1. Upstream, EGR-1 superexpression binds to the promoter and induces miR-99b and miR-100 expression, and downstream, AKT-1 silencing replicates the effect of overexpression of miR-99, showing the mechanism by which this regulation occurs through this AT-enriched family of miRNAs (Ramasamy et al., 2018).

Therefore, a clipping was performed here to demonstrate the potentiality of the crosstalk between AT and heart *via* miRNAs. There is a vast field to be clarified in this sense, with very comprehensive clinical perspectives regarding therapies and detection methods. In the next topic, we will discuss the other side of bidirectional crosstalk from the heart to AT.

Cardiac Enriched MicroRNAs: The Heart as an Endocrine Organ

The evidence of the heart as an endocrine organ emerged from studies that showed that the atrial cardiomyocytes in the mammalian heart could perform roles similar to endocrine cells, by the expression of ANF, BNP, and CNP in circulation.

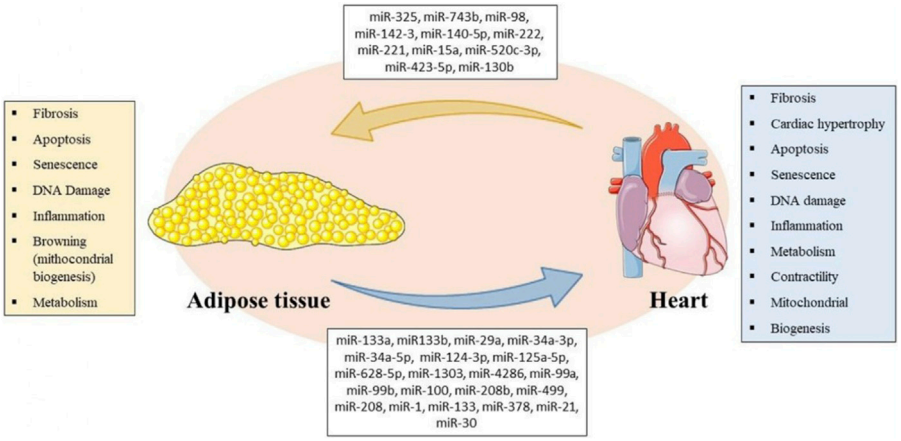

FIGURE 1 | Representative Scheme of miRNAs secreted by AT and heart with their respective biological processes involved in bidirectional crosstalk between tissues. Parts of the figure were drawn using pictures from Servier Medical Art (https://smart.servier.com/). Servier Medical Art by Servier is licensed under a Creative Commons Attribution 3.0 Unported License.

These molecules, known as natriuretic peptides, displayed paracrine functions related to blood volume regulation, cardiac output, and serum concentrations of sodium and total body water. These studies were the guideline for identifying new molecules linked to the contractile function of the heart (Garciá-Arias et al., 2020).

The first evidence of a miRNA as a regulator of systemic metabolism related to the endocrine role of the heart emerged by miR-208a, which pharmacologic inhibition by injections induced resistance to obesity in animals fed with a high-fat diet (Grueter et al., 2012). MiR-208a is cardiac-specific and is encoded by the α-myosin heavy chain (MHC) gene. This miRNA up-regulates β-MHC by directly targeting PURβ and SOX-6 together with miR-208b and miR-499, also called myomiRs, which share a similar seed sequence. β-MHC has an ATPase activity slower than α-MHC and is a pathological CH and cardiac stress marker (Van Rooij et al., 2007; van Rooij et al., 2009). Therefore, miR-208a is considered an epigenetic biomarker of myocardial stress, having a high predictive potential in several pathological conditions (Callis et al., 2009; Ji et al., 2009; Boštjančič et al., 2010; Satoh et al., 2010). Grueter et al. (2012) by several mechanism studies, including transgenic mice models, showed that MED13 is a target of miR-208, which triggers systemic and cardiac metabolic actions of miR-208a, and indirectly regulates β-MHC expression. In addition, cardiac-specific gain and loss of function of MED13 in mice established a crucial role in the governance of whole metabolism and the control of energy expenditure pathways by regulating the action of nuclear receptors. Cardiomyocyte-specific overexpression of MED13 in mice conferred a lean phenotype by enhancing metabolism in white AT and the liver, and O_2 consumption, without increasing food consumption. The epigenetic mechanism of systemic metabolism regulation *via* miR-208 is not yet fully elucidated. However, miR-208a increases in several cardiovascular diseases, including heart failure. Considering the systemic, cardiac, and metabolic changes arising from severe cardiac diseases, there is evidence of a systemic-metabolic down-regulation of transcription role performed by nuclear receptors on metabolic genes profile and a possible relationship with mitochondrial dysfunction (Gan et al., 2013). Additionally, there is a glimpse of miR-208a inhibition in a clinical perspective for OBT and CVD by metabolic gene expression, considering that the challenge to therapies towards miRNAs lies in controlling the expression in an acceptable physiological range, beyond improved oligonucleotides, deliveries, and vectors.

Other noncardiac-specific myomiRs that are highly expressed and involved in AT regulation are miR-1, and miR-133, miR-378. In addition, there are others that present lower baseline expression, such as miR-208a, and for which the studies show involvement in metabolism in disease, such as miR-21, and the miR-34 and miR-30 families, which may play a reinforcing role in regulating phenotypes.

MiR-133 was first characterized in mice. Its homologs were identified in several other species, including the human genome in which miR-133 genes comprise miR-133a-1, miR-133a-2, and miR-133b located on chromosomes 18, 20, and 6. Importantly, miR-133a-1 and miR-133a2 have identical nucleotide sequences, whereas miR-133b differs in the last 2 nucleotides at the 3′-terminus. MiR-133a-1, miR-133a-2, and miR-133b are bicistronically transcribed with miR-1-2, miR-1-1, or miR-206, with low genomic distances between the miRNA coding regions. Cardiac miR-133 has a crucial role in cardiac remodeling in response to several stresses (Matkovich et al., 2013). The decreased expression of miR-133 is correlated with the increased severity of HF and a high NT-proBNP concentration (Danowski et al., 2013). In animal models, miR-133 also regulates cardiac fibrosis, electrical activities apoptosis, and gene reprogramming by targeting a plethora of targets (Li et al., 2018). Outside CVS, miR-133 controls BAT fate determination in skeletal muscle satellite cells (SMSC) targeting the *PRDM16* gene, regulating the choice between myogenic and brown adipose determination. Since brown adipocytes derive from myogenic

TABLE 1 | miRNAs secreted by adipose tissue and heart and targets potentially involved in bidirectional crosstalk.

Adipose tissue-enriched miRNAs with cardiovascular functions			
miR	**Target**	**Model**	**References**
miR-325	UCP-1 TRPV4	Mice	Thomou et al. (2017)
miR-743b		Rat	Feng et al. (2014)
		cells	Cheng et al. (2017)
			Zhou et al. (2021)
miR-98	PGC1α TGFβR1	Mice cells	Cheng et al. (2017)
			Song, et al. (2017)
			Neiburga et al. (2021)
			Sun et al. (2017)
miR-142-3p	LIFR VEGFA	Humans	Lörchner et al. (2021)
miR-140-5p			
miR-222			
miR-221			
miR-15a			Ortega et al. (2013)
miR-520c-3p			
miR-423-5p			
miR-130b			
miR-200a	TSC1	Cells	Fang et al. (2016)
miR-130b-3p	AMPLα1/α2BIRC6 UCP3	Mice	Gan et al. (2013)
Epicardial and Pericardial Adipose Tissue miRNAS			
miR	Target	Model	References
miR-133a		Human explants	Shaihov-Teper et al. (2021)
miR-133b			
miR 29a			
miR-34a-3p	PNUTSKLF4 SEM4b BCL6 ALD2	Humans mice	Mari-Alexandre et al. (2019)
miR-34a-5p			Bernardo et al. (2012)
miR-124-3p			Boon et al. (2013)
miR-125a-5p			Li et al. (2015) Qipshidze
miR-658-5p			Kelm et al. (2018)
miR-1303			
miR-4286			
miR-99a	AKT-1	rat cells	Ramasamy et al., 2015, 2018
miR-99b			
miR-100			
Cardoac-enriched miRNAs			
miR	Target	Model	References
miR-208a	PURβ	Mice	Van Rooij et al. (2007)
miR-208b	SOX-6		Van Rooij et al. (2009)
miR-499	MED13		Grueter et al. (2012)
miR-1	PRCM16	cells	Yin et al. (2013)
miR-133			
miR-378	MAPK1	Cells	Fisher et al. (2011)
	IGF1		
	GRB2		
	KRS1		
miR-21	PTEN	Cells	Cheng and Zhang, (2010a)
	PDCD4		
	SPRY2		
miR-30	RUNX2	Cells	Zaragosi et al. (2011)
	RIP140		Hu et al. (2015)

progenitors during embryonic development, *PRDM16*, highly expressed in WAT and myogenic cells, performs the role of a crucial regulator in BAT adipogenesis. Thus, miR-133 also becomes an important therapeutic target to treat obesity, in addition to cardiovascular function (Yin et al., 2013). As the miR-133 family is highly expressed in muscle tissues and decreases both CH and skeletal muscle hypertrophy, and this miRNA regulates the differentiation and proliferation by cell cycle targets and transcription factors, this family is an interesting target for whole approaches for CVD, metabolic disease and obesity.

The miR-378 family also is highly expressed in heart and has 11 members (miR-378a-3p/b/c/d/e/f/g/h/i/j and miR-422a). Although they are encoded by different genomic *loci*, they share identical seed sequences, and the family is conserved between humans and rodents. MiR-378 family targets 4 mRNAs of the MAPK pathway: MAPK1, IGF1, and GRB2 displaying epigenetic regulation of CH in cardiomyocytes.

Concomitantly, the metabolic regulation is mediated by PGC1α and KSR1, being ERRα-dependent and MAPK-independent, suggesting that common molecular regulatory points intersect CH and metabolism (Fisher et al., 2011). Plus, the PGC-1β gene encodes miR-378-3p and miR-378-5p, with the latter being responsible for counterbalancing its metabolic actions. Knockout mice for miR-378-3p and miR-378-5p, like miR-208a, are resistant to high-fat diet-induced obesity and exhibit a higher oxidative capacity for fatty acid metabolism in insulin-target tissues. This role seems to be performed by multiple targets, pointing out carnitine O-acetyltransferase (CRAT) and MED13, both increased in the livers of miR-378-3p/378-5p KO mice (Carrer et al., 2012).

MiR-21 is highly expressed in CVS. It is encoded by the VMP1 gene in chromosome 17 and is highly conserved between vertebrates. MiR-21, different from other tissue-specific miRNAs, is expressed in several mammal organ systems: heart, spleen, the small intestine, and colon, and many functional studies have identified miR-21 as an oncomiR. In the CVS, it is associated with the regulation of proliferative vascular disease, atherosclerosis, coronary heart disease, post angioplasty restenosis, and transplantation arteriopathy by targeting PTEN and PDCD4, and CH by targeting SPRY2 (Cheng and Zhang, 2010a). In this regard, some authors already showed that miR-21 inhibition in mouse hearts reduced cardiomyocyte size and the heart weight under CH conditions, and that pathological CH was induced by miR-21 by stimulating MAPK signaling in cardiac fibroblasts (Thum et al., 2008). If, on the one hand, miR-21 inhibition is therapeutic for cardiomyocytes, the same does not happen to adipocytes. An *in vitro* study shows that overexpression of miR-21 in glucose-insulin overloaded cells significantly increased insulin-induced glucose uptake and decreased PTEN protein expression, improving the metabolic phenotype of adipose cells, and the underlying mechanisms of versatile miRNA-21 in both tissues and their communication by circulation need further investigation (Cheng and Zhang, 2010b).

Finally, another cardiac-enriched family also implicated in the regulation of AT is the miR-30. This family is involved in ventricular CH by several mechanisms: autophagy, apoptosis, oxidative stress, and inflammation, associated with ischemic heart disease, hypertension, diabetic cardiomyopathy, and antineoplastic drug cardiotoxicity. The miR-30 family expression decreases in CH and myocardial ischemia/reperfusion, being permissive to a variety of targets to perform roles in the disease and also compensatory effects (Zhang X. et al., 2019). Beyond the role in CVS, the miR-30 family plays a role in AT regulating adipocyte differentiation, since its expression increases in the differentiation of human AT-derived stem cells into adipocytes. The inhibition of miR-30a and miR-30d in human multipotent adipose-derived stem cells reduced lipogenesis, and inversely, the overexpression of miR-30a and miR-30d family members promoted lipogenesis by targeting the transcription factor RUNX2 (Zaragosi et al., 2011). The miR-30b and -30c also increase thermogenic gene expression in primary adipocytes during adipocyte differentiation, cold exposure, or by the β-adrenergic receptor. Furthermore, the knockdown of miR-30 family members (including miR-30b and miR-30c), inhibited the expression of uncoupling protein 1 (UCP1) and cell death-inducing DFFA-like effector a (CIDEA) in brown adipocytes, by directly targeting RIP140, a nuclear receptor that acts as a co-regulator of lipid and glucose metabolism, showing a clear role in regulating BAT function (Hu et al., 2015). In summary, the miR-30 family performs a role in adipogenesis and regulates BAT function, showing that it may be another potential therapeutic target for regulating and clarifying lipid metabolism.

CONCLUSION

We elucidated some regulatory miRNAs and their endocrine roles by bidirectionally acting on the CV system and AT to regulate metabolism and several biological processes between phenotypes in health and disease (**Figure 1**; **Table 1**). The epigenetic relationship between tissues and the whole role performed by miRNAs and other regulatory RNAs remains a very complex field with several gaps to be investigated. It is worth mentioning that this bidirectional relationship is carried out through the circulation, and it is likely that the miRNAs that are part of crosstalk come not only from the AT and the heart and their cells but also from other tissues such as skeletal muscle, liver and the neuroendocrine axis. In addition, free or within EVs, miRNAs are not the only molecules involved in crosstalk, and genes, proteins, and other effector molecules can be carried, such as myokines and adipokines. Thus, the crosstalk is multilevel and involves not only the heart and AT, but is systemic. We discussed an interesting molecular basis that could partially explain the intricate, frequent and worldwide relationship between obesity and CVD. It remains unclear if the cardiac miRNAs are released within EVs, and publications regarding the role of EVs in these miRNAs mechanisms are emerging. These issues are of great interest, both mechanistically in a basic science view as in a clinical perspective, since CVD also may induce metabolic and morphological changes, and inversely, metabolic and morphological changes may induce CVD.

Mapping common, antagonistic, and/or parallel regulatory targets in the health status of different organisms by epigenetic mechanisms is also highly dependent on biotechnology, bioinformatics, confirmatory approaches from the bench, and effective gain and loss of function protocols. Translational approaches from the bench to clinical confirmation are also crucial to show how mechanisms can interact or be changed in different complexity grades. We are moving towards a science where all the knowledge produced in these inter areas converge, thus generating increasingly accurate and individualized approaches for treatment, prevention, and detection of diseases that globally affect humanity.

AUTHOR CONTRIBUTIONS

UPRS - Survey, Writing and Review BRRC - Survey, Writing, Review, Table and Figure ACI-C - Survey, Writing and Review LR - Writing and Review.

REFERENCE

Ambros, V. (2004). The Functions of Animal microRNAs. *Nature* 431, 350–355. doi:10.1038/nature02871

Arner, P., and Kulyté, A. (2015). MicroRNA Regulatory Networks in Human Adipose Tissue and Obesity. *Nat. Rev. Endocrinol.* 11, 276–288. doi:10.1038/nrendo.2015.25

Avogaro, A. (2006). Insulin Resistance: Trigger or Concomitant Factor in the Metabolic Syndrome. *Panminerva Med.* 48, 3–12.

Bartel, D. P. (2018). Metazoan MicroRNAs. *Cell.* 173, 20–51. doi:10.1016/j.cell.2018.03.006

Battineni, G., Sagaro, G. G., Chintalapudi, N., Amenta, F., Tomassoni, D., and Tayebati, S. K. (2021). Impact of Obesity-Induced Inflammation on Cardiovascular Diseases (Cvd). *Ijms* 22, 4798. doi:10.3390/ijms22094798

Bernardo, B. C., Gao, X.-M., Winbanks, C. E., Boey, E. J. H., Tham, Y. K., and Kiriazis, H. (2012). Therapeutic Inhibition of the miR-34 Family Attenuates Pathological Cardiac Remodeling and Improves Heart Function. *Proc. Natl. Acad. Sci. U. S. A.* 109, 17615–17620. doi:10.1073/pnas.1206432109

Boon, R. A., Iekushi, K., Lechner, S., Seeger, T., Fischer, A., Heydt, S., et al. (2013). MicroRNA-34a Regulates Cardiac Aging and Function. *Nature* 495, 107–110. doi:10.1038/nature11919

Boštjančič, E., Zidar, N., Štajer, D., and Glavač, D. (2010). MicroRNAs miR-1, miR-133a, miR-133b and miR-208 Are Dysregulated in Human Myocardial Infarction. *Cardiology* 115, 163–169. doi:10.1159/000268088

Brandes, R. P. (2014). Endothelial Dysfunction and Hypertension. *Hypertension* 64. doi:10.1161/HYPERTENSIONAHA.114.03575

Buechler, C., Krautbauer, S., and Eisinger, K. (2015). AT Fibrosis. *World J. Diabetes* 6. doi:10.4239/wjd.v6.i4.548

Callis, T. E., Pandya, K., Hee, Y. S., Tang, R. H., Tatsuguchi, M., Huang, Z. P., et al. (2009). MicroRNA-208a Is a Regulator of Cardiac Hypertrophy and Conduction in Mice. *J. Clin. Invest.* 119, 2772–2786. doi:10.1172/JCI36154

Carè, A., Catalucci, D., Felicetti, F., Bonci, D., Addario, A., Gallo, P., et al. (2007). MicroRNA-133 Controls Cardiac Hypertrophy. *Nat. Med.* 13, 613–618. doi:10.1038/nm1582

Carrer, M., Liu, N., Grueter, C. E., Williams, A. H., Frisard, M. I., Hulver, M. W., et al. (2012). Control of Mitochondrial Metabolism and Systemic Energy Homeostasis by microRNAs 378 and 378. *Proc. Natl. Acad. Sci. U. S. A.* 109, 15330–15335. doi:10.1073/pnas.1207605109

Caus, M., Eritja, À., and Bozic, M. (2021). Role of Micrornas in Obesity-Related Kidney Disease. *Int. J. Mol. Sci.* 22, 11416. doi:10.3390/ijms222111416

Chait, A., and den Hartigh, L. J. (2020). AT Distribution, Inflammation and its Metabolic Consequences, Including Diabetes and Cardiovascular Disease. *Front. Cardiovasc. Med.* 7, 22. doi:10.3389/fcvm.2020.00022

Chakravarthy, S., Sternberg, S. H., Kellenberger, C. A., and Doudna, J. A. (2010). Substrate-specific Kinetics of Dicer-Catalyzed RNA Processing. *J. Mol. Biol.* 404, 392–402. doi:10.1016/j.jmb.2010.09.030

Cheng, R., Dang, R., Zhou, Y., Ding, M., and Hua, H. (2017). MicroRNA-98 Inhibits TGF-B1-Induced Differentiation and Collagen Production of Cardiac Fibroblasts by Targeting TGFBR1. *Hum. Cell.* 30, 192–200. doi:10.1007/s13577-017-0163-0

Cheng, Y., and Zhang, C. (2010a). MicroRNA-21 in Cardiovascular Disease. *J. Cardiovasc. Transl. Res.* 3, 251–255. doi:10.1007/s12265-010-9169-7

Cheng, Y., and Zhang, C. (2010b). MiRNA-21 Reverses High Glucose and High Insulin Induced Insulin Resistance in 3T3-L1 Adipocytes through Targeting Phosphatase and Tensin Homologue. *J. Cardiovasc. Transl. Res.* 3, 553–559. doi:10.1055/s-0032-1311644

Christensen, R. H., von Scholten, B. J., Lehrskov, L. L., Rossing, P., and Jørgensen, P. G. (2020). Epicardial AT: an Emerging Biomarker of Cardiovascular Complications in Type 2 Diabetes? *Ther. Adv. Endocrinol. Metab.* 11, 2042018820928824. doi:10.1177/2042018820928824

Corrêa, L. H., Heyn, G. S., and Magalhaes, K. G. (2019). The Impact of the Adipose Organ Plasticity on Inflammation and Cancer Progression. *Cells* 8, 662. doi:10.3390/cells8070662

Danowski, N., Manthey, I., Jakob, H. G., Siffert, W., Peters, J., and Frey, U. H. (2013). Decreased Expression of miR-133a but Not of miR-1 Is Associated with Signs of Heart Failure in Patients Undergoing Coronary Bypass Surgery. *Cardiol* 125. doi:10.1159/000348563

Davis, B. N., Hilyard, A. C., Nguyen, P. H., Lagna, G., and Hata, A. (2010). Smad Proteins Bind a Conserved RNA Sequence to Promote MicroRNA Maturation by Drosha. *Mol. Cell.* 39. doi:10.1016/j.molcel.2010.07.011

Denli, A. M., Tops, B. B. J., Plasterk, R. H. A., Ketting, R. F., and Hannon, G. J. (2004). Processing of Primary microRNAs by the Microprocessor Complex. *Nature* 432. doi:10.1038/nature03049

Ding, J., Kritchevsky, S. B., Harris, T. B., Burke, G. L., Detrano, R. C., Szklo, M., et al. (2008). The Association of Pericardial Fat with Calcified Coronary Plaque. *Obesity* 16. doi:10.1038/oby.2008.278

Eichhorn, S. W., Guo, H., McGeary, S. E., Rodriguez-Mias, R. A., Shin, C., Baek, D., et al. (2014). MRNA Destabilization Is the Dominant Effect of Mammalian microRNAs by the Time Substantial Repression Ensues. *Mol. Cell.* 56. doi:10.1016/j.molcel.2014.08.028

Fang, X., Stroud, M. J., Ouyang, K., Fang, L., Zhang, J., Dalton, N. D., et al. (2016). Adipocyte-specific Loss of PPARγ Attenuates Cardiac Hypertrophy. *J. Clin. Invest.* 1. doi:10.1172/jci.insight.89908

Feng, B., Chen, S., Gordon, A. D., and Chakrabarti, S. (2017). miR-146a Mediates Inflammatory Changes and Fibrosis in the Heart in Diabetes. *J. Mol. Cell. Cardiol.* 105, 70–76. doi:10.1016/J.YJMCC.2017.03.002

Feng, H. J., Ouyang, W., Liu, J. H., Sun, Y. G., Hu, R., Huang, L. H., et al. (2014). Global microRNA Profiles and Signaling Pathways in the Development of Cardiac Hypertrophy. *Braz. J. Med. Biol. Res.* 47. doi:10.1590/1414-431X20142937

Fisher, K. W., Das, B., Kortum, R. L., Chaika, O. V., and Lewis, R. E. (2011). Kinase Suppressor of Ras 1 (KSR1) Regulates PGC1α and Estrogen-Related Receptor α to Promote Oncogenic Ras-dependent Anchorage-Independent Growth. *Mol. Cell. Biol.* 31. doi:10.1128/mcb.05255-11

Fu, T., Seok, S., Choi, S., Huang, Z., Suino-Powell, K., Xu, H. E., et al. (2014). MicroRNA 34a Inhibits Beige and Brown Fat Formation in Obesity in Part by Suppressing Adipocyte Fibroblast Growth Factor 21 Signaling and SIRT1 Function. *Mol. Cell. Biol.* 34. doi:10.1128/mcb.00596-14

Gan, L., Xie, D., Liu, J., Bond Lau, W., Christopher, T. A., Lopez, B., et al. (2020). Small Extracellular Microvesicles Mediated Pathological Communications Between Dysfunctional Adipocytes and Cardiomyocytes as a Novel Mechanism Exacerbating Ischemia/Reperfusion Injury in Diabetic Mice. *Circulation* 141 (12), 968–983. doi:10.1161/CIRCULATIONAHA.119.042640

Gan, Z., Rumsey, J., Hazen, B. C., Lai, L., Leone, T. C., Vega, R. B., et al. (2013). Nuclear receptor/microRNA Circuitry Links Muscle Fiber Type to Energy Metabolism. *J. Clin. Invest.* 123, 2564–2575. doi:10.1172/JCI67652

Ganz, P., and Hsue, P. Y. (2013). Endothelial Dysfunction in Coronary Heart Disease Is More Than a Systemic Process. *Eur. Heart J.* 34. doi:10.1093/eurheartj/eht199

Garciá-Arias, M. R., Gómez-Acosta, S. A., Medina-Galindo, J., Alavez-Torres, E., Cedillo-Urbina, M. R., Azuara-Negrete, N. D., et al. (2020). Heart as an Endocrine Organ. *Med. Interna Mex.* 36. doi:10.24245/mim.v36i2.2911

Grueter, C. E., Van Rooij, E., Johnson, B. A., Deleon, S. M., Sutherland, L. B., Qi, X., et al. (2012). A Cardiac MicroRNA Governs Systemic Energy Homeostasis by Regulation of MED13. *Cell* 149 (3), 671–683. doi:10.1016/j.cell.2012.03.029

Han, M. S., White, A., Perry, R. J., Camporez, J. P., Hidalgo, J., Shulman, G. I., et al. (2020). Regulation of at Inflammation by Interleukin 6. *Proc. Natl. Acad. Sci. U. S. A.* 117. doi:10.1073/pnas.1920004117

Hartwig, S., De Filippo, E., Göddeke, S., Knebel, B., Kotzka, J., Al-Hasani, H., et al. (2019). Exosomal Proteins Constitute an Essential Part of the Human at Secretome. *Biochim. Biophys. Acta - Proteins Proteomics* 1867 (12), 140172. doi:10.1016/j.bbapap.2018.11.009

Hashim, M. J. (2017). Global Burden of Obesity. *Int. J. Growth Dev.* 1. doi:10.25081/ijgd.2017.v1i1.46

Hassan, M. B., Nafakhi, H., and Al-Mosawi, A. A. (2020). Pericardial Fat Volume and Coronary Atherosclerotic Markers Among Body Mass Index Groups. *Clin. Cardiol.* 43. doi:10.1002/clc.23396

Heindel, J. J., and Blumberg, B. (2019). Environmental Obesogens: Mechanisms and Controversies. *Annu. Rev. Pharmacol. Toxicol.* 59. doi:10.1146/annurev-pharmtox-010818-021304

Heyn, G. S., Corrêa, L. H., and Magalhães, K. G. (2020). The Impact of AT–Derived miRNAs in Metabolic Syndrome, Obesity, and Cancer. *Front. Endocrinol. (Lausanne)* 11. doi:10.3389/fendo.2020.563816

Horman, S. R., Janas, M. M., Litterst, C., Wang, B., MacRae, I. J., Sever, M. J., et al. (2013). Akt-mediated Phosphorylation of Argonaute 2 Downregulates Cleavage and Upregulates Translational Repression of MicroRNA Targets. *Mol. Cell.* 50. doi:10.1016/j.molcel.2013.03.015

Hu, F., Wang, M., Xiao, T., Yin, B., He, L., Meng, W., et al. (2015). MiR-30 Promotes Thermogenesis and the Development of Beige Fat by Targeting RIP140. *Diabetes* 64. doi:10.2337/db14-1117

Hutvágner, G., McLachlan, J., Pasquinelli, A. E., Bálint, É., Tuschl, T., and Zamore, P. D. (2001). A Cellular Function for the RNA-Interference Enzyme Dicer in the Maturation of the Let-7 Small Temporal RNA. *Science* 80, 293. doi:10.1126/science.1062961

Iacobellis, G. (2009). Epicardial and Pericardial Fat: Close, but Very Different. *Obesity* 17. doi:10.1038/oby.2008.575

Improta Caria, A. C., Nonaka, C. K. V., Pereira, C. S., Soares, M. B. P., Macambira, S. G., and Souza, B. S. de. F. (2018). Exercise Training-Induced Changes in MicroRNAs: Beneficial Regulatory Effects in Hypertension, Type 2 Diabetes, and Obesity. *Int. J. Mol. Sci.* 19 (11), 3608 doi:10.3390/ijms19113608

Improta-Caria, A. C., Aras, M. G., Nascimento, L., De Sousa, R. A. L., Aras-Júnior, R., and Souza, B. S. D. F. (2021). MicroRNAs Regulating Renin-Angiotensin-Aldosterone System, Sympathetic Nervous System and Left Ventricular Hypertrophy in Systemic Arterial Hypertension. *Biomolecules* 11. doi:10.3390/biom11121771

Improta-Caria, A. C., de Sousa, R. A. L., Roever, L., Fernandes, T., de Oliveira, E. M., Júnior, R. A., et al. (2022). MicroRNAs in Type 2 Diabetes Mellitus: Potential Role of Physical Exercise. *Rev. Cardiovasc. Med.* 23. doi:10.31083/j.rcm2301029

Ji, C., and Guo, X. (2019). The Clinical Potential of Circulating microRNAs in Obesity. *Nat. Rev. Endocrinol.* 15. doi:10.1038/s41574-019-0260-0

Ji, X., Takahashi, R., Hiura, Y., Hirokawa, G., Fukushima, Y., and Iwai, N. (2009). Plasma miR-208 as a Biomarker of Myocardial Injury. *Clin. Chem.* 55 (11), 1944–1949. doi:10.1373/clinchem.2009.125310

Kershaw, E. E., and Flier, J. S. (2004). AT as an Endocrine Organ. *J. Clin. Endocrinol. Metabolism* 89 (6), 2548–2556. doi:10.1210/jc.2004-0395

Ketting, R. F., Fischer, S. E. J., Bernstein, E., Sijen, T., Hannon, G. J., and Plasterk, R. H. A. (2001). Dicer Functions in RNA Interference and in Synthesis of Small RNA Involved in Developmental Timing in *C. elegans*. *Genes. Dev.* 15. doi:10.1101/gad.927801

Kim, V. N. (2005). MicroRNA Biogenesis: Coordinated Cropping and Dicing. *Nat. Rev. Mol. Cell. Biol.* 6 (5), 376–385. doi:10.1038/nrm1644

Kozomara, A., Birgaoanu, M., and Griffiths-Jones, S. (2019). MiRBase: From microRNA Sequences to Function. *Nucleic Acids Res.* 47. doi:10.1093/nar/gky1141

Kranendonk, M. E., de Kleijn, D. P., Kalkhoven, E., Kanhai, D. A., Uiterwaal, C. S., van der Graaf, Y., et al. (2014). Extracellular Vesicle Markers in Relation to Obesity and Metabolic Complications in Patients with Manifest Cardiovascular Disease. *Cardiovasc. Diabetol.* 13, 37. doi:10.1186/1475-2840-13-37

Krol, J., Loedige, I., and Filipowicz, W. (2010). The Widespread Regulation of microRNA Biogenesis, Function and Decay. *Nat. Rev. Genet.* 11. doi:10.1038/nrg2843

Lázár, L., Nagy, B., Molvarec, A., Szarka, A., and Rigó, J. (2012). Role of Hsa-miR-325 in the Etiopathology of Preeclampsia. *Mol. Med. Rep.* 6. doi:10.3892/mmr.2012.954

Lee, R. C., Feinbaum, R. L., and Ambros, V. (1993). The *C. elegans* Heterochronic Gene Lin-4 Encodes Small RNAs with Antisense Complementarity to Lin-14. *Cell.* 75, 843–854. doi:10.1016/0092-8674(93)90529-Y

Lee, Y., Jeon, K., Lee, J. T., Kim, S., and Kim, V. N. (2002). MicroRNA Maturation: Stepwise Processing and Subcellular Localization. *The EMBO journal* 21 (17), 4663–4670. doi:10.1093/emboj/cdf476

Lee, Y., Kim, M., Han, J., Yeom, K. H., Lee, S., Baek, S. H., et al. (2004). MicroRNA Genes Are Transcribed by RNA Polymerase II. *EMBO J.* 23. doi:10.1038/sj.emboj.7600385

Lei, P., Baysa, A., Nebb, H. I., Valen, G., Skomedal, T., Osnes, J. B., et al. (2013). Activation of Liver X Receptors in the Heart Leads to Accumulation of Intracellular Lipids and Attenuation of Ischemia-Reperfusion Injury. *Basic Res. Cardiol.* 108. doi:10.1007/s00395-012-0323-z

Li, H., Li, S., Yu, B., and Liu, S. (2012). Expression of miR-133 and miR-30 in Chronic Atrial Fibrillation in Canines. *Mol. Med. Rep.* 5, 1457–1460. doi:10.3892/MMR.2012.831

Li, N., Wang, K., and Li, P. F. (2015). MicroRNA-34 Family and its Role in Cardiovascular Disease. *Crit. Rev. Eukaryot. Gene Expr.* 25. doi:10.1615/CritRevEukaryotGeneExpr.2015015396

Li, N., Zhou, H., and Tang, Q. (2018). miR-133: A Suppressor of Cardiac Remodeling? *Front. Pharmacol.* 9. doi:10.3389/fphar.2018.00903

Longo, M., Zatterale, F., Naderi, J., Parrillo, L., Formisano, P., Raciti, G. A., et al. (2019). AT Dysfunction as Determinant of Obesity-Associated Metabolic Complications. *Int. J. Mol. Sci.* 20. doi:10.3390/ijms20092358

Lörchner, H., Adrian-Segarra, J. M., Waechter, C., Wagner, R., Góes, M. E., Brachmann, N., et al. (2021). Concomitant Activation of OSM and LIF Receptor by a Dual-specific hlOSM Variant Confers Cardioprotection after Myocardial Infarction in Mice. *Int. J. Mol. Sci.*23 (1), 353. doi:10.3390/ijms23010353

Marí-Alexandre, J., Barceló-Molina, M., Sanz-Sánchez, J., Molina, P., Sancho, J., Abellán, Y., et al. (2019). Thickness and an Altered miRNA Expression in the Epicardial at Is Associated with Coronary Heart Disease in Sudden Death Victims. *Rev. Española Cardiol.* 72 (1), 30–39. doi:10.1016/j.rec.2017.12.007

Mathieu, M., Martin-Jaular, L., Lavieu, G., and Théry, C. (2019). Specificities of Secretion and Uptake of Exosomes and Other Extracellular Vesicles for Cell-To-Cell Communication. *Nat. Cell. Biol.* 21. doi:10.1038/s41556-018-0250-9

Matkovich, S. J., Hu, Y., and Dorn, G. W. (2013). Regulation of Cardiac microRNAs by Cardiac microRNAs. *Circ. Res.* 113, 62–71. doi:10.1161/CIRCRESAHA.113.300975

Maurizi, G., Della Guardia, L., Maurizi, A., and Poloni, A. (2018). Adipocytes Properties and Crosstalk with Immune System in Obesity-Related Inflammation. *J. Cell. Physiol.* 233. doi:10.1002/jcp.25855

Montaigne, D., Hurt, C., and Neviere, R. (2012). Mitochondria Death/survival Signaling Pathways in Cardiotoxicity Induced by Anthracyclines and Anticancer-Targeted Therapies. *Biochem. Res. Int.*, 951539 doi:10.1155/2012/951539

Morlando, M., Ballarino, M., Gromak, N., Pagano, F., Bozzoni, I., and Proudfoot, N. J. (2008). Primary microRNA Transcripts Are Processed Co-transcriptionally. *Chemtracts* 21. doi:10.1038/nsmb.1475

Muralimanoharan, S., Guo, C., Myatt, L., Maloyan, A., Romina, F., Manti, M., et al. (2015). Comparative Proteome Profile of Human Placenta from Normal and Preeclamptic Pregnancies. *ProQuest Diss. Theses* 7.

Neiburga, K. D., Vilne, B., Bauer, S., Bongiovanni, D., Ziegler, T., Lachmann, M., et al. (2021). Vascular Tissue Specific miRNA Profiles Reveal Novel Correlations with Risk Factors in Coronary Artery Disease. *Biomolecules* 11. doi:10.3390/biom11111683

Okada, C., Yamashita, E., Lee, S. J., Shibata, S., Katahira, J., Nakagawa, A., et al. (2009). A High-Resolution Structure of the Pre-microrna Nuclear Export Machinery. *Science* 80, 326. doi:10.1126/science.1178705

Ortega, F. J., Mercader, J. M., Catalán, V., Moreno-Navarrete, J. M., Pueyo, N., Sabater, M., et al. (2013). Targeting the Circulating microRNA Signature of Obesity. *Clin. Chem.* 59. doi:10.1373/clinchem.2012.195776

Pan, Y., Hui, X., Chong Hoo, R. L., Ye, D., Cheung Chan, C. Y., Feng, T., et al. (2019). Adipocyte-secreted Exosomal microRNA-34a Inhibits M2 Macrophage Polarization to Promote Obesity-Induced Adipose Inflammation. *J. Clin. Invest.* 129. doi:10.1172/JCI123069

Pasquinelli, A. E., Reinhart, B. J., Slack, F., Martindale, M. Q., Kuroda, M. I., Maller, B., et al. (2000). Conservation of the Sequence and Temporal Expression of Let-7 Heterochronic Regulatory RNA. *Nature* 408. doi:10.1038/35040556

Patel, V. B., Shah, S., Verma, S., and Oudit, G. Y. (2017). Epicardial at as a Metabolic Transducer: Role in Heart Failure and Coronary Artery Disease. *Heart fail. Rev.* 22. doi:10.1007/s10741-017-9644-1

Pfeffer, S., Sewer, A., Lagos-Quintana, M., Sheridan, R., Sander, C., Grässer, F. A., et al. (2005). Identification of microRNAs of the Herpesvirus Family. *Nat. Methods* 2. doi:10.1038/nmeth746

Pilkington, A. C., Paz, H. A., and Wankhade, U. D. (2021). Beige at Identification and Marker Specificity—Overview. *Front. Endocrinol. (Lausanne)* 12. doi:10.3389/fendo.2021.599134

Pu, Y., Zhao, Q., Men, X., Jin, W., and Yang, M. (2021). MicroRNA-325 Facilitates Atherosclerosis Progression by Mediating the SREBF1/LXR axis via KDM1A. *Life Sci.* 277. doi:10.1016/j.lfs.2021.119464

Qipshidze Kelm, N., Piell, K. M., Wang, E., and Cole, M. P. (2018). MicroRNAs as Predictive Biomarkers for Myocardial Injury in Aged Mice Following Myocardial Infarction. *J. Cell. Physiol.* 233. doi:10.1002/jcp.26283

Ramasamy, S., Velmurugan, G., Rajan, K. S., Ramprasath, T., and Kalpana, K. (2015). MiRNAs with Apoptosis Regulating Potential Are Differentially Expressed in Chronic Exercise-Induced Physiologically Hypertrophied Hearts. *PLoS One* 10, 1–12. doi:10.1371/journal.pone.0121401

Ramasamy, S., Velmurugan, G., Rekha, B., Anusha, S., Shanmugha Rajan, K., Shanmugarajan, S., et al. (2018). Egr-1 Mediated Cardiac miR-99 Family Expression Diverges Physiological Hypertrophy from Pathological Hypertrophy. *Exp. Cell. Res.* 365. doi:10.1016/j.yexcr.2018.02.016

Reilly, J. J. (2017). Health Effects of Overweight and Obesity in 195 Countries. *N. Engl. J. Med.* 377, 1496. doi:10.1056/nejmc1710026

Reinhart, B. J., Slack, F. J., Basson, M., Pasquienelll, A. E., Bettlnger, J. C., Rougvle, A. E., et al. (2000). The 21-nucleotide Let-7 RNA Regulates Developmental Timing in *Caenorhabditis elegans*. *Nature* 403. doi:10.1038/35002607

Ren, J., Wu, N. N., Wang, S., Sowers, J. R., and Zhang, Y. (2021). Obesity Cardiomyopathy: Evidence, Mechanisms, and Therapeutic Implications. *Physiol. Rev.* 101. doi:10.1152/physrev.00030.2020

Rosen, E. D., and Spiegelman, B. M. (2014). What We Talk about when We Talk about Fat. *Cell.* 156. doi:10.1016/j.cell.2013.12.012

Roush, S., and Slack, F. J. (2008). The Let-7 Family of microRNAs. *Trends Cell. Biol.* 18. doi:10.1016/j.tcb.2008.07.007

Sala, L. La., Crestani, M., Garavelli, S., de Candia, P., and Pontiroli, A. E. (2021). Does microRNA Perturbation Control the Mechanisms Linking Obesity and Diabetes? Implications for Cardiovascular Risk. *Int. J. Mol. Sci.* 22. doi:10.3390/ijms22010143

Samanta, S., Balasubramanian, S., Rajasingh, S., Patel, U., Dhanasekaran, A., Dawn, B., et al. (2016). MicroRNA: A New Therapeutic Strategy for Cardiovascular Diseases. *Trends cardiovasc. Med.* 26. doi:10.1016/j.tcm.2016.02.004

Satoh, M., Minami, Y., Takahashi, Y., Tabuchi, T., and Nakamura, M. (2010). Expression of microRNA-208 Is Associated with Adverse Clinical Outcomes in Human Dilated Cardiomyopathy. *J. Card. Fail.* 16, 404–410. doi:10.1016/j.cardfail.2010.01.002

Scheja, L., and Heeren, J. (2019). The Endocrine Function of ATs in Health and Cardiometabolic Disease. *Nat. Rev. Endocrinol.* 15. doi:10.1038/s41574-019-0230-6

Shaihov-Teper, O., Ram, E., Ballan, N., Brzezinski, R. Y., Naftali-Shani, N., Masoud, R., et al. (2021). Extracellular Vesicles from Epicardial Fat Facilitate Atrial Fibrillation. *Circulation* 143, 2475–2493. doi:10.1161/CIRCULATIONAHA.120.052009

Sluijter, J. P. G., Davidson, S. M., Boulanger, C. M., Buzás, E. I., De Kleijn, D. P. V., Engel, F. B., et al. (2018). Extracellular Vesicles in Diagnostics and Therapy of the Ischaemic Heart: Position Paper from the Working Group on Cellular Biology of the Heart of the European Society of Cardiology. *Cardiovasc. Res.* 114. doi:10.1093/cvr/cvx211

Small, E. M., and Olson, E. N. (2011). Pervasive Roles of microRNAs in Cardiovascular Biology. *Nature* 469, 336–342. doi:10.1038/nature09783

Sohel, M. H. (2016). Extracellular/Circulating MicroRNAs: Release Mechanisms, Functions and Challenges. *Achiev. Life Sci.* 10. doi:10.1016/j.als.2016.11.007

Song, J., Su, W., Chen, X., Zhao, Q., Zhang, N., Li, M. G., et al. (2017). Micro RNA-98 Suppresses Interleukin-10 in Peripheral B Cells in Patient Post-cardio Transplantation. *Oncotarget* 8. doi:10.18632/oncotarget.16000

Sun, C., Liu, H., Guo, J., Yu, Y., Yang, D., He, F., et al. (2017). MicroRNA-98 Negatively Regulates Myocardial Infarction-Induced Apoptosis by Down-Regulating Fas and Caspase-3. *Sci. Rep.* 7. doi:10.1038/s41598-017-07578-x

Thomou, T., Mori, M. A., Dreyfuss, J. M., Konishi, M., Sakaguchi, M., Wolfrum, C., et al. (2017). Adipose-derived Circulating miRNAs Regulate Gene Expression in Other Tissues. *Nature* 542. doi:10.1038/nature21365

Thompson, M. D., Cismowski, M. J., Serpico, M., Pusateri, A., and Brigstock, D. R. (2017). Elevation of Circulating microRNA Levels in Obese Children Compared to Healthy Controls. *Clin. Obes.* 7. doi:10.1111/cob.12192

Thum, T., Gross, C., Fiedler, J., Fischer, T., Kissler, S., Bussen, M., et al. (2008). MicroRNA-21 Contributes to Myocardial Disease by Stimulating MAP Kinase Signalling in Fibroblasts. *Nature* 456. doi:10.1038/nature07511

Torres, N., Vargas-Castillo, A. E., and Tovar, A. R. (2015). "AT: White at Structure and Function," in *Encyclopedia of Food and Health*. doi:10.1016/B978-0-12-384947-2.00006-4

Treiber, T., Treiber, N., and Meister, G. (2019). Regulation of microRNA Biogenesis and its Crosstalk with Other Cellular Pathways. *Nat. Rev. Mol. Cell. Biol.* 20. doi:10.1038/s41580-018-0059-1

Turchinovich, A., Weiz, L., and Burwinkel, B. (2012). Extracellular miRNAs: the Mystery of Their Origin and Function. *Trends biochem. Sci.* 37, 460–465. doi:10.1016/j.tibs.2012.08.003

van Rooij, E., Quiat, D., Johnson, B. A., Sutherland, L. B., Qi, X., Richardson, J. A., et al. (2009). A Family of microRNAs Encoded by Myosin Genes Governs Myosin Expression and Muscle Performance. *Dev. Cell.* 17, 662–673. doi:10.1016/j.devcel.2009.10.013

Van Rooij, E., Sutherland, L. B., Qi, X., Richardson, J. A., Hill, J., and Olson, E. N. (2007). Control of Stress-dependent Cardiac Growth and Gene Expression by a microRNA. *Science* 316 (5824), 575–579. doi:10.1126/science.1139089

Van Rooij, E., Sutherland, L. B., Thatcher, J. E., DiMaio, J. M., Naseem, R. H., Marshall, W. S., et al. (2008). Dysregulation of microRNAs after Myocardial Infarction Reveals a Role of miR-29 in Cardiac Fibrosis. *Proc. Natl. Acad. Sci. U. S. A.* 105, 13027–13032. doi:10.1073/pnas.0805038105

Vegiopoulos, A., Rohm, M., and Herzig, S. (2017). AT: between the Extremes. *EMBO J.* 36. doi:10.15252/embj.201696206

Wang, Y., Medvid, R., Melton, C., Jaenisch, R., and Blelloch, R. (2007). DGCR8 Is Essential for microRNA Biogenesis and Silencing of Embryonic Stem Cell Self-Renewal. *Nat. Genet.* 39. doi:10.1038/ng1969

Wightman, B., Ha, I., and Ruvkun, G. (1993). Posttranscriptional Regulation of the Heterochronic Gene Lin-14 by Lin-4 Mediates Temporal Pattern Formation in C. elegans. *Cell* 75 (5), 855–862. doi:10.1016/0092-8674(93)90530-4

Yi, R., Qin, Y., Macara, I. G., and Cullen, B. R. (2003). Exportin-5 Mediates the Nuclear Export of Pre-microRNAs and Short Hairpin RNAs. *Genes. Dev.* 17. doi:10.1101/gad.1158803

Yin, H., Pasut, A., Soleimani, V. D., Bentzinger, C. F., Antoun, G., Thorn, S., et al. (2013). MicroRNA-133 Controls Brown Adipose Determination in Skeletal Muscle Satellite Cells by Targeting Prdm16. *Cell. Metab.* 17, 210–224. doi:10.1016/J.CMET.2013.01.004

Zaragosi, L. E., Wdziekonski, B., Brigand, K. L., Villageois, P., Mari, B., Waldmann, R., et al. (2011). Small RNA Sequencing Reveals miR-642a-3p as a Novel Adipocyte-specific microRNA and miR-30 as a Key Regulator of Human Adipogenesis. *Genome Biol.* 12. doi:10.1186/gb-2011-12-7-r64

Zeng, Y., and Cullen, B. R. (2004). Structural Requirements for Pre-microRNA Binding and Nuclear Export by Exportin 5. *Nucleic Acids Res.* 32. doi:10.1093/nar/gkh824

Zhang, P., Konja, D., and Wang, Y. (2020). AT Secretory Profile and Cardiometabolic Risk in Obesity. *Endocr. Metab. Sci.* 1. doi:10.1016/j.endmts.2020.100061

Zhang, X., Dong, S., Jia, Q., Zhang, A., Li, Y., Zhu, Y., et al. (2019). The microRNA in Ventricular Remodeling: The MIR-30 Family. *Biosci. Rep.* 39. doi:10.1042/BSR20190788

Zhang, Y., Liu, Y., Liu, H., and Tang, W. H. (2019). Exosomes: Biogenesis, Biologic Function and Clinical Potential. *Cell. Biosci.* 9. doi:10.1186/s13578-019-0282-2

Zhou, Y., Li, X., Zhao, D., Li, X., and Dai, J. (2021). Long Non-coding RNA MEG3 Knockdown Alleviates Hypoxia-Induced Injury in Rat Cardiomyocytes via the miR-325-3p/TRPV4 axis. *Mol. Med. Rep.* 23. doi:10.3892/mmr.2020.11656

Zoico, E., Rubele, S., De Caro, A., Nori, N., Mazzali, G., Fantin, F., et al. (2019). Brown and Beige at and Aging. *Front. Endocrinol. (Lausanne).* 10. doi:10.3389/fendo.2019.00368

Conflict of Interest: The authors declare that the research was conducted in the absence of any commercial or financial relationships that could be construed as a potential conflict of interest.

Publisher's Note: All claims expressed in this article are solely those of the authors and do not necessarily represent those of their affiliated organizations, or those of the publisher, the editors, and the reviewers. Any product that may be evaluated in this article, or claim that may be made by its manufacturer, is not guaranteed or endorsed by the publisher.

GLOSSARY

ABCA1, ATP-binding cassette transporter A
ADicerKO, Knockout Dicer-deficient
AF, Atrial Fibrillation
Akt, Protein kinase B (PKB)
ALDH2, Aldehyde dehydrogenase
AMPK, AMP-activated protein kinase (α1 and α2 subunit)
ANF, Atrial natriuretic factor
ApoE-/-, Apolipoprotein E knockout mice
AT, AT
BAT, Brown AT
BCL6, B-cell lymphoma 6
BeAT, Beige AT
BIRC, Baculoviral IAP Repeat Containing 6
BMI-, Body mass index
BNP, Brain natriuretic peptide
CAD, Coronary vascular disease
CH-, Cardiac hypertrophy
CNP, Cardiac natriuretic peptides
CRP-, C-Reactive Protein
CVD, Cardiovascular disease
CVS, cardiovascular system
CIDEA, Cell Death Inducing DFFA Like Effector A
CRAT, Carnitine O-acetyltransferase
EAT, Epicardial AT; epicardial fat
EGR-1, Early growth response protein 1
ERR-α, Estrogen-related receptor α
EVs, Extracellular vesicles
Fas, Fas ligand protein
FGF21, Fibroblast Growth Factor
FLT, Follistatin
GDF-15, Growth differentiation factor-15
GRB2, Growth factor receptor-bound protein
HF, Heart failure
Hif1α, Hypoxia-inducible factor 1-alpha
hiPSC, Human induced pluripotent stem cells
IGF1, Insulin Growth Factor 1
IGFR1, Insulin-like growth factor receptor
IHF, Intrahepatic fat
IL-6, Interleukin 6
IL-10, Interleukin 10
IL-1β, Interleukin-1 beta
KDM1A, Lysine-specific histone demethylase 1A (LSD1)
KLF4, Krüppel-like factor 4
KRS1 Kinase suppressor of ras 1
KO, Knockout
LIFR, Leukemia inhibitory factor receptor
LV, left ventricle
LXR, The liver X receptor
MAPK, Mitogen-Activated Protein Kinases
MEG3, Maternally Expressed Gene 3
MED13, Mediator of RNA polymerase II transcription subunit 13
MHC, myosin heavy chain
MII, Myocardial infarct injury
miRNAs, microRNAs
mRNA, messenger RNA
mTOR, Mammalian target of rapamycin
OBT, Obesity
PAT, Pericardial AT
PDCD4, Programmed cell death 4
PGC1α, Peroxisome proliferator-activated receptor gamma coactivator 1α
PI3Ks, Phosphoinositide-3 kinases
PNUTS, Protein phosphatase 1 binding protein
PPARγ, Peroxisome proliferator-activated receptor gamma
PRDM16, PR/SET Domain 16
PTEN, Phosphatase and tensin homolog
PURβ, Transcriptional activator protein Pur-beta
PVAT, Perivascular AT; perivascular fat
RIP140, Receptor-interacting protein 140
RNA, ribonucleic acid
RUNX, Runt-related transcription factor X
SEMA4b, Semaphorin 4B
SIRT1, Sirtuin 1
SMSC, Skeletal muscle satellite cells
SMSC, skeletal muscle satellite cells
SOX-6, SRY-Box Transcription Factor 6
SPRY-2, Sprouty homolog 2
SREBF1, Sterol response element-binding factor-1
TGFβ, Transforming growth factor beta
TGFβR1, Transforming growth factor beta receptor
TNFα, Tumor Necrosis Factor α
TRPV4, Potential cation channel subfamily V member 4
TSC1, Tuberous Sclerosis Complex 1
WAT, White AT
UCP-1, Uncoupling protein-1
UCP-3, Uncoupling protein-3

3'-UTR, 3' untranslated region

VAT, Visceral AT; visceral fat

VGFA, Vascular endothelial growth factor A

VMP1, Vacuole Membrane Protein 1

Advantages of publishing in Frontiers

OPEN ACCESS
Articles are free to read for greatest visibility and readership

FAST PUBLICATION
Around 90 days from submission to decision

HIGH QUALITY PEER-REVIEW
Rigorous, collaborative, and constructive peer-review

TRANSPARENT PEER-REVIEW
Editors and reviewers acknowledged by name on published articles

Frontiers
Avenue du Tribunal-Fédéral 34
1005 Lausanne | Switzerland

Visit us: www.frontiersin.org
Contact us: frontiersin.org/about/contact

REPRODUCIBILITY OF RESEARCH
Support open data and methods to enhance research reproducibility

DIGITAL PUBLISHING
Articles designed for optimal readership across devices

FOLLOW US
@frontiersin

IMPACT METRICS
Advanced article metrics track visibility across digital media

EXTENSIVE PROMOTION
Marketing and promotion of impactful research

LOOP RESEARCH NETWORK
Our network increases your article's readership